

Title	The investigation of potentially toxic elements (PTE) and particulates absorbed on particle filters exposed to vehicle emissions at road level
Authors	Spellissy, Fiona
Publication date	2016
Original Citation	Spellissy, F. 2016. The investigation of potentially toxic elements (PTE) and particulates absorbed on particle filters exposed to vehicle emissions at road level. PhD Thesis, University College Cork.
Type of publication	Doctoral thesis
Rights	© 2016, Fiona Spellissy. - <a href="http://creativecommons.org/licenses/by-nc-nd/3.0/">http://creativecommons.org/licenses/by-nc-nd/3.0/</a>
Download date	2023-05-07 21:34:58
Item downloaded from	<a href="http://hdl.handle.net/10468/3880">http://hdl.handle.net/10468/3880</a>

The Investigation of Potentially Toxic Elements (PTE) and  
Particulates Absorbed on Particle Filters Exposed to Vehicle  
Emissions at Road Level.

Fiona Spellissy B.Sc. M.Sc.

Doctoral Thesis

Chemistry Department  
University College Cork

Submitted:

Supervisor: Dr. Dara Fitzpatrick

Head of Department: Prof. Martyn Pemble

**Declaration:**

I declare that the following thesis is my own work and that it has not been previously submitted with the intension of obtaining a third level qualification.

---

Fiona Spellissy

**Abstract:**

The main focus of this study is to determine the levels of potentially toxic elements (PTE) collected from cabin particle filters in and around Cork city. Cabin particle filters are used in motor vehicles to extract toxins from air coming through the ventilation system. A systematic study of pollutants captured over fixed mileages on cabin filters has not previously been reported in literature, despite being an obvious and widespread sample source to measure potential exposure in traffic streams. This study presents quantitative data for a range of analytes from filters harvested from vehicles at set mileages.

Different open and closed vessel acid digestion methods were compared to determine which extraction method yields optimum recoveries for a known standard reference material (NIST 1648a Urban Particulate Matter). Analyte concentrations from filter samples were determined using inductively coupled plasma emission spectroscopy (ICP-OES). SEM analysis was used to provide imagery of the filter surface to determine the size of particulates being extracted by the filters.

The extraction efficiencies of particle filters were analysed with respect to the following variables: filter manufacturer, car model, varying kilometerages and different filter types. Air purifiers were also placed in the car's cabins to analyse the concentrations of analytes passing through the ventilation system into the cabin, with and without a particle filter in place. Cycling filters, worn by a cyclist for 500 km intervals, were also tested to analyse the difference between exposures in a vehicle compared to at the roadside.

From SEM images obtained there appears to be degradation in the filter structure with use, this degradation affects the filters ability to retain particulates. This degradation has a direct impact on the retention of certain PTEs which are bound to coarse or fine particulates.

It was found that for all analytes, the level of capture increases steadily between 0 and 15,000 km, followed by a significant increase between 15,000 and 30,000. The capture rate levels off between 30,000 and 45,000 km. Cabin filters with an activated carbon layer (combination filters) demonstrate a significant increase in pollutant capture. The possible health implications of exposure to reported analytes captured on the filters is also discussed due to the prevalence of convertible cars in warmer climates. This study leads to a recommendation of the use of combination filters in all vehicles.



<b>Declaration:</b>	1
<b>Abstract:</b>	2
<b>Chapter 1: Introduction</b>	
1.1 Particulate Matter: (PM)	6
1.2 Ambient Air Monitoring	8
1.3 Potentially toxic elements of Concern	14
1.4 Particle/Cabin Air Filters	24
1.5 Instrumentation	39
<b>Chapter 2: Materials and Methods</b>	
2.1 Materials: Acids used for microwave digestion	52
2.2 Acid Digestion Methods	53
2.3 Instrumentation	54
2.4 Representative sampling of pollen filters	55
2.5 Portable in cabin air purifier	56
2.6 Respro® City™ Cycle Mask	57
<b>Chapter 3: Method development for acid digestion of filter samples</b>	
3.1 Closed vs Open Vessel Digestion Methods	61
3.2 Microwave Multiwave Closed Vessel Acid Digestion	64
3.3 Reproducibility of analytical method	77
3.4 The effect of acid concentration on Acid Digestion Recoveries	78
<b>Chapter 4: Data Comparison between ICP and GFAAS</b>	89
<b>Chapter 5: Cabin filter analysis.</b>	
5.1 Analyte Concentrations from Exposed Cabin Air Filters	97
5.2 Aluminium	98
5.3 Chromium	107
5.4 Copper	114
5.5 Iron	121
5.6 Lead	128
5.7 Manganese	135
5.8 Zinc	142

5.9	Analyte concentrations in relation to particulate sizes.	149
 <b>Chapter 6: Internal Cabin Filters and Cycle Filters.</b>		
6.1	Internal filtration filters Introduction	158
6.2	Aluminium	159
6.3:	Chromium	165
6.4:	Copper	168
6.5:	Iron	173
6.6:	Lead	178
6.7:	Manganese	183
6.8:	Zinc	188
6.9:	Filters collected from cycling masks	193
6.10	A comparison between cycle filters and internal cabin filters	203
 <b>Chapter 7: SEM Imagery &amp; EDX quantitative analysis</b>		
7.1:	SEM imagery of Micronair Standard Particle Filters	208
7.2:	SEM imagery of Micronair Combination Filter	218
7.3:	EDX: Micronair Standard Particle Filters	222
 <b>Conclusion</b>		228
 <b>Further study</b>		230
 <b>References</b>		231
 <b>Appendix</b>		237

# **Chapter 1:**

## **Introduction**

## Chapter 1

### Introduction

#### **Atmospheric Pollution:**

The increasing volume of traffic on our roads is contributing to ever increasing levels of pollutants in the air at ground level. Potentially toxic elements (PTEs) can be bound to solid particles, liquid droplets or gases found in ambient roadside air. The levels of atmospheric pollutants are of interest due to the toxic effects they can have on human health. Trends in air pollution are monitored to identify the sources of pollutants. Particulate matter is of interest because it can absorb/adsorb gas, analytes and other carcinogenic compounds [1].

#### **1.1 Particulate Matter: (PM)**

A direct link exists between the size of pollutant particles and their toxicity. Particulate matter [2] refers to a mixture of solid particles and liquid drops found in the air. Air contains inhalable coarse particles with diameters between 2.5  $\mu\text{m}$  and 10  $\mu\text{m}$  and fine particles with diameters  $<2.5 \mu\text{m}$ . Fine particles that are  $<2.5 \mu\text{m}$  in diameter can remain in the air for weeks because of their light weight. Particles that pose the greatest risk are  $<10 \mu\text{m}$  in diameter because they can travel into the lungs and enter the bloodstream. Inhalable coarse particles found near roadways and as industrial by-products are generally  $>2.5 \mu\text{m}$  and  $<10 \mu\text{m}$ . While fine particles released during combustion (e.g. wood burning, vehicle emissions and power plants) are generally  $\leq 2.5 \mu\text{m}$  in diameter, these particles pose the greatest risk because they can penetrate deep into the lungs. Health problems arise from inhaling these particles such as decreased lung function, aggravated asthma, chronic bronchitis, non-fatal heart attacks and even death in people suffering from heart/lung disease [3].

Particulates come from primary sources emitted directly from a source e.g. construction sites, fires and unpaved roads. Secondary sources arise from reactions that occur in the air, mainly involving sulfur dioxide and nitrogen oxides that are emitted from factories and vehicles [4]. The release of pollutants is due to either human activity or natural sources. Sources from human activity include stationary sources e.g. power plants or waste incinerators, mobile sources include motor vehicles, aircraft, dust and controlled burning practices in agriculture. Natural sources, from non-human activity e.g. dust from areas with no vegetation and radon from radioactive decay within the earth's crust [5].

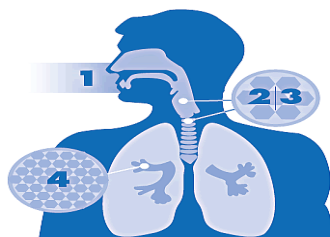


**Figure 1.1.1** Diagram of particulate matter entering the body: 1, PM enters through the respiratory system through the nose and mouth, 2/3, Larger particles are eliminated through coughing and sneezing. 4. PM 2.5 and smaller enter deep into the lungs causing lung, heart problems and release harmful chemicals into the bloodstream. [6]

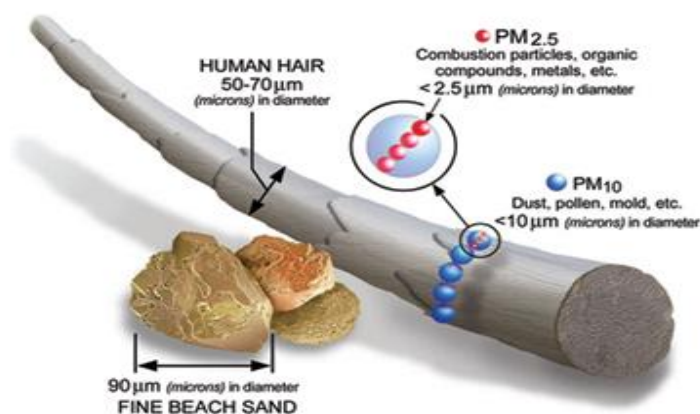


Figure 1.1.2: A human hair is shown to be ~70  $\mu\text{m}$  in diameter which makes it ~30 times larger than the largest fine particle (2.5 $\mu\text{m}$ ). [7]

Table 1.1.1 and Table 1.1.2 show the world's most polluted countries (2014). Air pollution is measured here by the concentration of fine particulate matter (i.e. particles  $\leq 2.5$  (PM 2.5) present in ambient air.[8]

**Table 1.1.1** The World Health Organisation's (WHO) ranking of the most polluted countries in terms of PM<sub>2.5</sub> concentrations.

Country	Annual mean PM <sub>2.5</sub> $\mu\text{g}/\text{m}^3$	Year	Urban population coverage (%)
Botswana	216	2005	27%
India	109	2008	91% by state
Mongolia	279	2008	70%
Pakistan	198	2004	40
Senegal	145	2010	50%

Table 1.1.2 Comparison by the World Health Organisation of major cities in Central and Southeast Asia.[8]

Country	Annual mean PM2.5 $\mu\text{g}/\text{m}^3$
Delhi (India)	153
Karachi (Pakistan)	117
Dhaka (Bangladesh)	86
Beijing (China)	56
Colombo (Sri Lanka)	28

## 1.2 Ambient Air Monitoring:

A report on Irish air quality Index for Health (AQIH) was generated by the EPA/HSE in 2013. The reporting procedure was developed in 2004 (used from 2005) by the EPA to investigate the health impact of air pollution and examine the air quality across Ireland.

Air quality is ranked from Good (ranked No. 1)  $\longrightarrow$  fair  $\longrightarrow$  poor  $\longrightarrow$  very poor (ranked No. 10) based on the quantities of the five measured air pollutants, ozone, nitrogen dioxide, sulfur dioxide, PM2.5 and PM10 [9].

Table 1.2.1: Air Quality Index Criteria

Band	Index	Ozone	Nitrogen Dioxide	Sulfur Dioxide	PM2.5	PM10
		Running 8hr mean ( $\mu\text{g}/\text{m}^3$ )	1hr mean ( $\mu\text{g}/\text{m}^3$ )	1hr mean ( $\mu\text{g}/\text{m}^3$ )	Running 24hr mean ( $\mu\text{g}/\text{m}^3$ )	Running 24hr mean ( $\mu\text{g}/\text{m}^3$ )
Good	1	0-33	0-67	0-29	0-11	0-16
	2	34-66	68-134	30-59	12-23	17-33
	3	67-100	135-200	60-89	24-35	34-50
Fair	4	101-120	201-267	90-119	36-41	51-58
	5	121-140	268-334	120-149	42-47	59-66
	6	141-160	335-400	150-179	48-53	67-75
Poor	7	161-187	401-467	180-236	54-58	76-83
	8	188-213	468-534	237-295	59-64	84-91
	9	214-240	535-600	296-354	65-70	92-100
Very poor	10	$\geq 241$	$\geq 601$	$\geq 355$	$\geq 71$	$\geq 101$

Table 1.2.2: Health Precautions: [9]

Band	Index	Health Messages for at Risk Groups	
		At Risk Individuals	General Population
Good	1 - 3	Partake in usual outdoor activities	Partake in usual outdoor activities
Fair	4 - 6	Adults/children with heart/lung problems should partake in less strenuous activities.	Partake in usual outdoor activities
Poor	7 - 9	Adults/children with heart/lung problems should partake in less strenuous activities especially outdoors. Asthma sufferers may need to use inhalers more often.	May experience sore eyes, coughing or sore throats. Should consider partaking in less strenuous activities.
Very poor	10	Adults/children with heart/lung problems should avoid strenuous activities.	Should consider reducing outdoor activities.

Several geographical areas were sampled, the results of which are shown in Table 1.2.3, these included Dublin City, large towns (referring to areas with populations >15,000 people e.g. Cork City), small towns (referring to areas with population between 5,000 and 15,000 people), rural west (towns with population less than 5,000 people, on the west coast) and Rural East (Towns with population less than 5,000, on the east coast). The geographical area of interest is Cork City because the filter samples analysed as part of this study were collected in and around Cork City. The pollutants of interest are PM<sub>2.5</sub> and PM<sub>10</sub> because it is assumed that PTE extracted from filter samples are bound to particulate matter on filters.

Table 1.2.3: Shows the results of EPA monitoring of PM<sub>2.5</sub> & PM<sub>10</sub> in 2005 ranked per the criteria set out in Table 1.2.1 [9]

	No. Fair days		No. Poor days		No. Very Poor days	
	PM <sub>2.5</sub>	PM <sub>10</sub>	PM <sub>2.5</sub>	PM <sub>10</sub>	PM <sub>2.5</sub>	PM <sub>10</sub>
Dublin City	12	10	2	2	0	0
Large Towns	21	15	6	5	6	4
Small Towns	11	11	0	0	0	0
Rural West	1	0	0	0	0	0
Rural East	1	0	0	0	0	0

Table 1.2.4 shows locations of monitors placed around Cork City. With regard to this report Cork city figures relate to areas incorporating Cork City Council jurisdiction with additional built up areas [9].

Table 1.2.4 Cork City EPA Monitor Locations [9].

	Ozone	Nitrogen Dioxide	Sulfur Dioxide	PM2.5	PM10
Cork City	Cork - Old Station Road	Cork - Old Station Road	Cork – Old Station Road	None - Small town used (Longford town*)	None - Small town used (Longford town*)

\*No real-time PM2.5 or PM10 monitor exists in Cork City. It is assumed that concentrations are comparable to small town concentrations rather than Dublin City.

PM2.5 originates from a mixture of solids and liquids made of nitrates, sulfates, VOCs, PTE and soil/dust particles and PM10 originates from dust emissions from burning solid fuels or vehicle emissions.

Figures for annual qualitative analyses of PM 2.5, PM10 and PTE (arsenic, lead, cadmium and nickel) carried out by the EPA are shown below. Figures 1.2.1 and Figure 1.2.2 show annual mean concentrations for PM2.5 and PM10 analysis at various sampling locations. Average PM2.5 & PM10 levels in Cork City are comparable on average to the other locations and are significantly less than the annual limit value.

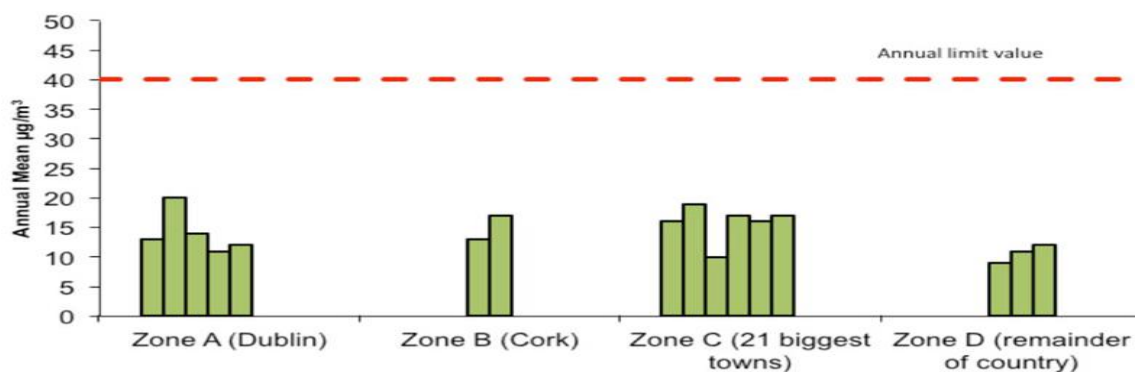


Figure 1.2.1: PM10 Concentrations[10]

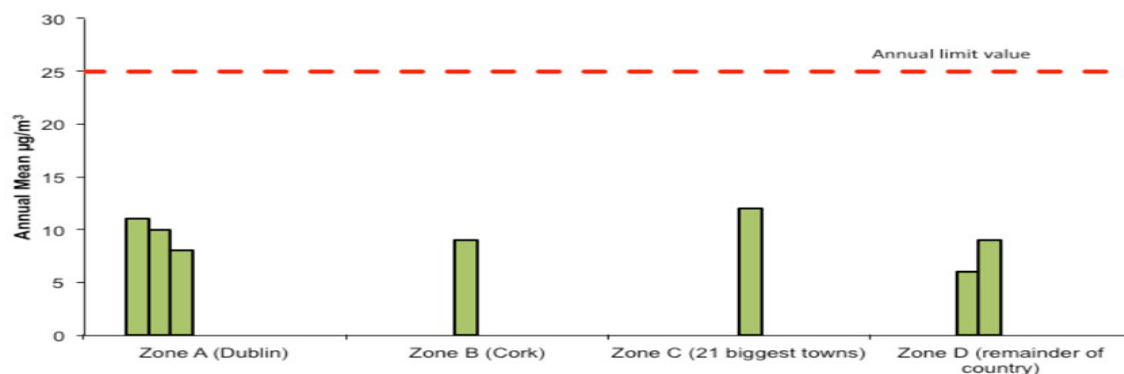


Figure 1.2.2: PM2.5 Concentrations[10]



Potentially toxic elements in air: Figures 1.2.2, 1.2.4, 1.2.5 and 1.2.6, show annual mean concentrations for arsenic, lead, cadmium and nickel respectively at sampling locations. Table 1.2.5 shows threshold limits for the four PTE tested. Average levels for arsenic, lead, cadmium and nickel in Cork city are comparable to the other locations and are significantly less than the annual limit value.

Table 1.2.5: Shows PTE exposure limits in air [10].

Pollutant	EU Limit or Target Value ( $\text{ng}/\text{m}^3$ )	Upper Assessment Threshold Value ( $\text{ng}/\text{m}^3$ )	Lower Assessment Threshold Value ( $\text{ng}/\text{m}^3$ )
Arsenic	6	3.6	2.4
Lead	500	3	2
Nickel	20	14	10
Cadmium	5	3	2

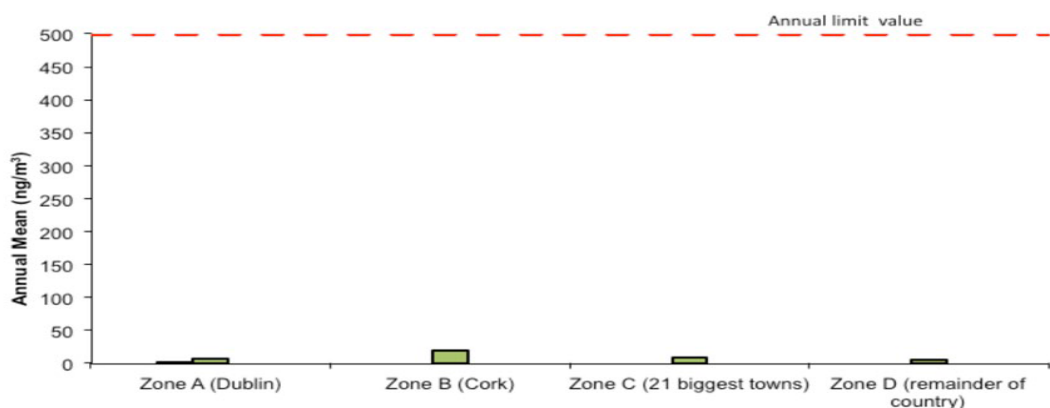


Figure 1.2.3: Pb Concentrations [10].

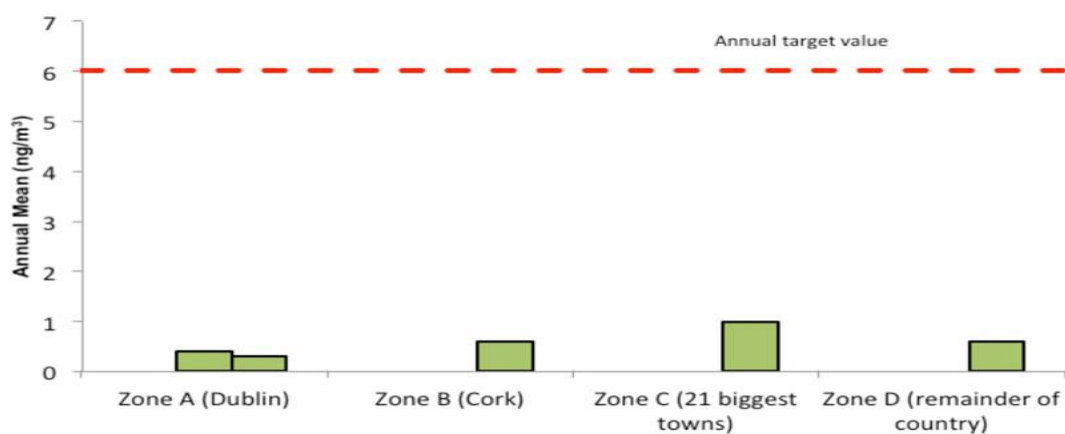


Figure 1.2.4: As Concentrations [10].

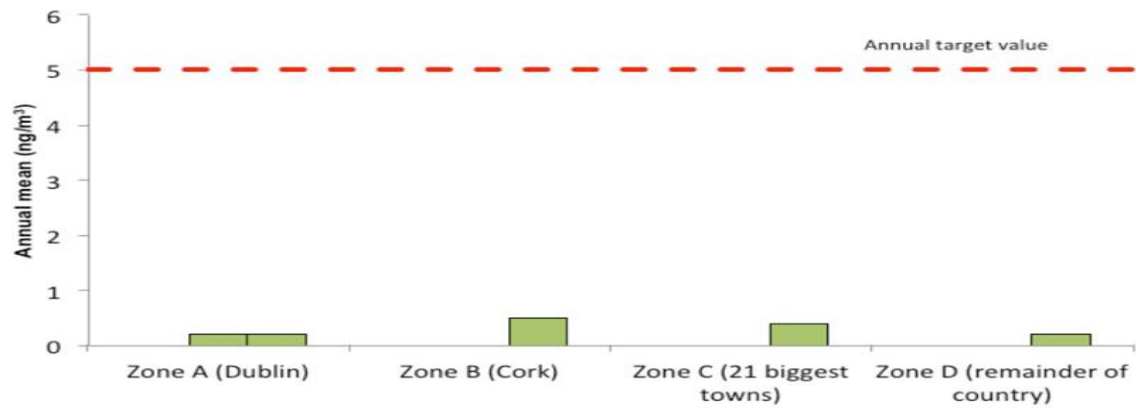
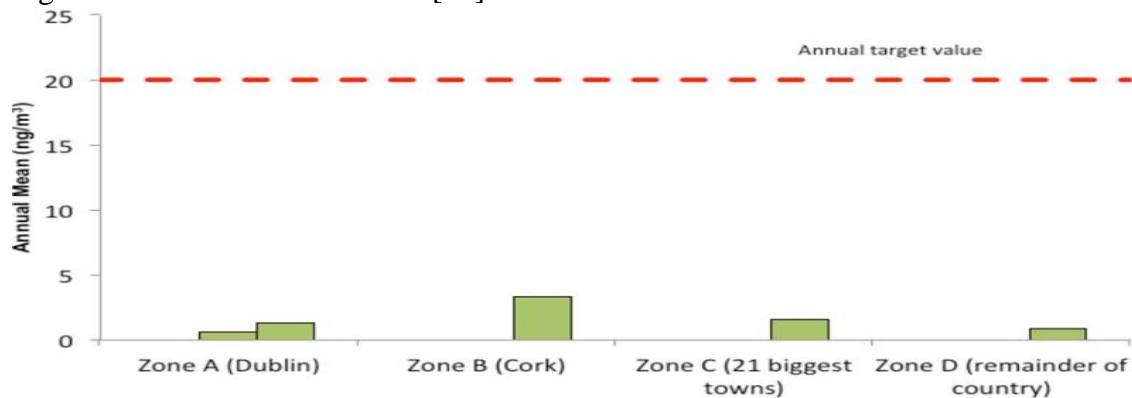


Figure 1.2.5: Cd Concentrations [10].



Figure

e 1.2.6: Ni Concentrations [10].

### Ambient Air Monitoring Legislation:

The European Commission set out an Air Quality Framework Directive in 1996, with four daughter directives outlining the requirement to monitor specific pollutants. The monitoring of Particulate Matter (PM) is a requirement of the 1<sup>st</sup> daughter directive.

Table 1.2.6 Shows EPA particulate matter guidelines regarding legislation on the monitoring and reporting of PM levels in ambient air. The public must be informed of the following exceedences [11].

Table 1.2.6 EPA legislation guidelines regarding particulate matter. 4<sup>th</sup> daughter directive

Pollutant	Averaging Period	Limit Value $\mu\text{g}/\text{m}^3$	Basis of Application of the Limit Value	Limit Value Attainment Date
PM10	24 hours	50	Not to be exceeded more than 35 times in a calendar year	Since 2005
PM10	calendar year	40	Annual mean	Since 2005
PM2.5	calendar year	25	Annual mean	From 2015
PM2.5	calendar year	20	Annual mean	From 2020

Table 1.2.7 shows the monitoring of PTE required by legislation arsenic, nickel, cadmium and mercury in air as a requirement of the 4<sup>th</sup> daughter directive.

Table 1.2.7 4<sup>th</sup> Daughter Directive Requirements for Monitoring of potentially toxic elements.[12]

Pollutant	Averaging Period	Limit Value $\mu\text{g}/\text{m}^3$	Basis of Application of the Limit Value	Limit Value Attainment Date
Lead	Calendar Year	0.5	Annual mean	Since 2005
Arsenic	Calendar Year	5	Annual mean	Since 2012
Cadmium	Calendar Year	6	Annual mean	Since 2012
Nickel	Calendar Year	20	Annual mean	Since 2012

Automobiles on our roads emit high levels of pollutants e.g. particulates, CO, NO<sub>x</sub> and volatile organic compounds (VOC's) all of which can have an adverse effect on our air quality.

Vehicle numbers have increased significantly in recent decades. However, there has been a decrease in large particulate emission levels due to the introduction of catalytic converters but emissions still pose a problem to human health because of the increasing number of smaller particulates ( $<2.5 \mu\text{g}/\text{m}^3$ ) which catalytic converters are unable to convert [12].

Motor vehicles release potentially toxic elements (PTEs) into the environment. These can absorb onto particulate matter and can be transported into the lungs. Many of these PTEs have toxic and carcinogenic effects. Brake and clutch dust are very fine powder residues. Brake dust occurs as a result of abrasion of the brake pads and brake shoes and clutch dust is produced when the surface of the clutch discs slip during clutch lock up processes. Vehicle exhaust emissions contain PTEs which are present due to the wear and tear of internal engine parts and the use of old brakes. These PTEs can include nickel, lead and cadmium all of which are known to be toxic. Engine oil also contains PTEs due to direct contact with engine parts and also because it contains additives in order to keep the engine clean, to inhibit corrosion or to act as an acid neutraliser. Typical additives include zinc and calcium additives. Therefore an oil leak may also facilitate the transport of PTEs to the atmosphere.

Engines are composed of different types of PTEs e.g. aluminium and aluminium alloys are commonplace engine materials due to the lightweight nature of aluminium. A number of studies have been published on PTE emissions from road traffic. Table 1.2.9 is a summary of the findings from studies which have been conducted on PTE emissions from traffic sources.

Table 1.2.9 Common PTEs found in the environment from automobiles:

Aluminium	Corrosion of engine parts and body work, asphalt[13]
Cadmium	Burning of fuel[14], battery, road marking paint and wear of tyres[15]
Chromium	Diesel soot [15], yellow road paint[13], Tyre wear [16]
Copper	Brake wear, Wear of bearings, engine oil [17], fuel additives [15], Tyre wear [17]
Iron	Rusty body work, engine parts, brake dust[13], tyre wear [16]
Lead	Brake wear, Tyre wear, bearing wear, engine oil, fuel burning [17]
Manganese	Road marking paint and diesel soot [15]
Nickel	Petrol & diesel, lubricating oil, brake abrasion, asphalt[15], Asphalt[13]
Zinc	Tyre wear, engine oil, brake abrasion, corrosion of galvanised parts, burning of fuel [17], diesel soot [15].

### 1.3 Potentially Toxic Elements (PTEs) of Concern

Potentially toxic elements (PTEs) in the environment are a cause of concern, due to the impact they can have on the quality of ecological systems and human health. Industries are required through operating licences to carry out environmental sampling which are generally submitted to third party laboratories for routine analysis, to monitor PTE releases. In modern laboratories the most common methods for the analysis of PTEs, in environmental samples, involves spectroscopic techniques such as FAAS, GFAAS, ICP-OES and ICP-MS. The only drawback with these techniques is that they all require solid samples to be converted into a liquid to perform analysis. An average ICP-OES can operate with a maximum suspended solid concentration of 3%. However, high solid kits are available which can function with suspended solids up to 20% [18].

Certain PTEs such as lead, aluminium, mercury and cadmium are present in significant quantities in the environment through pollution sources. The bio-accumulation of PTEs in the body is a gradual slow process. Sufferers may feel fatigue, headaches, upset stomachs and anaemia. The central nervous system experiences the most adverse effects to PTE over exposure. This usually manifests itself in the appearance of muscular tremors, dizziness and insomnia. Many developmental disorders in new born infants have been linked to PTE exposure.

There are 23 different PTE that are a concern to humans namely antimony, arsenic, bismuth, cadmium, cerium, chromium, cobalt, copper, gallium, gold, iron, lead, manganese, mercury, nickel, platinum, silver, tellurium, thallium, tin, uranium, vanadium, and zinc. Significant levels of these PTEs can cause chronic toxicity.

PTEs are elements that cannot be metabolized in the body and therefore accumulate in soft tissues. These PTEs may enter the body through food, water, air or by absorption through the skin. Most exposure to PTEs is through diet, medication, occupational or from the environment.

PTEs can be introduced into the food chain when they are absorbed by plants which are the foundation of the food chain [20]. Plants need essential transition metals such as iron, manganese, molybdenum, copper, zinc, nickel and micronutrients required in small quantities. They also absorb elements that have no biological function within the plant e.g. arsenic, cadmium, chromium, mercury and lead. They become toxic if absorbed in high quantities. Elements such as cobalt and aluminium are known to inhibit plant growth [21].

Exposure to PTEs when left untreated leads to illness and in extreme cases death, usually from encephalopathy of the brain. PTEs tend to bind to oxygen, nitrogen and sulfhydryl groups which alter enzyme activity [22]. Some PTEs also compete with ionised species like calcium and zinc to move through membrane channels in ionic form e.g. lead competes with calcium in the body. The age of a person is another influence on toxicity e.g. young children are at greater risk to lead exposure because they absorb more ingested lead than adults and their brains are also more susceptible to lead poisoning. Route of exposure is also a factor, e.g. mercury is not toxic in the gastrointestinal tract and is poorly absorbed through the skin but it is highly toxic if inhaled or injected [23].

Environmental contamination occurred in the 1950's in Minimate bay, Japan. Industrial waste from acetaldehyde production was consistently dumped into Minimate bay causing mercury to accumulate over time leading to high levels in local fish. Adults showed signs of toxic exposure but the main effect was on the next generation being born with neurologic defects.

There is an issue with arsenic exposure in Bangladesh due to high levels in the water supply. High levels of arsenic are present in the drinking water due to high concentrations of arsenic in deeper levels of groundwater.[24]

Occupational exposure of workers exposed to PTE fumes suffer from metal fume fever (MFF) characterised by fever headache, fatigue, coughing and a metallic taste. The usual cause of this is zinc oxide but it also occurs with magnesium, cobalt and copper oxides. These dusts are known carcinogens [25]. Table 1.3.1 shows the properties of some of the PTEs of concern.

Table 1.3.1 Physical and chemical characteristics of common metals of concern found in the polluted air.

	At No.	Atomic Wt g/mol	Appearance	Density g/cm <sup>-3</sup>	Melting Point (K)	Boiling Point (K)
Aluminium (Al)	13	26.98	Grey	2.70	933.47	2792
Cadmium (Cd)	48	112.41	Silvery grey metallic	8.65	594.22	1040
Chromium (Cr)	24	52	Silvery metallic	7.19	2180	2944
Copper (Cu)	29	63.55	Metallic bronze	8.96	1357.77	2835
Iron (Fe)	26	55.85	Metallic with greyish tinge	7.874	1811	3134
Lead (Pb)	82	87.62	Bluish grey	11.34	600.61	2022
Manganese (Mn)	25	54.94	Silvery metallic	7.21	1519	2334
Nickel (Ni)	28	58.69	Lustrous, metallic & silvery with a gold tinge	8.908	1728	3186
Zinc (Zn)	30	58.69	Bluish pale grey	7.14	692.68	1180

Chapter 5, Section 5.1. covers the reason why these elements were chosen for analysis.

### 1.3.1 Aluminium

Aluminium is the most abundant metal in the earth's crust making up approximately 8% of it. It is not as toxic as lead or cadmium but due to its abundance it is a concern. It is a silver coloured, ductile, lightweight metal. It does not occur in its elemental state because it is reactive. It has three oxidation states  $Al^{+1}$ ,  $Al^{+2}$  and  $Al^{+3}$  etc. It is a good conductor of heat and electricity. It is the most popular non-ferrous metal used in industrial processes, due to its lightweight, it's easy to weld and resistant to corrosion. The development of a thin (0.01 $\mu$ m) layer of aluminium oxide on the metal surface, acts as a protective barrier when it is exposed to air. The main source of aluminium is bauxite ore [26].

**Health Effects:** Aluminium has no known function in living cells but it can damage human tissues. It has not been classified as a carcinogen by the EPA. It is number 186 on the Agency for Toxic Substances and Disease Registry (ATSDR) priority list. It is generally ingested through food additives, antacids, buffered aspirin and from using aluminium foil and cookware. It is thought to play a role in the onset of Alzheimer's disease because increased amounts of aluminium were found in the brains of Alzheimer patients. Although there is no conclusive evidence for or against aluminium being a cause of Alzheimer's disease, it is thought it plays a role in the dementia aspect of the disease. Aluminium damages the central nervous system, the kidneys and the digestive system. [27]

The use of aluminium in some antiperspirants and food additives is controversial. Some researchers have linked aluminium in antiperspirants to breast cancer [27]. Aluminum

deposits have been found in the bones and the central nervous system of those suffering from renal dysfunction. It competes with calcium for absorption and increased levels leads to calcium deficiencies. Small percentages of the population are allergic to aluminium and suffer from contact dermatitis, an itchy rash and digestive disorders as a result. However these allergies are very rare. [27]

The occupational exposure limit for aluminium as set out by the Occupational Safety and Health Authority (OSHA) is  $15 \text{ mg/m}^3$  for an eight hour work day, 40 hour working week. The level of aluminium allowed in drinking water as set out by the US EPA is 50-200  $\mu\text{g/L}$  [28].

### 1.3.2 Cadmium:

Cadmium is a soft, malleable, ductile, toxic, bluish-white transition metal. Its most common oxidation state is  $\text{Cd}^{+2}$  with a less common state of  $\text{Cd}^{+1}$  also occurring. In areas of low zinc concentrations biological species have been known to use cadmium as a replacement for zinc. It is number 7 on the ATSDR priority list. cadmium is a by-product of mining and smelting of lead and zinc. It is used in batteries, as a paint pigment, in insecticides, fungicides and fertilizers [29].

**Health Effects:** Cadmium has no known function in the human body. The EPA has classified cadmium as a group B1 Carcinogen, which means it is a probable human carcinogen. It is known to cause recurring kidney stones. It is also capable of replacing zinc stores in the body. It can cause liver damage and high blood pressure. cadmium is found in different tobacco products and pesticides. There are high levels of cadmium in cigarette smoke which is one of the reasons cigarette smoke is so toxic (cigarette smoke also contains arsenic and lead). Food is also a source of cadmium exposure. High levels can be found in the liver and kidneys of older animals and plants grown in industrial areas can contain small amounts of cadmium. There is generally less cadmium in cigarettes than in food but the lungs absorb cadmium more efficiently than the stomach. It targets the liver, placenta, kidneys, lungs, brain and bones. Inhalation is the most common source of exposure with initial development of metal fume fever leading to chemical pneumonitis, pulmonary edema and death [29].

Workers can be exposed to cadmium from the smelting of metals or in factories that make cadmium products e.g. batteries. Industrial exposure to workers has been reduced since more has been learned about cadmium poisoning. However, in industrial areas there is a build-up of cadmium in the water, air and soil. Some phosphate fertilizers contain cadmium which also increases cadmium levels in the soil.

The occupational exposure limit for cadmium in the workplace in air as set out by OSHA is 100  $\mu\text{g}/\text{m}^3$  as cadmium fumes and 200  $\mu\text{g}/\text{m}^3$  as cadmium dust for an eight hour work day, 40 hour work week. The level of cadmium allowed in drinking water as set out by the US EPA is 5  $\mu\text{g}/\text{L}$  and the Food and Drug Authority (FDA) has set a limit of 15  $\text{mg}/\text{L}$  of cadmium in food colourings [28].

### 1.3.3. Chromium

Chromium is a steel like, grey hard metal. As a group VI transition metal it exhibits a wide range of possible oxidation states. The most common oxidation states are  $\text{Cr}^{+2}$ ,  $\text{Cr}^{+3}$ ,  $\text{Cr}^{+6}$  and less common oxidation states:  $\text{Cr}^{+1}$ ,  $\text{Cr}^{+4}$ ,  $\text{Cr}^{+5}$ . Chromium is number 76 on the ATSDR priority list. It is odourless and tasteless. It is found as fine dust particles in air, water and soil mainly in the form of chromium  $\text{Cr}^{+3}$  and chromium  $\text{Cr}^{+6}$ . It exists in nature as chromite ( $\text{FeCr}_2\text{O}_4$ ). It is also released during industrial processes such as polishing, painting, pigment manufacture and wood preservation [30].

**Health effects:** Trivalent chromium  $\text{Cr}^{+3}$  is an essential nutrient in trace amounts for the metabolism of sugar, protein and fat, with an RDA of 50-200 $\mu\text{g}$ . The body loses the ability to use sugar, protein and fat without  $\text{Cr}^{+3}$  resulting in weight loss/decreased growth, disorders of the nervous system and diabetes. The natural acidity of the body is enough to maintain a  $\text{Cr}^{+3}$  state. However  $\text{Cr}^{+3}$  in high quantities can be coordinated with two guanine bases from DNA causing DNA mutations.

In comparison hexavalent chromium  $\text{Cr}^{+6}$  is toxic in the body if ingested or inhaled. It is a known carcinogen. The US dietary guidelines suggest a daily maximum intake of 35  $\mu\text{g}$  (male) and 25  $\mu\text{g}$  (female). Breathing high levels of chromium  $\text{Cr}^{+6}$  causes irritation to the nose causing nosebleeds, ulcers and holes in the nasal septum. Ingesting large amounts of chromium  $\text{Cr}^{+6}$  causes stomach upsets, ulcers, kidney and liver damage and even death.

$\text{Cr}^{+6}$  is not in a very stable state compared to chromium  $\text{Cr}^{+3}$ . Chromium  $\text{Cr}^{+6}$  is a strong oxidising agent. This is one of the reasons chromium  $\text{Cr}^{+6}$  is so toxic, it is reduced to  $\text{Cr}^{+5}$  which is a known carcinogen (according to the World Health Organisation (WHO), the EPA and the International Agency for Research on Cancer) and will lodge in kidney, intestine or lung tissue forming cancerous growths. This reduction is promoted by the acidity levels and action of enzymes in the body.

People that have worked handling  $\text{Cr}^{+6}$  have developed skin ulcers. In animals chromium exposure has caused damage to the respiratory system and a reduced ability to fight disease. It has been known to cause birth defects, fewer offspring and a reduced sperm count in mice



that were exposed to extremely high levels of chromium.  $\text{Cr}^{+5}$  is extremely toxic and promotes the formation of reactive oxygen species which cause damage to human DNA. The main source of human exposure is through smoking. Humans are also exposed through contaminated food and drinks packaging.

The occupational exposure limit for chromium in workplace air as set out by OSHA is  $500 \mu\text{g}/\text{m}^3$  as water soluble  $\text{Cr}^{+3}$ ,  $1000 \mu\text{g}/\text{m}^3$  as  $\text{Cr}^0$  and  $52 \mu\text{g}/\text{m}^3$  as  $\text{Cr}^{+5}$  for an eight hour work day, 40 hour work week. The level of  $\text{Cr}^{+6}$  allowed in drinking water as set out by the US EPA is  $100 \mu\text{g}/\text{L}$  as  $\text{Cr}^{+6}$  [28].

### 1.3.4 Copper:

Copper is also a transition metal. It is one of the few metals that occur naturally in its elemental form. It is an electrically conductive, malleable, ductile metal. It has a pinkish appearance uncommon for metals. It is used as a heat and electrical conductor, as a building material and as a constituent of various metal alloys. It is an essential nutrient in plants and animals in trace amounts. It can be poisonous and even fatal in high quantities. It is found in the bloodstream, as a cofactor in various enzymes and in copper based pigments. It does not react with water but it will react slowly with oxygen at room temperature forming a brown-copper oxide on the surface. It is used in piping systems, as copper wire, as electromagnets (motors, generators and transformers), printed circuit boards, musical instruments and coins. It is incorporated into alloys (e.g. brass; copper-zinc and bronze; copper-tin) because it is often too soft for its general applications. Some molluscs, arthropods and crabs use a copper containing pigment hemocyanin instead of iron carrying haemoglobin to transport oxygen in the blood and therefore their blood adapts a blue colour. It has four different ions  $\text{Cu}^{+1}$  (common),  $\text{Cu}^{+2}$  (common),  $\text{Cu}^{+3}$  (rare) and  $\text{Cu}^{+4}$  (extremely rare) [31].

**Health Effects:** Copper is carried in the bloodstream by ceruloplasmin a plasma protein. When absorbed in the gut it is then carried to the liver bound to albumin. The EPA has not classified copper as a human carcinogen. It is found in several enzymes and is involved in biological electron transport. Zinc and copper compete for absorption in the body so an excess of one of these minerals leads to a deficiency in the other. It is recommended that an adult's daily intake of copper not exceed  $3 \text{ mg}/\text{day}$ . Copper facilitates the uptake of iron so copper deficiencies can lead to anaemia like symptoms. Deficiencies can also lead to abnormalities in the metabolism of fats, fatty liver disease, poor melanin and dopamine synthesis causing depression and sunburn.

Copper is known to block the absorption of milk/egg proteins. Symptoms of copper poisoning are similar to arsenic poisoning. Death is usually caused by convulsion, palsy and insensibility. The main factor in copper's toxicity is its ability to accept and donate single electrons while changing oxidation states, this catalyses the production of reactive radical ions. A Kayser Fleischer ring, where copper deposits, are found in the iris indicated improper metabolism of copper in the body. Wilson's disease is an inherited disorder which causes the body to retain copper, where copper is not excreted by the liver into bile as it should be, if untreated it can lead to brain and liver damage. People that suffer from mental illnesses like schizophrenia are known to have high copper levels in their systems. It is not known if the copper is a contributor to the mental illness or if the illness is causing the body to retain copper. High levels of copper in water is known to damage marine life.[31]

The occupational exposure limit for copper in workplace air as set out by OSHA is  $100 \mu\text{g}/\text{m}^3$  as copper fumes and  $1000 \mu\text{g}/\text{m}^3$  as copper dusts for an eight hour work day, 40 hour work week. The level of copper allowed in drinking water as set out by the US EPA is  $<1300 \mu\text{g}/\text{L}$  [28].

### 1.3.5 Iron:

Iron does not appear on the ATSDR priority list but is a PTE of interest. Iron is the most abundant transition metal in the earth's crust and the fourth most abundant metal in the earth's crust over all. It is a shiny metal which is silvery in colour. Iron is perhaps the most widely used of all metals this is partly due to the fact that it is cheap and very strong. It is mainly used in the construction of machinery, tools, ships, motor vehicles and it is also used as a structural support in buildings. Iron in its pure form can be quite soft so it is generally used as a steel alloy, cast iron, wrought iron and carbon steel. The main problem associated with iron and steel alloys is that they are very prone to rusting unless they have been previously treated. Ferric ( $\text{Fe}^{+3}$ ) and Ferrous ( $\text{Fe}^{+2}$ ) compounds also find widespread applications and can be used in; clothes dying, insecticides, water treatment, additives added to human and animal food, paint pigments and wood preservatives amongst other things. [32]

**Health Effects:** Iron is an essential nutrient in the body and is necessary for survival. Exposure to iron overloading can result in damage to organs such as the heart and liver and in extreme cases it may even lead to organ failure. Occupational exposure can result in the development of a benign condition known as siderosis. Ingestion is the most common form of poisoning because iron is very rapidly absorbed into the gastrointestinal tract. Iron targets the liver, cardiovascular system and the kidneys. Iron toxicity can be either corrosive or cellular.

Corrosive toxicity occurs in the gastrointestinal tract. It acts on muscle tissues and causes diarrhoea and hematemesis (a vomiting of blood). In the case of cellular toxicity, exposure can cause phosphorylation (the addition of a phosphate ( $\text{PO}_4$ ) group to a protein or other organic molecule) or cell damage and in extreme cases it can cause cellular death. The liver is mainly affected but infection can also occur in the kidneys, lungs and heart [32].

The occupational exposure limit for iron in workplace air as set out by OSHA is  $10 \text{ mg/m}^3$  as iron oxide fumes for an eight hour work day, 40 hour work week [28].

### 1.3.6. Lead:

Lead is number 2 on the ATSDR priority list. It is a soft, malleable PTE. When freshly cut it is a bluish/white colour and becomes a dull/grey colour on exposure to air. Lead is used in building construction, batteries and bullets. It is also used as a shielding device from x rays for people working in the nuclear radiography industry. Metallic lead rarely occurs in nature. It usually found in an ore with zinc, silver and copper. The use of lead in gasoline, paints and ceramic products has been reduced because of health concerns. It was used as a common building material in houses built before 1940. Now lead is most commonly used in batteries, ammunition and fuel additives. The main source of lead release is from metal smelting [33].

**Health Effects:** Lead has no known function in biological systems. The complexation of lead determines the toxicity. Lead ( $\text{Pb}^{+2}$ ) acetate is considered to cause dementia. Like mercury it is a neurotoxin damaging nervous connections and accumulating in soft tissue and bone. The most common source of exposure in humans is through ingesting contaminated food and drinking water. Lead poisoning usually occurs when the lead is dispersed e.g. when sanding lead based paint. Testing for lead in blood indicates recent exposure while testing for lead in the bones indicates cumulative exposure.

Lead poisoning is usually indicated by a blue lining on the sufferer's gums. Sufferers will also experience muscle weakness and mental disorders. The build-up of lead leads to tissue paralysis leading to blindness, memory loss, mental disturbances and eventually mental retardation. Lead poisoning can affect both male and female reproduction. Initial symptoms are indigestion, dryness of the mouth, nausea, and vomiting and appetite loss.

It generally targets the bones, blood, kidneys and the thyroid gland. Poisoning usually occurs from environmental sources. Detection is vital due to the hazardous side effects. Lead exposure can also cause learning difficulties. Children are more susceptible to lead poisoning because of their neurological and behavioral characteristics. It may lead to a reduced intelligence quotient (IQ), slow development or hyperactivity. Lead in the environment can

be absorbed by the human body by breathing or swallowing lead dust, lead based paint or food, water or soil that has been contaminated by lead.

The occupational exposure limit for lead in workplace air as set out by OSHA is  $50 \mu\text{g}/\text{m}^3$  for an eight hour work day, 40 hour work week. The National Ambient Air Quality Standard (NAAQS) limit for lead in ambient air is  $1.5 \mu\text{g}/\text{m}^3$ . The level of lead allowed in drinking water as set out by the Irish EPA is  $10 \mu\text{g}/\text{L}$  [28].

### 1.3.7 Manganese:

The EPA has not classified manganese as a human carcinogen. It is the 12th most abundant metal on the earth's surface. Its colour depends on its oxidation state because of this it is often used as a pigment in industry. Manganese dioxide is used as a cathode material in dry cell batteries. It is found naturally in the environment in rocks. Pure manganese however does not occur naturally and is generally bound to other substances. Manganese is required in trace amounts by all organisms, in humans several enzymes have manganese as a cofactor and in plants it is essential for photosynthesis. Organic manganese compounds are found in pesticides and are used as additives in petrol. It can however be toxic causing neurological damage, impaired motor skills and cognitive disorders in higher quantities. Exposure should not exceed  $5 \mu\text{g}/\text{m}^3$ . Its most common oxidation states are  $\text{Mn}^{+2}$ ,  $\text{Mn}^{+3}$ ,  $\text{Mn}^{+4}$ ,  $\text{Mn}^{+6}$  and  $\text{Mn}^{+7}$  with less common  $\text{Mn}^{+1}$  and  $\text{Mn}^{+5}$ . An oxidation state of  $\text{Mn}^{+2}$  is the most stable and has a pink colour. This is the state that is used by living organisms. All other oxidation states are toxic.  $\text{Mn}^{+4}$  &  $\text{Mn}^{+7}$  are oxides used as laboratory reagents.  $\text{Mn}^{+4}$  is used in dry batteries [34].

**Health Effects:** Exposure to high levels of manganese for long time periods can cause mental and emotional problems and result in slow awkward body motions. These are all the symptoms of a disease called Manganism. Exposure to high levels of airborne manganese effects motor skills and high levels of manganese metal can affect respiratory function.

The occupational exposure limit for manganese in workplace air as set out by OSHA is  $5 \text{mg}/\text{m}^3$  for an eight hour work day, 40 hour work week. The level of manganese allowed in drinking water as set out by the US EPA is  $50 \mu\text{g}/\text{L}$  [28].

### 1.3.8 Nickel

Nickel is one of the four metals that are magnetic at room temperature. It is a silvery-white, hard, ductile transition metal. Nickel is corrosion resistant it forms a protective oxide layer on exposure to air for this reason it is used in coin manufacture, stainless steel, magnets and household utensils. In certain organisms it is an active centre in enzymes e.g. urease (an

enzyme that assists the hydrolysis of urea) contains nickel. The most common oxidation state is +2.

**Health effects:** The EPA has classified both nickel and nickel dust as a human carcinogens. Nickel sulfide fumes are regarded as carcinogenic. A nickel allergy known as dermatitis affects the skin causing an itchy rash. In 2002, it was found that the amount of nickel in 1 & 2 euro coins is above the recommended level. The American Contact Dermatitis Society voted it 'allergen of the year' in 2008. [35].

Allergic reactions are a common side effect of exposure to nickel and typically take the form of skin rash that is why a lot of jewellery today, especially wrist watches, are nickel free. People who are exposed to nickel in their work environment have developed chronic bronchitis and also have experienced reduced lung function as a direct result of inhaling the nickel. Ingestion of water containing high levels of nickel can result in stomach ache and in extreme cases can cause kidney damage.

The occupational exposure limit for nickel in workplace air as set out by OSHA is  $1 \text{ mg/m}^3$  for metallic nickel and nickel compounds for an eight hour work day, 40 hour work week. The level of nickel allowed in drinking water as set out by the US EPA is  $0.1 \text{ mg/L}$  [28].

### 1.3.9 Zinc

Zinc is a bluish-white, hard, brittle diamagnetic transition metal. It is the 24<sup>th</sup> most abundant metal on the earth's crust. It has only one common oxidation state  $\text{Zn}^{+2}$ . Zinc deficiency affects 2 billion people in the developing world. A deficiency can cause growth retardation, chromes liver disease, renal disease, diabetes, impaired appetite, impotence, diarrhoea and causes about 800,000 deaths a year. Plants that grow in areas that are zinc deficient tend to be more susceptible to disease but excess zinc can be toxic to plants. Zinc can speed up the healing process after injury and is used in throat lozenges/tablets to reduce the duration/severity of colds. It is also used in anti-dandruff shampoos. Many alloys contain zinc, the most common being brass an alloy of zinc and copper. It is used in galvanising to protect iron and steel against corrosion. It is essential to plants, animals and microorganisms. It is found in several enzymes. The US RDA is  $8 \text{ mg/day}$  for women and  $11 \text{ mg/day}$  for men. Sources of zinc in the diet are red meats, beans, nuts and seeds. Excess zinc suppresses copper and iron absorption. The hydrochloric acid in the stomach dissolves zinc giving off corrosive zinc chloride which causes damage to the stomach and in extreme cases can be fatal [36].

**Health Effects:** EPA has not classified zinc as a human carcinogen because the information to date from both human and animal studies has proven inconclusive. Exposure to high levels of zinc can lead to nausea, loss of appetite, cramps and headache. Intakes of 150–450 mg of zinc per day have been associated with such effects. Over exposure to zinc results in a copper deficiency because zinc and copper compete for absorption in the body. It also results in altered iron function and impaired immune function [36].

The occupational exposure limit for zinc in workplace air as set out by OSHA is  $1 \text{ mg/m}^3$  for zinc chloride fumes and  $5 \text{ mg/m}^3$  for zinc oxide dust and fumes, for an eight hour work day, 40 hour work week. The level of zinc allowed in drinking water as set out by the US EPA is 5 mg/L. [28]

#### 1.4. Particle/Cabin Air Filters

There are two principal types of particle filters, filter manufacturers provide a wealth of information on-line, some of which is presented here for standard particle filters and combination filters. If pollen gets inside the car unfiltered, allergy sufferers are particularly at risk. Streaming eyes, dripping noses, shortness of breath or sneezing attacks reduce concentration levels and increase the risk of an accident. A sneeze when you're driving at 60 miles an hour means you're driving blind for 30 meters [37].

**Particle Filters:** The earliest particle filters were all standard particle filters. Particle filters protect against fine dusts, and also against particles, road dust, abraded particles, soot, bacteria, industrial dusts and other respirable ultra-fine particles. Figure 1.4.1 shows a standard particle filter. Filter shapes differ depending on the vehicle type. Figure 1.4.2 shows a three layer filter cross section of a filter fold within the filter.



Figure 1.4.1 (A) – Standard Particle Filter [38]

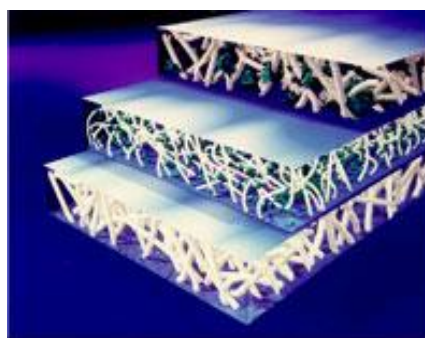


Figure 1.4.1 (B) - Filter cross section [38]

**Combination Filters** were introduced in the ninties, shown as Figure 1.4.2. (A). They have a activated layer of carbon in addition to the particle filter as shown in Figure 1.4.2 (B). Figure 1.4.3 shows an enlarged depiction of a Micronair activated-carbon medium in a combination filter.

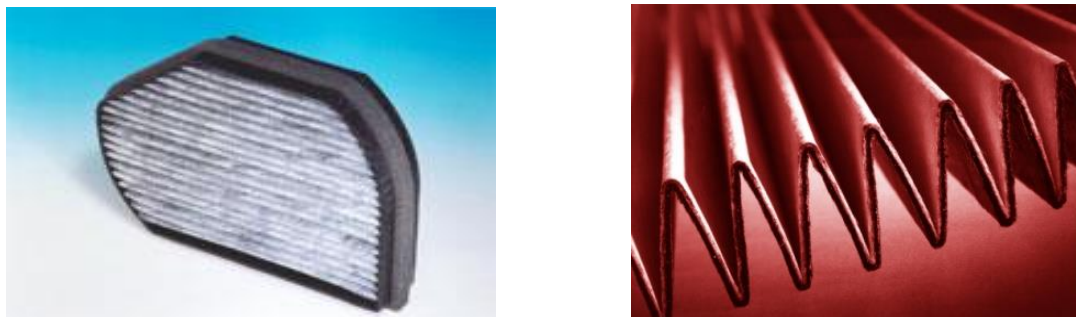


Figure 1.4.2 (A) – Combination filter. [39] Figure 1.4.2 (B). – Activated charcoal layer [39]

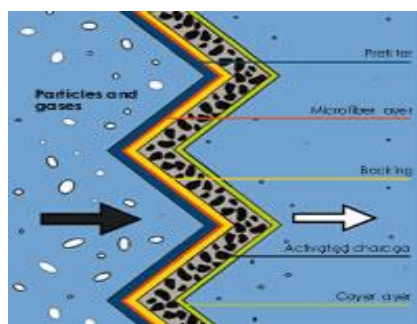


Figure 1.4.3: Activated-carbon medium in combination filter. [40]

The carbon layer provides additional protection against harmful gases like benzene and toluene. Gaseous pollutants and odours bond to the surface of the activated carbon. Although combination filters offer more protection they need to be replaced more often than particle filters, due to a breakdown in the filters surface with use. [39] The activated-carbon layer in a combination filter also breaks down in up to 99% of ozone.

Particle filters can be replaced with combination filters. Both filters are identical in dimension and have the same installation instructions. Some manufactures have begun installing combination filters as standard.

Combination and standard particle filters extract dust and mineral particles from incoming air, they also extract particles of biological origin (bacteria, fungal spores and pollen). A pathogenic bacterium which is bound to combustion particles can cause serious health problems e.g. tuberculosis. Fungi spores and pollen can cause respiratory problems. Extractor systems can remove these particles but they can also be a breeding ground for bacterial growth. Microorganisms are able to multiply in the filter media. Analysis of particles in

fibrous filters, used for general ventilation purposes, shows that the fibrous filters are equally efficient in extracting biological and non-biological particles. The surface structure of the particles effects adhesion, as opposed to filtration velocities and particles sizes [41].

Figure 1.4.4 shows the increase in the installation of combination filters due to demands made by car owners for 'healthier' cars [42]. This shows an increase in the demand for filters over time and a dramatic increase in the demand for combination filters in recent years.

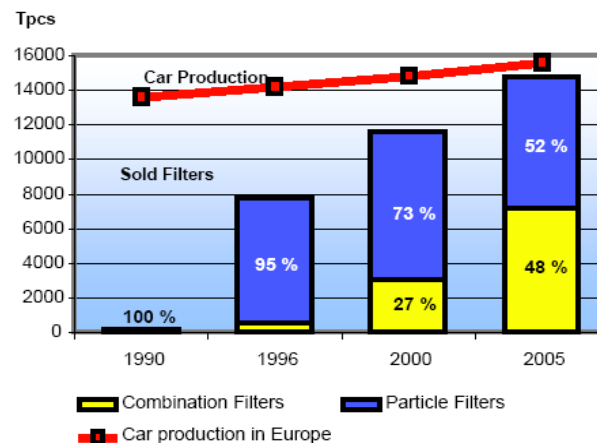


Figure 1.4.4: Combination filter demands from 1990 to 2005 [40].

### Cabin air filter development:

95% of all cabin air filters are standard particle filters. They have been installed in vehicles in Europe since 1988 and in the US since 1993. The aim of standard particle filters is not just to extract coarse road dust but to extract small particles capable of penetrating into the lungs [43].

The occurrence of filters in European cars is higher than in American cars. This is due to the fact that the population in America is less dense than in Europe therefore concern about pollution levels are lower in the US. Originally particle filters were made of a heat bonded, non-woven, synthetic fibres that were creased in plastic frames. The media is pleated to maximise the surface area available for airflow. This increases the filters performance and the lifetime of the filter. Most modern filters no longer have the plastic frame but have a synthetic card frame.

The first companies to use particle filters were Mercedes Benz and BMW in Germany in 1989. Of the 60 million cars manufactured in Europe every year 95% of them are equipped with filters (particle or combination). 70 % of these filters are Micronair.



Originally only luxury cars are fitted with combination filters as standard. According to Micronair the roll out of combination filters will not make particle filters obsolete. Micronair are continuing to develop both particle and combination filters.

Companies began developing combination filters in 1991. Initially there were problems binding the layers of activated charcoal to the filter surface. It was found that the binded layer matrix allowed for good filter performance but also stopped the charcoal granules being blown into the cabin, see Figures 1.4.5 (A) & (B). In Figure 1.4.5 (B) the activated charcoal layer is clearly visible between the filter layers.

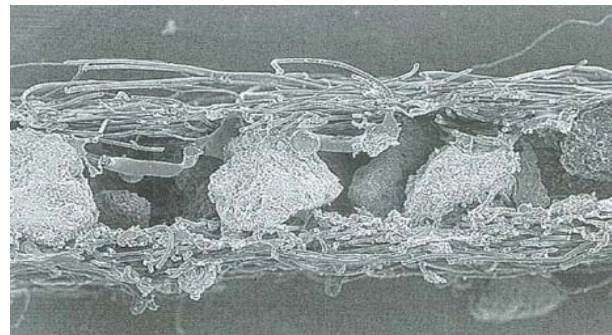
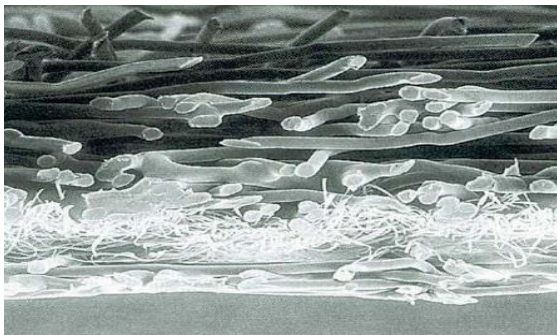


Figure 1.4.5 (A) SEM: particle filter image

Figure 1.4.5 (B) SEM combination filter image

Filters also prolong the lifetime of air conditioning systems by preventing them being soiled. There is interdependence between the filter material and pleat pitch and height. Heavy turbulence can cause the filter material to collapse. The poor absorption capacity of a filter is overcome by increasing the filter area, which diminishes the pitch of the folds.

Particle filter materials face several demands. The structure should remain unchanged during the lifetime of the filter even when exposed to high humidity, chemicals, water and extreme temperatures. The filters must be microbiologically inactive and they must emit no odour or materials and must also be non-flammable.

Particle filters are made of pleated paper as shown in Figure 1.4.6. Paper is used because it is cost effective, efficient and easy to service. As long as the pleated paper fits the vehicles compartment and it is appropriate for the air flow in the vehicle there will not be any significant restriction to air flow, unless the filter becomes clogged or dirty [44].

Particle/Cabin air filters are placed in the outside air intake for the vehicles passenger compartment. Filters are typically located in one of three locations under the hood, inside the glove box or under the dashboard. Filter manufacturers recommend replacement every 12,000 km to 15,000 km or at least once a year. Depending on general driving conditions and taking

into account pollutant levels in areas where most driving has been done. The filters are uniquely shaped to fit the available space in the particular vehicles outside air-intake compartment. Filters that have become clogged or dirty because they have not been regularly changed result in a reduced air flow from the cabin's vents but also result in allergens entering the cabin by de-absorption.

Filter material has three different layers consisting of micro-fibres which are excellent filters. North American car manufactures mainly use particle filters and European manufactures mainly use combination filters. Installation levels seem to be dependent on consumer awareness, consumer awareness in America is low from a consumer standpoint whereas in Europe/Japan the awareness levels are considerably higher. In countries where consumers are aware of the need for filter installation levels are higher.

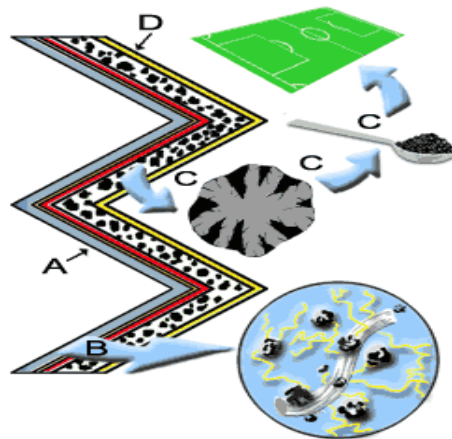


Figure 1.4.6 Detailed Particle filter design [44]:

- A. Prefilter – Blue Layer: This is the first layer of filters to meet the incoming air and this layer extracts the largest particles mainly road dust and pollen. This layer is electrostatically charged which attracts large dust particles. When loaded with particles the efficiency of this layer is increased because the particles themselves act as a filter.
- B. Secondary - Red Layer: This layer consists of finer electrostatically charged fibres that are densely packed. Fine particles are trapped here e.g. soot and finer road dust.
- C. Carbon Layer – Black Spotted: This layer consists of tiny granules of porous, activated carbon. Pollutant gases are absorbed in this layer. It has a large surface layer within the microscopic pores of the activated carbon. Pollutant gases are attracted to the activated carbon surface by Van Der Waal's forces.

- D. Strength Layer – Yellow Layer: This is the layer at the back of the filter consisting of coarse synthetic fibres. This layer is not a filter layer but gives support and shape to the filter.

### **Research carried out into the health risks of not using filters:**

Researchers in Lancaster University have said that 15 million people would suffer from health problems caused by traffic fumes, and exposure would lead to 10,000 premature deaths per year. The BBC's world service report (March, 2001) said that particles emitted from cars are causing premature deaths and illness by causing bronchitis and asthma. Dr. Michele De Rosa at the University of Naples studied the effects of traffic fumes on male fertility. The findings demonstrated that continuous exposure impairs sperm quality in young and middle aged men. Researchers in the University of California studied the development of asthma in monkeys exposed to ozone. Exposure was shown to trigger asthma attacks [45].

### **Why use particle filters?**

Micronair studies have shown that the contaminant levels in the traffic stream can be up to six times the level at the roadside. A jam jar of city air contains 35 million particles of dust. Filters are made up of non-woven filtration media designed to trap pollen spores, dust and soot and are used to reduce the contaminants that aggravate respiratory problems e.g. asthma and hay fever. Most filters take 5-10 minutes to change, replacement is relatively easy and replacement details can be found on manufactures websites. The particle filter selection is not dependant on a models engine size, or body type (e.g. estate, hatch, saloon etc).

### **The benefits of particle filters:**

A historical customer research study conducted in 2003 for a non-woven filter manufacturer, Freudenberg in Dohring County, North America found that 95% of people questioned said they were concerned about pollutants in their cars. 91% of people questioned said they would like to see particle filters as a standard feature in new cars. 83% of people questioned said they would prefer that their next car be equipped with a cabin filter. 85% said they were concerned about the health effects of exhaust gases and vapours entering their vehicles. 82% of people questioned said they would be willing to pay extra for the addition of a particle filter. 67% of people questioned said they suffer from allergies or respiration problems or that

they live with someone that does. This suggested that people are becoming increasingly aware of the quality of air in their cars [48].

The two filter types tested in this study were obtained from 2 different makes and model of car, namely, Skoda Octavia and Toyota Aventis, both are popular family cars.

Figure 1.4.7 (A) shows a particle filter designed for a Skoda Octavia Size: 199 x 217 x 18 mm:

The particle filter is on the passenger side behind the glove box.

Figure 1.4.7 (B) shows a particle filter designed for a Toyota Aventis, Size: 287 x 218 x 57 mm. The particle filter is on the passenger side behind access plate in the footwell.



Figure 1.4.7 (A) Skoda Octavia filter [46]



(B) Toyota Aventis filter [47]

During the spring and autumn there are high levels of pollen in the air. During the summer & autumn there are high levels of particulates. When a particle filter becomes clogged with dust/dirt the cars defroster becomes ineffective. This results in increased humidity within the cabin causing windows to fog up and reducing visability. During the winter, clean particle filters are vital, from a safety perspective [49]. Figure 1.4.8 illustrates an annual timeline of the prevalence of pollutants and misting up of car windows.

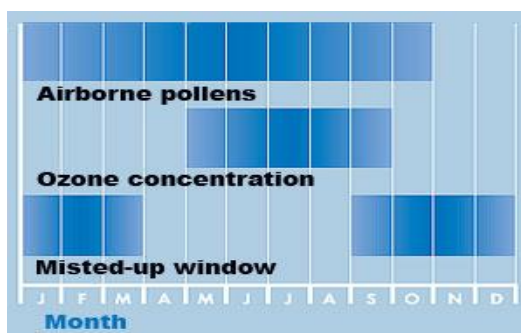


Figure 1.4.8 Demand for particle filters all year around [50]

All year long particle filters keep the ventilation and air conditioning systems clean increasing their lifespan and effectiveness. Filter samples were examined over the course of a year, with separate filters run and extracted during the spring, summer, autumn and winter. [50]

Figure 1.4.9 (A) shows a particle filter run during the spring months. In spring, one notices pollen, grass seed and relatively coarse dirt particles. These can lead to clogging on the surface of the pleated bellows – while the pleats further down remain comparatively clean. While Figure 1.4.9 (B) shows a particle filter run during the summer months. During the summer period there is an increase in the levels of pollen, dust particles and pollutants in the air. This results in an increasing need for particle filters. In summer, significantly more soot and fine dust can be found in the filter.



(A) Spring period.



(B) Summer period



(C) autumn period



(D) winter months.

Figure 1.4.9: Visual examination of filters used at different times of the year [50].

Figure 1.4.9 (C) shows a particle filter run during the autumn months. In autumn, the situation is similar to that of summer – however, due to high humidity, even more dust and particles are collected. While Figure 1.4.9 (D) shows a particle filter run during the winter months. The filter is so dirty that it can no longer fulfil its intended purpose and needs replacement.

### **Protection against gases and odours:**

Weinheim *et al.*, found that the higher the temperature rises the higher the level of ozone in ambient air. Ozone is converted by the action of UV light on pollutants released by vehicles

e.g. nitrogen oxide. This reaction is accelerated at high temperature. Each second 10/150 litres of air passes through these filters. These filters must be replaced at regular intervals to obtain adequate filtering levels [51].

Air born particles can be classified into three classes' course, fine and ultrafine. Catalytic converters are used to break down exhaust emission into fine particles. These fine particles are in significant amounts to cause serious damage to health. They are small enough to be inhaled into the human lungs. Air needs to be exchanged between the car's interior and exterior to maintain adequate oxygen levels in the car. Exhaust fumes and allergens enter the cabin when this exchange occurs.

Car manufactures are catering for the 50 million allergy sufferers in the US [52]. They are now using these modifications as selling points for their cars. Lexus had, in the past, an advertisement for it LS 430 model depicting a person driving through a greenhouse and not sneezing till they got out of the car.

Reyton Eggteston professor at John Hopkins University and environmental allergy expert said approximately 20% of his patients have problems with their allergies while travelling by car.

Toyota & Lexus have particle filters to remove dust and pollen but they also have an optional rear seat air purifier which uses ultraviolet light to break down bacteria, mould and odours. This feature has been available from Lexus (as part of their 'Ultra Luxury Selection') for several years but they only started advertising them in the last 4/5 years. [53]

The most common allergens found in the car are dust mites, pet dander, pollen, road dust and mould spores. All of which occur on damp surfaces and leaking air conditioning systems. These can enter the car through the air conditioning or ventilation systems, can be carried in by passengers or may be released from car materials especially in new cars.

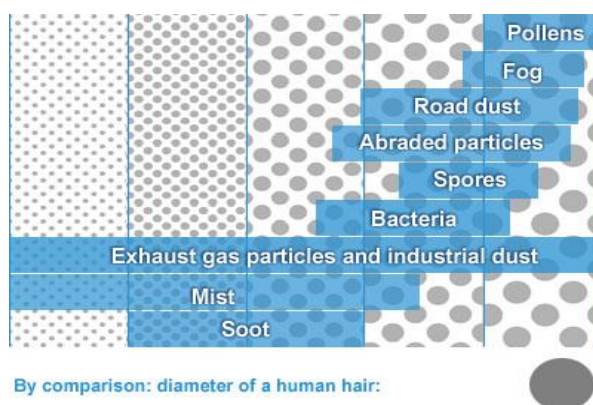


Figure 1.4.10 – Comparison of particulate sizes [54].



Figure 1.4.10 shows a comparison of particulate sizes relative to the size of a human hair. A cubic meter of particulate matter may contain up to 80 billion particles depending on the weather conditions and locality. A distinction is drawn between two different particle sizes: ones  $>2.5\ \mu\text{m}$  and ones  $<2.5\ \mu\text{m}$ .

### Filter Tests:

Different filter manufactures commission tests on their filters. Generally, research is carried out by manufactures with a majority share in the market, namely Micronair.

Tests on combination filters generally take place at 50% humidity and at  $23^{\circ}\text{C}$  even though in reality filters are exposed to a wider range of temperatures and humidity and air input concentrations. These factors influence the absorption capacity of the cabin filters. Experiments were carried out on filters at the department of chemical engineering at the University of Duisburg with varying temperatures, relative humidity and input concentrations. These investigations showed that the absorbance capacity of the filters is significantly reduced at higher temperatures and humidity. When the temperature and humidity rise and the input concentration falls this leads to desorption of previously absorbed pollutants [55].

The activated charcoal layer on combination filters is very thin and typically a few millimetres thick. There is a restricted amount of space for cabin filters therefore they are pleated to increase their surface size. The filter's surface is exposed to air velocities up to  $0.44\ \text{m/s}$ . The filter surface is relatively thin resulting in low resistance times, minimised mass transfer and reduced absorption because it prevents a mass transfer zone developing. Absorption is an exothermic process and is more efficient at lower temperatures. Increases in temperatures can lead to desorption. Therefore conditions during the winter are good for absorption while in the summer the absorption capacity can be reduced. The hydrophobic properties of the activated charcoal layer on combination filters decrease at high humidity. Input concentrations vary depending on the cars surroundings, which may lead to de-absorption of a loaded filter.

The gases n-butane, toluene, sulfur dioxide ( $\text{SO}_2$ ) and nitrogen dioxide ( $\text{NO}_2$ ) were selected. The concentrations of gases drawn through the filters during tests were  $80\ \text{mg L}^{-1}$  n-butane and toluene with  $30\ \text{mg L}^{-1}$  sulfur dioxide ( $\text{SO}_2$ ) and nitrogen Dioxide ( $\text{NO}_2$ ). These levels are over 104 times the concentrations found in car emissions.

It was found that increasing the humidity causes the lifetime of the filter to be cut in half. The humidity levels were increased from 20% to 50% to 95%, while the temperature was held constant at  $23^{\circ}\text{C}$ . Increasing the temperature from  $23^{\circ}\text{C}$  to  $43^{\circ}\text{C}$  causes a reduction of one

third in breakthrough time. The input concentration was varied while the temperature and humidity were held constant at 23°C and 50%. The filter was loaded for five minutes and then rinsed with nearly clean air to simulate the conditions in a car travelling through a polluted area. The concentrations of PTEs in the cabin are lower when clean air is passed through a loaded filter than when clean air is passed through a saturated filter. This indicates de-absorption occurs when filters are overloaded/saturated, which results in PTEs being released into the cars cabin.[55]

Regulations such as Verein Deutscher Ingenieure (VDI) 6032 (English: Association of German Engineers) ‘Hygiene standards for ventilation technologies in passenger vehicles’ are in place to insure careful construction and use of filter systems in cars. VDI 6032 have implemented regulation of filter designs with the intention of preventing possible hygiene irritation to passengers. Filters are specified by minimum filter capacity efficiency and the maximum two year service interval. Although in cases where there are heavy pollution levels it is recommended that filters be changed more frequently [56].

The DIN EN ISO 846 standard regulates if a filter media provides nutrition to promote the growth of microorganisms or if it is inert? Two tests are carried out on the filter exposing them to various fungi and bacteria. The samples are incubated for four weeks at defined thermal conditions and fungal and bacterial growths are then investigated. The results are rated in a class from 0-5. A result of 0-1 is considered as harmless for use in ventilation systems. However these tests do not reflect real life conditions [57].

### **Pollution scenarios and impact on filtration requirements:**

A decrease in particle emissions of approximately 70% has been reported between 1990 and 1996. This is mainly due to the fact that particles are only monitored to PM 10. Therefore, it suggests that the total mass of particles is decreasing when in fact the number of particles being emitted are increasing but particles are just getting smaller [56].

It’s now known that particles as large as 2.5  $\mu\text{m}$  can deposit in the lungs therefore, testing needs to be extended to include particles of <PM 2.5. The increase in PM 2.5 has been attributed to the increase in the number of diesel cars on the road. This has led to a reduction in CO<sub>2</sub> output but an increase in NO<sub>x</sub> emissions and an increase in the number of fine particles released by a factor of 1,000 [56].

The tests described below were carried out under laboratory conditions on cabin filters and are described in DIN 71460-1 [56]. The test results therefore don’t reflect real atmospheric conditions but they allow for a comparison of filters under laboratory conditions, therefore



giving an overview about filter performance. The tests evaluate particles size between 0.002-0.5  $\mu\text{m}$ .

The test methods used for Combination filters is DIN 71460-1. Tests are effective at determining a filter's ability to improve a passengers comfort or health. DIN 13725 tests odour reduction due to the installation of combination cabin filters. The odour threshold is defined at an odour concentration at which 50% of a surveyed population perceive an odour. The odour thresholds of four test persons were determined using an odfactometer. The odfactometer dilutes the samples with clean/neutral air and decreases the dilution in steps of a factor of 2. Just four test subjects noticed an odour in two successive dilution steps.

Cabin filters manufactured by JVC were installed in the HVAC ("heating, ventilating, and air conditioning") of a car and were compared with other commercially available filters. Both combination and particle filters were tested [58].

The ambient air in urban areas contains more toxins that are harmful to human health than air in rural areas. Pollen/particle filters have been used in Europe for over a decade and since 1997, Japanese cars have been equipped with them.

Table 1.4.1 shows the results of Japanese Environmental Agency monitoring roadside gas concentrations.

Table 1.4.1 - Japanese Environmental Agency monitors roadside gas concentrations [58].

		Mean value per year ( $\text{mg}/\text{m}^3$ )
SO <sub>2</sub>	National Average	0.007
	Maximum	0.013
NO <sub>2</sub>	National Average	0.04
	Maximum	0.056
HC	National Average	0.43 $\text{mg}/\text{m}^3 \text{C}$
	Maximum	0.96 $\text{mg}/\text{m}^3 \text{C}$

Odour tests were carried on JVC standard particle and combination filters using a panel of three people including the driver. They were compared to filters from unnamed manufacturers.

The odour tests were classed into 6 categories. 0: No Odour, 1: Slight Odour, 2: Mild Odour, 3: easily perceived odour, 4: Strong Odour, 5: Intense odour.

The test filters were replaced every half an hour. Maximum concentrations were measured but disappeared after about 10 secs. These peaks were attributed to exhaust fumes from vehicles in front of the test car. The panellists perceived an odour when the peak concentrations were measured.[58]

Table 1.4.2 – Results of filter analysis [59]

JVC Filters	Average Efficiency %
Particulate I	70
Particulate II	45
Combination I	79
Combination II	46
Other Companies	Average Efficiency %
Combination I	16
Combination II	23
Combination III	39
Combination IV	88

The efficiency was measured from:  $\text{Efficiency \%} = (1 - \text{Concentration downstream} / \text{Concentration upstream}) \times 100$  Mean efficiencies are shown in Table 1.4.2.

While combination (IV) is high at 88% it shows low efficiency for  $0.3 \mu\text{m}$  atmospheric dust. It was found the combination filter removed practically all odours while the particle filters were successful in removing some degree of odour because they remove particulate matter/dust.

### Analysis of substances bound to particles

Increased air pollution tends to increase allergic diseases. Four different European cities were studied at different times of the year [60]. Polycarbonate filters were used to collect samples and samples were analysed using a scanning electron microscope. The presence of pollen allergens, latex and  $\beta$ -glucans were analysed. SEM analysis showed positive signs of carbon particles which are thought to originate from exhaust emissions. Pollen allergens, latex and  $\beta$ -glucans were found to be bound and transported by combustion particles in air. Pollen allergies from trees, grass or weeds are submicron particles which can be bound to other particles. Differences between urban and rural areas was analysed. Vehicle traffic is the main source of pollutant particles in urban areas. The presence of latex particles released from tyres and the presence of Beta-glucans from the cell walls of plants were investigated. Particles were collected using a high cascade impactor. The impactor was set to collect samples at the same time and place for analysis using the electron microscope [60].

The levels of ambient air particles were found to be highest during the winter months and lowest during spring for all locations tested. The samples collected from the filters mainly contained carbon particles. Heavy rain fall caused a decrease in particle levels in samples. Typically grass pollen allergens were found to bind weakly to carbon particles. Combustion

particles from vehicle exhausts are the main source of carbon particles. Namork *et al.*, [59] concluded that combustion particles from vehicle exhaust emissions bind to and transport airborne antigens from pollen, latex and  $\beta$ -glucans.

### **Tunnel Effect:**

The exposure to toxins in traffic increases due to the tunnel effect. The vehicle in front causes an exhaust fume tunnel which results in pollutants being drawn into the cabin in concentrated amounts, shown in Figure 1.4.11.[61] Therefore the toxins concentrations in the cabin are greater than at the roadside. In fact the levels can be up to six times the levels at the roadside.



Figure 1.4.11 – Tunnel Effect [61].

Micronair claim to supply 70% of all particle filters sold worldwide. They produce over 300 different products for over 700 different vehicle makes. They claim to offer more protection over time and extraction of smaller sized particles than other suppliers. Figure 1.4.12 shows a comparison between different filter manufactures.

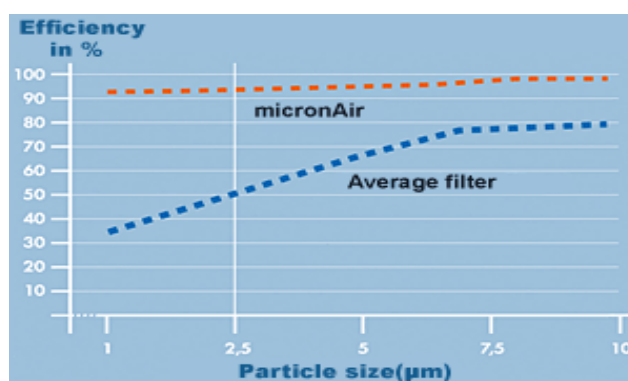


Figure 1.4.12. Different Filter Manufactures:[62]

There has been a continuous increase in the amount of Micronair filters sold from the late nineties till 2005 with a projected sharp increase post 2005, shown in Figure 1.4.13.

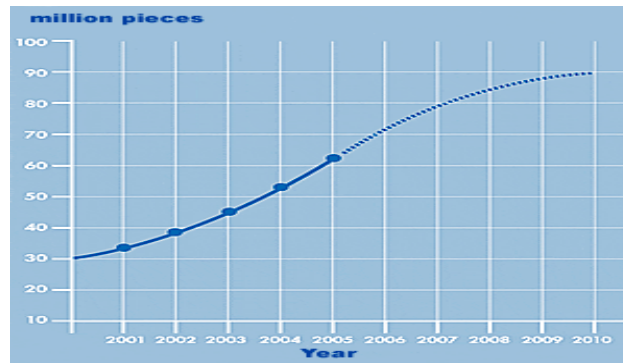


Figure 1.4.13– Micronair filter sales increasing with time [63].

Micronair have earned the Greenguard indoor air quality certification [64]. Micronair was the first company to achieve this third party certification for automotive cabin air filters. The Greenguard Environmental Institute is an independent non-profit organisation that oversees the Greenguard certification programme. The Greenguard product guide lists products that are low emitting and will not compromise indoor air quality. Micronair filters were subjected to Greenguard testing procedures and it was found that they do not contribute to chemical emission within the vehicles cabin. Automotive users are becoming increasingly concerned with the quality of air within the vehicles cabin according to Carl E Smith former CEO of Greenguard Environmental Institute.

#### **Other filter manufacturers:**

Mann filters, shown in Figure 1.4.14 are non-woven and are made up of several small fibres as small as  $0.1\ \mu\text{m}$ . The pores on combination filters are 10,000 times finer than human hair. Their structures provide almost complete extraction of dust and soot particles. They have no chemicals impregnated on them and they are odour free.

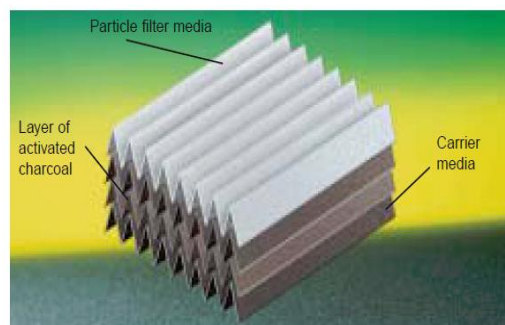


Figure 1.4.14 –Mann filter [65]

Puravent: claim that their filters will trap 100% of particles  $\geq 3$  micron or larger and will trap 80% of particles  $< 3$  and  $> 0.3$  microns in size.

## 1.5: Instrumentation

Graphite Furnace Atomic Absorption Spectrometry (GFAAS) and Inductively Coupled Plasma-Optical Emission Spectrometry (ICP-OES) are used in this study to analyse pollen filter samples impregnated with a standard reference material (SRM). The results of each analytical technique were compared to determine which is more efficient at PTE detection.

### Graphite Furnace Atomic Absorption Spectrometry

Light of a specific wavelength is passed through the atomic vapour of an element of interest. A measurement is made of the decrease in the intensity of the light as a result of absorption. Samples are vaporized/atomized using a graphite furnace at temperatures as high as 3,000°C. Ground-state atoms absorb energy, in the form of light, and are elevated to an excited state. The amount of light energy absorbed increases as the concentration of the selected element increases. Samples are generally entered as dilute aqueous solutions in 10-20 mL quantities. This process is performed by starting a pre-programmed heating sequence.

GFAAS Steps, shown in Figure 1.5.1: [66]

1. Injection: the sample is placed via syringe into the furnace.
2. Drying: the sample is evaporation at a low temperature typically around 110°C in order to remove the solvent. This temperature must be kept low enough in order to avoid spattering of the sample and ultimately loss of analyte.
3. Pyrolysis: this temperature is then increased to approximately 300°C and after that it is further increased to 1200°C where the pyrolysis step takes place. The function of the pyrolysis step is to volatilise any organic and inorganic matrix components.
4. Atomisation: Once the pyrolysis is complete the temperature is increased rapidly to 2000-3000°C and as a result of this rapid increase in temperature, atomisation and vaporisation of the sample occurs. The function of this step is to produce an atomic vapour of the analyte to facilitate the measurement of atomic absorption. Temperature is also critical in this step because it must be high enough to facilitate efficient atomisation and low enough to ensure optimum analyte residence times in the optical path.
5. Measurement
6. Clean out and Cool down. The clean out and cool down steps of the analytical programme are essential in order to prevent contamination from a previous sample.

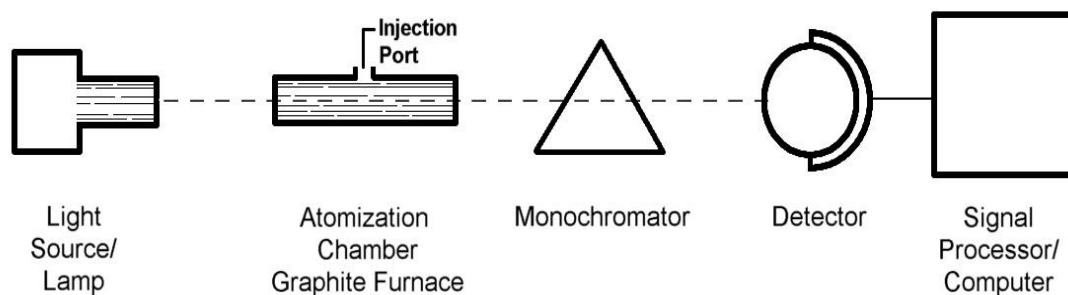


Figure 1.5.1 – GFAAS schematic [67].

An interference results in a change of the analyte signal while the analyte concentration remains unchanged. GFAAS interference can arise from a number of sources e.g. chemical, ionisation and spectral sources.

**Chemical interferences:** A reaction of the analyte ion with a matrix produces a signal leading to a loss of analyte signal. It can be rectified by the addition of a matrix modifier. This is added to the sample and it can either increase the volatility of the matrix or decrease the volatility of the analyte. The addition of a chemical modifier results in a more efficient pyrolysis step.

**Spectral interferences** lines from different elements are at the same wavelength as the analyte and the spectrometer cannot differentiate between them. It can be corrected by using secondary or tertiary wavelengths ( $\lambda$ ).

**Ionization interferences:** if the temperature is too high causing the ionisation of certain elements. Emission interference is encountered when ‘Black body’ radiation from a hot graphite tube or L’Vov platform reaches the detector. It causes an increase noise in the signal which results in a distorted measurement. Emission interference can be controlled by keeping away from high atomisation temperatures, ensuring the furnace is kept clean and also by making certain that the furnace is properly aligned.

### **Advantages:**

Electrothermal atomisers offer a better degree of sensitivity when compared to traditional flame atomisers because the entire sample is atomised quickly and the atoms have a residence time of one second or more in the optical path. The sample size required for electrothermal atomisers is only a few microlitres.

### Disadvantages

The disadvantages associated with GFAAS are that there is a possibility of cross contamination. Samples need to be in solution and individual source lamps are required for each element, therefore multi-element analysis is not possible [68].

### Applications

GFAAS is applicable to the determination of trace elements in various sample types. Environmental samples such as water, sediments, plant material and particulates, industrial samples such as steel, petroleum products and clinical and biological samples such as blood, plasma and urine.

### Inductively Coupled Plasma Emission Spectrometry:

ICP works on the principle that excited atoms emit energy (electromagnetic radiation ( $h\nu$ )) at a given wavelength as they return to a ground state, shown in Figure 1.5.2. The sample is subjected to high temperatures causing dissociation to occur. This radiation is emitted in the plasma and analysed in an inert gas in the ultraviolet, ultraviolet-visible, and near infrared regions. The intensity of the energy emitted is proportional to the concentration of the element being analysed.

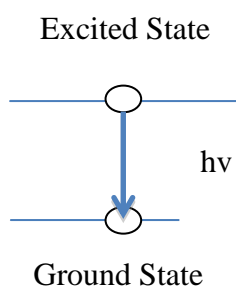


Figure 1.5.2 – Atomic Emissions Process of Electron De-excitation. [69]

Detection systems are more sensitive to VUV, UV, VIS, and NIR regions. The vacuum ultraviolet region needs an environment devoid of air.

Ionisation of an electron occurs when the energy absorbed by an atom is sufficiently high and caused the electron to become dissociated and leave the atom as an ion with a positive charge.

Excitation source: In ICP-OES the plasma is a gas that has been ionised and is electrically neutral. The main advantage of plasma over furnace or flame analysis is the high temperature of the plasma and the electrically neutral environment which reduces analyte ionisation.

Table 1.5.1: ICP Operation Steps. [69]

Nebulisation	Liquid samples are converted to aerosol
Desolvation/Volatilisation	Water is driven off and the remaining solid and liquid is converted to gases.
Atomization	Gas phase bonds are broken and only atoms are present.
Excitation/Emission	Atoms gain energy from collisions and emit light of characteristic wavelengths.
Separation/Detection	Grating disperses light that is quantitatively measured.

Sample introduction is shown in Table 1.5.1, where samples are introduced as liquids or fine solids (particle diameters should not exceed 10 microns). A peristaltic pump conveys the sample into the nebulizer. The nebulizer converts the aqueous sample into an aerosol [69]. This mist accumulates in the spray chamber where the larger droplets settle out to the waste outlet by gravity with the remaining fine aerosol proceeding to the torch assembly. Torch consists of three tubes: An external (Outer) tube: is used to make the gas spiral tangentially around the chamber. The function of the gas is to keep the walls of the torch cool. An Intermediate (Inner) tube: sends gas directly into the plasma to lift the plasma tip away from the injector. A central tube: carries the sample into the plasma through the injector [70]. The light emitted by the atoms of an element is converted to an electrical signal so they can be measured quantitatively. The light is resolved into its component radiation (usually by the use of diffraction grating) the light intensity is then measured using a photomultiplier tube at a specific wavelength for each element line. The intensity of the electron signal is compared to previous measured intensities of known standards for each element.

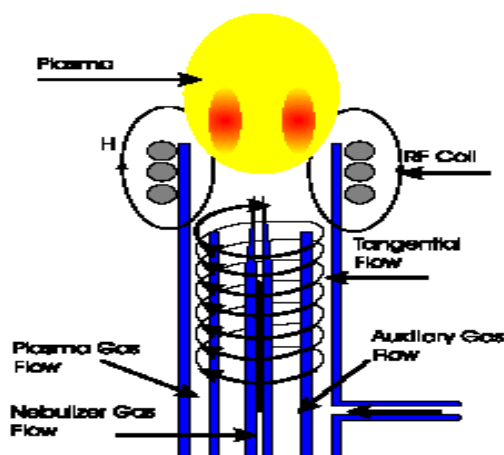


Figure – 1.5.3 – Sample introduction [70]

A radio frequency generator, shown in Figure 1.5.3, is used to deliver the power required to obtain and maintain the plasma. It is made up of copper tubing and is cooled by water during



operation. There are two types of spectrometers, sequential and simultaneous, which carry out multi-element analyses by scanning rapidly from one emission line to the other or measure all emission lines at once.

### Radial/Axial viewed plasma

Radial View, shown in Figure 1.5.4 (A) the spectrometer views the analyte emission from the side of the plasma through the background argon emissions. The spectrometer is designed to image a vertical slit in the plasma. The slit averages the analyte emission intensity over the height of the slit. Used for highly concentrated samples.

Axial view, shown in Figure 1.5.4 (B) the spectrometer views the analyte down the central channel of the plasma and collects analyte emissions over the entire length of the plasma. As a result the emission path length is increased relative to the radially viewed plasma. This improves sensitivity but doesn't extend the dynamic measurement range available. Axially viewed plasma improves detection limits by 5-10 times and is used for low concentration samples. However, interferences are greater with axial viewing.

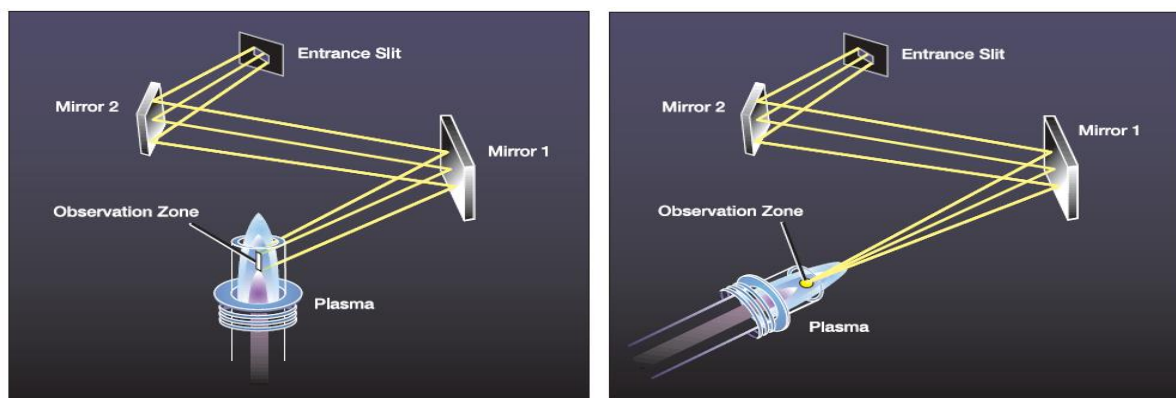


Figure 1.5.4 (A) – Radial View of ICP Torch [71] (B) – Axial View of ICP Torch [71]

Using a shear gas (nitrogen) to reduce axially viewed plasma interferences: Self-absorption occurs when the analyte emission is absorbed by ground state atoms in the plasma. In axially viewed plasma this occurs at high analyte concentrations resulting non-linear calibration plots. The blue colour is the normal emission and the red zone is the plasma's cooler tail plume. The emissions from the analyte atoms are absorbed by ground state atoms. This is not an issue in radially viewed plasma because the tail plume is not in the optical path. In axially viewed plasma a shear gas displaces the tail plume out of the optical path, shown in Figure 1.5.5 (A) and (B).

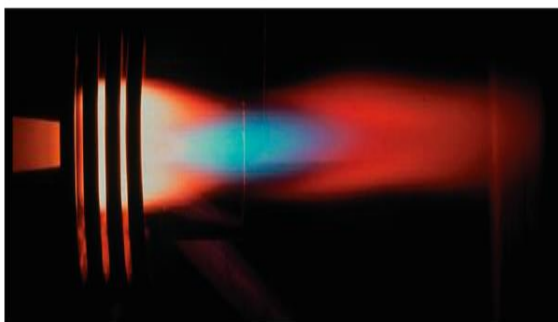


Figure 1.5.5 (A) - Without shear gas. [71]

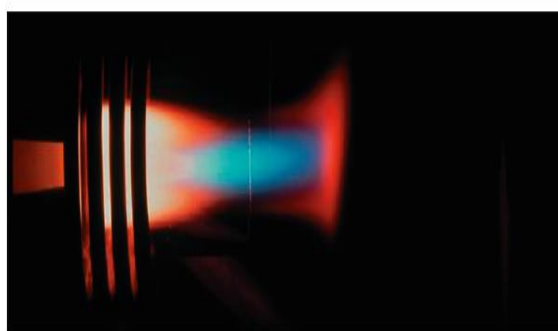


Figure 1.5.5 (B) - With Shear Gas. [71]

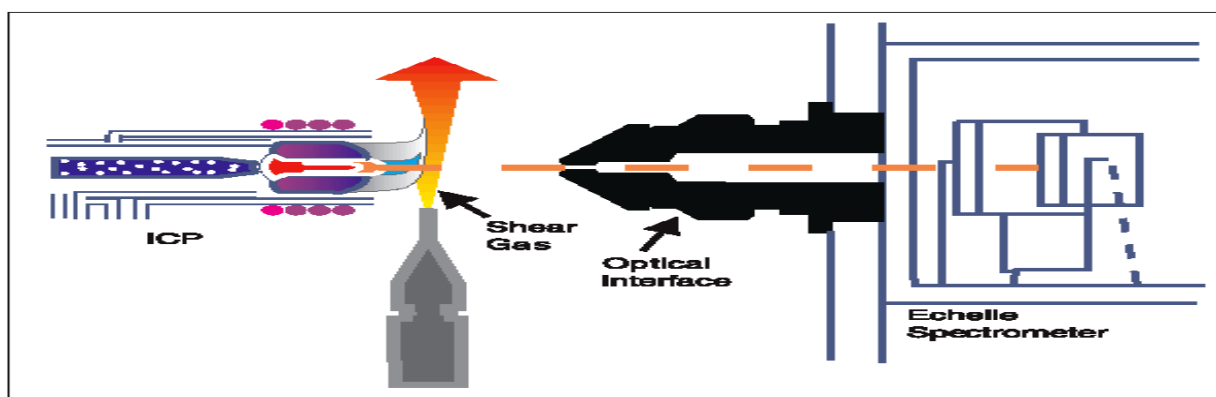


Figure 1.5.6 – ICP schematic showing the use of a shear gas, to remove the tail plume of the torch.

Analysis was carried out using a Perkin Elmer Optima 2000 DV ICP-AES, shown in Figure 1.5.8. Win lab 32 operating software was used to interpret analytical results. A AS-90 series auto sampler is used for sample delivery. The 2000 DV has a dual plasma viewing option and a free-running 40-MHz solid-state RF generator. A double monochromator spectrometer, shown in Figure 1.5.7, is used to separate and measure light according to its wavelengths.

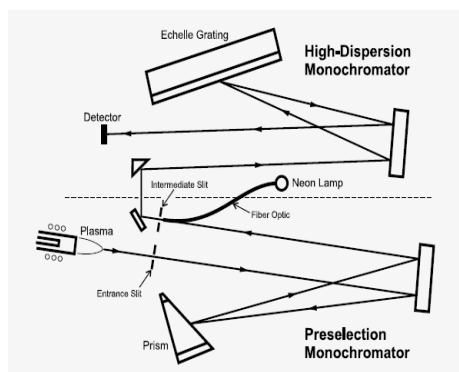


Figure 1.5.7 – A double monochromator detector [72]

A pneumatic nebuliser was used for analysis. The nebuliser gas (argon) draws the sample through a capillary. The aerosol generated is separated by size in the spray chamber with smaller drops being carried into the plasma. The larger drops are drained off. The sample and the nebulizer gas combine at a right angle forming an aerosol. The aerosol then strikes an impact beam causing the drops to break apart.



Figure 1.5.8 – Perkin Elmer Optima 2000 DV ICP-AES [73]

An ICP can simultaneously view emissions from several (approximately 70 at a time) elements.

Interferences:

Plasma interferences occur when a spectral overlap of emission lines from different elements are at the same (or close) wavelengths and the spectrometer cannot differentiate between them. Alternative lines should be used to overcome this interference, spectral overlap is not an issue in practical terms.

Argon interferences occur when the plasma emits spectra bands from NO, OH and NH radicals between 200 and 350nm. Argon also emits at wavelengths that are identical to the atomic lines of elements being analysed. This results in a non-uniform background.

Matrix interferences result from high concentrations of dissolved solids in sample solutions. The effects can be minimised by the use of an internal standard to detect any shift in results.

### **Microwave Multiwave 3000:**

A Microwave Multiwave 3000 was used to carry out acid digestions on filter samples as a pretreatment for ICP-OES and GFAAS analysis.

The microwave Multiwave has two microwave generators (magnetrons) that generate a frequency of 2.45 GHz.

Sealed vessels with a screw cap and a self-sealing lip-type seals are used. The microwave vessels are made up of a porcelain exterior, with a plastic liner. These vessels prevent contamination and loss of volatile analyte. Each screw cap has a safety lid which is designed to burst at a pressure of 22 bar. As a result, the operational pressure is limited to 18 bar. The vessels are placed in the rotor and the rotor is placed in the Multiwave 3000. The reaction is controlled using a microcontroller, which holds the method information and documents the reaction process and results. The measured data is transmitted wirelessly from the rotor to the built in microprocessor. The surface temperature of the reaction vessels is measured using an infrared sensor. The Multiwave has an integrated cooling system that cools the reaction vessels preventing overheating of the rotor components by passing air over the vessels during analysis. It reduces cooling times and omits the need for external cooling and limits the need to handle hot vessels and offers improved parts lifetimes. A built in cookbook with a library of preset microwave methods is available. These methods can be adapted to suit the user's needs.

A dual temperature sensor is shown in Figure 1.5.9: The microwave multiwave 3000 has an immersing temperature probe that is inserted into a reference vessel and a rotor IR sensor under the oven cavity which measures each vessel through ports in the rotor base.



Figure 1.5.9 - Dual temperature sensor [74]

A sensor in the base of the oven sends an infrared beam onto the bottom plate of the rotor, shown in Figure 1.5.10. The bottom plate reflects this beam to the sensor, where the beam is then electronically analysed. The beam provides information on the rotor type, the rotors revolution (to sustain uniform microwave heating), vessel temperature (enabling the display of individual vessel temperatures) and detection of the rotor lid (as a safety mechanism).

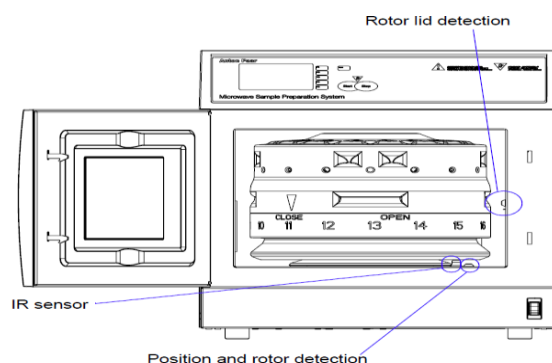


Figure 1.5.10 – Microwave temperature sensor [74].

The microwave Multiwave has an exhaust unit, shown in Figure 1.5.11 that carries off the reaction heat during analysis.

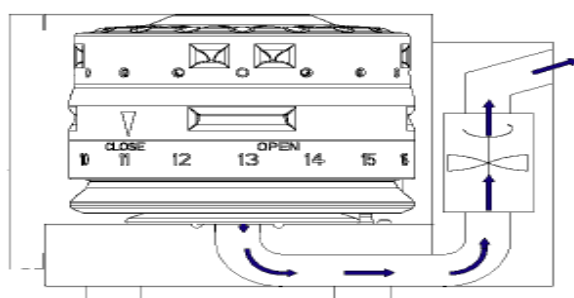


Figure 1.5.11 – Microwave exhaust unit [74].

Table 1.5.2: Reaction vessel used: [75]

Pressure vessel	Operation Pressure	Vessel Material	Filling volume max.	Typical application	Maximum temperature
HF100	70bar (1000 psi)	Liner of TFM or PTA and supporting vessel of ceramics	50 ml	Sediments, Rocks, Ashes, metals and pigments.	260 °C

When starting a digestion programme the following should be considered, sample being digested, that the method being used matches the properties of the sample material and that the method can be modified to optimise recoveries. [75]

The following properties should be considered when developing an digestion method, analyte, sample matrix, sample weight, reagents, measuring methods and their accuracy.[75]

Permissible parameter values:[75]

Power: 0....1400 [W] (Initial and end powers of the microwave)

Time: 0:00....99:58 [mm:ss]

Fan: 0,1,2,3 (Power step of exhaust module)

Digestion time should be between 30 and 60 minutes. Longer digestion times will not have a significant impact on recoveries. [75]

The cooling phase should be at least 10/15 minutes. A security cooling cycle will activate if cooling time is set too low to cool the solution to below 60°C.

A cool down period is added to the end of each programmes to cool the vessels for extraction. Different fan settings, shown in Table 1.5.3, can be selected during the cool down period depending on requirements. Generally setting 0 (reduced cooling) is selected, it offers a slow gradual cool. Setting 1 to 3 are used if rapid cooling is required.

Table 1.5.3: Power step of exhaust module (Fan):[75]

Fan	Power	Remark
0	25%	Reduced cooling power (pulsed cooling)
1	25%	Normal cooling power.
2	50%	Increased cooling power at the beginning of power program to compensate for spontaneous reaction when decomposing reacting samples.
3	100%	Maximum cooling power to rapidly cool down reagents once heating has completed.
-	5%	This is not programmable it runs automatically after the end of a program to extract possible escaping fumes

### **Principles of Scanning electron microscope (SEM):**

SEM was used in this study to determine the minimum particle size retained by particle filters at different kilometerages. The ability of filters tested to remove small particulates is significant given that particles <2.5 µm can pass into the lungs and that particles <1 µm can pass from the lungs into the bloodstream. EDX was used to determine if it could be used as an alternative method of PTE analysis to investigate if filter analysis could be carried out without carrying out acid digestions on filters.

SEM is used to observe particle size, shape and arrangement down to nanometer levels. It uses electrons rather than light to form a three dimensional image. In order to analyse samples they must be conductive. If not they can be layered with a thin layer of gold.

The samples are placed in the vacuum column of the microscope, once prepared, through an air tight door. Once the air has been pumped out of the vacuum column the electron gun emits a high-energy beam of electrons. The beam is directed down through the column and travels through a series of magnetic lenses which focus the beam on one fine spot. The scanning coils facilitate the back and forth motion of the focused beam across the sample surface. As the electron beam hits each spot on the surface it results in the release of

backscattered and secondary electrons from the sample surface. The detectors then count these electrons and in turn produce a signal which is sent to an amplifier and a three dimensional image of the sample surface is produced.

An electron gun (the visual source), shown in Figure 1.5.15 produces a stream of monochromatic electrons. A condenser lens then condenses the electron stream into a beam and limits the amount of current contained in the beam. A condenser aperture is used to eliminate high angle electrons. A second condenser lens forms a tighter coherent beam of electrons. The objective lens focuses the scanning beam on the sample being investigated. The scan coils then sweep the sample in a grid fashion. The scan speed determines the amount of time spent reading a particular area.

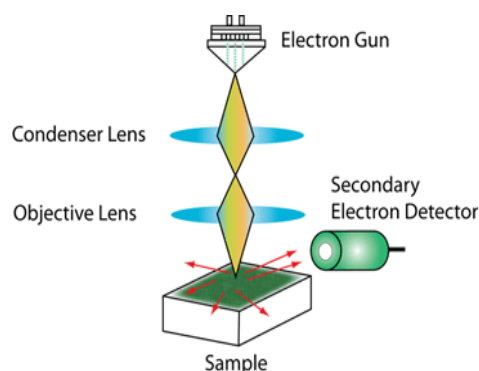


Figure 1.5.15 - Scanning electron microscope (SEM) [76].

### **Advantages:**

Magnifications of over 100,000 times can take place. Artificial colour can be added to samples using computer software.

### **Disadvantages:**

Images (without modification) can only be displayed in black and white because light is needed to carry colour information. Only images of inanimate objects can be analysed as only surface information can be obtained.

### **Energy dispersive x-ray spectrometry (EDS):**

An x-ray analyzer is beamed onto the sample particles and an energy dispersive pattern is generated which gives the elemental composition of the particles. An electron from the SEM strikes an atom due to the size of the electron (generally  $\sim 1.0 \times 10^{-5} \text{ m}$  ( $10 \text{ }\mu\text{M}$ )) it can penetrate the atom. The force of the collision creates enough energy to force the inner core electron to leave the atom. As the electron returns from an orbital of higher energy level to an

orbital of lower energy, it causes a release of energy in the form of an x-ray. Each element detected in an EDS emits x-rays that have a unique energy for that element.

The overall objectives of the research carried out are as follows:

- (a) Develop and optimise an acid digestion method for car pollen filters using a Microwave Multiwave 3000.
- (b) Investigate the optimum analysis method for digested samples by comparing recoveries using ICP-OES and GFAAS.
- (c) Use an SEM to observe particles retained on different types of filter.
- (d) To investigate the use of EDX as an alternative method of PTE detection.
- (e) Determine the capture rates of various filters, at varying kilometerages for a range of PTEs with significant environmental and health concerns.
- (f) To compare exposure to these PTEs in the absence of a pollen filter, with the use of a particle filter and a combination filter by measuring PTE levels within the cabin.
- (g) To determine the level of exposure to analytes for cyclists travelling in city traffic.



## **Chapter 2:**

### **Material and Methods**

## Chapter 2

### Materials

#### 2.1 Materials: Acids used for microwave digestion

The following Analar grade reagents were purchased from Merck, (Darmstadt Germany). nitric acid 69% concentrated ( $\text{HNO}_3$ ), a strong oxidant when hot, used in the decomposition of biological samples, also used in combination with  $\text{HCl}$ , perchloric acid or  $\text{HF}$  [77]. Hydrogen peroxide 30%, it is used in combination with other acids to speed up digestions. It is used with  $\text{HNO}_3$  or  $\text{H}_2\text{SO}_4$  for digestion of organic samples and with  $\text{HF}$  and  $\text{HCl}$  for digestions of inorganic samples (e.g. metals)

The following Analar grade reagents were purchased from Sigma Aldrich, (Buchs, Switzerland).

Hydrochloric acid 37% concentrated ( $\text{HCl}$ ) is used in conjunction with  $\text{HNO}_3$  (Aqua regia - 3  $\text{HCl}$ :1 part  $\text{HNO}_3$ ). Aqua regia is a strong oxidising agent making it useful for the digestion of solid sample matrices. [78] It is used for the decomposition of organic samples but acts as a complexing agent for  $\text{Fe}$ ,  $\text{Sb}$ ,  $\text{Sn}$ ,  $\text{Ag}$  and  $\text{Zn}$  (thus inhibiting their extraction).

Hydrofluoric acid (47-51%) is generally used to digest samples containing silicate and is commonly applied with other acids (e.g.  $\text{HNO}$  or  $\text{HCl}$ ).

Hydrofluoric acid Safety - Hydrofluoric acid was supplied in and stored in a plastic polyethylene bottle, contained in a metal canister. All work with hydrofluoric acid was carried out in a fume hood with a Calgonate 2.5% calcium gluconate gel on hand for use in the event of contact with the users skin.

Perchloric Acid 70% concentrated ( $\text{HClO}_4$ ) is a strong oxidising agent. A mixture of nitric acid and perchloric acid is more powerful than either acid on its own and is less hazardous than perchloric acid on its own [77].

Boric acid 99% ( $\text{H}_3\text{BO}_3$ ) is used to decompose fluorides. Boric acid is used after the digestion with  $\text{HF}$  to decompose fluoride formed during  $\text{HF}$  digestions. The concentration of boric acid used matches the concentration of  $\text{HF}$  used (in the original  $\text{HF}$  digestion) and solution is heated again using the same digestion method as the original digestion.

Glassware used was cleaned by soaking it in a  $\text{HNO}_3$ : $\text{H}_2\text{O}$  (10%:90%) wash bath overnight and then soaking it in a deionised water bath for an hour.

ICP calibration standards were prepared using a made to order 11 element ICP OES standard purchased from Spex Certiprep with element concentrations of  $1000 \text{ mg L}^{-1}$  in 10%  $\text{HNO}_3$ .

An element specific GFAAS master standard was prepared using an AAS standard, purchased from Sigma Aldrich, Buchs, Switzerland containing  $1000 \text{ mg L}^{-1} \pm 4 \text{ mg L}^{-1}$  in a 2% nitric acid solution.

**GFAAS Matrix modifiers:** The function of a matrix modifier in graphite furnace atomic absorption spectrometry is to eliminate interfering components and reduce volatility of the analyte.

An ammonium nitrate matrix modifier was used for Lead and Copper analysis by GFAAS. A  $10 \text{ mg L}^{-1}$  modifier solution was prepared by adding 1 g of ammonium nitrate to a 100 ml volumetric flask and made up with 2% Nitric acid.

A magnesium nitrate matrix modifier was used for chromium, iron, manganese and zinc analysis by GFAAS. A  $10 \text{ mg L}^{-1}$  modifier solution was prepared by adding 1g of magnesium nitrate to a 100 ml volumetric flask and made up with 2% Nitric acid.

A standard reference material (SRM 1648a) [79] was purchased from the National Institute of Standards and Technology (NIST). NIST is a measurement standards laboratory which is a non-regulatory agency of the United States Department of Commerce. SRM 1648a is composed of particulate matter, collected in an urban areas and containing known quantities of elements of interest, shown in Table 2.1.1.

Table 2.1.1: Element quantities present in SRM 1648a

Element	Al	Cd	Cr	Cu	Fe	Mg	Ni	Pb	Zn
Quantity (mg/L)	34,300	73.7	402	610	39,200	813	81.1	655	4,800

## 2.2 Acid Digestion Methods:

Microwave digestions of filter samples were carried out using 6 ml  $\text{HNO}_3$ , 2 ml HF and 1 ml HCl and operation settings shown in Table 2.2.1.

Table 2.2.1 – Microwave digestion method:

Power (W)	Ramp (mins)	Time (mins)	Fan Setting
500	5.00	10	1
1000	5.00	10	1
1400	5.00	10	1
0		15	3

**Preparation of Calibration Standards for ICP-OES:**

ICP-OES calibrations were carried out using a calibration range of 0-1000  $\mu\text{g/L}$  for each element. Calibration standards were prepared from a made to order 11 element ICP OES standard purchased from Spex Certiprep with element concentrations of 1000  $\text{mg L}^{-1}$  in 10% Nitric acid solution. This standard was then diluted to prepare the following calibration standards in  $\mu\text{g L}^{-1}$ ; 0, 50, 100, 250, 500 and 1000. 10% Nitric acid was used as a diluent in the preparation of the working standards. The 10% Nitric acid prepared by slowly adding 144 ml of 69% nitric acid to a 1L volumetric flask containing 500 ml of deionised water. The solution was then made up to the 1 L mark with deionised water.

**Preparation of Calibration Standards for GFAAS:**

GFAAS calibrations were carried out for Cr, Cu, Fe, Pb, Mn, Ni and Zn. Master standards were prepared using a AAS standards, purchased from Sigma Aldrich, Buchs, Switzerland, containing  $1000 \text{ mg L}^{-1} \pm 4 \text{ mg L}^{-1}$  in a 2% nitric acid solution. 2% Nitric acid was used as a diluent in the preparation of all the master standards for GFAAS. The 2% Nitric acid was prepared by slowly adding 28.8 mL of 69% nitric acid to a 1 L volumetric flask containing 500 mL of deionised water. The solution was then made up to the 1 L mark with deionised water.

**2.3 Instrumentation:**

ICP-OES: Elemental analysis by ICP-OES was performed using the Perkin Elmer Optima 2000 DV optical emission spectrometer. The Spectrometer was also equipped with a pneumatic nebuliser, a Scott spray chamber and an AS-90 Series Auto sampler. The system was run on PE WINLAB32 software.

Table 2.3.1: ICP settings used: The gases used to operate the ICP were ultrapure argon and nitrogen

Operating Conditions	Units	Value
Source Equilibration time	s	15
Viewing Height	mm	15
Read Delay	s	40
Rinse Delay	s	40
Number of Replicates	-	2
RF Power	W	1350
Nebuliser Flow	ml/min	800
Auxiliary Flow	ml/min	15,000
Plasma Flow	ml/min	500
Sample Flow	ml/min	1800

GFAAS: Elemental analysis by GFAAS was performed using the thermo electron M series Graphite furnace atomic absorption spectrometer. The spectrometer was equipped with an automated FS95/97 autosampler and pyrolytically coated graphite tube. The system was run on SOLAAR Data Station V10.11 software.

Table 2.3.3 Furnace operation conditions for thermo electron M series Graphite Furnace Atomic Absorption Spectrometer:

Phase	Temp ( $^{\circ}\text{C}$ )	Time (s)	Ramp (s)	Gas Flow L/min
1	100	30	10	0.2
2	1200	20	150	0.2
3	2500	3	0	Off
4	2600	3	0	0.2

## 2.4 Representative sampling of pollen filters:

Representative samples were collected from both filter types to accurately represent the dispersal of PTEs over the surface of the filter.

Table 2.4.1 shows representative sampling for Skoda Octavia: Skoda Octavia filters have 29 folds which are 1” high and the filter is 10” wide. Samples were taken from fold number 8, 19 and 25 at 2”, 5” and 8” along the width of the filter, thus creating 1” square filter samples.

Table 2.4.1: Representative analysis of Skoda Octavia particle filters.

	2"	5"	8"
Fold 8	A	B	C
Fold 19	D	E	F
Fold 25	G	H	I

Table 2.4.2 shows representative sampling for a Toyota Aventis: a Toyota Aventis filters have 40 folds, which are 1" high and the filter is 8" wide. Samples were taken from fold number 9, 19, 29 and 39 at 2", 4" and 6" along the width of the filter which also creates 1" square filter samples.

Table 2.4.2: Representative analysis of a Toyota Aventis particle filters.

	2"	4"	6"
Fold 9	A'	B'	C'
Fold 19	D'	E'	F'
Fold 29	G'	H'	I'
Fold 39	J'	K'	L'

Table 2.4.3 shows representative sampling for Ford Fiesta filters: Ford Fiesta filters have 50 folds which are 1" high and the filter is 7" wide. Samples were taken from fold number 12, 24, 36 and 48 at 2", 4" and 6" along the width of the filter, creating 1" square filter samples.

Table 2.4.3: Representative analysis of Ford Fiesta particle filters.

	2"	4"	6"
Fold 12	A*	B*	C*
Fold 24	D*	E*	F*
Fold 36	G*	H*	I*
Fold 48	J*	K*	L*

1" square samples were collected and digested. Once digested the samples were filtered through a 25 mm syringe filter with 0.45  $\mu\text{m}$  filter cellulose acetate membrane.

## 2.5: Portable in cabin air purifier:

In cabin air purifiers were used to determine the levels of PTEs entering the cabin firstly without a filter in place, secondly with a standard particle filter in place and finally with a combination filter in place.

Internal filtration system: An Amaircare XR-100 Car Air Purifier was used and is shown in Figure 2.5.1. The unit is mounted behind the headrest, this position allows for optimum filtration efficiency. In an average sized car the air will be exchanged 10 times per hour, it filters at 20 cubic feet per minute. Filters should be changed every 4 to 6 months.

### Three-Stage Air Purifier Filtration Operation

Stage 1: Activated Carbon. This pre filter captures large particulates and odours.

Stage 2: Electrically charged media. This electrically charged filter captures sub-micron particles such as dust, pollen, cigarette smoke, and bacteria.

Stage 3: Zeolite V.O.C. filter. Removes gases, fumes and odours.



Figure 2.5.1 Amaircare XR-100 Car Air Purifier[80]

Representative samples were collected from all the circular internal filters to accurately represent the dispersal of PTEs over the surface of the filter.

The internal filters were split into 9 equal sections shown in Figure 2.5.2. Samples were taken from segments 1, 3, 5, 7 and 9 to get an even representation of quantities present. Once digested the samples were filtered through a 0.45µm cellulose syringe filter.

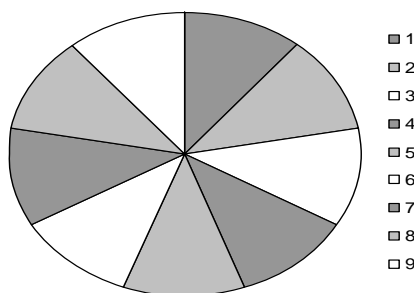


Figure 2.5.2: Internal Filters digestion sections.

## 2.6: Respro® Citytm Cycle Mask,

Cycling masks were worn by a volunteer to investigate a cyclists exposure to PTE when travelling in Cork city traffic and to compare the concentrations of analytes at the roadside to those in the traffic stream.

The mask shown in Figure 2.6.1 uses an activated charcoal material to filter inhaled air. The masks are made from hypo-allergenic neoprene. It is recommended that the filters be changed monthly.



Figure 2.6.1 - Respro® City™ Cycle Mask [81]

The filters taken from the cycle mask are folded, circular filters, 2½” in diameter. Two 1” square samples were collected and digested from the front and back fold of the filter. The front and back folds were divided as shown in Figure 2.6.2. Front: F1, F2, F3 & F4 and Back: B1, B2, B3 & B4. Samples were taken from F1 & F4 and B1 & B4. Once digested the samples were filtered through a 0.45µm cellulose syringe filter.

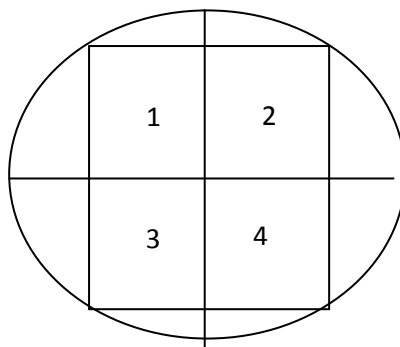


Figure 2.6.2: Cycle filters digestion sections.



**Chapter 3:**  
**Method development for microwave acid digestion of filter**  
**samples:**

## Chapter 3

### Method development for acid digestion of filter samples

#### Introduction:

The increasing levels of potentially toxic elements (PTEs) in the environment is becoming a growing concern. The European Union (EU) and the United States Environmental Protection Agency (US EPA) have set out specific guidelines for acceptable levels of PTE contaminants in the environment. There is, however, a small difference between acceptable and toxic levels for some PTEs, therefore, it is vital to develop an effective method for PTE detection. The measurement of PTEs in soil/air samples is essential to monitor these levels.

#### 3.1: Closed Vs Open Vessel Digestion Methods

The first requirement is for a samples to undergo acid digestions to extract the PTEs. There are two principal approaches to acid digestion, open digestion or closed digestion. Table 3.1.1 outlines the differences between open and closed acid digestion.

Table 3.1.1: Closed Vs Open Acid digestion

	<i>Open System</i>	<i>Closed System</i>
<b>Maximum Temp.</b>	Limited by acid boiling point	260-300°C
<b>Sample Size</b>	Large sample weights allowed	Limited by sample nature
<b>Acid consumption</b>	High acid consumption	Reduced acid consumption
<b>Time</b>	2-15 hours	20-60 minutes
<b>Digestion Quality</b>	Loss of volatile elements, risk of contamination. Costly due to high acid consumption.	Reduced loss of volatile elements, low risk of contamination due to closed system. Cost effective due to low acid consumption.

**Results:** An open digestion is one which is carried out under atmospheric pressure. Three different extractions were carried out on pollen filter samples using a nitric acid digestion and two National Institute for Occupational Safety and Health (NIOSH) acid extraction methods with two different acid combinations with a view to establishing an optimum open vessel acid digestion method, the results are shown in Table 3.1.2. and Figure 3.1.1. [82] The acids combinations tested were (i): Nitric acid ( $\text{HNO}_3$ ) (ii): Aqua regia ( $\text{HNO}_3$ :  $\text{HCl}$ ) 1:3 [82] and

(iii): Nitric:Perchloric ( $\text{HNO}_3:\text{HClO}_4$ ) 4:1 [83]. The efficiency of the extraction methods were evaluated using a NIST urban particulate matter standard reference material 1648a. The PTEs tested, of environmental concern, were Al, Cd, Cr, Cu, Fe, Mn, Ni & Pb.

(All glassware was soaked in a  $\text{HNO}_3:\text{H}_2\text{O}$  (10%:90%) wash bath overnight and then soaked in a deionised water bath for an hour).

Table 3.1.2: Recoveries (%) of PTEs based on certified values

Element	Certified Value ( $\text{mg kg}^{-1}$ )	% Recovery		
		$\text{HNO}_3$	$\text{HNO}_3:\text{HCl}$	$\text{HNO}_3:\text{HClO}_4$
Aluminium	34,300	8.61	10.50	10.26
Cadmium	73.7	68.16	66	60.06
Chromium	402	8.77	8.77	11.95
Copper	610	59.85	59.86	29.81
Iron	39,200	11.47	21.34	21.40
Lead	6,500	41.64	36.20	36.97
Manganese	790	65.09	62.19	61.78
Nickel	81.1	58.76	56.11	50.42

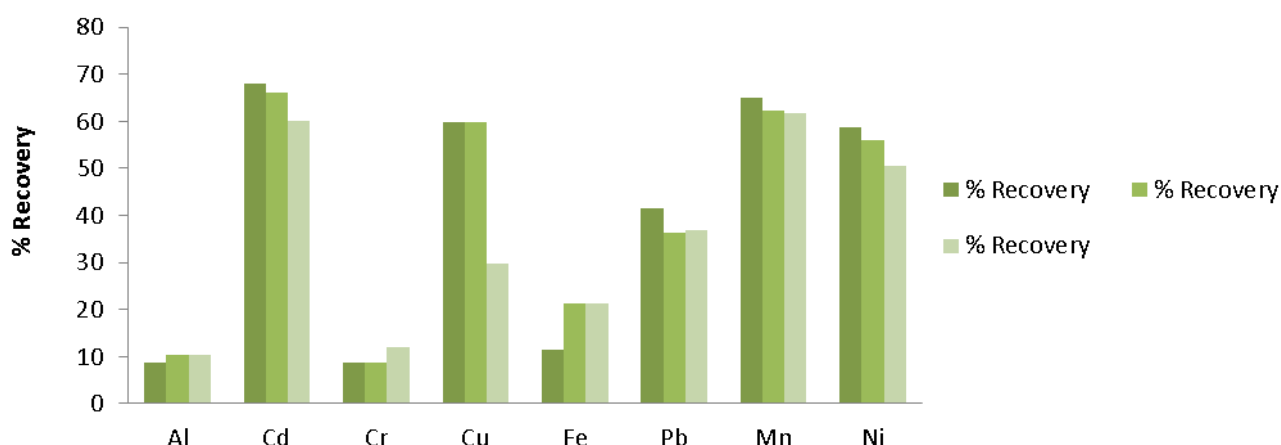


Figure 3.1.1 - % recoveries for NIOSH open vessel digestion methods.

#### Filter Sample Preparation:

Blank filters were prepared from an unused micronair particulate filter. 1" square blank filter samples were compared to 1" square filter samples spiked with SRM. Spiked filter samples were prepared by accurately weighing 10 mg of SRM 1648a onto a blank 1" square filter

The blank & spiked filter samples were placed in 100 ml beakers and placed in a fume hood. 5 ml of Nitric acid was added to the beakers. The beakers were covered with a watchglass and left to stand for 30 minutes in the fume hood. The beakers were then placed on a hotplate and heated at 120°C until all but 0.5 ml of solutions had evaporated off. A further 2 ml of

nitric acid was then added and the heat was increased to 150°C until all but 0.5 ml of solutions had again evaporated off. The watchglass was then removed and the beakers were washed with 10% nitric acid. The beakers were removed from the heat and allowed to cool. The residue was dissolved in 5 ml of 10% nitric acid and the solution was transferred to 25 ml volumetric flasks and made up to the mark with 10% nitric acid. All blank and spiked filter samples were prepared in triplicate.

It was observed that when using nitric acid the filter was not dissolved after the digestion but the SRM was completely dissolved. When aqua regia was used the filter was not dissolved after the digestion but the SRM was completely dissolved. However, a mixture of nitric:perchloric ensured both the filter and the SRM dissolve. The solution also effervesced. Special care must be taken nitric:perchloric samples to maintain low temperature levels because if the solution is too hot the nitric acid will evaporate off before complete oxidation of the organic sample material which can result in an explosion.

The EPA set 80-120% as an acceptable recovery level for NIST 1648a [84]. However according to The Royal Society of Chemistry an acceptable % recovery level from microwave acid digestions used universally is 80-110% [85]. Therefore all methods will be reviewed with respect to a 80-110% limit.

The recoveries shown in Table 3.1.2 are based on the certified values supplied with NIST SRM 1648a according to the following calculation: An acceptable recovery is 80-110%, shown as Equation 3.1.

Equation 3.1: %Recovery = (Actual result x 100)/Certified value

### **Discussion:**

Aluminium (8.61-10.26%), chromium (8.77-11.95%) and iron (11.47-21.40%) yield similar results. The recoveries for all three methods are significantly low for aluminium, chromium and iron. The low recoveries may be due to nitric acid's inability to digest all three analytes even when heated. These analytes do not react with concentrated nitric acid because a thick, hard to dissolve oxidation layer builds and protects the analytes against further oxidation (a process called passivation) [86]. This oxide layer prevents these analytes from further reaction [86]. The low recoveries for these analytes may also be due to the fact that these digestions were performed in an open system so some of the sample may have been lost to the environment.

Cadmium (60.06-68.16%), copper (29.81-59.86%), lead (41.64-36.97%), manganese (62.19-65.09%) and nickel (50.42-58.76%), yield similar results. The three methods do not provide sufficient recoveries for these five analytes.

**Conclusion:**

The analytes that form an oxidation layer with nitric acid (Al, Cr and Fe) appear to give the lowest overall recoveries. The formation of this layer prevents further digestion of the analyte, resulting in lower extraction recoveries [86]. The low recoveries for the other analytes may be due to the fact that the digests were performed in an open system. Some of the samples may be lost to the surrounding environment.

The filters were not digested in two of the three acid digestions. Incomplete digestion of the filter sample indicates that these methods are not applicable to this field of research. The samples to be analysed using these digestion methods require complete digestion for use in a ICP-OES or GFAAS, both analytical instruments require liquid samples. The use of partially digested samples is not feasible and any filtration or centrifuging of the acid digests to remove undigested filter samples could lead to further sample loss. The % recoveries are consistent across all three acid combinations tested for each element.

**3.2 Microwave Multiwave Closed Vessel Acid Digestion:**

Atmospheric particulate matter is difficult to dissolve at atmospheric pressure. Generally the application of digestion methods at higher pressures is necessary to completely dissolve these samples. Closed vessel acid digestion is a common method for the dissolution of solid samples. Closed vessel digestion is favourable over open vessel digestion because it minimises the loss of volatile elements to the surrounding environment. It also enables digestion at high temperatures. Digestion efficiency is dependent on the method of heating, working pressure and reagents used. Microwave digestion methods have been successful in dissolving a NIST 1648 standard reference material and giving recoveries from 80-110% [79].

**Microwave closed vessel digestion**

The sample and acid mixture when using microwave digestion is heated internally by dipole rotation and ion conduction caused by an oscillating electromagnetic field which results in rapid, safe and efficient digestion. Microwave digestion vessels have an added safety

protection by monitoring pressure and temperature during the digestion process. Higher working temperatures can be attained as a result of a change in the reaction kinetics caused by the closed system. The increased reaction kinetics allows digestions to be completed in a shorter time period. The temperature influences the quality of the digestion but also causes a significant increase in pressure inside the vessel. The pressure build-up in closed system acid digestion occurs as a consequence of the vapour pressure of the acid mixture, the operating temperature and the likely formation of gases such as CO<sub>2</sub> released during the digestion of organic samples [74].

Microwave assisted digestions are useful in cases where liquid samples are required e.g. ICP-OES and GFAAS. There is a higher probability of contamination with open vessel extraction methods and they generally take longer. There is also a lower reagent and sample usage, reduced loss of volatile species, better operational safety and more reproducible results with the multiwave microwave compared to other conventional methods. It is possible to reach higher temperatures with closed vessels due to increased pressure and temperature control [87]. This temperature control option also makes inter laboratory comparisons of results possible. Complete digestion can be achieved in a short operation time. Microwaves can pass through the PTFE vessels allowing rapid heating of sample and reagents. Reagents which condense on the vessel wall return to the sample causing a reflux inside the vessel. The optimum oxidising power of the digestion mixture is obtained during this process. Samples are efficiently digested with low contamination levels [88]

Cleaning of digest vessels is essential between digests. Background contaminates are generally due to contamination of the vessel containers or a memory effect left on containers from previous digestions. For this reason a cleaning run is carried out between analyses. The reagents used for the cleaning run are 4 ml of nitric acid and 4 ml of deionised water, using the microwave operation settings shown in Table 3.2.1.

Table 3.2.1: Microwave cleaning method:

Power (W)	Ramp (mins)	Time (mins)	Fan
1200	5	15	1
500	5	10	1
0		15	3

Very small amounts of airborne particulate can be collected on filters and for this reason a highly sensitive, accurate analytical method is necessary [88]. Microwave digestion reagents need to be selected so they completely digest the samples but also so elements are stable in

solution [89]. The use of HCl, HClO<sub>4</sub> and H<sub>2</sub>SO<sub>4</sub> are generally avoided because they introduce interfering species which affect ICP analysis [87].

The Investigation of different Microwave digestion methods on % recoveries: Filter samples: 1" square blank filter samples were compared to 1" square filter samples spiked with SRM. The efficiency of the extraction methods were evaluated using a NIST urban particulate matter standard reference material 1648a. The analytes tested were Al, Cd, Cr, Cu, Fe, Mn, Ni, Pb and Zn. (All glassware was soaked in a HNO<sub>3</sub>:H<sub>2</sub>O (10%:90%) wash bath overnight and then soaked in a deionised H<sub>2</sub>O bath for one hour)

### Microwave Methods with Various Power Settings

Microwave digestion Method 1 was used initially to digest the filters spiked with NIST SRM 1968a. The acid combination used was 6ml HNO<sub>3</sub>, 2 mL HF and 1 mL HCl and operation settings are outlined in Table 3.2.2.

Table 3.2.2: Microwave digestion Method 1

Power (W)	Ramp (mins)	Time (mins)	Fan
1400	10.00	30	1
0		15	3

Microwave digestion Method 1, 2 and 3: Microwave digestion Method 1 is an instrument pre-set microwave method shown in Table 3.2.2 designed for the digestion of filter samples. Sandroni *et al.*, [90] suggested that a gradual increase in power yields the most efficient results. Method 1 was therefore modified to include extra power steps: Method 2 shown in Table 3.2.3 and Method 3 shown in Table 3.2.4.

Microwave digestion Method 2: The pre-set microwave was modified to include an extra heating step outlined in Table 3.2.3 using the same acid combination and concentration:

Table 3.2.3: Microwave digestion Method 2

Power (W)	Ramp (mins)	Time (mins)	Fan
700	5.00	15	1
1400	5.00	15	1
0		15	3

Microwave digestion Method 3: The pre-set microwave was modified to include two extra heating steps outlined in Table 3.2.4 using the same acid combination and concentration.

Table 3.2.4: Microwave digestion Method 3

Power (W)	Ramp (mins)	Time (mins)	Fan
500	5.00	10	1
1000	5.00	10	1
1400	5.00	10	1
0		15	3

Microwave Method 4 and 5: Zhou *et al.*, [91] suggested that 15 minutes is sufficient time for complete digestion and Robache *et al.*, [86]. suggested that digestion times beyond 11 minutes lead to vessel leakage. However Link *et al.*, [88] suggested that the higher the working pressure employed then the quicker and more efficient the digestion procedure. Method 1 was modified to hold the highest power step for longer periods to test the effect of digestion times on sample recovery.

Microwave Method 4 is a modification of microwave Method 1 modified to hold the initial step at 1400 W for 40 minutes and is outlined in Table 3.2.5. It uses the same acid combination and concentration.

Table 3.2.5: Microwave digestion Method 4

Power (W)	Ramp (mins)	Time (mins)	Fan
1400	10	40	1
0		15	3

Microwave Method 5: The microwave method was modified to hold the initial step at 1400W for 50 minutes outlined in Table 3.2.6 using the same acid combination and concentration.

Table 3.2.6: Microwave digestion Method 5

Power (W)	Ramp (mins)	Time (mins)	Fan
1400	10.00	50	1
0		15	3



Method 6 & 7: Sandroni *et al.*, investigated two different programmes which yield optimum recoveries. Firstly a microwave program with a maximum power of 650 W and secondly a microwave program with a maximum power of 1000 W. Method 1 was therefore modified to create Method 6 (maximum power 650 W) and Method 7 (maximum power 1000 W).

#### Microwave Method 6

The microwave method was modified to include two heating steps at lower power shown in Table 3.2.7, with the maximum power being 650W.

Table 3.2.7: Microwave digestion Method 6

Power (W)	Ramp (mins)	Time (mins)	Fan
325	5.00	15	1
650	5.00	30	1
0		10	3

Microwave Method 7: The microwave method was modified to include three heating steps at lower powers shown in Table 3.2.8, with the maximum power being 1000 W.

Table 3.2.8: Microwave digestion Method 7

Power (W)	Ramp (mins)	Time (mins)	Fan
325	5.00	15	1
650	5.00	15	1
1000	5.00	30	1
0		10	3

#### Result for Microwave Methods 1 to 7:

ICP-OES analysis was used to analyse the digests, from methods 1 to 7, of SRM impregnated standard particle filters, the results are shown in Figure 3.2.1 to Figure 3.2.9.

**Aluminium:** The percentage recovery levels for aluminium are low for all of the seven methods tested, as shown in Figure 3.2.1. The maximum recovery was 58.88% for Method 7 a three step, 60 minute method with a maximum power of 1000 W and the minimum was 21.41% for Method 2, a two-step, 30 minute method with a maximum power of 1400 W. Adjusting the heat settings and run times does not have a significant effect on aluminium extraction recoveries.

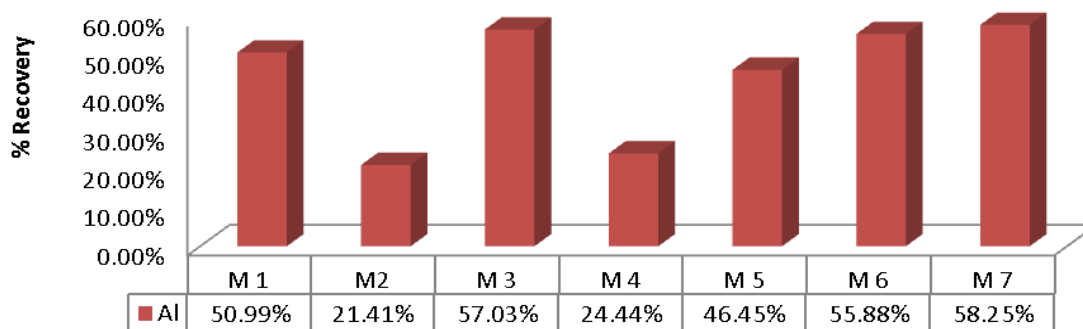


Figure 3.2.1 - Comparison of aluminium % recoveries for modified closed vessel microwave digestions Methods 1 to 7.

**Cadmium:** The percentage recovery levels for cadmium are within an acceptable range for Methods 1, 3, 4 and 5, shown in Figure 3.2.2. The maximum recovery was 105.28% for Method 5 a one step, 50 minute method with a maximum power of 1400 W and the minimum was 58.03% for Method 6 a two-step, 45 minute method with a maximum power of 650 W. More aggressive heating methods (e.g. Method 1, 3, 4, and 5) yield significantly greater % recoveries than the less aggressive methods.

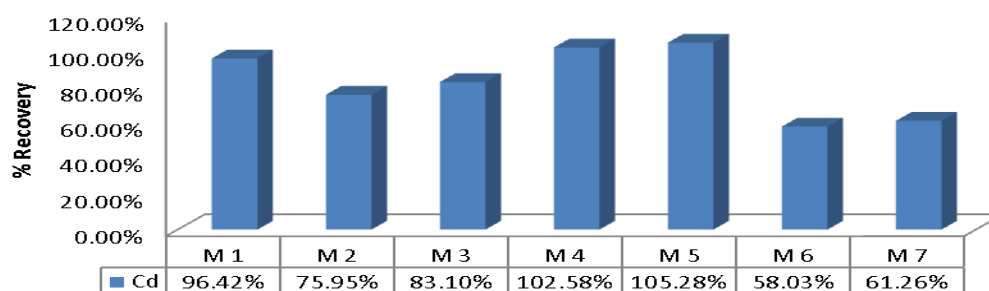


Figure 3.2.2 - Comparison of cadmium % recoveries for modified closed vessel microwave digestions Methods 1 to 7.

**Chromium:** The percentage recovery level for chromium is within an acceptable level for Method 3 only, shown in Figure 3.2.3. The maximum recovery was 91.39% for Method 3, a three step, 30 minute method with a maximum power of 1400 W and the minimum was 65.01% for Method 2 a two-step, 30 minute method with a maximum power of 1400 W. This indicates that chromium extraction recoveries are significantly improved using a high power method but a gradual increase to this power is necessary.

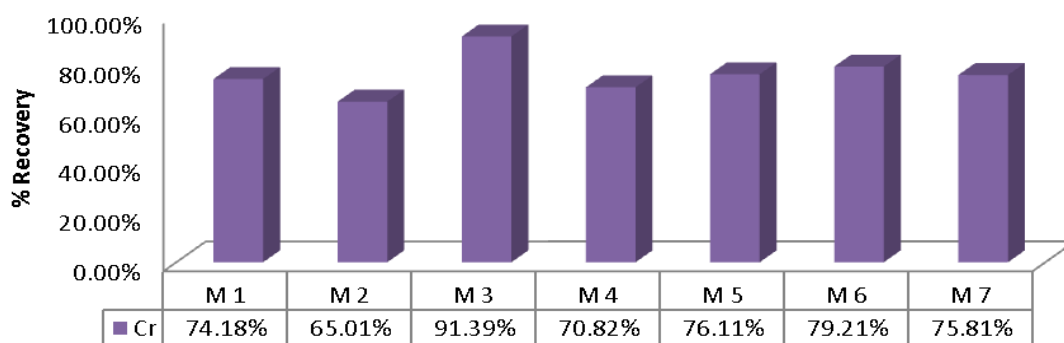


Figure 3.2.3 - Comparison of chromium % recoveries for modified closed vessel microwave digestions Methods 1 to 7.

**Copper:** The percentage recovery levels for Copper are within an acceptable range for Method 1, 2 & 3, shown in Figure 3.2.4. The recoveries for Methods 1, 2 and 3 are relatively consistent. The maximum recovery was 85.53% for Method 1 a one step, 30 minute method with a maximum power of 1400 W and the minimum was 61.58% for Method 4 a one step, 40 minute method with a maximum power of 1400 W. This indicates that copper extractions increase with more aggressive methods to a point. The recoveries decrease for Methods 4 and 5 indicating that heating the sample at a higher power for longer periods of time results in the loss of copper samples.

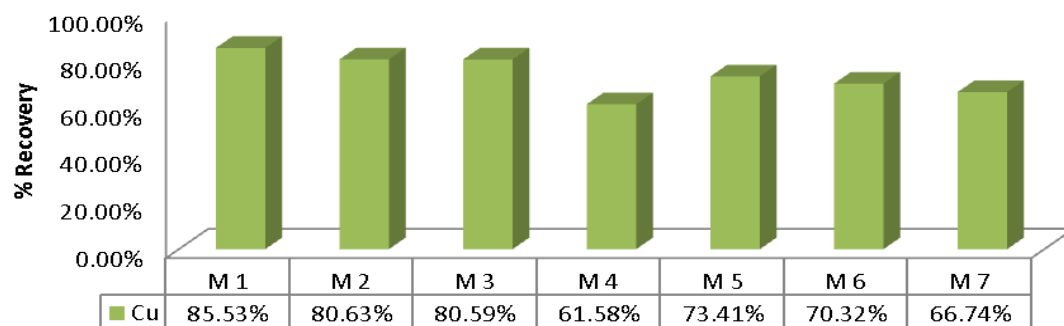


Figure 3.2.4 - Comparison of copper % recoveries for modified closed vessel microwave digestions methods 1 to 7.

**Iron:** The % recovery concentrations for iron are within an acceptable range for Method 1, 3 & 5, shown in Figure 3.2.5. The maximum recovery was 93.23% for Method 1 a one step, 30 minute method with a maximum power of 1400 W and the minimum was 68.26 % for Method 4 a one step, 40 minute method with a maximum power of 1400 W. This indicates that like copper iron extractions increase with more aggressive methods to a point. The recoveries decrease for Methods 4 and 5 indicating that heating the sample at a higher power for longer periods of time results in the loss of iron from samples.

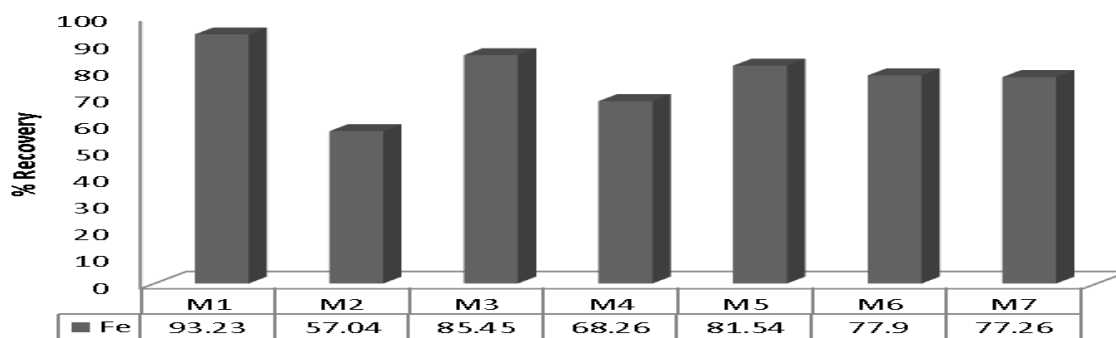


Figure 3.2.5 - Comparison of iron % recoveries for modified closed vessel microwave digestions Methods 1 to 7.

**Lead:** The percentage recovery levels for lead are within an acceptable range for Method 1, 3 & 5, shown in Figure 3.2.6. The maximum recovery was 92.85% for Method 1 a one step, 30 minute method with a maximum power of 1400 W and the minimum was 61.52 % for Method 2 a two-step, 30 minute method with a maximum power of 1400 W. This indicates that, like copper and iron, lead extractions increase with more aggressive methods to a point. The recoveries decrease for Methods 4 and 5 indicating that heating the sample at a higher power for longer periods of time results in the loss of lead from the SRM samples.

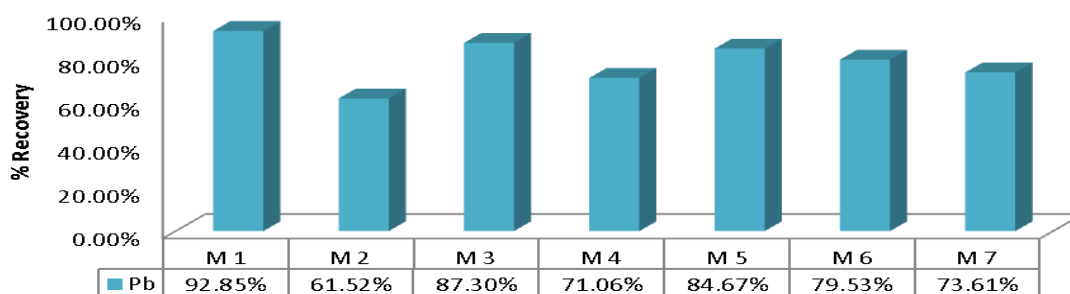


Figure 3.2.6 - Comparison of lead % recoveries for modified closed vessel microwave digestions Methods 1 to 7.

**Manganese:** The percentage recovery levels for manganese shown in Figure 3.2.7 are within an acceptable range for Methods 2, 3, 5 & 6, shown in Figure 3.2.7. However, the recoveries for all methods are relatively consistent. The maximum recovery was 84.47% for Method 5 a one step, 50 minute method with a maximum power of 1400 W and the minimum was 72.52% for Method 4, a one step, 40 minute method with a maximum power of 1400 W.

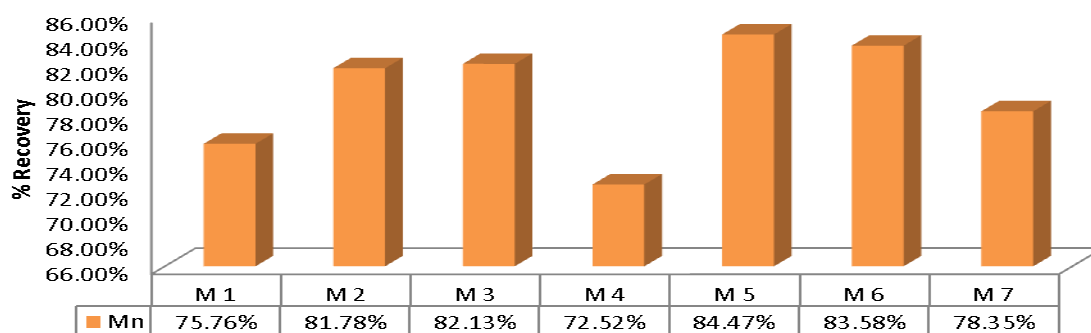


Figure 3.2.7 - A comparison of manganese % recoveries for modified closed vessel microwave digestions Methods 1 to 7.

**Nickel:** The percentage recovery for nickel shown in Figure 3.2.8 are within an acceptable range for Methods 2 & 3, shown in Figure 3.2.8. The maximum recovery was 88.52% for Method 3, a three step, 30 minute method with a maximum power of 1400 W and the minimum was 40.4% for Method 5 a one step, 50 minute method with a maximum power of 1400 W. This indicates that nickel extractions increase with the use of an aggressive method (e.g. continuous max power 1400 W) however a gradual increase to this power is necessary for optimum results.

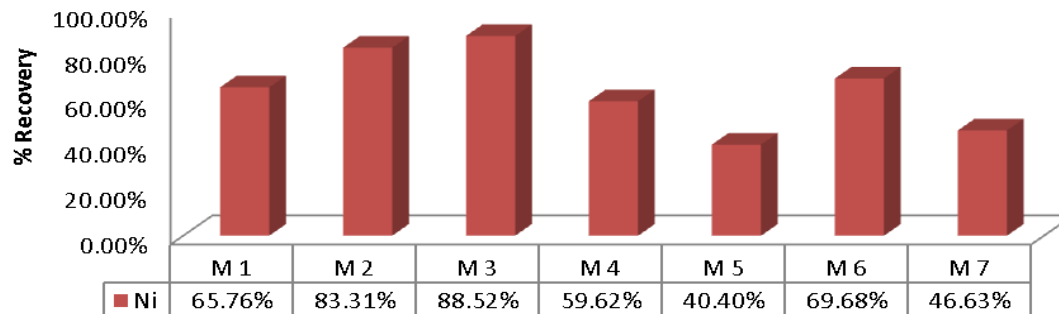


Figure 3.2.8 - Comparison of nickel % recoveries for modified closed vessel microwave digestions methods 1 to 7.

**Zinc:** The percentage recoveries for zinc are within an acceptable range for all methods except 6 & 7, shown in Figure 3.2.9. The maximum recovery was 95.64% for Method 1, a one step, 30 minute method with a maximum power of 1400 W and the minimum was 65.92% for Method 6 a two-step, 45 minute method with a maximum power of 650 W. This indicates that zinc recoveries are optimised by the use of an aggressive method to a point. The recoveries decrease for methods 4 and 5 indicating that heating the sample at a higher power for longer periods of time results in the loss of zinc from the SRM samples through venting.

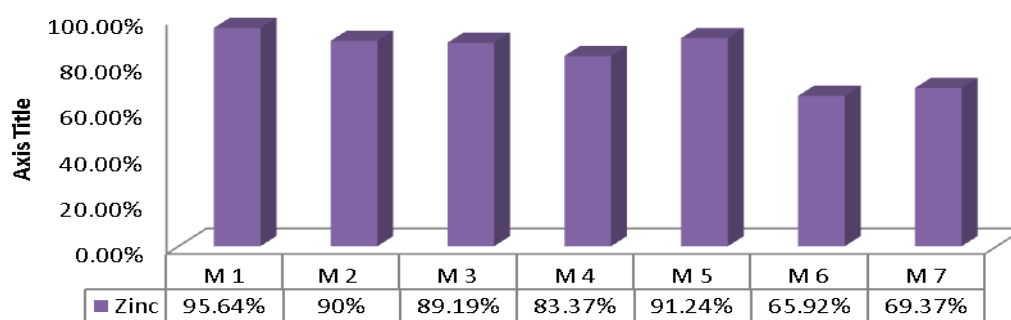


Figure 3.2.9 - Comparison of zinc % recoveries for modified closed vessel microwave digestions methods 1 to 7.

**Conclusion:** Method three gives optimum recoveries for 8 of the 9 analytes analysed with the highest efficiency having an average % recovery of 82.41%, shown in Table 3.2.9.

Table 3.2.9 – Average % recoveries for all analytes for Methods 1 to 7.

	M1	M2	M3	M 4	M5	M6	M 7
Average	81.15	68.57	82.41	68.25	75.95	71.12	66.92

### Digestion Methods 8 & 9

When digestions are carried out and samples are removed from digestion vessels a considerable amount of vapour is observed when the vessels are opened. For Methods 8 & 9 samples were left to sit in digestion vessels for an hour after digestion to see if letting sample vapours settle would result in higher sample recoveries the results of which are detailed below in Figures 3.2.10 to 3.2.18. Method 8 is a re-run of Method 3, a three step, 30 minute method with a maximum power of 1400 W and Method 9, is a re-run of Method 5 a one step, 50 minute method with a maximum power of 1400 W with the samples being allowed to sit for an hour after digestion.

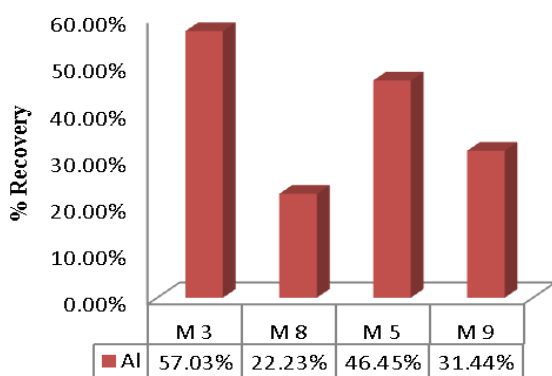


Figure 3.2.10 Comparison of % recoveries of Al with modified cool down times for methods 3 and 5

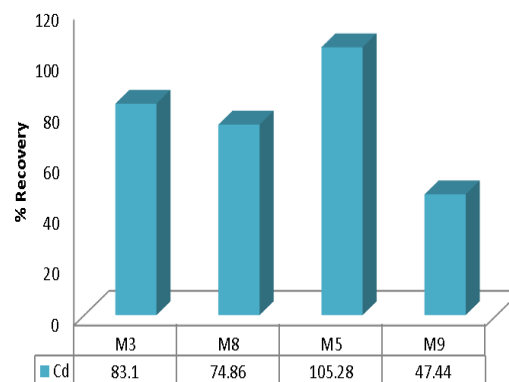


Figure 3.2.11 Comparison of % recoveries of Cd with modified cool down times for methods 3 and 5

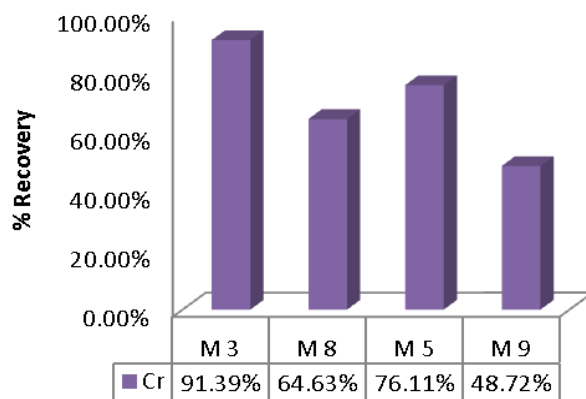


Figure 3.2.12 Comparison of % recoveries of Cr with modified cool down times for methods 3 and 5

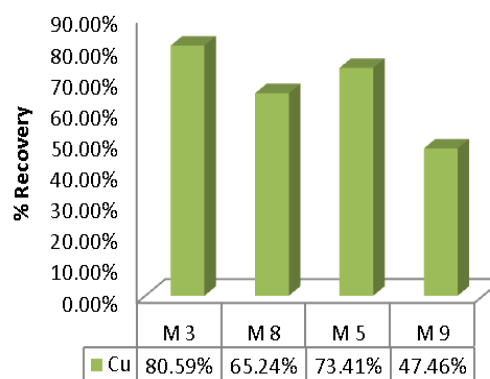


Figure 3.2.13 Comparison of % recoveries of Cu with modified cool down times for methods 3 and 5

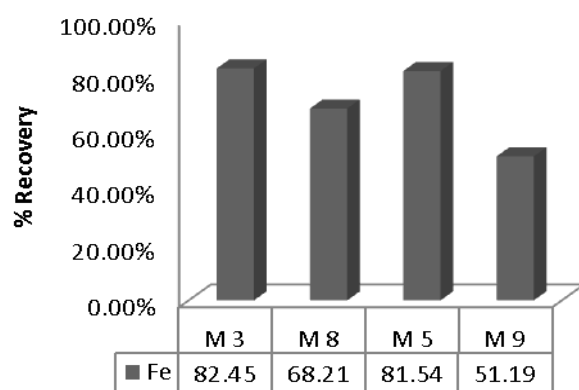


Figure 3.2.14 Comparison of % recoveries of Fe with modified cool down times for methods 3 and 5

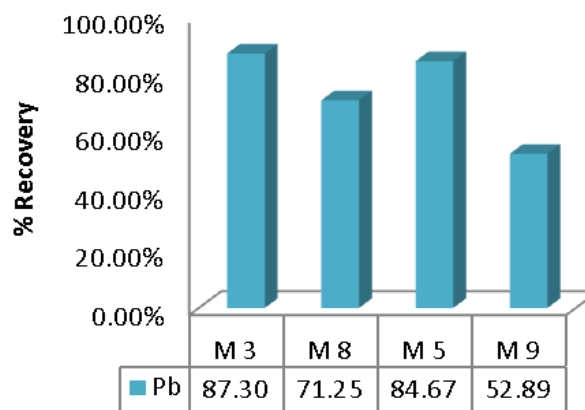


Figure 3.2.15 Comparison of % recoveries of Pb with modified cool down times for methods 3 and 5

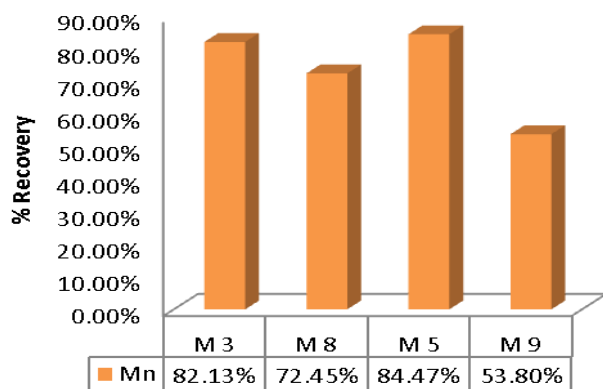


Figure 3.2.16 Comparison of % recoveries of Mn with modified cool down times for methods 3 and 5

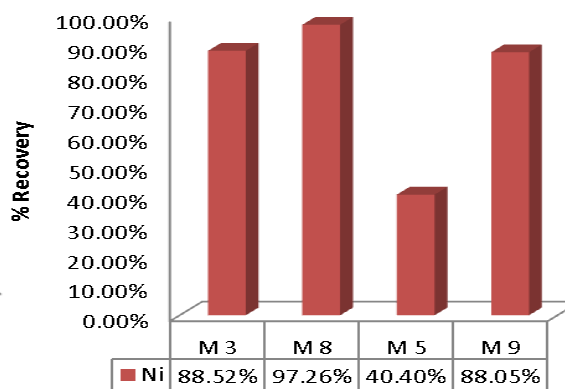


Figure 3.2.17 Comparison of % recoveries of Ni with modified cool down times for methods 3 and 5

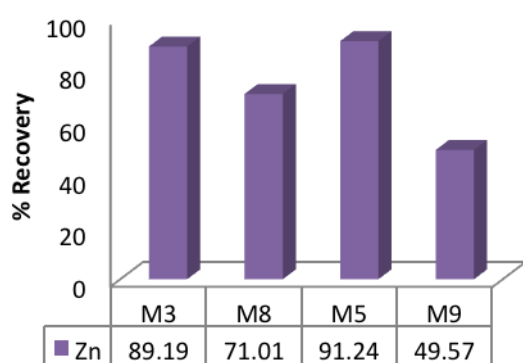


Figure 3.2.18 Comparison of % recoveries of Zn with modified cool down times for methods 3 and 5

**Conclusion:** The addition of a cool down step does not have a positive effect on the % recovery of aluminium, cadmium, chromium, copper, iron, lead, manganese or zinc as shown in Figures 3.2.10-3.2.16 & 3.2.18. The % recoveries of these elements decreased with the addition of the cool down step, this may be due to leakage from the microwave vessel while it was left to cool for one hour. However, the use of digestion Method 5 with an extended cool down period significantly improved the recovery of nickel, shown in Figures 3.2.17. However the extraction recoveries for nickel are still higher and are within an acceptable range using heating Method 3 without a cool down period.

**Microwave Digestion Method 10:** A un-programmed drop in power is observed while running method three, during the final step. While at 1400 W the power drops to 0 W for 5 minutes, shown by the dark blue line in Figure 3.2.19. Method 3 was modified to run the last step for 5 minutes instead of 10 minutes to investigate if the sample is still being digested during the final five minutes of the run.



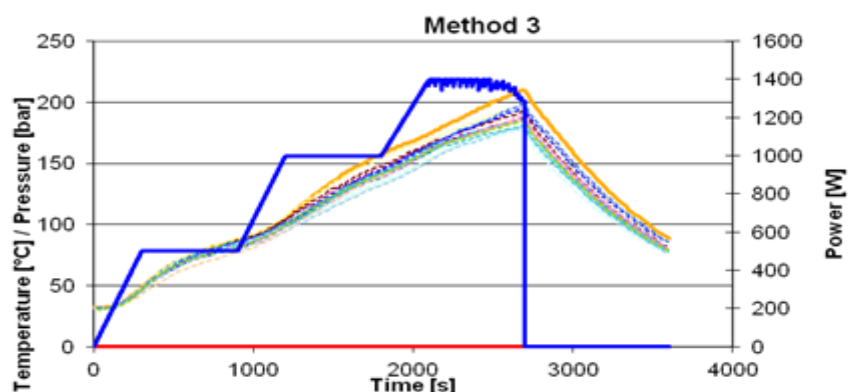


Figure 3.2.19 – Method 3 shown power drop off during the final step, at 25 minutes, for 5 minutes.

Table 3.2.10: Microwave digestion Method 10

Power (W)	Ramp (mins)	Time (mins)	Fan
500	5.00	10	1
1000	5.00	10	1
1400	5.00	5	1
0		15	3

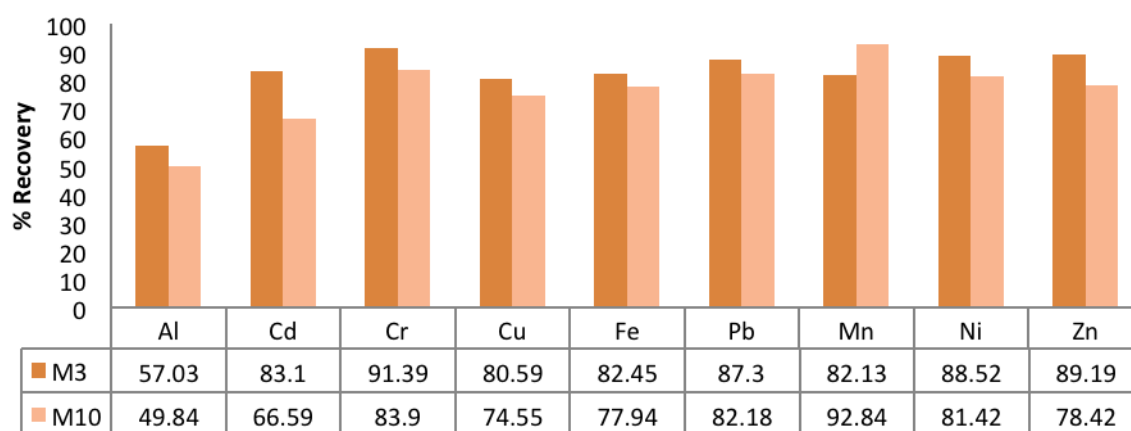


Figure 3.2.20 – Comparison of SRM analytes % recoveries between Method 3 & 10.

**Conclusion:** For all analytes except manganese the extraction recovery for Method 3 is higher than for Method 10 indicating that digestion is still occurring during the 5 minutes at the end of the run when the drop in power occurs, shown in Figure 3.2.20.

**Microwave Digestion Method 11:** Method three was modified to investigate if starting the run at a higher power and decreasing the power in steps during the run as opposed to starting

at a low power and increasing the power to a maximum in steps (as in Method 3) would lead to more efficient digestions with higher recoveries. Method 11 is outlined in Table 3.2.11.

Table 3.2.11: Microwave digestion Method 11

Power (W)	Ramp (mins)	Time (mins)	Fan
1400	5.00	10	1
1000	5.00	10	1
500	5.00	10	1
0		15	3

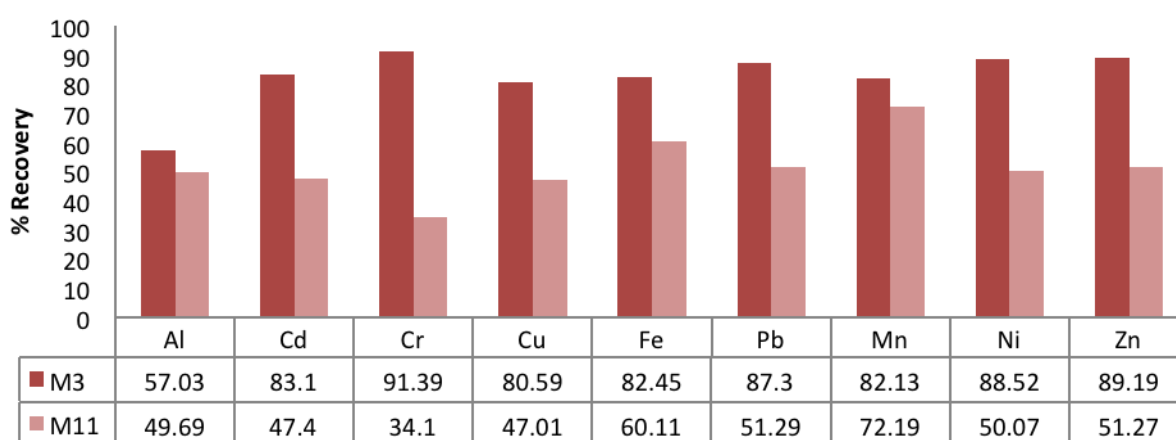


Figure 3.2.21 – Comparison of SRM analyte % recoveries between Method 3 & 11.

**Conclusion:** For all analytes the extraction percentage recovery for Method 3 is higher than for Method 11 indicating that a gradual increase in power during digestion leads to more efficient digestion than a gradual decrease in power during the course of a digestion, shown in Figure 3.2.21. The % recoveries for aluminium and manganese for both methods are comparable but for all other analytes the % recoveries for Method 3 are almost double those of Method 11.

### 3.3. Reproducibility of an analytical method:

An analytical method should only be used if it is reproducible. Therefore microwave Method 3, with the acid combination 6ml HNO<sub>3</sub>, 2 ml HF and 1 ml HCl was run 3 times and the results compared for reproducibility, shown in Table 3.3.1. The standard deviation between replicates, shown in 6, are significantly low and indicate that there is no significant difference between replicates.

Table 3.3.1: Percentage Recoveries of Method 3 SRM.

Analytes	Run 1	Run 2	Run 3	Average	St Dev
	% Recovery				
Aluminium	64.47	57.64	48.99	57.1	7.7
Cadmium	82.82	91.95	74.53	83.1	8.7
Chromium	94.9	93.44	85.84	91.3	4.9
Copper	80.14	81.27	80.37	80.5	0.6
Iron	84.22	85.3	77.84	82.4	4
Lead	88.42	89.202	84.28	87.3	2.6
Manganese	90.62	82.1	73.66	82.1	8.5
Nickel	91.22	90.81	83.51	88.5	4.3
Zinc	85.69	86.63	78.32	83.5	4.5

### 3.4 The effect of acid concentration on Acid Digestion Recoveries:

Method 3 (Table 3.2.4) has been established as the optimum settings for closed vessel microwave acid digestion using a Microwave Multiwave 3000, demonstrated in section 3.2. An acid combination of 6ml HNO<sub>3</sub>, 2 ml HF and 1 ml HCl was used during the optimisation process. In section 3.4 the use of alternative acid combinations will be reviewed to determine the optimum acid combination for acid digestions of particle filters.

#### Microwave Digestion Method 3, Acid combination 1, Method 12: The use of Hydrogen peroxide

Method 3 (Table 3.2.4) was used to investigate the following acid combination 1 ml HCl, 1 ml H<sub>2</sub>O<sub>2</sub>, 2 ml HF and 5 ml HNO<sub>3</sub>. This acid combination was analysed to determine the effect of the addition of H<sub>2</sub>O<sub>2</sub>.

Karthikeyan *et al.*, [93] suggested the use of a HNO<sub>3</sub>:H<sub>2</sub>O<sub>2</sub> combination because it reduces matrix effects and both are strong oxidising agents.

The use of hydrogen peroxide decreased the recoveries of all elements except aluminium, shown in Figure 3.4.1. Pekney *et al.*, [87] suggested that the use of hydrogen peroxide reduces the concentration of NO fumes from nitric acid; this reduction in fumes may have caused the increase in aluminium levels by decreasing the oxidation effect of nitric acid on aluminium recovery. However, using H<sub>2</sub>O<sub>2</sub> presents a risk of Al, Fe, and Zn contamination.

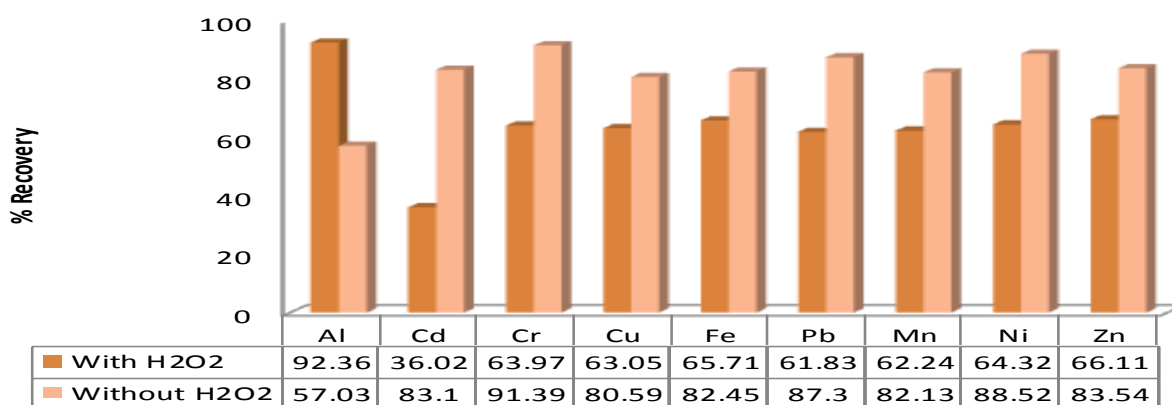


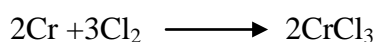
Figure 3.4.1 – % recoveries of elements using 1 ml hydrogen peroxide in the acid combination, HCl, H<sub>2</sub>O<sub>2</sub>, HF and HNO<sub>3</sub>.

### Microwave Digestion Method 3, Acid combination 2, Method 13: The use of Hydrochloric acid

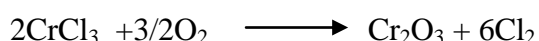
Method 3 (Table 3.2.4) using a different acid combinations of (A), 1 ml HCl, 2 ml HF and 6ml HNO<sub>3</sub>, (B) 0.5 ml HCl, 2 ml HF and 6ml HNO<sub>3</sub> and (C) 0 ml HCl, 2 ml HF and 6ml HNO<sub>3</sub>, shown in Table 3.4.1.

Karthikeyan *et al.*, [93] suggest avoiding the use of HCl, HClO<sub>4</sub> and H<sub>2</sub>SO<sub>4</sub> because they introduce interfering species which affect ICP analysis.

Wang *et al.*, [89] examined the recovery levels of sixteen analytes using an urban particulate matter standard reference material. They investigated using an acid mixture of HNO<sub>3</sub>-HClO<sub>4</sub>-HF in closed vessels. Elements can be lost because of the pressure relief mechanism in vessels during digestion. The formation of certain compounds during the digestion step can also lead to sample loss e.g. CrO<sub>2</sub> is formed when chloride species are present and can result in the loss of Cr, shown in Equation 3.4.1 and 3.4.2. This is avoided by decreasing the amounts of problematic reagents used. [94]



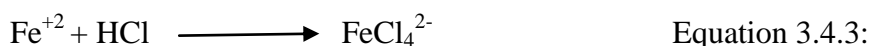
Equation 3.4.1:



Equation 3.4.2:

Link *et al.*, [89] suggested that the use of HCl should be avoided because of its effect on detection methods e.g. GFAAS and ICP. This is recommended to avoid the production of volatile species. The addition of HCl increases the pressure in the vessel during digestion. HCl addition also results in the formation of additional species (Cl<sub>2</sub> and NO). The gas bi-products increase the pressure and reactivity of the digestion reagents. A mixture of acid

reagents in digestion also results in higher pressure as a result of the acid themselves heating. Acids need to be added in concentrated forms, mixing the  $\text{HNO}_3$  and  $\text{HCl}$  before digestions results in the formation of gases e.g. chlorine gas and these gases may be violently released when heated. Therefore, the presence of  $\text{HCl}$  reduces a methods effectiveness for the extraction of certain analytes. e.g. iron extraction: in the presence of  $\text{Cl}^-$  results in  $\text{Fe(II)}$  forming a  $\text{FeCl}_4^{2-}$  anion, shown by equation 3.4.3.



Yang *et al.*, stated that the use of  $\text{HCl}$  and  $\text{H}_2\text{SO}_4$  should be avoided because they increase  $\text{Cl}$  and  $\text{S}$  into the ICP system. [95] The presence of  $\text{S}$  in the solution affects the recovery of  $\text{Se}$  by producing  $\text{SO}_3$  in the plasma. Arsenic recoveries are affected by the presence of  $\text{ArCl}$ .

Table 3.4.1: Reagents used to optimise Method 3.

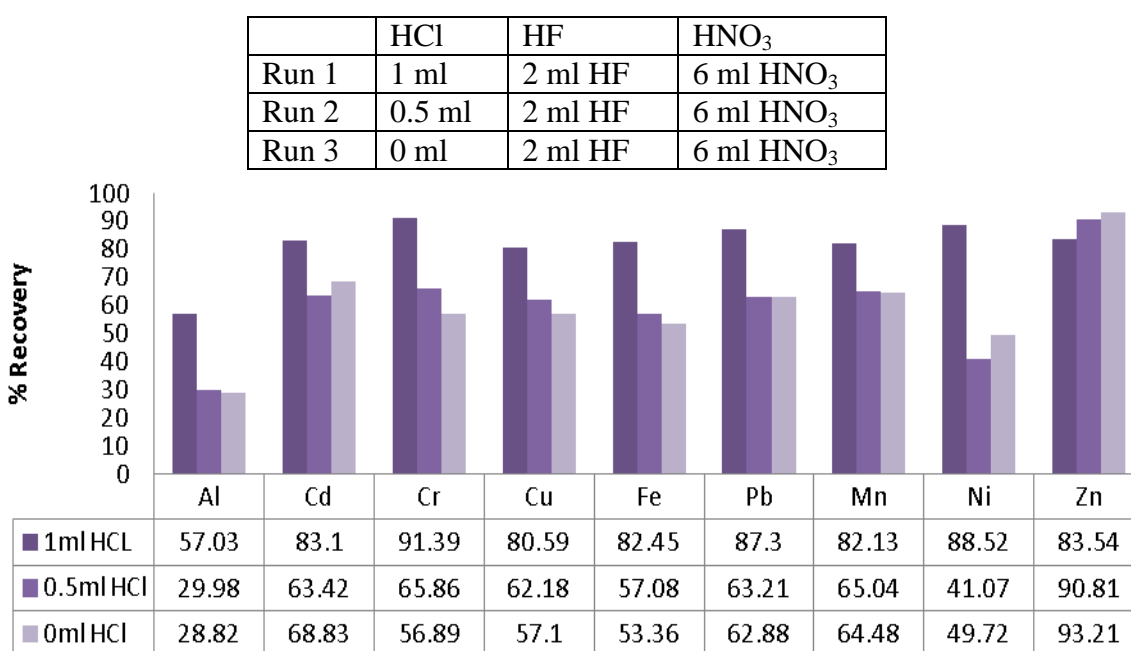
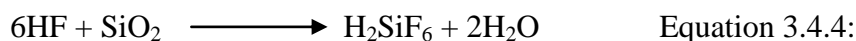


Figure 3.4.2 – % recoveries of elements when altering the concentration of hydrochloric acid in the acid combination, using 1 ml, 0.5 ml and 0 ml of hydrochloric acid.

The reduction in  $\text{HCl}$  concentrations has an adverse effect on all % recoveries of analytes except zinc. The increase in zinc concentrations due to the addition of  $\text{HCl}$  is ~10%, shown in Figure 3.4.2. a significant increase but due to the decreases observed for the other analytes tested the use of  $\text{HCl}$  is advised.

**Microwave Digestion Method 3, Acid combinations 3 & 4, Method 13 and 14: The use of hydrofluoric acid and boric acid.**

Karanasiou *et al.*, [96] suggested that HF is needed in digestion to dissolve silicate shown in equation 3.2.4. This allows for better recoveries of certain analytes e.g. Cr and Ni. More rigorous digestion methods need to be used for the digestion of Cr and V.



Pekney *et al.*, [87] digested a standard reference material, NIST 1648 Urban Dust, using HNO<sub>3</sub>, HF and H<sub>2</sub>O<sub>2</sub>. They found that HNO<sub>3</sub> is effective in digestion of most elements but is unsuccessful in the digestion of siliceous material. Therefore, HF must be used for digestion of siliceous material. Samples were run with and without HF to test recoveries. A batch of seven samples were tested with three having HF and four without HF. Recoveries of K, Ti, Cr, Rb, Sb, Cs and Ba were improved with the addition of HF. The recovery of Mg decreased with the addition of HF. Results showed that trace amounts of HF are needed for complete digestion. Analysis results were within 15% of certified values except for Na, Al, Cr and Cs. The recoveries of aluminium are lower in the absence of HF. HF is required for the destruction of aluminosilicates (minerals composed of aluminium, silicon, and oxygen) in soil and sediment samples.

Pekney *et al.*, [87] found that using a small amount of HF can eliminate the need to use H<sub>3</sub>BO<sub>3</sub>, therefore, eliminating B interferences. Boric acid is used to complex HF at higher concentration to reduce potential damage to the ICP.

Kulkarni *et al.*, investigated using HNO<sub>3</sub>, HF and H<sub>3</sub>BO<sub>3</sub> using an urban particulate matter standard reference material NIST 1648 [97]. A two stage method was tested using HNO<sub>3</sub> and HF in the first stage and H<sub>3</sub>BO<sub>3</sub> in the second stage. H<sub>3</sub>BO<sub>3</sub> is used to re-dissolve fluoride precipitates prior to ICP analysis. Four different reagent combinations were used (I) A single stage using 3ml HNO<sub>3</sub>, (II) A single stage with 3ml HNO<sub>3</sub> and 0.3ml HF (III) a dual stage with 2.4ml HNO<sub>3</sub> and 1 ml HF in the first stage and in the second stage 8ml H<sub>3</sub>BO<sub>3</sub>. The temperature was ramped to 200°C within 20 minutes with a dwell time of 20 minutes in the first stage and the second stage had the same power settings. The use of HNO<sub>3</sub> alone did not yield recoveries within 15% of certified values. An increase in the % recoveries for some analytes using HNO<sub>3</sub> and HF was observed but the recoveries for other analytes were lowered due to the formation of fluoride precipitates. The addition of H<sub>3</sub>BO<sub>3</sub> reduced the formation of these precipitates thus yielding better % recoveries for the effected analytes. The addition of

larger amount of HF didn't increase % recoveries. The optimum recovery levels were obtained from a dual stage method with 2.4ml HNO<sub>3</sub> and 1 ml HF in the first stage and 8ml H<sub>3</sub>BO<sub>3</sub> in the second stage. The recoveries of Cr were below the expected recovery levels but there was a significant improvement when HF and H<sub>3</sub>BO<sub>3</sub> were used [96].

Wang *et al.*, [89] found the use of HF may cause significant damage to the ICP torch. The elemental analysis of particulate matter on filter membranes may be considered as difficult samples to digest because of the various matrix components involved e.g. organic compounds, oxides, silicates. The addition of HF coupled with high temperatures and pressures aid in the digestion of silicates and organic compounds. The recovery of chromium is also improved with the addition of HF however the concentrations of Cu, Mn, S, Pb & Zn remained similar with and without the addition of HF.

Robache *et al.*, [86] found that the use of hydrofluoric acid improved the % recoveries of Cr, Ni, K, Na and Ti. HNO<sub>3</sub> is effective in digestion for most elements but is unsuccessful in the digestion of siliceous material, HF must be used for these compounds. Samples were run with and without HF to test recoveries. Robache *et al.*, also used boric acid to complex HF at higher concentrations to reduce damage to the ICP.

Yang *et al.*, [95] investigated the use of a HF-HNO<sub>3</sub>-H<sub>2</sub>O<sub>2</sub>-H<sub>3</sub>BO<sub>3</sub> combination was used in analysis. The detection of most analytes is adversely affected by the presence of B and F ions. HF is used to break down silica matrices. The addition of HF improved the recovery of Cr but decreased the recoveries for Se. This decrease in Se recovery is due to the formation and volatilization of SeF<sub>6</sub>. Ideally HF needs to be removed after the digestion due to the formation of insoluble fluorides. The presence of HF can also damage the silica based sampler tube, the ICP torch and the Ni interface leading to signal drift, contamination and the eventual destruction of the torch. To avoid the adverse effects of HF a further step needs to be carried out using H<sub>3</sub>BO<sub>3</sub> which removes excess HF from the solution according to Equation 3.4.5.



The addition of H<sub>3</sub>BO<sub>3</sub> to the solution increases the amount of dissolved matter, however it can also affect the signal due to presence of boron containing species. It was found that the best acid combination was 5 ml HNO<sub>3</sub>, 4ml H<sub>2</sub>O<sub>2</sub>, 0.5 ml HF and 5 ml H<sub>3</sub>BO<sub>3</sub>.

Kulkarni *et al.*, [97] found that the addition of HF is essential to recover elements from silicate matrices.

Melaku *et al.*, [98] tested three different acid combinations HCl/HNO<sub>3</sub>, HClO<sub>4</sub>/HNO<sub>3</sub> and HF/HCl/HNO<sub>3</sub>/H<sub>3</sub>BO<sub>3</sub>. The best combination was found to be HF/HCl/HNO<sub>3</sub>/H<sub>3</sub>BO<sub>3</sub>. HF is needed to completely digest trace amounts of Al from an alumina-silicate phase. Diluting the initial digest 50 fold reduces the potential damage caused by HF. The use of HF can lead to sample loss due to the possible formation of fluoride precipitates.

### Microwave Digestion Method 3, Acid combination 3 - Method 13: Determining the optimum HF Concentration:

Digestion Method 3 (Table 3.2.4) run with a different acid combination is used 1 ml HCl, 2 ml HF and 6ml HNO<sub>3</sub>, 1 ml HCl, 1.5 ml HF and 6ml HNO<sub>3</sub>, 1 ml HCl, 1 ml HF and 6ml HNO<sub>3</sub>, 1 ml HCl, 0.5 ml HF and 6ml HNO<sub>3</sub> and 1 ml HCl, 0 ml HF and 6ml HNO<sub>3</sub>, shown in Table 3.4.3.

Table 3.4.2: Acid Combinations for HF Optimisation.

	HCl	HF	HNO <sub>3</sub>
Run 1	1 ml	2 ml	6 ml
Run 2	1 ml	1.5 ml	6 ml
Run 3	1 ml	1 ml	6 ml
Run 4	1 ml	0.5 ml	6 ml
Run 5	1 ml	0 ml	6 ml

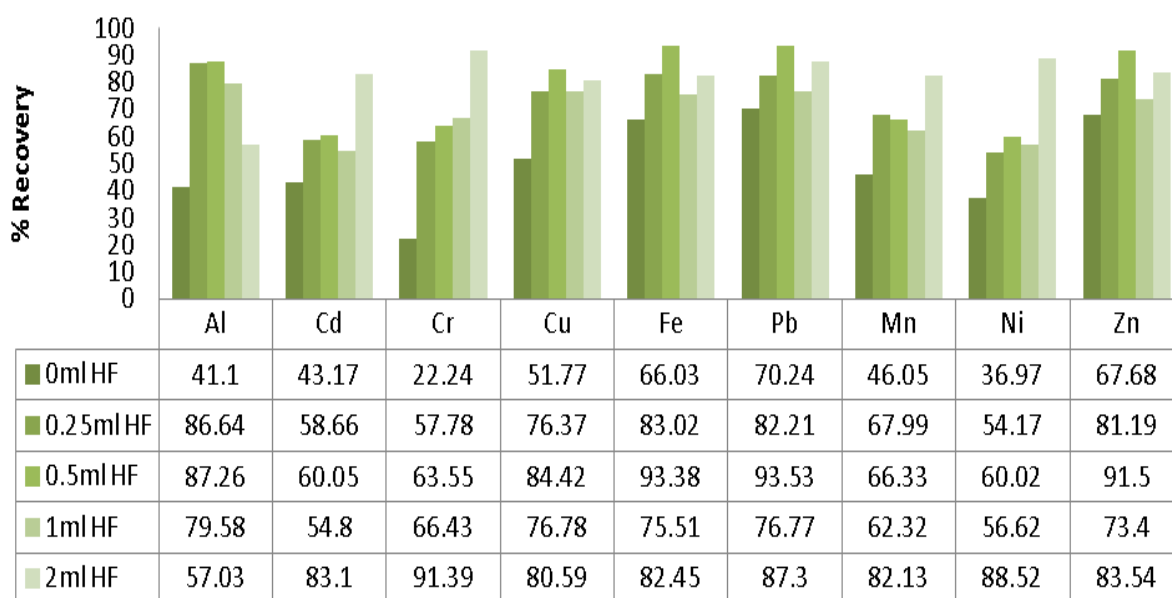


Figure 3.4.3 – % recoveries of elements when altering the quantity of hydrofluoric acid in the acid combination, using 2 ml, 1 ml, 0.5 ml, 0.25 ml and 0 ml hydrofluoric acid.



There is a decrease in the % recoveries for all analytes except aluminium with a reduction in the concentration of HF used. A small amount of HF (0.25 - 0.5 ml) results in a significant increase in percentage recovery of Al. A further increase in HF leads to a significant reduction in Al concentrations. The highest recovery for Cd, Cr, Mn and Ni are found using an acid combination with 2 ml HF. Higher % recoveries are observed for Cu, Fe and Pb using an acid combination with 0.5 ml HF but % recoveries are comparable with % recoveries using an acid combination with 2 ml HF. The % recoveries for all analytes except Al are within the acceptable recovery range for an acid combination with 2 ml HF. Therefore it is recommended that at least 2 ml of HF be used, however the use of higher concentrations of HF is not recommended due to the potential damage HF can cause to the ICP torch.

### **Microwave Digestion Method 3, Acid combination 4 - Method 14: Investigating the use of boric acid**

To investigate the effects of using boric acid a comparison was made between running acid digestion Method 3 without boric acid (0 ml  $\text{H}_3\text{BO}_3$ , 1 ml HCl, 1.5 ml HF), running acid digestion Method 3 with a concentration of boric acid matching the concentration of HF, i.e. 2 ml (2 ml  $\text{H}_3\text{BO}_3$ , 1 ml HCl, 2 ml HF and 6 ml  $\text{HNO}_3$ ) and finally running the same digest sample through acid digestion Method 3 twice, initially with 1 ml HCl, 2 ml HF and 6 ml  $\text{HNO}_3$  and then adding 2 ml  $\text{H}_3\text{BO}_3$  to the digest and running the sample through acid digestion Method 3 a second time, shown in Table 3.4.3.

Table 3.4.3: Acid Combinations for Boric Acid Optimisation.

	HCl	HF	$\text{HNO}_3$	$\text{H}_3\text{BO}_3$
Run 1	1 ml	2 ml	6 ml	0 ml
Run 2	1 ml	2 ml	6 ml	2 ml
Run 3	1 ml	2 ml	6 ml	2 ml

Aluminium is the only element that shows improved extraction recoveries with the addition of boric acid in Figure 3.4.4. The extraction recoveries for aluminium are just within the acceptable range of 80-110%. The improvement in recovery occurs with the addition of an extra  $\text{H}_3\text{BO}_3$  step. However the decrease in extraction % recoveries for the other eight analytes of interest means that this is not a viable method for urban particulate matter analysis.

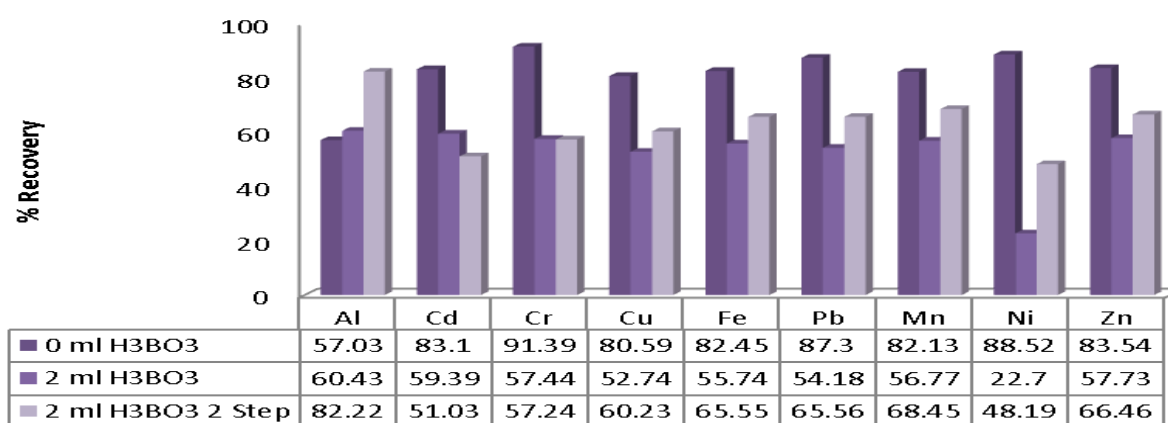


Figure 3.4.4 – % recoveries of elements when adding boric acid to the acid combination, initially running the method with boric acid added and secondly running the digestion method with the original acid combination and then re-running the digest with an additional 2 ml of boric acid.

Table 3.4.4: Shows Optimum recoveries for each analyte tested:

Method 1	Copper	85.53%	Method 3 80.59%
	Iron	93.23%	Method 3 82.45%
	Zinc	95.64%	Method 3 89.19%
	Lead	92.85%	Method 3 87.30%
Method 3	Chromium	91.39%	
	Manganese	82.13%	
	Nickel	88.52%	
Method 5	Cadmium	105.23%	M3 83.10%
Method 12	Aluminium	92.35%	

Method 3 and Method 1 yield the highest results for the majority of analytes tested. Method 3 yields the highest recoveries for Cr (91.39%), Mn (82.13%) and Ni (88.52%) and Method 1 yields the highest recoveries for Cu (85.53%), Fe (93.23%), Zn (95.64%) and Pb (92.85%). Method 1 yields higher recoveries for more analytes than Method 3, the recoveries for all analytes except Aluminium, are however within the acceptable level of 80-110% for Method 3, for Method 1 Cd, Cu, Fe, Pb and Zn are the only analytes with the acceptable level. Aluminium is within the acceptable level of 80-110% for Method 12 but all other analytes yield recoveries below 80% using Method 12, it is therefore not a viable method. When using digestion Method 3, SRM recoveries for Al are consistently 57%, aluminium concentrations can therefore be correlated from SRM recoveries.

## **Chapter 4:**

Comparison between ICP-OES and GFAAS as a suitable detection method for Cabin Particle Filters.

## Chapter 4

### Data Comparison between ICP and GFAAS

A data comparison was made between ICP-OES and GFAAS to determine the optimum analytical method for the analysis of analytes under investigation. The calibration plots are presented below in Figures 4.1 to 4.14 for the following elements Cr, Cu, Fe, Pb, Mn, Ni and Zn, correlation coefficients and limits of detection were investigated for both analytical methods. GFAAS linearity tends to level off after 1 AU, limiting the linearity range of the calibration plot. All GFAAS calibration plots were run to the maximum linear range. All analytes examined are present in the SRM in mg/L concentrations and require dilution for analysis by ICP-OES and GFAAS, to fall within the range of the calibration plot.

**Chromium:** Note, the dynamic linear range of ICP-OES from 0 µg/L to 1 mg/L for Cr, shown in Figure 4.1 (A) as opposed to the restricted linear range of GFAAS from 0 µg/L to 50 µg/L, shown in Figure 4.1 (B).

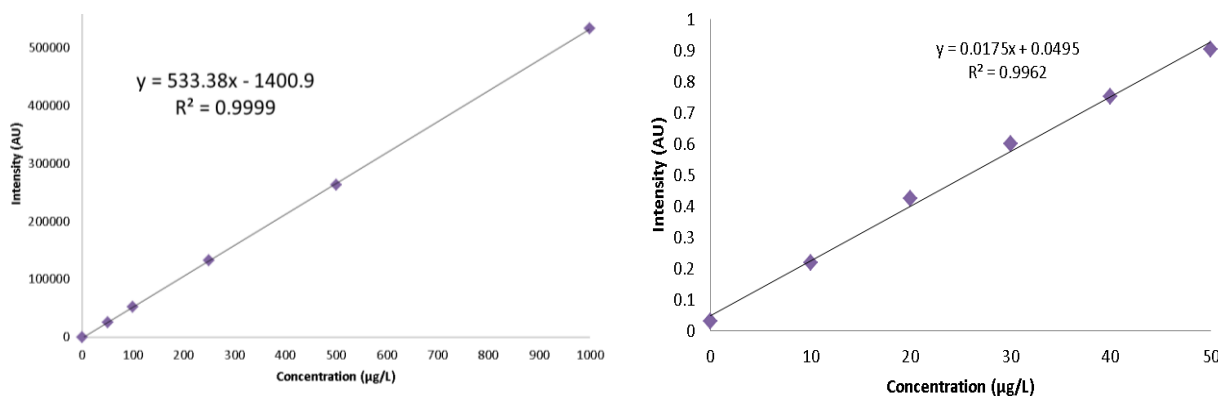


Figure 4.1 (A) – Cr ICP-OES Calibration Curve      Figure 4.1 (B) – Cr GFAAS Calibration Curve

The % recovery of SRM samples for Method 3 and 6 are shown in Figure 4.2. Method 3 and 6 were chosen for a data comparison between the two instruments. Method 3 was found to be the optimum preparation method and Method 6 was found to be the second best method of extraction. The extraction % recoveries for ICP-OES are higher for Method 3 and 6, 91.39% and 79.21%, than for GFAAS 89.9% and 72.96%, respectively, indicating that ICP-OES is the preferred analysis method.

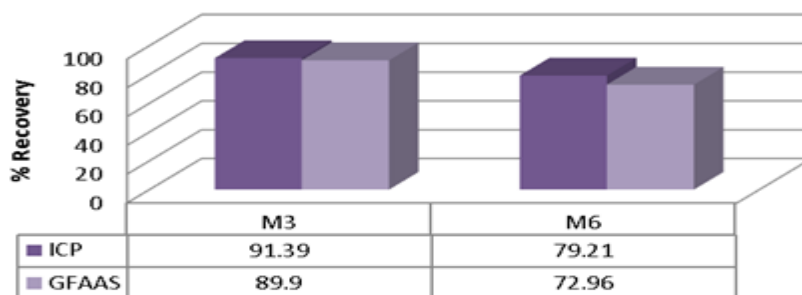


Figure 4.2 – Comparison of Cr recoveries for Method 3 and 6 using GFAAS and ICP-OES.

**Copper:** The linear range of ICP-OES is comparable to the range for Cr from 0 µg/L to 1mg/L, shown in Figure 4.3 (A), the linear range of GFAAS is also comparable to Cr from 0 µg/L to 50 µg/L, shown in Figure 4.3 (B).

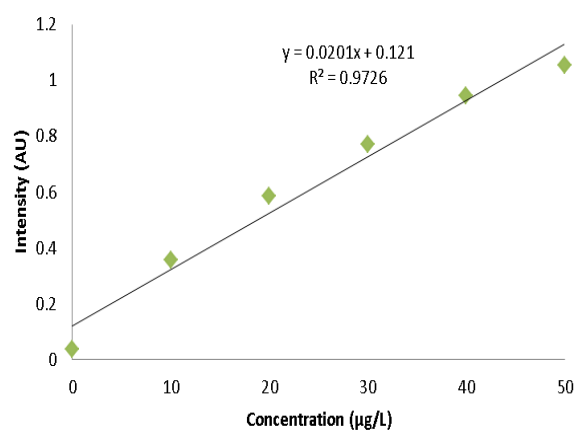
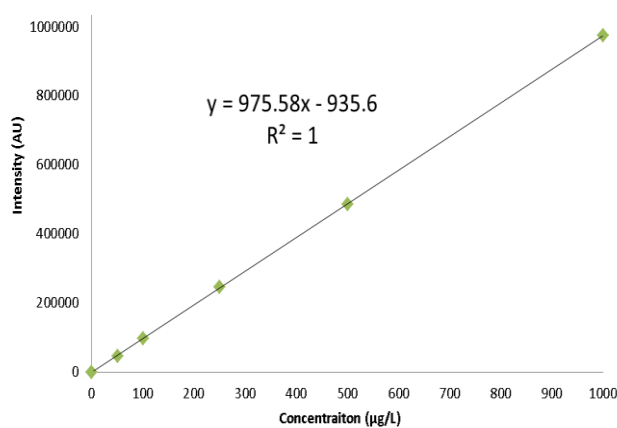


Figure 4.3 (A) – Cu ICP-OES Calibration Curve      Figure 4.3 (B) – Cu GFAAS Calibration Curve

Methods 3 and 6 were chosen for a data comparison between the two analytical methods, shown in Figure 4.4. The extraction % recoveries for ICP-OES are higher (~double) for Method 3 and 6 80.59% and 70.32% than for GFAAS 49.95% and 36.09%, respectively, indicating that ICP-OES is the preferred analysis method for Cu

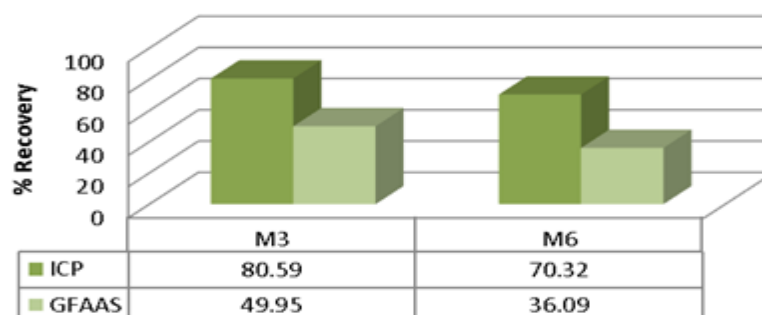


Figure 4.4 – Comparison of Cu % recoveries between GFAAS & ICP-OES.

**Iron:** The linear range of ICP-OES is comparable to the range for previous analytes from 0 µg/L to 1 mg/L, shown in Figure 4.5 (A), the linear range of GFAAS is also comparable to previous analytes from 0 µg/L to 50 µg/L, shown in Figure 4.5 (B).

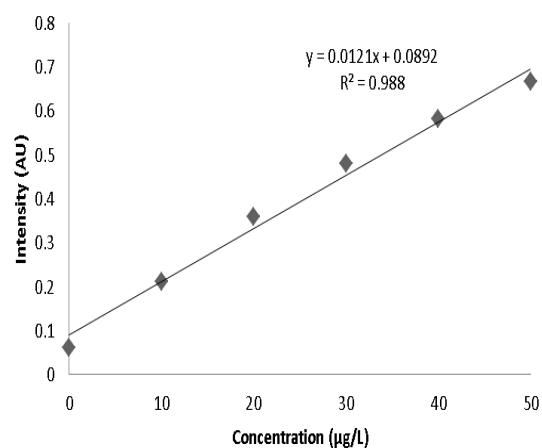
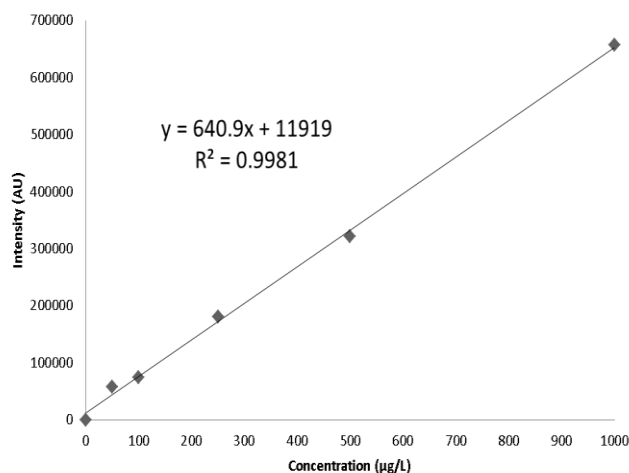


Figure 4.5 (A) – Fe ICP-OES Calibration Curve      Figure 4.5 (B) – Fe GFAAS Calibration Curve

Methods 3 and 6 were chosen for a data comparison between the two analytical methods for Fe, shown in Figure 4.6. The extraction % recoveries for ICP-OES are higher for Method 3, 85.45% compared to 77.90% for GFAAS but the recovery for Method 6 using GFAAS, 91.92% is higher than the recovery using ICP-OES 83.98%, indicating that when using Method 3 ICP-OES is the preferred analysis method.

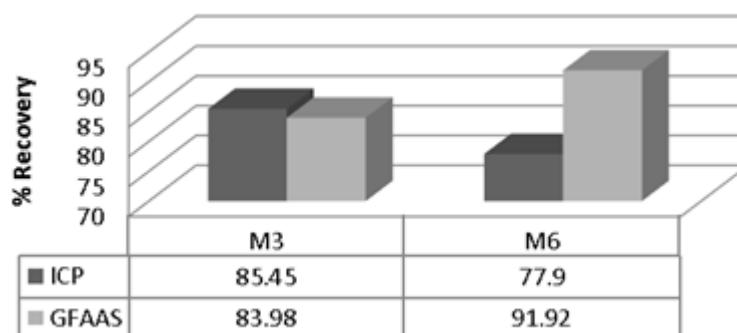


Figure 4.6 – Comparison of Fe % recoveries between GFAAS & ICP-OES.

**Lead:** The linear range of ICP-OES is comparable to the range for previous analytes from 0 to 1 mg/L, shown in Figure 4.7 (A), the linear range of GFAAS is also comparable to previous analytes from 0 µg/L to 50 µg/L, shown in Figure 4.7 (B).

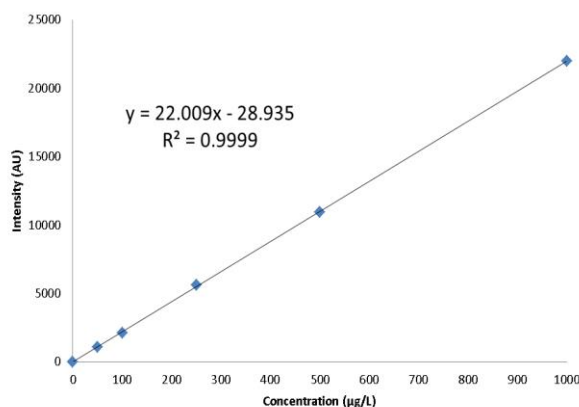


Figure 4.7 (A) – Pb ICP-OES Calibration Curve

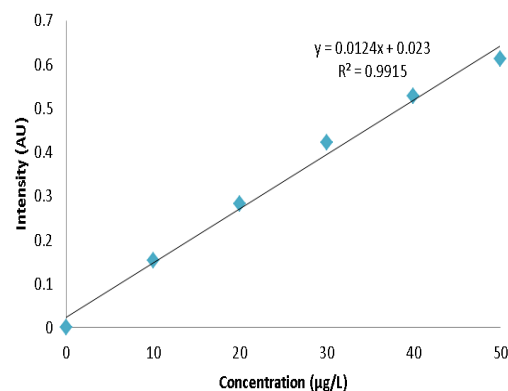


Figure 4.7 (B) – Pb GFAAS Calibration Curve

Methods 3 and 6 were chosen for a data comparison between the two analytical methods for Pb, shown in Figure 4.8. The extraction % recoveries for ICP-OES are higher for Method 3 and 6, 87.3% and 79.51% than for GFAAS 11.77% and 21.01%, respectively, indicating that ICP-OES is the preferred analysis method.

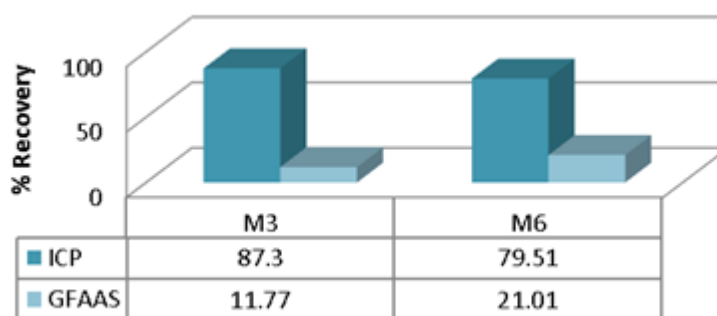


Figure 4.8 – Comparison of Pb % recoveries between GFAAS &amp; ICP-OES.

**Manganese:** The linear range of ICP-OES is comparable to the range for previous analytes from 0 µg/L to 1 mg/L, shown in Figure 4.9 (A), but the linear range of GFAAS is significantly lower than previous analytes from 0 µg/L to 20 µg/L, shown in Figure 4.9 (B).

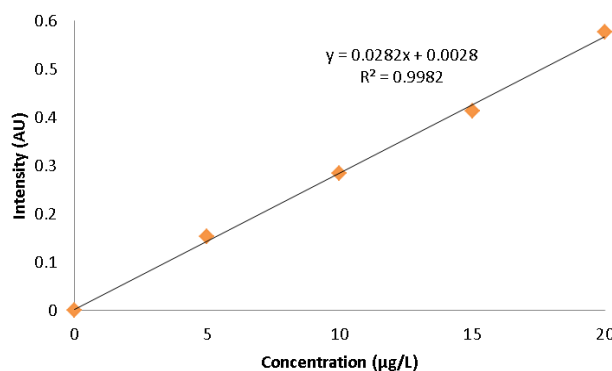
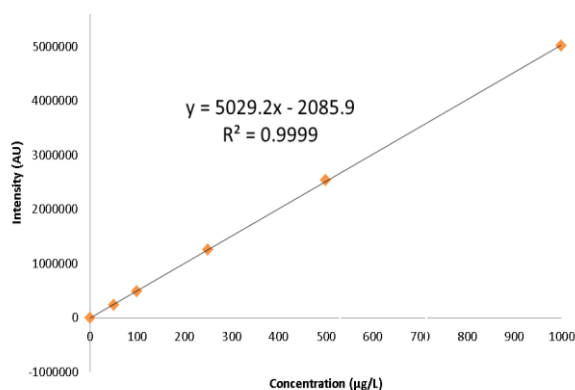


Figure 4.9 (a) – Mn ICP-OES Calibration Curve

Figure 4.9(b) – Mn GFAAS Calibration Curve

Analyte Methods 3 and 6 were chosen for a data comparison between the two analytical methods for Mn, shown in Figure 4.10. The extraction % recoveries for ICP-OES are higher for method 3 and 6, 82.13% and 83.58% than for GFAAS 39.9% and 55.58%, respectively, indicating that ICP-OES is the preferred analysis method.

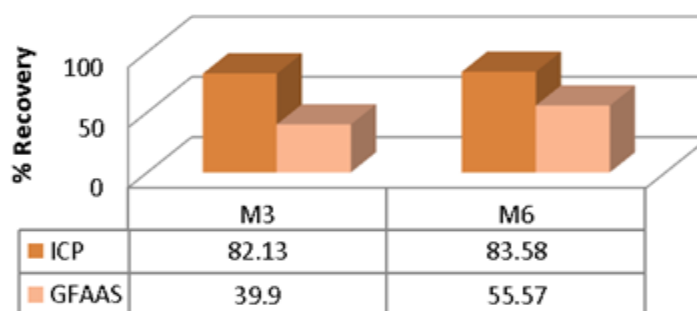


Figure 4.10 – Comparison of Mn % recoveries between GFAAS &amp; ICP-OES.

**Nickel:** The linear range of ICP-OES is comparable to the range for previous analytes from 0  $\mu\text{g/L}$  to 1 mg/L, shown in Figure 4.11 (b), the linear range of GFAAS is also comparable to previous analytes from 0  $\mu\text{g/L}$  to 50  $\mu\text{g/L}$ , shown in Figure 4.11 (a).

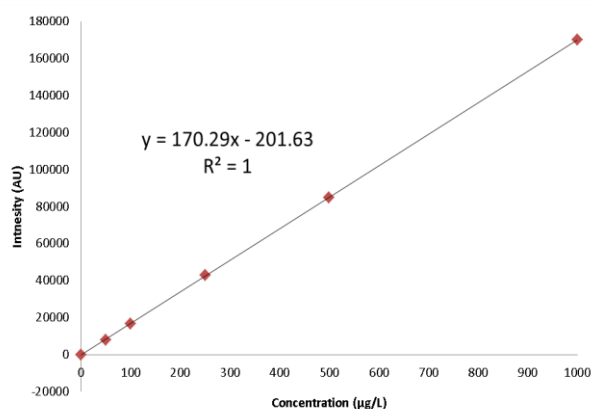


Figure 4.11(a) – Ni ICP-OES Calibration Curve

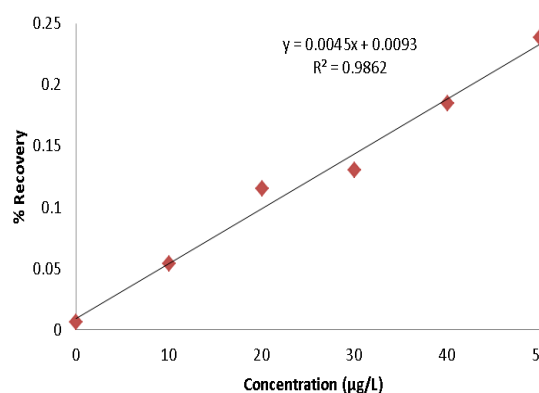


Figure 4.11(b) – Ni GFAAS Calibration Curve

Methods 3 and 6 were chosen for a data comparison between the two analytical methods for Ni, shown in Figure 4.12. The extraction % recoveries for ICP-OES are higher for Method 3 and 6, 88.52% and 69.68% than for GFAAS 63.02% and 59.60%, respectively, indicating that ICP-OES is the preferred analysis method.



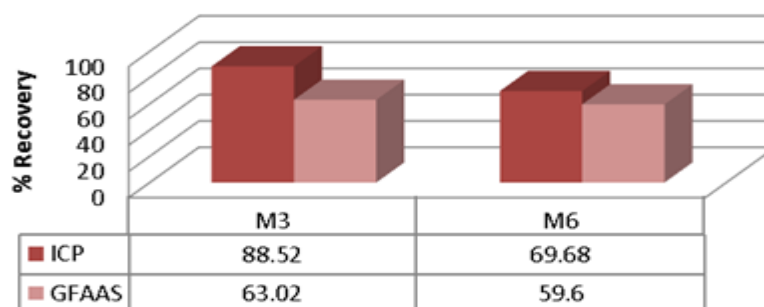


Figure 4.12 – Comparison of Ni % recoveries between GFAAS & ICP-OES.

**Zinc:** The linear range of ICP-OES is comparable to the range for previous analytes from 0 µg/L to 1mg/L, shown in Figure 4.13 (b), but the linear range of GFAAS is double that of previous analytes from 0 µg/L to 100 µg/L, shown in Figure 4.13 (a).

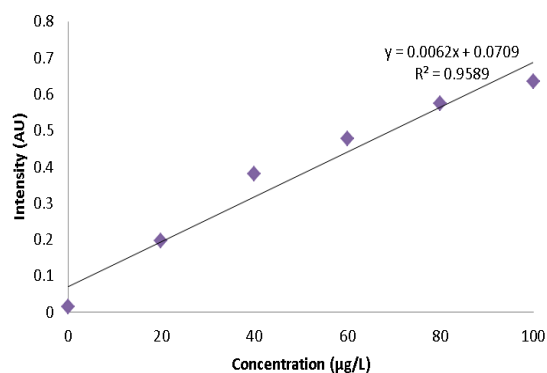
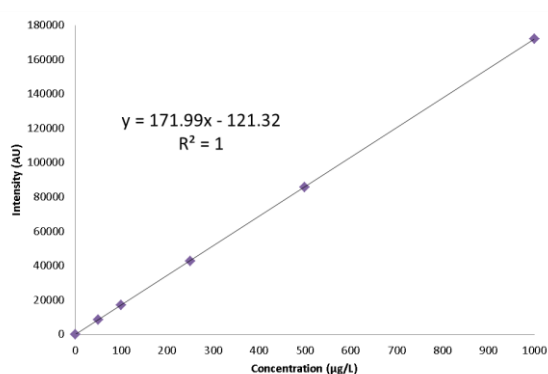


Figure 4.13(a).20 – Zn GFAAS Calibration Curve      Figure 4.13(b) – Zn ICP-OES Calibration Curve

Methods 3 and 6 were chosen for a data comparison between the two analytical methods for Zn, shown in Figure 4.14. The extraction % recoveries for ICP-OES are higher for Method 3 89.19% compared to 61.75% for GFAAS but the recoveries using Method 3 are comparable for both analytical methods, 65.92% for ICP-OES and 63.29% for GFAAS, indicating that when using digestion Method 3 ICP-OES is the preferred analysis method.

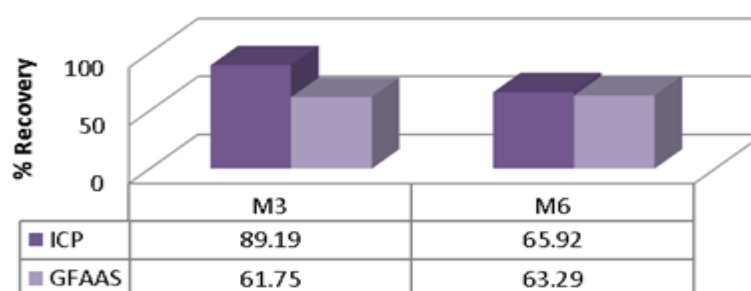


Figure 4.14 – Comparison of Zn % recoveries between GFAAS & ICP-OES.

The % recoveries are generally higher using ICP-OES detection than for GFAAS detection for all elements except iron. The recoveries for Iron are similar for both ICP-OES detection and GFAAS detection using Method 3. GFAAS calibration plots tend to level off, lose linearity after an absorption  $>1$  AU is reached. 1 AU is reached at a maximum of 50  $\mu\text{g/L}$  for the analytes tested, except Zn. The difference in recoveries between ICP-OES and GFAAS detection can be attributed to interferences present. The use of alternative wavelengths, to overcome the presence of spectral interferences and the use of matrix modifiers to overcome the presence of chemical (matrix) interferences were investigated. Overcoming spectral and matrix interferences did not result in increased recoveries, indicating that recovery issues are related to atomisation interferences. These interferences can be overcome by reducing atomisation temperatures.

### **Detection Limit:**

Most instruments produce a signal even when a blank sample is being analysed. This signal is what is commonly referred to as noise or background. The concentration of analyte required to produce a signal that is 3 times greater than the standard deviation (relative to the slope) of this noise level is known as the limit of detection (LOD). The Limit of Quantitation (LOQ) on the other hand is measured as 10 times the standard deviation of the noise signal and this represents the lowest analyte concentration which can be determined with confidence.

The LOD is the lowest concentration at which an analyte can be observed. It is defined by the EPA as 'the minimum concentration that can be determined, with 99% confidence that true concentration is greater than zero'. The LOD of a method can be affected by the equipment, chemicals, methodology, materials, sample compositions and analysts. It differs from an instrument's limit of detection in that an instrument's limit of detection is defined under optimum conditions but in reality there are other factors that affect the results e.g. matrix interferences or the sample introduced may be contaminated [92]. It is determined as 3 times the standard deviation of 10 replicate blank determinations/the slope ( $3\sigma/s$ ). The LOQ [96], is the level above which the concentration can be determined with acceptable precision. It is determined as ten times the standard deviation of 10 replicate blank determinations/the slope ( $10\sigma/s$ ).

These LOD and LOQ values are also subject to environmental conditions and serve only as a guide. Ideally they should be re-established at least every six months or so. If the relative standard deviation is not between 0.5 and 2% there may be a problem with the instrument.

The use of an internal standard can help identify these issues. It can highlight the variation in power, temperature, changes in density, viscosity or surface tension. The standard deviation should never be zero.

Limit of detection analysis was run for both analytical methods, shown in Table 4.1. A significant difference is not observed between the detection limits for GFAAS and ICP-OES either method can be used to analyse samples. The limits of detection for ICP-OES are generally lower than the GFAAS limits. Therefore due to the discrepancies between detection methods and the difference between limits of detection for detection methods, ICP-OES will be used for analysis going forward.

Table 4.1: ICP-OES & GFAAS LOD/LOQ

	Limit of Detection ( $3\delta$ )		Limit of quantisation ( $10\delta$ )	
	GFAAS	ICP-OES	GFAAS	ICP-OES
Aluminium		0.63		2.13
Cadmium		0.57		1.9
Copper	0.45	0.73	1.51	2.42
Iron	0.72	0.73	2.4	2.46
Lead	0.06	7.23	0.19	24.11
Manganese	0.02	0.04	0.06	0.15
Nickel	0.04	4.19	0.14	13.99
Zinc	1.53	4.11	5.1	13.71

**Chapter 5:**  
Cabin filter analysis.

## Chapter 5

### Cabin filter analysis.

#### Introduction:

The main objectives of the overall study is to determine the levels of analytes trapped on vehicular particle filters. The results of the method developments in chapter 3 now allows confident measurement of analytes residues/deposits.

#### 5.1: Analytes Concentrations from Exposed Standard Particle Cabin Air Filters.

Preliminary tests were carried out on particle cabin filters taken at 15,000 km from a Skoda Octavia, they were then analysed using Method 3, shown again in Table 5.1.1.

Table 5.1.1: Microwave digestion Method 3, used to digest the samples.

Power (W)	Ramp (mins)	Time (mins)	Fan
500	5.00	10	1
1000	5.00	10	1
1400	5.00	10	1
0		15	3

A broad range of analytes were analysed including aluminium, antimony, arsenic, cadmium, calcium, chromium, cobalt, copper, iron, lead, magnesium, manganese, mercury, molybdenum, nickel, silicon, sulfur, tin, titanium, vanadium and zinc. From the analytes tested the following were the only analytes present in significant quantities, aluminium, cadmium, chromium, copper, iron, lead, magnesium, nickel and zinc.

Cabin filters were then placed in two different car models until specific kilometerages of 15,000 km, 30,000 km & 45,000 km were attained. The filters were collected and then replaced. Different makes of filter were also examined to determine if filtration efficiency is brand dependent.

The collected samples were prepared using microwave digestion. The following acid combination was used, 2 ml HF, 1 ml HCl and 6ml HNO<sub>3</sub> and settings for the microwave digestion method used are shown in Table 5.1.1.

Two different car models were used for the collection of samples discussed in this chapter, a Skoda Octavia and a Toyota Aventis. Representative samples were taken from the filter samples, details of are given below.

Table 5.1.2. shows representative sampling for Skoda Octavia: Skoda Octavia filters have 29 folds which are 1" high and the filter is 10" wide. Samples were taken from fold number 8, 19 and 25 at 2", 5" and 8" along the width of the filter, thus creating 1" square filter samples.

Table 5.1.2.: Representative analysis of Skoda Octavia particle filters.

	2"	5"	8"
Fold 8	A	B	C
Fold 19	D	E	F
Fold 25	G	H	I

Table 5.1.3. shows representative sampling for a Toyota Aventis: a Toyota Aventis filters have 40 folds, which are 1" high and the filter is 8" wide. Samples were taken from fold number 9, 19, 29 and 39 at 2", 4" and 6" along the width of the filter which also creates 1" square filter samples.

Table 5.1.3.: Representative analysis of a Toyota Aventis particle filters.

	2"	4"	6"
Fold 9	A'	B'	C'
Fold 19	D'	E'	F'
Fold 29	G'	H'	I'
Fold 39	J'	K'	L'

## 5.2: Aluminium: Concentrations from Standard Filters.

### 5.2.1: Concentrations of Al at Different Kilometerages from a Skoda Octavia.

Figure 5.2.1 shows a comparison between Micronair particle filters taken from a Skoda Octavia at kilometerages of 15,000 km, 30,000 km and 45,000 km.

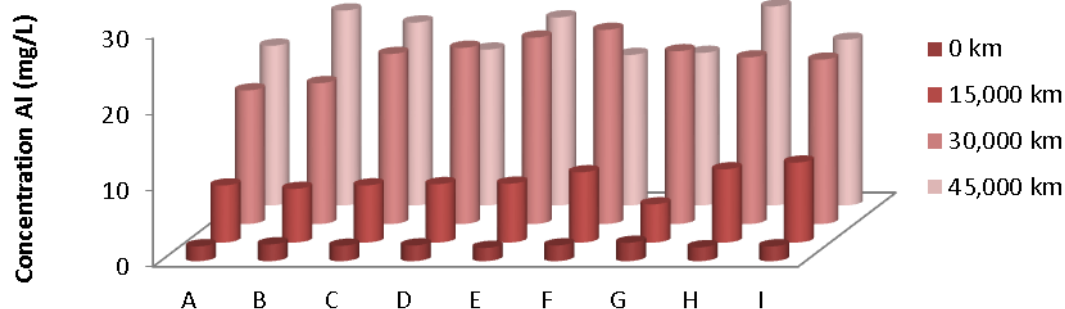


Figure 5.2.1: Al average concentrations for a Skoda Octavia, standard particle filter from 0 km to 45,000 km in increments of 15,000 km, manufactured by Micronair. The legend key for the x axis is shown in Table 1.4.1, pg. 34. All samples were collected in triplicate.

Column 3 of Table 5.2.1 shows concentrations corrected to 100% based on SRM recoveries of aluminium using Method 3 shown in Figure 3.2.1, page 78, estimated to be 57.03% of the overall quantities of aluminium on the filter. Three different filter samples were collected for each kilometerage.

Table 5.2.1: The average concentrations of Al for filters samples, with standard deviation errors between replicates are shown in column 2. With corrected concentrations based on percentage recoveries from SRM samples shown in column 3. Column 4 shows recoveries for the entire area of the filter.

Kilometerage (km)	Al concentrations from filter sample ( $\mu\text{g}$ )	Corrected based on SRM % recovery ( $\mu\text{g}$ )	Recovery of Al for entire filter area (mg)
0 km	$18.18 \pm 1.71$	31.95	9.27
15,000 km	$71.82 \pm 10.62$	125.91	36.54
30,000 km	$197.64 \pm 62.91$	346.5	100.53
45,000 km	$203.4 \pm 40.68$	356.76	103.5

A blank filter was also analysed as a background reference, background levels of Al were found to be  $18.18 \pm 1.71 \mu\text{g}$ . Exposure of the filter over 15,000 km increased Al levels to  $71.82 \pm 10.62 \mu\text{g}$  per sample area. An exposure of a further 15,000 km (i.e. to 30,000 km) resulted in an increase of Al levels to  $197.64 \pm 62.91 \mu\text{g}$ . However a further increase of 15,000 km to 45,000 km resulted in moderate increases in aluminium levels to  $203.4 \pm 40.68$ .

This indicates that filter extraction efficiency is increasing up to 30,000 km but from 30,000 km to 45,000 km the extraction efficiency levels off.

It is important to compare filters made by different manufacturers. Different manufacturing material and processes may lead to different performance. To investigate this different brands of filter were run in the same vehicle for the same kilometerage.

### 5.2.2: Concentration variations for Al between Different Standard Particle Filter Manufacturers.

Figure 5.2.2 shows a comparison between Airforce and Micronair standard particle filters taken at 15,000 km from a Skoda Octavia. Airforce particle filters were run to 15,000 km to investigate the relationship between different brands of standard particle filters over 15,000 km.

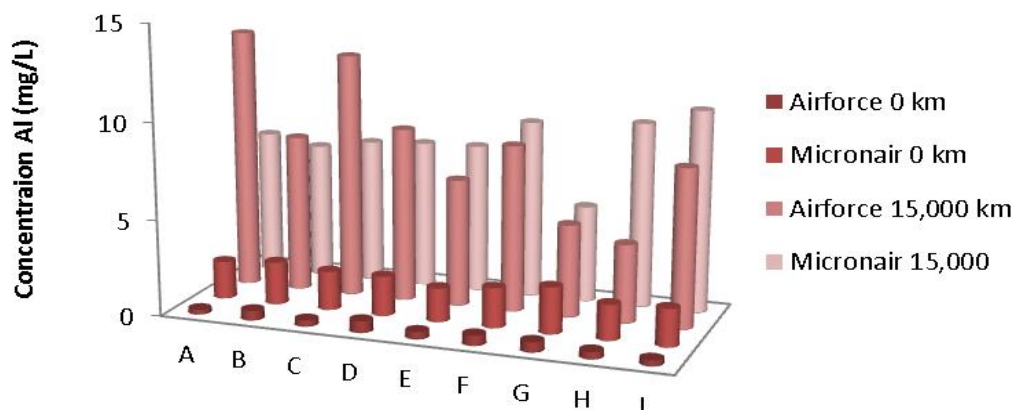


Figure 5.2.2: A comparison of average Al concentrations from standard particle filters manufacturers by comparing Micronair and Airforce from 0 km to 15,000 km for a Skoda Octavia. All samples were collected in triplicate.

Background Al levels of Airforce particle filters are significantly lower, ( $3.6 \pm 0.99 \mu\text{g}$ ) than for Micronair particle filters, ( $18.27 \pm 1.71 \mu\text{g}$ ). A significant difference is observed between blank filters samples and those taken at 15,000 km,  $3.6 \pm 0.99 \mu\text{g}$  to  $75.69 \pm 76.14 \mu\text{g}$  for Airforce compared to  $18.27 \pm 1.71$  to  $71.82 \pm 10.62 \mu\text{g}$  for Micronair filters. A difference is observed between the different brands of particle filter,  $72.09 \pm 5.15 \mu\text{g}$  for Airforce and  $53.55 \pm 8.91 \mu\text{g}$  for Micronair, indicating that for aluminium, Airforce filters are more efficient than Micronair filters.



Table 5.2.2: The average concentrations of Al for filters samples, with standard deviation errors between replicates are shown in column 2. With corrected concentrations based on percentage recoveries from SRM samples shown in column 3. Column 4 shows recoveries for the entire area of the filter.

Kilometerage (km)	Al concentrations from filter sample ( $\mu\text{g}$ )	Corrected based on SRM % recovery ( $\mu\text{g}$ )	Recovery of Al for entire filter area (mg)
0 km - Airforce	$3.6 \pm 0.99$	6.3	1.8
0 km - Micronair	$18.27 \pm 1.71$	31.95	9.27
15,000 km - Airforce	$75.69 \pm 6.14$	132.66	38.43
15,000 km - Micronair	$71.82 \pm 10.62$	126	36.54

### 5.2.3 Al Concentrations from Combination Filters from Two Different Manufactures.

It is also important to compare other filter products made by different manufacturers. Figure 5.2.3 shows a comparison between Airforce and Micronair combination filters taken at 15,000 km from a Skoda Octavia. Airforce combination filters were run to 15,000 km to investigate the relationship between different brands of combination filters over 15,000 km. Combination filters consist of a particle filter with an additional charcoal layer. The charcoal layer is added to increase the filters ability to extract gases/odours.

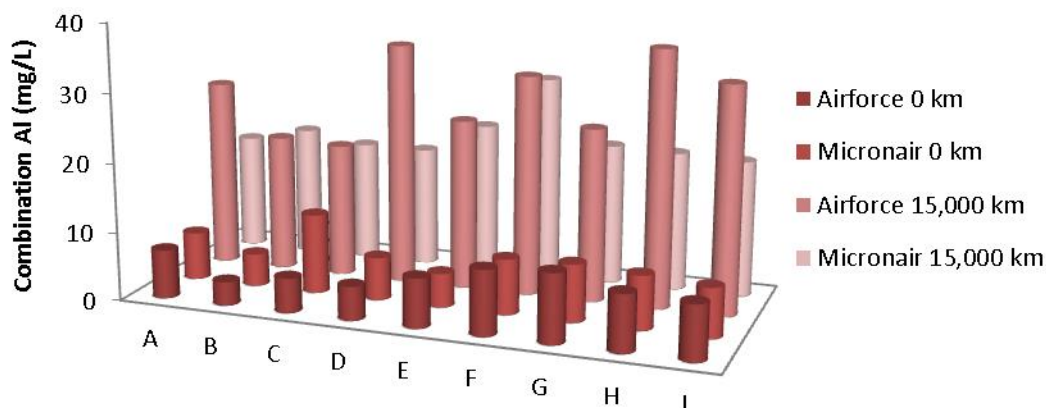


Figure 5.2.3: A comparison of average Al concentrations from combination filters manufacturers by comparing Micronair and Airforce from 0 km to 15,000 km for a Skoda Octavia All samples were collected in triplicate.

A significant difference is observed between blank filters which give an average reading of  $64.485 \pm 15.12 \mu\text{g}$  and those taken at 15,000 km which give an reading of  $253.08 \pm 78.84$  and  $182.43 \pm 86.94$  for Airforce and Micronair filters, respectively. A significant difference is

observed between the different brands of combination filter tested, taking error into consideration and subtracting background readings. Indicating that for aluminium extraction using combination filters, filter make does plays a significant role.

Table 5.2.3: The average concentrations of Al for filters samples, with standard deviation errors between replicates are shown in column 2. With corrected concentrations based on percentage recoveries from SRM samples shown in column 3. Column 4 shows recoveries for the entire area of the filter.

Kilometerage (km)	Al concentrations from filter sample ( $\mu\text{g}$ )	Corrected based on SRM % recovery ( $\mu\text{g}$ )	Recovery of Al for entire filter area (mg)
0 km - Airforce	$63.27 \pm 14.49$	110.88	32.13
0 km - Micronair	$65.7 \pm 15.75$	115.29	33.39
15,000 km - Airforce	$253.08 \pm 78.84$	443.79	128.7
15,000 km - Micronair	$182.43 \pm 86.94$	319.86	92.7

#### 5.2.4 Al Concentrations of Standard Particle Filters from Two Different Suppliers in Two Different Car Models.

It's important to investigate if the car manufacturer plays a role in PTE concentrations but also important to see if filter shape or orientation plays a significant role. Filters from the same manufacturer have different shapes and orientations when installed in different car models.

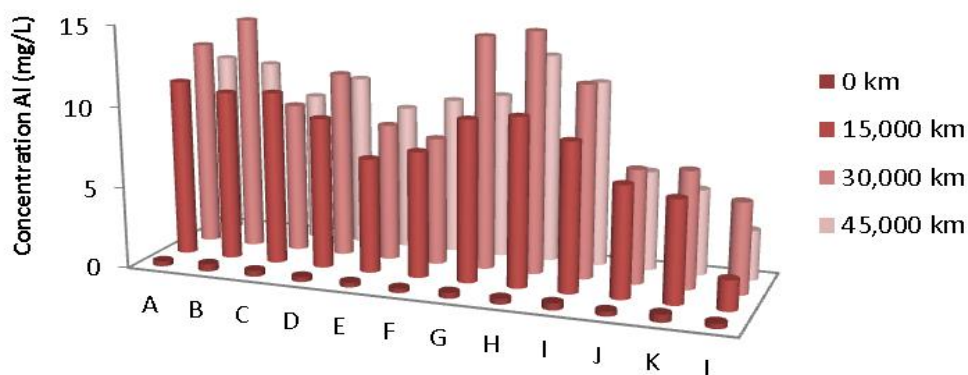


Figure 5.2.4: Al average concentrations for a Toyota Aventis, standard particle filter from 0 km to 45,000 km in increments of 15,000 km, manufactured by Micronair. The legend key for the x axis is shown in Table 1.4.2. All samples were collected in triplicate.

Figure 5.2.4 shows a comparison of Micronair particle filters taken at kilometerages of 15,000 km, 30,000 km and 45,000 km from a Toyota Aventis. This figure is a straight comparison to Figure 5.2.1 but a different car model was utilised.

Table 5.2.4: The average concentrations of Al for filters samples, with standard deviation errors between replicates are shown in column 2. With corrected concentrations based on percentage recoveries from SRM samples shown in column 3. Column 4 shows recoveries for the entire area of the filter.

Kilometerage (km)	Al concentrations from filter sample ( $\mu\text{g}$ )	Corrected based on SRM % recovery ( $\mu\text{g}$ )	Recovery of Al for entire filter area (mg)
0 km	$3.15 \pm 2.61$	5.49	1.71
15,000 km	$75.6 \pm 21.51$	172.8	55.26
30,000 km	$94.05 \pm 31.95$	201.15	64.35
45,000 km	$82.71 \pm 22.32$	179.82	57.51

A significant difference is observed between blank filters samples,  $3.15 \pm 2.61 \mu\text{g}$  and those taken at 15,000 km,  $75.6 \pm 21.51 \mu\text{g}$ . However, a significant difference is not observed between 15,000 km,  $75.6 \pm 21.51 \mu\text{g}$ , 30,000 km,  $94.05 \pm 31.95 \mu\text{g}$  and 45,000 km,  $82.71 \pm 22.32 \mu\text{g}$  indicating that the filters becomes less effective for aluminium extraction after 15,000 km in a Toyota Aventis. Concentrations at 15,000 km are comparable for both car models,  $75.6 \pm 21.51 \mu\text{g}$  for a Toyota Aventis and  $71.82 \pm 10.62 \mu\text{g}$  for a Skoda Octavia filters. Omitting background values  $18.18 \pm 1.71 \mu\text{g}$  for a Skoda Octavia and  $3.15 \pm 2.61 \mu\text{g}$  for a Toyota Aventis. Toyota Avenits filters yeild slightly higher concentrations. Filters from a Toyota Aventis are slightly more efficient than the same filter make placed in a Skoda Octavia over the same kilometerage intervals, (see Figure 5.2.1). At 30,000 km the filter in a Skoda Octavia yields a higher concentrations of  $197.64 \pm 62.91 \mu\text{g}$  over a filter from the same manufacturer in a Toyota Aventis over the same kilometerage which yields a concentration of  $94.05 \pm 31.95\mu\text{g}$ . A moderate decrease is observed in concentrations from filters taken at 45,000 km for a Toyota Aventis and a moderate increase is observed in Skoda Octavia at 45,000 km.

Filters in a Toyota Aventis are positioned horizontally while filters in a Skoda Octavia are placed vertically; suggesting that filter orientation plays a significant role in extraction efficiency, with vertical filters having a higher extraction efficiency after 15,000 km.

### 5.2.5: Concentrations for a Third Standard Particle Filter Manufacturer in a Toyota Aventis.

Figure 5.2.5: shows a comparison of Nip & Denso particle filters taken at 15,000 km, 30,000 km and 45,000 km from a Toyota Aventis.

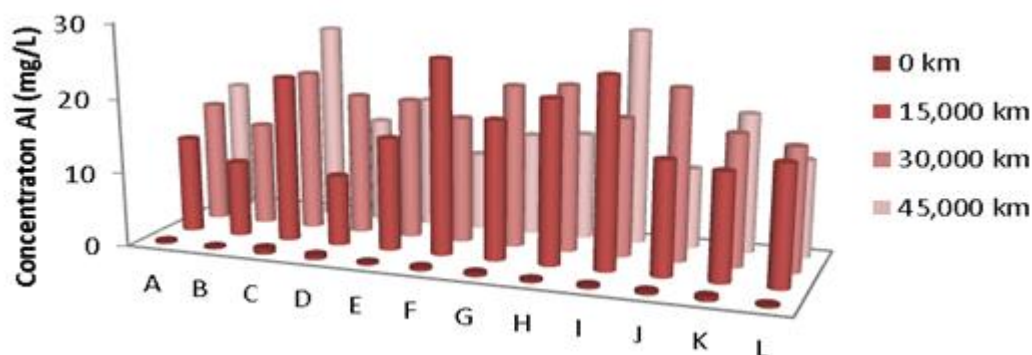


Figure 5.2.5: Al average concentrations for a Toyota Aventis, standard particle filter from 0 km to 45,000 km in increments of 15,000 km, manufactured by Nip & Denso. All samples were collected in triplicate.

Table 5.2.5: The average concentrations of Al for filters samples, with standard deviation errors between replicates are shown in column 2. With corrected concentrations based on percentage recoveries from SRM samples shown in column 3. Column 4 shows recoveries for the entire area of the filter.

Kilometerage (km)	Al concentrations from filter sample ( $\mu\text{g}$ )	Corrected based on SRM % recovery ( $\mu\text{g}$ )	Recovery of Al for entire filter area (mg)
0 km	$3.87 \pm 1.35$	6.84	2.16
15,000 km	$155.79 \pm 113.58$	203.67	65.16
30,000 km	$169.47 \pm 29.97$	256.23	81.99
45,000 km	$152.73 \pm 80.55$	279	89.28

This filter is manufactured by the car manufacturer and comes as standard in a Toyota Aventis. As seen for all filter types thus far, a significant difference is observed between blank filters samples,  $3.87 \pm 1.35 \mu\text{g}$  and those taken at 15,000 km,  $155.79 \pm 113.58 \mu\text{g}$ . However a

significant difference is not observed between 15,000 km, ( $155.79 \pm 113.58 \mu\text{g}$ ), 30,000 km, ( $169.47 \pm 29.97 \mu\text{g}$ ) and 45,000 km, ( $152.73 \pm 80.55 \mu\text{g}$ ) indicating that for aluminium, filters become less effective after 15,000 km. The decreased extraction efficiency can be attributed to the filter orientation because a decreased efficiency is observed across both filter makes in a Toyota Aventis, where filters lie horizontally.

### **Aluminium Conclusions:**

An increase in aluminium concentrations of  $53.64 \pm 8.91 \mu\text{g}$  is observed between 0 km and 15,000 km and an increase of  $125.82 \pm 52.29 \mu\text{g}$  is observed between 15,000 km and 30,000 km for Micronair standard particle filters but an increase of only  $5.76 \pm 11.61$  is observed between 30,000 km and 45,000 km.

Airforce particle filters have a higher extraction efficiency than micronair standard particle filters from 0 km to 15,000 km,  $72.09 \pm 5.15 \mu\text{g}$  and  $53.55 \pm 8.91 \mu\text{g}$ , respectively.

Airforce combination filters have a higher extraction efficiency than Micronair particle filters from 0 km to 15,000 km,  $188.59 \pm 63.72 \mu\text{g}$  and  $117.95 \pm 71.82 \mu\text{g}$ . Concentrations for both Airforce and Micronair combination filters are over double those of standard particle filters. This shows that the extraction efficiency of combination filters in a Skoda Octavia is superior to standard particle filters for aluminium extraction.

Micronair particle filters in a Toyota Aventis yield a high concentration from 0 km to 15,000 km ( $72.45 \pm 18.9 \mu\text{g}$  in a Toyota Aventis compared to  $53.64 \pm 8.91 \mu\text{g}$  in a Skoda Octavia) but no significant increase in concentrations is observed between 15,000 km and 30,000 km. This indicates that the extraction efficiencies of Micronair standard particle filters in a Skoda Octavia and a Toyota Aventis are comparable up to 15,000 km and that filters placed in a Skoda Octavia are more efficient up to 30,000 km. This may be attributed to the orientation of the filter. In a Skoda Octavia filters are placed vertically and in a Toyota Aventis filters are placed horizontally.

Micronair and Nip and Denso standard particle filters run in a Toyota Aventis yield similar results up to 30,000 km. This shows a large increase in Al values from 0 km to 15,000 km for both car makes and moderate increase from 15,000 km to 30,000 km. From 30,000 km to 45,000 km Micronair filters show a decrease in Al levels from  $94.05 \pm 31.95 \mu\text{g}$  to  $82.71 \pm 22.32 \mu\text{g}$  and Nip & Denso filters show a decrease from  $169.47 \pm 29.97 \mu\text{g}$  to  $152.73 \pm 80.55$

µg. This indicates that different filter makes in the same vehicle behave similarly for all kilometerages covered.

#### 5.2.6: Al Concentrations at 15,000 km less blanks for all filter makes.

All makes of standard particle and combination filters were run to a minimum of 15,000 km in their respective car models. 15,000 km is the replacement interval recommended by filter manufactures. A comparison was made between all car models and filter manufacturers up to a kilometerage of 15,000 km, shown in Table 5.2.6.

Table 5.2.6: Al concentrations from complete filters run to 15,000 km minus blank filter concentrations, for all filter types tested (different filter brands, types and car models), extrapolated over the surface area of the filter.

Car and filter make	µg
Micronair Particle Filter - Skoda Octavia	53.64 ± 8.91
Airforce Particle Filter - Skoda Octavia	72.09 ± 5.15
Airforce Combination filters – Skoda Octavia	188.59 ± 63.72
Micronair Combination filters – Skoda Octavia	117.95 ± 71.82
Micronair Particle Filter - Toyota Aventis	72.45 ± 18.9
Nip & Denso Particle - Toyota Aventis	151.92 ± 112.23

The concentrations of aluminium on Micronair and Airforce standard particle filters (for a Skoda Octavia) are comparable and concentrations from Nip & Denso and Micronair standard particle filter (for a Toyota Aventis) are comparable. Concentrations of aluminium are consistent for car models up to 15,000 km, irrespective of filter manufacturer. Both combination filters have higher concentrations than standard particle filter in the same car model (for a Skoda Octavia) over the same kilometerage. Airforce combination filters (for a Skoda Octavia) are more efficient than Micronair combination filters (for a Skoda Octavia). Nip & Denso Particle (for a Toyota Aventis) have a higher concentration than Micronair Combination filters (for a Skoda Octavia) but the concentrations are lower than Airforce combination filters (for a Skoda Octavia). Airforce Combination filters (for a Skoda Octavia) have the highest concentration, 188.59 ± 63.72 µg. Nip & Denso particle standard filters (for a Toyota Aventis) are the most efficient standard particle filters for aluminium extraction up to 15,000 km.

### 5.3: Chromium: Concentrations from Standard Particle Filters.

**5.3.1: Concentrations of Cr at Different Kilometerages in Car Model 1 (a Skoda Octavia).** Figure 5.3.1 Shows a comparison between Micronair particle filters taken from (a Skoda Octavia) at kilometerages of 15,000 km, 30,000 km and 45,000 km.

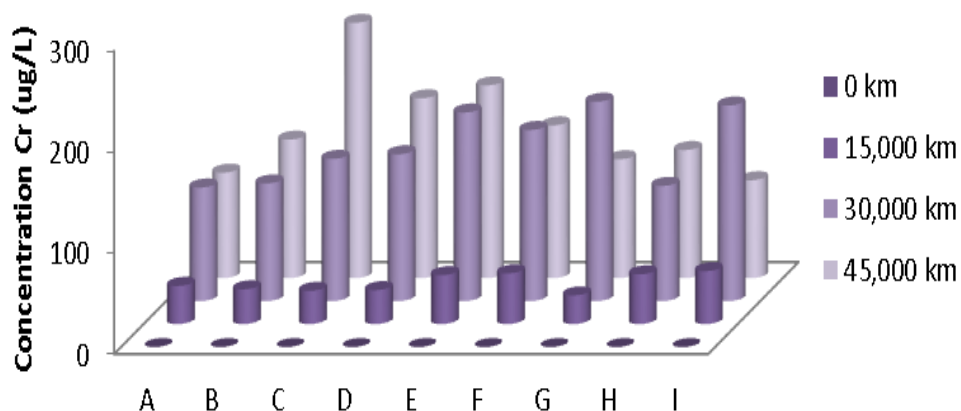


Figure 5.3.1: Average Cr concentrations for a Skoda Octavia, standard particle filter from 0 km to 45,000 km in increments of 15,000 km, manufactured by Micronair. All samples were collected in triplicate.

Column 3 in Table 5.3.1 shows corrected concentrations based on SRM recoveries of chromium using Method 3, estimated to be 91.3% of the overall quantities of chromium on the filter.

Table 5.3.1: The average concentrations of Cr for filters samples, with standard deviation errors between replicates are shown in column 2. With corrected concentrations based on percentage recoveries from SRM samples shown in column 3. Column 4 shows recoveries for the entire area of the filter.

Kilometerage (km)	Cr concentrations from filter sample (ng)	Corrected based on SRM % recovery (ng)	Recovery of Cr for entire filter area (µg)
0 km	0	0	0
15,000 km	367.56 ± 64.35	402.57	116.73
30,000 km	1,376.73 ± 416.97	1,507.95	437.22
45,000 km	1,356.12 ± 281.16	1,485.27	430.65

A blank filter was analysed as a background reference. Background levels of Cr were found to be 0 ng. Exposure of the filter over a kilometerage of 15,000 km increased Cr levels from 0 ng to  $367.56 \pm 64.35$  ng. An exposure of a further 15,000 km (i.e. 30,000 km) resulted in an increase in chromium to  $1,376.73 \pm 416.97$  ng. However a further increase of 15,000 km to 45,000 km did not show any increase in chromium levels,  $1,356.12 \pm 281.16$  ng. Indicating the filter extraction is most efficient between 15,000 km and 30,000 km.

### 5.3.2: Comparison of Concentrations of Cr between Standard Particle Filter Manufacturers.

Figure 5.3.2: Shows a Comparison between Airforce and Micronair Particle Filters taken at 15,000 km from a Skoda Octavia filters.

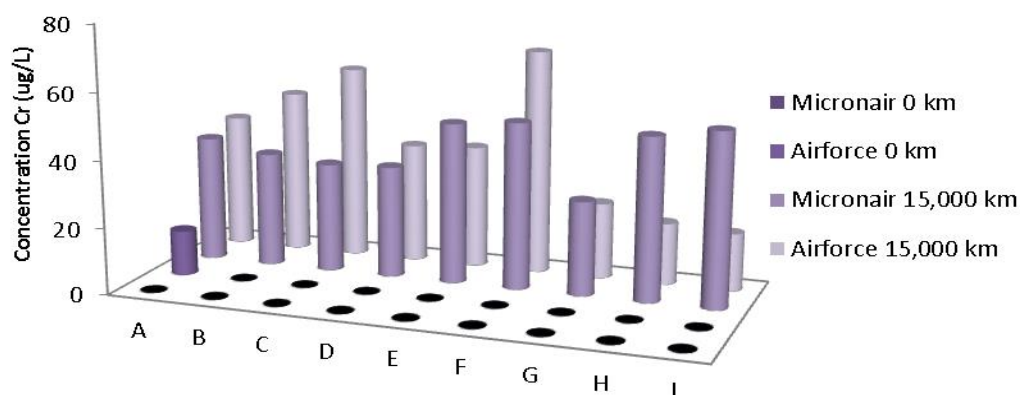


Figure 5.3.2: A comparison of average Cr concentrations from standard particle filters manufacturers by comparing Micronair and Airforce from 0 km to 15,000 km for a Skoda Octavia. All samples were collected in triplicate.

Background Cr levels of Airforce particle filters were found to be 0 µg/L. An increase in Cr levels is observed between blank Airforce filter samples and those taken at 15,000 km, from 0 ng to  $347.67 \pm 48.96$  ng. However no difference is observed between the different brands of particle filter,  $347.67 \pm 48.96$  ng for Airforce and  $367.56 \pm 64.35$  ng for Micronair. This indicates that for chromium, the extraction efficiency of Airforce and Micronair filters are comparable.



Table 5.3.2: The average concentrations of Cr for filters samples, with standard deviation errors between replicates are shown in column 2. With corrected concentrations based on percentage recoveries from SRM samples shown in column 3. Column 4 shows recoveries for the entire area of the filter.

Kilometerage (km)	Cr concentrations from filter sample (ng)	Corrected based on SRM % recovery (ng)	Recovery of Cr for entire filter area ( $\mu\text{g}$ )
0 km - Airforce	0	0	0
0 km - Micronair	0	0	0
15,000 km - Airforce	$347.67 \pm 48.96$	380.88	110.43
15,000 km - Micronair	$367.56 \pm 64.35$	402.57	116.73

### 5.3.3 Cr Concentrations from Combination Filters from Two Different Manufactures.

Figure 5.3.3 shows a comparison between Airforce and Micronair combination filters taken at 15,000 km from a Skoda Octavia.

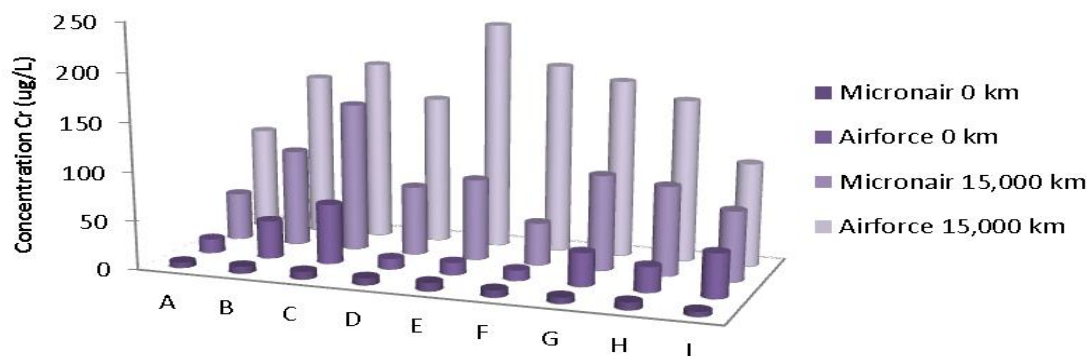


Figure 5.3.3: A comparison of average Cr concentrations from combination filters manufacturers by comparing Micronair and Airforce from 0 km to 15,000 km for a Skoda Octavia. All samples were collected in triplicate.

A significant difference is observed between blank filters  $253.17 \pm 96.75$  ng for Airforce and  $60.39 \pm 24.57$  ng for Micronair and those taken at 15,000 km,  $1,484.55 \pm 215.73$  ng for Airforce and  $757.35 \pm 422.73$  ng for Micronair. A significant difference is also observed between the different brands of combination filter tested,  $1,231.38 \pm 118.98$  ng and  $696.96 \pm 398.16$  ng for Airforce and Micronair filters, respectively, when background readings are subtracted. When using combination filters for chromium extraction, Airforce are more efficient than Micronair filters. This indicates that for chromium extraction filter brand plays a significant role in extraction efficiency.

Table 5.3.3: The average concentrations of Cr for filters samples, with standard deviation errors between replicates are shown in column 2. With corrected concentrations based on percentage recoveries from SRM samples shown in column 3. Column 4 shows recoveries for the entire area of the filter.

Kilometerage (km)	Cr concentrations from filter sample (ng)	Corrected based on SRM % recovery (ng)	Recovery of Cr for entire filter area ( $\mu\text{g}$ )
0 km - Airforce	$253.17 \pm 96.75$	277.29	80.37
0 km - Micronair	$60.39 \pm 24.57$	66.15	19.17
15,000 km - Airforce	$1,484.55 \pm 215.73$	1,626.03	471.51
15,000 km - Micronair	$757.35 \pm 422.73$	829.53	240.57

### 5.3.4 Cr Concentrations of Standard Particle Filters from Two Different Suppliers in Two Different Car Models.

Figure 5.3.4 shows a comparison of Micronair particle filters taken at kilometerages of 15,000 km, 30,000 km and 45,000 km from a Toyota Aventis.

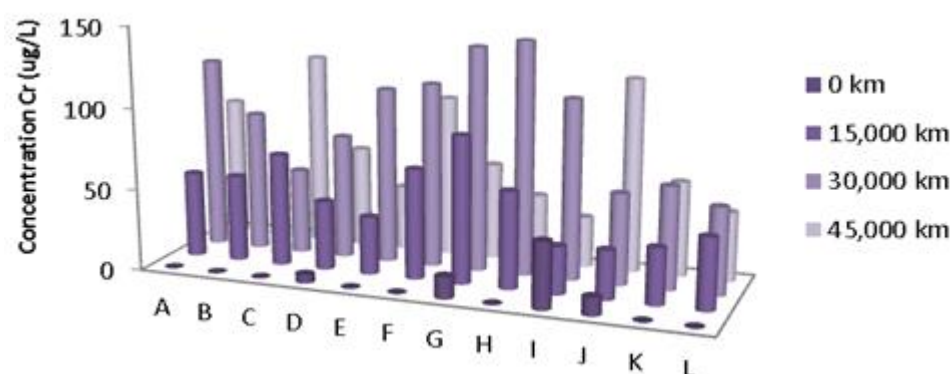


Figure 5.3.4: Average Cr concentrations for a Toyota Aventis, standard particle filter from 0 km to 45,000 km in increments of 15,000 km, manufactured by Micronair. All samples were collected in triplicate.

Filters in a Toyota Aventis are positioned horizontally while filters in a Skoda Octavia are placed vertically, the horizontal orientation of filters in a Toyota Aventis suggests that filter orientation plays a significant role in extraction efficiency/retention. Vertically mounted filters have higher extraction efficiency up to 30,000 km, almost triple that of horizontally mounted filters. De-absorption appears to occur in horizontally placed filters, demonstrated by

a decrease in concentrations,  $240.39 \pm 261.81$  ng between 30,000 km and 45,000 km. This decrease is not observed in vertically orientated filters.

Table 5.3.4: The average concentrations of Cr for filters samples, with standard deviation errors between replicates are shown in column 2. With corrected concentrations based on percentage recoveries from SRM samples shown in column 3. Column 4 shows recoveries for the entire area of the filter.

Kilometerage (km)	Cr concentrations from filter sample (ng)	Corrected based on SRM % recovery (ng)	Recovery of Cr for entire filter area ( $\mu\text{g}$ )
0 km	$26.1 \pm 75.06$	28.53	9.09
15,000 km	$457.29 \pm 140.31$	500.94	160.29
30,000 km	$839.79 \pm 540.99$	919.8	294.3
45,000 km	$599.4 \pm 279.81$	656.55	210.06

### 5.3.5: Concentrations for a Third Standard Particle Filter Manufacturer in a Toyota Aventis.

Figure 5.3.5: Shows a comparison of Nip & Denso particle filters taken at 15,000 km, 30,000 km and 45,000 km from a Toyota Aventis.

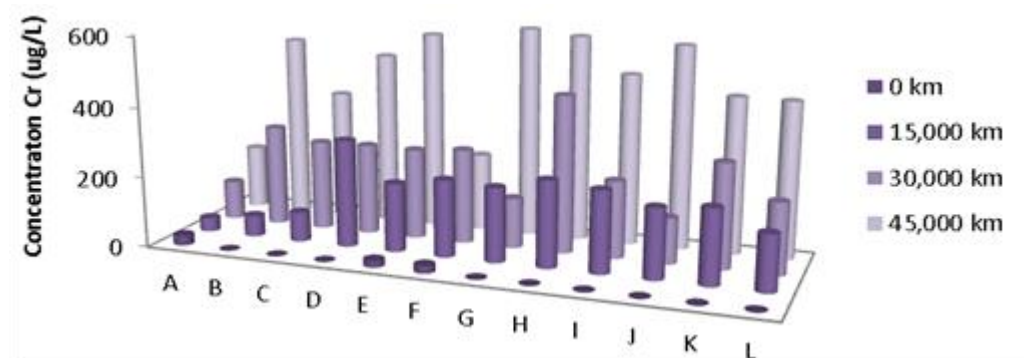


Figure 5.3.5: Average Cr concentrations for a Toyota Aventis, standard particle filter from 0 km to 45,000 km in increments of 15,000 km, manufactured by Nip & Denso. All samples were collected in triplicate.

A significant difference is observed between blank filters samples  $52.38 \pm 53.37$  ng and those taken at 15,000 km  $1,624.41 \pm 1,033.11$  ng. A moderate difference is observed between 15,000 km and 30,000 km,  $534.6 \pm 525.78$  ng. An increase of  $1,952.37 \pm 171.45$  ng is

observed between 30,000 km and 45,000 km. This indicates that for chromium extraction, the extraction efficiency improved with use, attributed to particle build up/filter blocking.

Table 5.3.5: The average concentrations of Cr for filters samples, with standard deviation errors between replicates are shown in column 2. With corrected concentrations based on percentage recoveries from SRM samples shown in column 3. Column 4 shows recoveries for the entire area of the filter.

Kilometerage (km)	Cr concentrations from filter sample (ng)	Corrected based on SRM % recovery (ng)	Recovery of Cr for entire filter area ( $\mu\text{g}$ )
0 km	$52.38 \pm 53.37$	57.42	18.36
15,000 km	$1,624.41 \pm 1,033.11$	1,779.21	569.34
30,000 km	$2,159.01 \pm 1558.89$	2,364.75	756.72
45,000 km	$4,111.38 \pm 1730.34$	4,503.15	1440.99

### Chromium Conclusions:

Micronair standard particle filters run in a Skoda Octavia show an increase from 0 km to 15,000 km of  $367.56 \pm 64.35$  ng and an increase from 15,000 km to 30,000 km to  $1009.17 \pm 352.62$  ng. A moderate decrease is observed between 30,000 km to 45,000 km of  $20.62 \pm 135.81$  ng.

Concentrations for Micronair and Airforce standard particle filters are comparable up to 15,000 km,  $367.56 \pm 64.35$  ng and  $347.67 \pm 48.96$  ng, respectively. Concentrations for Airforce combination filters are significantly higher than for Micronair,  $1231.38 \pm 118.98$  ng and  $696.96 \pm 398.16$  ng, respectively. This implies that different brands of standard particle filters have similar concentrations in a Skoda Octavia, while combination filter performance is dependent on filter make for a Skoda Octavia.

Micronair standard filters in a Skoda Octavia and in a Toyota Aventis show similar concentrations for Cr. There is an increase in concentrations from 0 km to 15,000 km and from 15,000 km to 30,000 km. A decrease is observed from 30,000 km to 45,000 for both car makes but the decrease for a Toyota Aventis is  $240.39 \pm 261.18$  ng compared to  $20.62 \pm 135.81$  ng for a Skoda Octavia. This indicates that filter orientation plays a role in particulate loss when filters become saturated. Filters in a Skoda Octavia are fitted vertically and filters

in a Toyota Aventis are fitted horizontally, horizontal placement seems to increase particulate loss.

Nip & Denso standard filters in a Toyota Aventis show higher concentrations than Micronair filters in the same car make. Nip & Denso filters, like Micronair filters, show increases in concentrations from 0 km to 15,000 km, 15,000 km to 30,000 km but unlike Micronair filters, Nip & Denso filters show an increase from 30,000 km to 45,000 km. This implies that Nip & Denso filter efficiency does not show the same diminished capacity with use.

### **5.3.6: Cr concentrations at 15,000 km less background levels for all filter makes.**

All makes of standard particle and combination filters were run to a minimum of 15,000 km in their respective car models. 15,000 km is the replacement interval recommended by filter manufactures. A comparison was made between all car models and filter manufacturers up to a kilometerage of 15,000 km, shown in Table 5.3.6.

Table 5.3.6. shows filter concentrations from filters run to 15,000 km minus blank filter concentrations, for all filter types tested (different filter brands, types and car models), extrapolated over the surface area of the filter.

Car and filter make	ng
Micronair Particle Filter - Skoda Octavia	$367.56 \pm 64.35$
Airforce Particle Filter - Skoda Octavia	$347.67 \pm 48.96$
Airforce Combination filters – Skoda Octavia	$1,231.38 \pm 118.98$
Micronair Combination filters – Skoda Octavia	$696.96 \pm 398.16$
Micronair Particle Filter - Toyota Aventis	$431.19 \pm 65.25$
Nip & Denso Particle - Toyota Aventis	$1,572.03 \pm 979.74$

The concentrations for Micronair standard particle filter (CW1) and Airforce standard particle filters (CW1) are comparable. This suggests that for chromium extraction, when using standard particle filters in a Skoda Octavia, filter make doesn't play a significant role. The concentrations for Micronair combination filters,  $696.96 \pm 398.16$  ng are lower than Airforce combination filters,  $1,231.38 \pm 118.98$  ng, suggesting that Airforce combination filters in the same car model are more efficient than Micronair filters. Concentrations for Micronair standard particle filters in a Toyota Aventis are comparable with Micronair standard particle filters in a Skoda Octavia, therefore car make or filter orientation does not play a significant

role up to 15,000 km. However Nip and Denso filter concentrations in a Toyota Aventis are significantly higher (almost 600 ng higher) than Micronair filters in the same car model. Airforce Combination filters (in a Skoda Octavia) yield the highest concentrations and Nip & Denso standard particle filters (in a Toyota Aventis) held the highest concentrations for particle filters.

## 5.4 Copper:

### 5.4.1: Concentrations of Cu at Different Kilometerages in Car Model 1 (a Skoda Octavia).

Figure 5.4.1 shows a comparison of percentage recoveries between Micronair particle filters taken from (a Skoda Octavia) at kilometerages of 15,000 km, 30,000 km and 45,000 km.

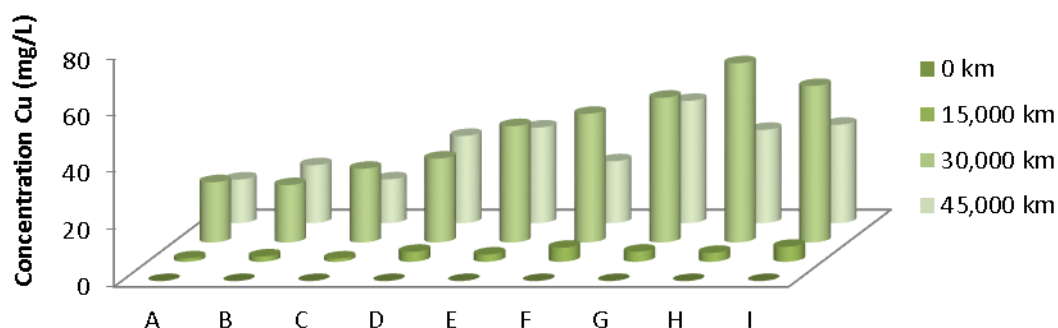


Figure 5.4.1: Average Cu concentrations for a Skoda Octavia, standard particle filter from 0 km to 45,000 km in increments of 15,000 km, manufactured by Micronair. All samples were collected in triplicate.

A blank filter was analysed as a background reference, background levels of Cu were found to be  $0.9 \pm 0.63 \mu\text{g}$ . Exposure of the filter over 15,000 km increased Cu levels to  $26.01 \pm 6.38 \mu\text{g}$ . A significant difference of  $325.26 \pm 76.23 \mu\text{g}$  is observed between 15,000 km and 30,000 km and a moderate decrease of  $80.37 \pm 131.49 \mu\text{g}$  is observed between 30,000 km and 45,000 km. This implies that filters are most efficient between 15,000 km and 30,000 km. The extraction efficiency diminishes between 30,000 km and 45,000 km and a loss of copper occurs.

Table 5.4.1 shows corrected concentrations based on SRM recoveries of copper using Method 3, estimated to be 80.5% of the overall quantities of copper on the filter. Column 2 shows

concentrations for one square inch of a filter with the standard deviation errors between sample replicates. All filter samples were collected in triplicate.

Table 5.4.1: The average concentrations of Cu for filters samples, with standard deviation errors between replicates are shown in column 2. With corrected concentrations based on percentage recoveries from SRM samples shown in column 3. Column 4 shows recoveries for the entire area of the filter. Column 4 shows recoveries for the entire area of the filter.

Kilometerage (km)	Cu concentrations from filter sample ( $\mu\text{g}$ )	Corrected based on SRM % recovery ( $\mu\text{g}$ )	Recovery of Cu for entire filter area (mg)
0	$0.9 \pm 0.63$	1.08	3.24
15,000	$26.91 \pm 7.01$	33.39	9.69
30,000	$352.17 \pm 147.24$	437.4	126.86
45,000	$271.8 \pm 278.73$	337.68	97.92

#### 5.4.2: Concentrations of Cu between Different Standard Particle Filter Manufacturers.

Figure 5.4.2 shows a comparison between Airforce and Micronair standard particle filters taken at 15,000 km from a Skoda Octavia filters.

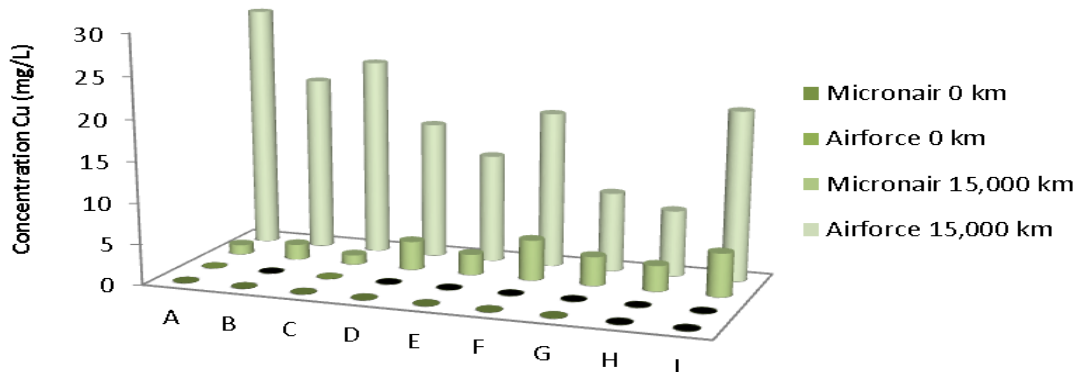


Figure 5.4.2: A comparison of average Cu concentrations from standard particle filters manufacturers by comparing Micronair and Airforce from 0 km to 15,000 km for a Skoda Octavia. All samples were collected in triplicate.

Background Cu levels of Airforce and Micronair standard particle filters are 0  $\mu\text{g}$ . A moderate difference is observed between blank Micronair standard filter samples, 0  $\mu\text{g}$  and those taken at 15,000 km,  $26.91 \pm 7.01$   $\mu\text{g}$ . A significant difference is observed between blank Airforce standard filter samples, 0  $\mu\text{g}$  and those taken at 15,000 km,  $161.91 \pm 96.65$   $\mu\text{g}$ . This indicates that for copper extraction Airforce filters are more efficient than Micronair filters.

Table 5.4.2: The average concentrations of Cu for filters samples, with standard deviation errors between replicates are shown in column 2. With corrected concentrations based on percentage recoveries from SRM samples shown in column 3. Column 4 shows recoveries for the entire area of the filter.

Kilometerage (km)	Cu concentrations from filter sample ( $\mu\text{g}$ )	Corrected based on SRM % recovery ( $\mu\text{g}$ )	Recovery of Cu for entire filter area (mg)
0 km - Airforce	0	0	0
0 km - Micronair	0	0	0
15,000 km - Airforce	$161.91 \pm 96.65$	201.15	58.32
15,000 km - Micronair	$26.91 \pm 7.01$	33.48	15.3

### 5.4.3 Cu Concentrations from Combination Filters from Two Different Manufactures.

Figure 5.4.3 shows a comparison between Airforce and Micronair combination filters taken at 15,000 km from a Skoda Octavia.

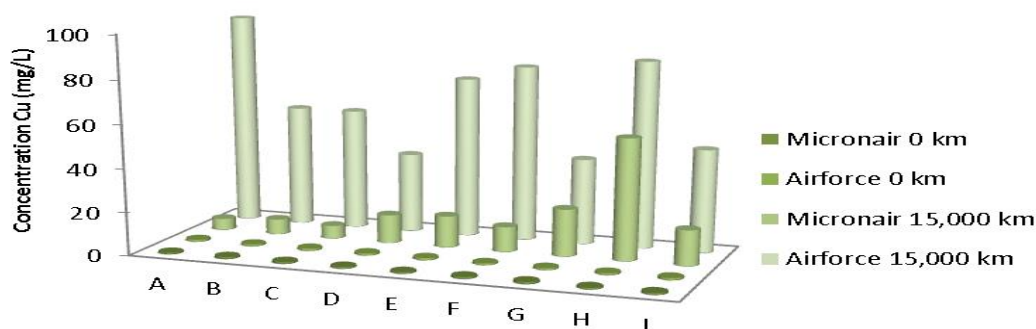


Figure 5.4.3: A comparison of average Cu concentrations from combination filters manufacturers by comparing Micronair and Airforce from 0 km to 15,000 km for a Skoda Octavia. All samples were collected in triplicate.

Combination filters show a significant increase in copper concentrations between blank filters and filters taken at 15,000 km for Airforce,  $566.1 \pm 11.67 \mu\text{g}$  than for Micronair filters,  $148.05 \pm 45.99 \mu\text{g}$ . Therefore extraction efficiency of Airforce combination filters is superior to the extraction efficiency of Micronair combination filters for copper. Implying that filter make plays a significant role in copper extraction when using combination filters for a Skoda Octavia.



Table 5.4.3: The average concentrations of Cu for filters samples, with standard deviation errors between replicates are shown in column 2. With corrected concentrations based on percentage recoveries from SRM samples shown in column 3. Column 4 shows recoveries for the entire area of the filter.

Kilometerage (km)	Cu recovered from filter sample ( $\mu\text{g}$ )	Corrected based on SRM % recovery ( $\mu\text{g}$ )	Recovery of Cu for entire filter area (mg)
0 km - Airforce	$7.65 \pm 12.3$	9.54	2.7
0 km - Micronair	$6.66 \pm 0.81$	8.28	2.43
15,000 km - Airforce	$573.75 \pm 0.63$	712.8	206.64
15,000 km - Micronair	$154.71 \pm 46.8$	192.15	55.71

#### 5.4.4 Cu Concentrations of Standard Particle Filters from Two Different Suppliers in Two Different Car Models.

Figure 5.4.4 shows a comparison of Micronair standard particle filters taken at kilometerages of 15,000 km, 30,000 km and 45,000 km from Car Model 2 (a Toyota Aventis).

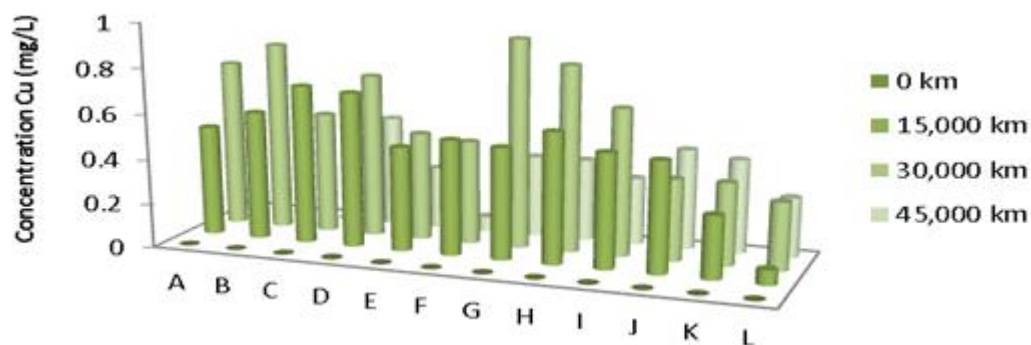


Figure 5.4.4: Average Cu concentrations for a Toyota Aventis, standard particle filter from 0 km to 45,000 km in increments of 15,000 km, manufactured by Micronair. All samples were collected in triplicate.

A moderate difference is observed between blank filters samples, 0  $\mu\text{g}$  and those taken at 15,000 km,  $4.32 \pm 3.87 \mu\text{g}$ . However a significant difference is not observed between 15,000 km  $4.32 \pm 3.87 \mu\text{g}$ , 30,000 km,  $5.4 \pm 2.34 \mu\text{g}$  and 45,000 km,  $6.3 \pm 2.79 \mu\text{g}$ . This indicates that for copper Micronair particle filters in a Toyota Aventis become less effective after 15,000 km. Filters from a Toyota Aventis are less efficient than for the same filter make placed in a Skoda Octavia over the same kilometerage intervals. From 0 km to 15,000 km Micronair standard particle filters in a Skoda Octavia extract  $26.91 \pm 71.01 \mu\text{g}$  while in a

Toyota Aventis they extract  $4.32 \pm 3.87 \mu\text{g}$ . Between 15,000 km and 30,000 km the filter in a Skoda Octavia yields a concentration of  $271.8 \pm 278.73$  but a filter from the same manufacturer in a Toyota Aventis over the same kilometerage yields a concentration of  $5.4 \pm 2.34 \mu\text{g}$ . Between 30,000 km and 45,000 km in a Skoda Octavia de-absorption occurs with a decrease in copper concentrations,  $80.37 \pm 131.49 \mu\text{g}$ , however the same filter in a Toyota Aventis doesn't appear to absorb a significant quantity of copper but de-absorption does not occur.

Table 5.4.4: The average concentrations of Cu for filters samples, with standard deviation errors between replicates are shown in column 2. With corrected concentrations based on percentage recoveries from SRM samples shown in column 3. Column 4 shows recoveries for the entire area of the filter.

Kilometerage (km)	Cu concentrations from filter sample ( $\mu\text{g}$ )	Corrected based on SRM % recovery ( $\mu\text{g}$ )	Recovery of Cu for entire filter area (mg)
0 km	0	0	0
15,000 km	$4.32 \pm 3.87$	5.31	1.69
30,000 km	$5.4 \pm 2.34$	6.75	2.16
45,000 km	$6.3 \pm 2.79$	7.83	2.49

Filters in a Toyota Aventis are positioned horizontally while filters in a Skoda Octavia are placed vertically, this suggests that filter orientation place a significant role in extraction efficiency. With vertical filters have higher extraction efficiency up to 30,000 km. However, loss of analyte does not appear to occur in horizontally orientated filters.

#### 5.4.5: Concentrations for a Third Standard Particle Filter Manufacturer in a Toyota Aventis.

Figure 5.4.5: Shows a comparison of Cu on Nip & Denso standard particle filters taken at 15,000 km, 30,000 km and 45,000 km from a Toyota Aventis.

A similar difference is observed between 0 km and 15,000 km and 15,000 km and 30,000 km  $5 \pm 3 \mu\text{g}$ . This indicates that for Nip & Denso filters in a Toyota Aventis extraction efficiency doesn't change over this kilometre range. The extraction efficiencies from 0 km to 30,000 km

are comparable to the same kilometre range for Micronair standard particle filtered sampled from a Toyota Aventis. The extraction efficiency at 45,000 km ( $59.49 \pm 18.18 \mu\text{g}$ ) is however ten times the extraction efficiency for a Micronair standard particle filtered sampled from a a Toyota Aventis ( $1.1 \pm 0.04$ ). For Nip & Denso filters in a Toyota Aventis, the efficiency improves with particle build up.

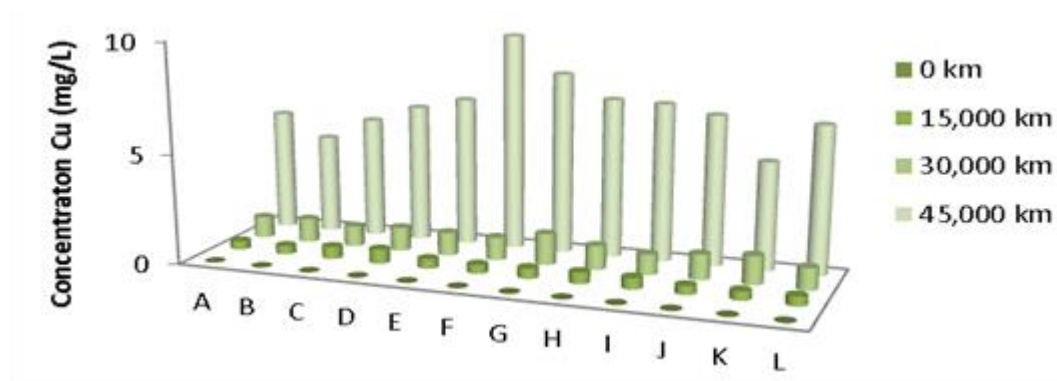


Figure 5.4.5: Average Cu concentrations for a Toyota Aventis, standard particle filter from 0 km to 45,000 km in increments of 15,000 km, manufactured by Nip & Denso. All samples were collected in triplicate.

Table 5.4.5: The average concentrations of Cu for filters samples, with standard deviation errors between replicates are shown in column 2. With corrected concentrations based on percentage recoveries from SRM samples shown in column 3. Column 4 shows recoveries for the entire area of the filter.

Kilometerage (km)	Cu concentrations from filter sample ( $\mu\text{g}$ )	Corrected based on SRM % recovery ( $\mu\text{g}$ )	Recovery of Cu for entire filter area (mg)
0 km	0	0	0
15,000 km	$4.86 \pm 2.16$	6.12	1.944
30,000 km	$9.81 \pm 4.68$	12.15	3.897
45,000 km	$59.49 \pm 18.18$	73.89	23.634

### Copper Conclusions:

Micronair standard particle filters show an increase in Cu values from 0 km to 15,000 km and from 15,000 km to 30,000 km of  $26.01 \pm 6.38 \mu\text{g}$  and  $325.26 \pm 140.23 \mu\text{g}$ , respectively. A decrease of  $80.37 \pm 131.49 \mu\text{g}$  in Cu values is observed from 30,000 km to 45,000 km.

Airforce particle filters yield concentrations over 3 times those of Micronair particle filters in a Skoda Octavia from 0 km to 15,000 km. Airforce combination filters also show concentrations over 3 times those of Micronair combination filters. This indicates that both particle and combination Airforce filters have superior extraction efficiencies for Cu.

Micronair standard particle filters in a Toyota Aventis show an increase from 0 m to 15,000, from 15,000 km to 30,000 km and from 30,000 km to 45,000 km. However, concentrations for all three kilometerage intervals are consistently low at  $4.32 \pm 3.87 \mu\text{g}$ ,  $5.4 \pm 2.34 \mu\text{g}$  and  $6.3 \pm 2.79 \mu\text{g}$ , respectively. Nip and Denso filters in a Toyota Aventis also show an increase from 0 m to 15,000, from 15,000 km to 30,000 km and from 30,000 km to 45,000 km. The concentrations from Nip and Denso are higher than from Micronair filters,  $4.86 \pm 2.16 \mu\text{g}$ ,  $9.81 \pm 4.68 \mu\text{g}$  and  $59.49 \pm 18.18 \mu\text{g}$ , respectively. This indicates that Nip and Denso filters in a Toyota Aventis yield higher concentrations than Micronair filters over the same kilometerage intervals.

#### 5.4.6: Cu concentrations at 15,000 km less blanks for all filter makes.

All makes of standard particle and combination filters were run to a minimum of 15,000 km in their respective car models. 15,000 km is the replacement interval recommended by filter manufactures. A comparison was made between all car models and filter manufacturers up to a kilometerage of 15,000 km, shown in Table 5.4.6.

Table 5.4.6. Shows filter concentrations from filters run to 15,000 km minus blank filter concentrations, for all filter types tested, extrapolated over the surface area of the filter.

Car and filter make	$\mu\text{g}$
Micronair Particle Filter - Skoda Octavia	$26.01 \pm 6.38$
Airforce Particle Filter - Skoda Octavia	$161.91 \pm 96.65$
Airforce Combination filters – Skoda Octavia	$566.1 \pm 11.67$
Micronair Combination filters – Skoda Octavia	$148.05 \pm 45.99$
Micronair Particle Filter - Toyota Aventis	$4.32 \pm 3.87$
Nip & Denso Particle - Toyota Aventis	$4.86 \pm 2.16$

Airforce Combination filters (in a Skoda Octavia) are the most efficient filters, extracting  $566.1 \pm 11.67 \mu\text{g}$  of copper and Airforce standard particle filters (in a Skoda Octavia) are

most efficient standard particle filters, extracting  $161.91 \pm 96.65 \mu\text{g}$  of copper. This implies that Airforce filters are the most efficient filters at copper extraction. Like Airforce filters, Micronair Combination filters (in a Skoda Octavia) are more efficient than Micronair standard particle filters (in a Skoda Octavia),  $148.05 \pm 45.99 \mu\text{g}$  and  $26.01 \pm 6.38 \mu\text{g}$ , respectively. The concentrations for Micronair Particle Filter (from a Toyota Aventis), and Nip & Denso Particle (from a Toyota Aventis), are comparable and poor relative to the other filters tested,  $4.32 \pm 3.87 \mu\text{g}$  and  $4.86 \pm 2.16 \mu\text{g}$ , respectively. This implies the design or orientation of filters in a Toyota Aventis (horizontal) is less effective than that of a Skoda Octavia filters (vertical) from 0 km to 15,000 km.

Filters in a Skoda Octavia are more efficient than filters in a Toyota Aventis for all filter makes. Filters in a Skoda Octavia are placed vertically while filters in a Toyota Aventis are placed horizontally. This implies that for copper extraction from 0 km to 15,000 km filter orientation plays a significant role and that vertically orientated filters are more efficient at retaining copper. It could also be speculated that the source of copper produces very fine particles which are trapped more efficiently by Airforce filters due to a tighter weave or higher accumulations at higher kilometerages. This may be enhanced further by the carbon layer of the combination filters to trap a very significant amount of available copper.

## 5.5: Iron:

### 5.5.1: Concentrations of Fe at Different Kilometerages in Car Model 1 (a Skoda Octavia).

Figure 5.5.1 shows a comparison of iron levels between Micronair particle filters taken from (a Skoda Octavia) at kilometerages of 15,000 km, 30,000 km and 45,000 km.

A blank filter was analysed as a background reference, background levels of Fe were found to be  $3.06 \pm 0.9 \mu\text{g}$ . A significant difference is observed between 0 km,  $3.06 \pm 0.9 \mu\text{g}$  and 15,000 km,  $56.7 \pm 15.97 \mu\text{g}$ . A significant difference of  $156.06 \pm 98.69 \mu\text{g}$  is observed between 15,000 km and 30,000 km, with an insignificant difference observed between 30,000 km and 45,000 km. The filters are most efficient between 15,000 km and 30,000 km. The extraction

efficiency diminishes between 30,000 km and 45,000 km. This suggests that as particulates build up on the filter the efficiency of the filter improves, to a point.

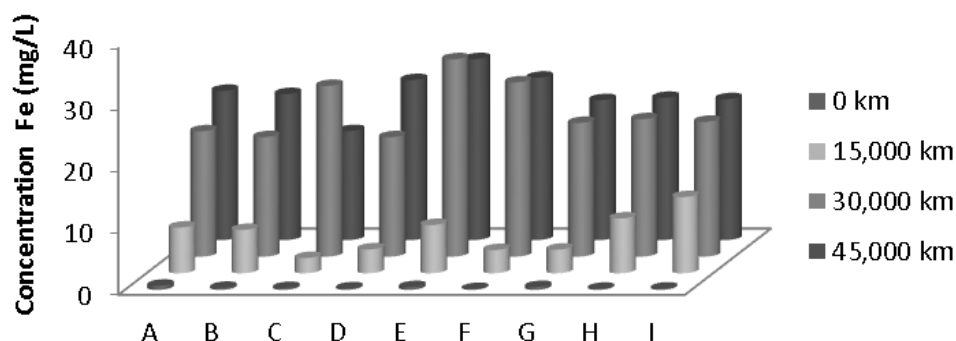


Figure 5.5.1: Average Fe concentrations for a Skoda Octavia, standard particle filter from 0 km to 45,000 km in increments of 15,000 km, manufactured by Micronair. All samples were collected in triplicate.

Table 5.5.1: The average concentrations of Fe for filters samples, with standard deviation errors between replicates are shown in column 2. With corrected concentrations based on percentage recoveries from SRM samples shown in column 3. Column 4 shows recoveries for the entire area of the filter.

Kilometerage (km)	Fe concentrations from filter sample ( $\mu\text{g}$ )	Corrected based on SRM % recovery ( $\mu\text{g}$ )	Recovery of Fe for entire filter area (mg)
0	$3.06 \pm 0.9$	3.69	1.08
15,000	$56.7 \pm 15.97$	68.85	19.98
30,000	$212.76 \pm 114.66$	258.21	74.88
45,000	$208.98 \pm 86.31$	253.62	73.53

Table 5.5.1 shows corrected concentrations for iron based on SRM recoveries using Method 3, estimated to be 80.5% of the overall quantities of iron on the SRM impregnated filter. Column 2 shows concentrations for one square inch of a filter, total filter concentrations have been calculated and shown in column 3 based on the overall filter area. All filter samples were collected in triplicate.

### 5.5.2: Concentrations of Fe between Different Standard Particle Filter Manufacturers.

Figure 5.5.2 Shows a comparison of percentage iron concentrations between Airforce and Micronair standard particle filters taken at 15,000 km from a Skoda Octavia filters.

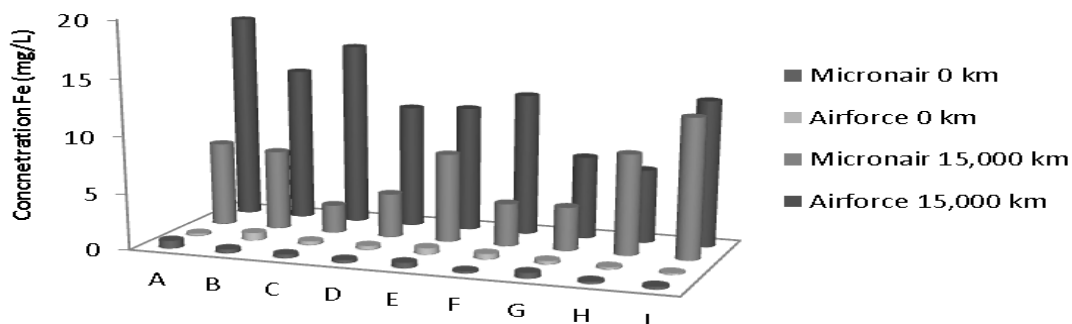


Figure 5.5.2: A comparison of average Fe concentrations from standard particle filters manufacturers by comparing Micronair and Airforce from 0 km to 15,000 km for a Skoda Octavia. All samples were collected in triplicate.

Background Fe levels of Airforce and Micronair standard particle filters are comparable; at  $3.06 \pm 1.26 \mu\text{g}$ . A significant difference is observed between blank samples and filter taken at 15,000 km for both Airforce and Micronair standard particle filter samples,  $3.06 \pm 1.26 \mu\text{g}$  for blank filters and  $56.7 \pm 6.97 \mu\text{g}$  and  $108.72 \pm 11.88 \mu\text{g}$  for Micronair and Airforce standard particle filters, respectively. The extraction efficiency for iron of Airforce is double that of Micronair standard particle filter.

Kilometerage (km)	Fe concentrations from filter sample ( $\mu\text{g}$ )	Corrected based on SRM % recovery ( $\mu\text{g}$ )	Recovery of Fe for entire filter area (mg)
0 km - Airforce	$3.06 \pm 1.26$	3.69	1.08
0 km - Micronair	$3.06 \pm 0.9$	3.69	1.08
15,000 km - Airforce	$108.72 \pm 11.88$	131.94	38.25
15,000 km - Micronair	$56.7 \pm 6.97$	68.85	19.98

Table 5.5.2: The average percentage concentrations of Fe for filters samples, with standard deviation errors between replicates are shown in column 2. With corrected concentrations based on percentage recoveries from SRM samples shown in column 3. Column 4 shows recoveries for the entire area of the filter.

### 5.5.3 Fe Concentrations from Combination Filters from Two Different Manufactures.

Figure 5.5.3: shows a comparison between Airforce and Micronair combination filters taken at 15,000 km from a Skoda Octavia.

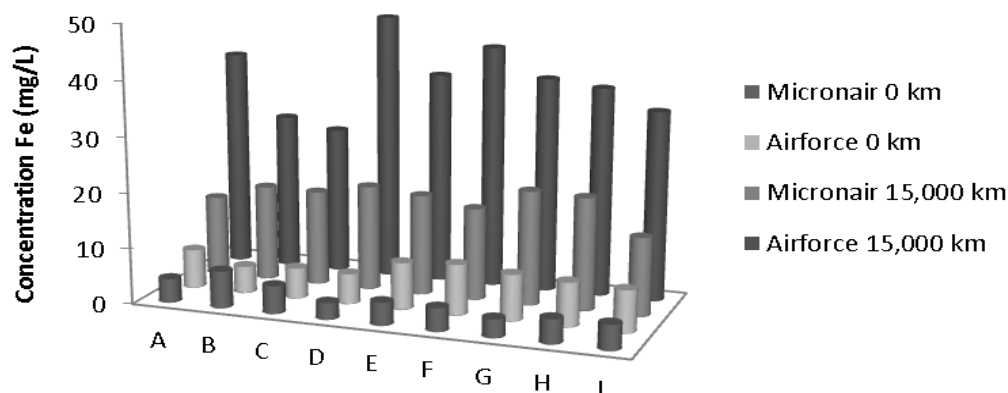


Figure 5.5.3: A comparison of average Fe concentrations from combination filters manufacturers by comparing Micronair and Airforce from 0 km to 15,000 km for a Skoda Octavia. All samples were collected in triplicate.

Combination filters show a greater increase between blank filters and filters taken at 15,000 km for Micronair filters  $270.24 \pm 88.56 \mu\text{g}$  than for Airforce filters,  $117.9 \pm 54.72 \mu\text{g}$  (15,000 km concentrations less blank filter concentrations). Indicating that filter manufacturer plays a significant role in iron extraction when using combination filters for a Skoda Octavia.

Table 5.5.3: The average concentrations of Fe for filters samples, with standard deviation errors between replicates are shown in column 2. With corrected concentrations based on percentage recoveries from SRM samples shown in column 3. Column 4 shows recoveries for the entire area of the filter.

Kilometerage (km)	Fe concentrations from filter sample ( $\mu\text{g}$ )	Corrected based on SRM % recovery ( $\mu\text{g}$ )	Recovery of Fe for entire filter area (mg)
0 km - Airforce	$39.42 \pm 9.27$	47.88	13.86
0 km - Micronair	$64.08 \pm 9.54$	77.85	22.59
15,000 km - Airforce	$157.32 \pm 63.99$	190.98	55.35
15,000 km - Micronair	$334.26 \pm 98.1$	405.72	117.63



#### 5.5.4 Fe Concentrations of Standard Particle Filters from Two Different Suppliers in Two Different Car Models.

Figure 5.5.4 Shows a comparison of Micronair particle filters taken at kilometerages of 15,000 km, 30,000 km and 45,000 km from a Toyota Aventis.

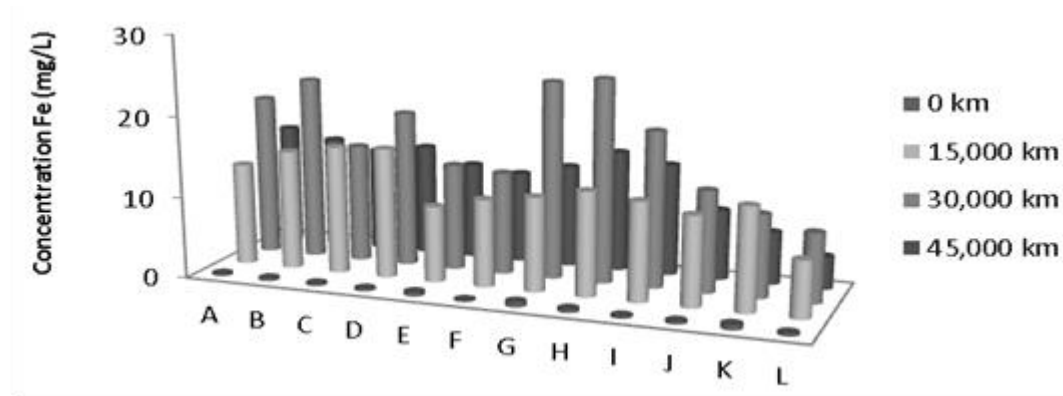


Figure 5.5.4: Average Fe concentrations for a Toyota Aventis, standard particle filter from 0 km to 45,000 km in increments of 15,000 km, manufactured by Micronair. All samples were collected in triplicate.

A significant difference is observed between blank filters samples,  $3.15 \pm 1.44 \mu\text{g}$  and those taken at 15,000 km  $99.54 \pm 63.72 \mu\text{g}$ . A difference is observed between 15,000 km  $99.54 \pm 63.72 \mu\text{g}$  and 30,000 km,  $152.19 \pm 60.21 \mu\text{g}$ . A decrease in iron levels is observed between 30,000 km and 45,000 km,  $152.19 \pm 60.21 \mu\text{g}$  and  $104.49 \pm 25.29$  respectively, which may imply that de-absorption has occurred when filters become saturated. It also indicates that for iron, Micronair standard particle filters in a Toyota Aventis are more effective between 0 km and 30,000 km but efficiency decreases from 30,000 km to 45,000 km.

Concentrations of iron from filters from a Toyota Aventis are comparable to the same filter make placed in a Skoda Octavia over the same kilometerage intervals. From 0 km to 15,000 km Micronair standard particle filters in a Skoda Octavia extract  $53.64 \pm 15.07 \mu\text{g}$  while in a Toyota Aventis they extract  $96.39 \pm 62.28 \mu\text{g}$ . Between 15,000 km and 30,000 km the filter in a Skoda Octavia yields a concentration of  $156.06 \pm 98.69 \mu\text{g}$  but a filter from the same manufacturer in a Toyota Aventis over the same kilometerage yields a concentration of  $52.65 \pm 3.51 \mu\text{g}$ . De-absorption occurs between 30,000 km and 45,000 km in a Toyota Aventis, with a decrease in iron concentrations of  $47.7 \pm 34.22 \mu\text{g}$ , however the same filter in a Skoda

Octavia doesn't appear to absorb a significant quantity of iron but de-absorption does not occur.

Table 5.5.4: The average concentrations of Fe for filters samples, with standard deviation errors between replicates are shown in column 2. With corrected concentrations based on percentage recoveries from SRM samples shown in column 3. Column 4 shows recoveries for the entire area of the filter.

Kilometerage (km)	Fe concentrations from filter sample ( $\mu\text{g}$ )	Corrected based on SRM % recovery ( $\mu\text{g}$ )	Recovery of Fe for entire filter area (mg)
0 km	$3.15 \pm 1.44$	3.87	1.26
15,000 km	$99.54 \pm 63.72$	120.78	38.61
30,000 km	$152.19 \pm 60.21$	184.68	59.13
45,000 km	$104.49 \pm 25.29$	126.9	40.59

Filters in a Toyota Aventis are positioned horizontally while filters in a Skoda Octavia are placed vertically, this suggests that filter orientation plays a significant role in extraction efficiency. With vertical filters having higher extraction efficiencies up to 30,000 km. De-absorption of iron does not appear to occur in vertically orientated filters.

#### 5.5.5: Concentrations for a Third Standard Particle Filter Manufacturer in a Toyota Aventis.

Figure 5.5.5 shows a comparison of Fe levels on Nip & Denso standard particle filters taken at 15,000 km, 30,000 km and 45,000 km from a Toyota Aventis.

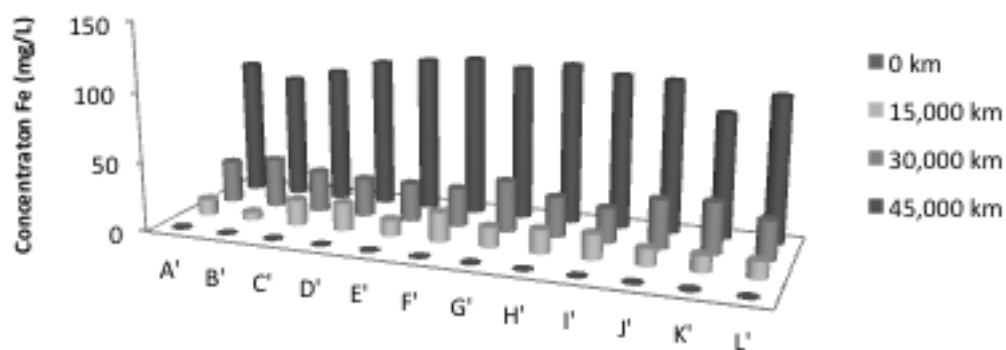


Figure 5.5.5: Average Fe concentrations for a Toyota Aventis, standard particle filter from 0 km to 45,000 km in increments of 15,000 km, manufactured by Nip & Denso. All samples were collected in triplicate.

A significant difference is observed between blank filters samples and those taken at 15,000 km,  $129.33 \pm 81.36 \mu\text{g}$ . A significant increase is observed between 15,000 km and 30,000 km,  $146.97 \pm 28.17 \mu\text{g}$  but the most significant increase is observed between 30,000 km and 45,000 km,  $665.64 \pm 57.42 \mu\text{g}$ . This implies that for Nip & Denso filters run in a Toyota Aventis the extraction efficiency for iron improves when the filters become saturated.

Table 5.5.5: The average concentrations of Fe for filters samples, with standard deviation errors between replicates are shown in column 2. With corrected concentrations based on percentage recoveries from SRM samples shown in column 3. Column 4 shows recoveries for the entire area of the filter.

Kilometerage (km)	Fe concentrations from filter sample ( $\mu\text{g}$ )	Corrected based on SRM % recovery ( $\mu\text{g}$ )	Recovery of Fe for entire filter area (mg)
0 km	$2.25 \pm 1.62$	2.7	0.9
15,000 km	$131.58 \pm 82.98$	159.75	51.12
30,000 km	$278.55 \pm 111.15$	338.13	108.18
45,000 km	$944.19 \pm 168.57$	1,145.88	366.66

### Iron Conclusions:

An increase of  $53.01 \pm 15.07 \mu\text{g}$  in iron levels is observed from 0 km to 15,000 km for Micronair standard particle filters run in a Skoda Octavia. An increase from  $56.7 \pm 15.97 \mu\text{g}$  to  $212.76 \pm 114.66 \mu\text{g}$  is observed from 15,000 km to 30,000 km. No significant change is observed between 30,000 km and 45,000 km.

Airforce standard particle filters show iron levels of  $105.66 \pm 10.62 \mu\text{g}$  and Micronair standard particle filters show iron concentrations of  $53.64 \pm 6.07 \mu\text{g}$ , run from 0 km to 15,000 km in a Skoda Octavia. This indicates that Airforce standard particle filters have a superior extraction efficiency than Micronair filters.

Airforce combination filters show a concentration of  $117.9 \pm 54.72 \mu\text{g}$ , comparable to standard particle filters. However, Micronair combination filters show a significant improvement over standard particle filters,  $270.18 \pm 88.54 \mu\text{g}$  and  $53.64 \pm 6.07 \mu\text{g}$ , respectively.

Micronair standard particle run in a Toyota Aventis show an increase from 0 km to 15,000 km ( $96.39 \pm 62.28 \mu\text{g}$ ) and from 15,000 km to 30,000 km ( $52.65 \pm 3.51 \mu\text{g}$ ). A decrease is observed from 30,000 km to 45,000 km of  $47.7 \pm 34.29 \mu\text{g}$ .

Nip and Denso filters in a Toyota Aventis show an increase from 0 km to 15,000 km of  $129.33 \pm 81.36 \mu\text{g}$  and an increase from 15,000 km to 30,000 km of  $146.97 \pm 28.17 \mu\text{g}$  (from  $131.58 \pm 82.98 \mu\text{g}$  to  $278.55 \pm 111.15 \mu\text{g}$ ). A significant increase is observed from 30,000 km to 45,000 km  $665.64 \pm 57.42 \mu\text{g}$  (from  $278.55 \pm 111.15 \mu\text{g}$  to  $944.19 \pm 168.57 \mu\text{g}$ ).

This indicates that for Nip and Denso filters, filtration improves with use, as particulates build up on the filters.

#### 5.5.6: Fe concentrations at 15,000 km less background levels for all filter makes.

All makes of standard particle and combination filters were run to a minimum of 15,000 km in their respective car models. A comparison was made between all car models and filter manufacturers up to a kilometerage of 15,000 km, shown in Table 5.5.6.

The concentrations for Airforce Particle Filters (from a Skoda Octavia),  $105.66 \pm 10.62 \mu\text{g}$ , Micronair Particle Filter (from a Skoda Octavia),  $53.64 \pm 15.07 \mu\text{g}$  and a Nip & Denso Particle (from a Toyota Aventis)  $129.33 \pm 81.36 \mu\text{g}$ , are comparable. Micronair Combination filters (from a Skoda Octavia) are the most efficient filter,  $270.18 \pm 88.56 \mu\text{g}$  and a Micronair standard particle filters (from a Toyota Aventis),  $96.39 \pm 62.28 \mu\text{g}$  are the least efficient filters, for the distance in kilometres covered by the vehicles.

Table 5.5.6. Shows filter concentrations from filters run to 15,000 km minus blank filter concentrations, for all filter types tested, extrapolated over the surface area of the filter.

Car and filter make	$\mu\text{g}$
Micronair Particle Filter - Skoda Octavia	$53.64 \pm 15.07$
Airforce Particle Filter - Skoda Octavia	$105.66 \pm 10.62$
Airforce Combination filters – Skoda Octavia	$117.9 \pm 54.72$
Micronair Combination filters – Skoda Octavia	$270.18 \pm 88.56$
Micronair Particle Filter - Toyota Aventis	$96.39 \pm 62.28$
Nip & Denso Particle - Toyota Aventis	$129.33 \pm 81.36$

## 5.6: Lead:

### 5.6.1: Concentrations of Pb at Different Kilometerages in Car Model 1 (a Skoda Octavia).

Figure 5.6.1 shows a comparison between Micronair particle filters taken from (a Skoda Octavia) at kilometerages of 15,000 km, 30,000 km and 45,000 km.

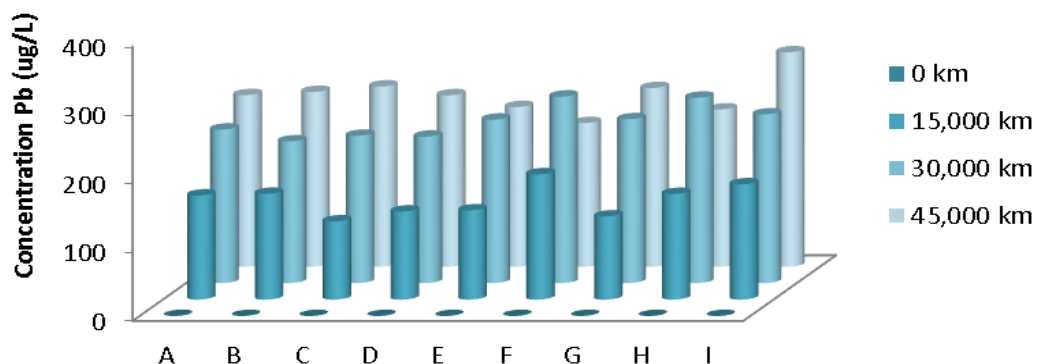


Figure 5.6.1: Average Pb concentrations for a Skoda Octavia, standard particle filter from 0 km to 45,000 km in increments of 15,000 km, manufactured by Micronair. All samples were collected in triplicate.

Table 5.6.1 shows corrected concentrations based on SRM recoveries of lead using Method 3, estimated to be 87.3% of the overall quantities of lead on the filter. Column 2 shows concentrations for one square inch of a filter. All filter samples were collected in triplicate.

Table 5.6.1: The average concentrations of Pb for filters samples, with standard deviation errors between replicates are shown in column 2. With corrected concentrations based on percentage recoveries from SRM samples shown in column 3. Column 4 shows recoveries for the entire area of the filter.

Kilometerage (km)	Pb concentrations from filter sample (ng)	Corrected based on SRM % recovery (ng)	Recovery of Pb for entire filter area (µg)
0	0 ± 1.08	0	0
15,000	1,303.2 ± 199.71	1,492.83	432.9
30,000	2,123.37 ± 520.74	2,432.25	705.33
45,000	2,259.9 ± 436.68	2,588.67	750.69

A blank filter was analysed as a reference. A significant difference in lead levels is observed between the blank,  $0 \pm 1.08$  ng, the sample taken at 15,000 km,  $1,303.2 \pm 199.71$  ng and 30,000 km,  $2,123.37 \pm 520.74$  ng. A moderate increase is observed between 30,000 km,  $2,123.37 \pm 520.74$  ng and 45,000 km,  $2,259.9 \pm 436.68$  ng. This implies that the extraction efficiency of the filter diminishes over time, with the peak extraction period being from 0 km to 15,000 km, followed closely by 15,000 km to 30,000 km but the extraction efficiency has significantly decreased from 30,000 km to 45,000 km.

### 5.6.2: Concentrations of Pb between Different Standard Particle Filter Manufacturers.

Figure 5.6.2 shows a comparison between Airforce and Micronair standard particle filters taken at 15,000 km from a Skoda Octavia filters.

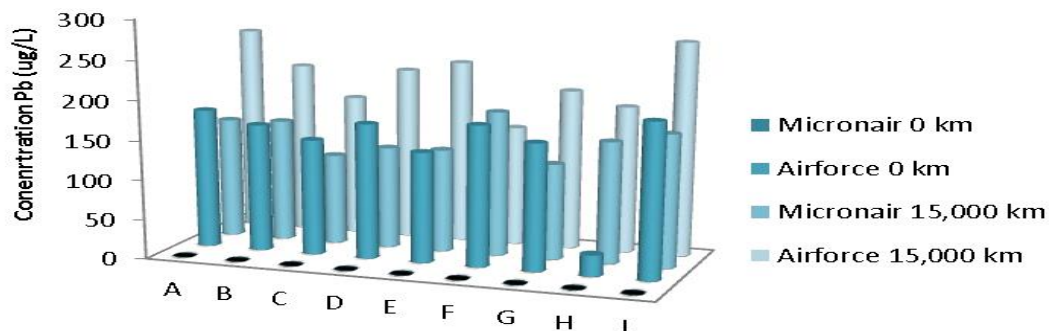


Figure 5.6.2: A comparison of average Pb concentrations from standard particle filters manufacturers by comparing Micronair and Airforce from 0 km to 15,000 km for a Skoda Octavia. All samples were collected in triplicate.

Table 5.6.2 The average concentrations of Pb for filters samples, with standard deviation errors between replicates are shown in column 2. With corrected concentrations based on percentage recoveries from SRM samples shown in column 3. Column 4 shows recoveries for the entire area of the filter.

Kilometerage (km)	Pb concentrations from filter sample (ng)	Corrected based on SRM % recovery (ng)	Recovery of Pb for entire filter area (µg)
0 - Airforce	$1,352.25 \pm 334.17$	1,548.99	449.19
0 - Micronair	0	0	0
15,000 - Airforce	$1,906.11 \pm 297.54$	2,183.49	633.15
15,000 - Micronair	$1,303.2 \pm 199.71$	1,492.83	432.9

A significant increase is observed between the blank samples and samples taken at 15,000 km for Micronair filters, from 0 ng to  $1,303.2 \pm 199.71$  ng. A difference is observed between blank samples and 15,000 km samples for Airforce filters, from  $1,352.25 \pm 334.17$  ng to  $1,906.11 \pm 297.54$  ng. An increase is observed between Micronair and Airforce filters at 15,000 km,  $1,303.2 \pm 199.71$  ng and  $1,906.11 \pm 297.54$  ng respectively, but taking into account the unexpected contribution of lead levels in the blank Airforce samples ( $580.86 \pm 36.63$  ng less blank) Micronair filters are observed to be more efficient.

### 5.6.3 Pb Concentrations from Combination Filters from Two Different Manufactures.

Figure 5.6.3 shows a comparison of Pb levels between Airforce and Micronair combination filters taken at 15,000 km from a Skoda Octavia.

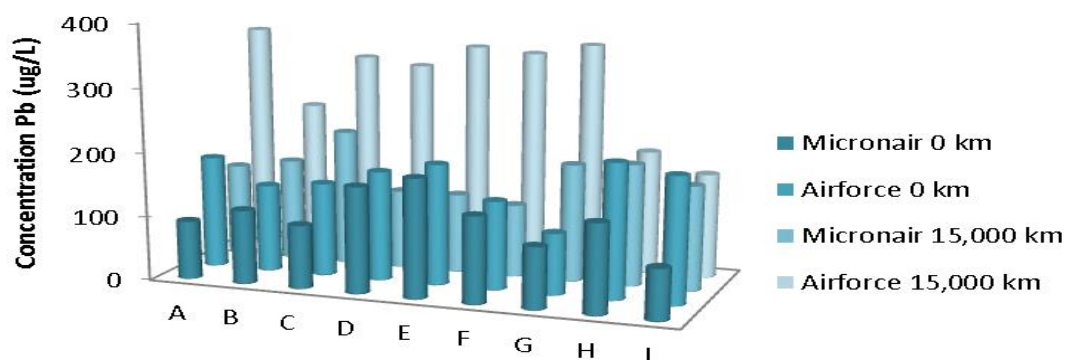


Figure 5.6.3: A comparison of average Pb concentrations from combination filters manufacturers by comparing Micronair and Airforce from 0 km to 15,000 km for a Skoda Octavia. All samples were collected in triplicate.

Table 5.6.3: The average concentrations of Pb for filters samples, with standard deviation errors between replicates are shown in column 2. With corrected concentrations based on percentage recoveries from SRM samples shown in column 3. Column 4 shows recoveries for the entire area of the filter.

Kilometerage (km)	Pb concentrations from filter sample (ng)	Corrected based on SRM % recovery (ng)	Recovery of Pb for entire filter area (µg)
0 - Airforce	$1,462.14 \pm 289.44$	1,674.81	485.64
0 - Micronair	$1,120.68 \pm 710.91$	1,283.67	372.24
15,000 - Airforce	$2,601.09 \pm 425.61$	2,979.45	864.9
15,000 - Micronair	$1,884.15 \pm 587.07$	2,158.29	625.86

A moderate increase is observed between the blank samples,  $1,120.68 \pm 710.91$  ng and those taken at 15,000 km,  $1,884.15 \pm 587.07$  ng for Micronair filters. A larger difference is observed between blank samples,  $1,462.14 \pm 289.44$  ng and 15,000 km samples,  $2,601.09 \pm 425.61$  ng for Airforce filters. A moderate difference is observed between Micronair and Airforce filters at 15,000 km ( $763.47 \pm 123.84$  ng and  $1,138.95 \pm 136.17$  ng respectively minus background levels). Based on these concentrations Airforce combination filters are marginally more efficient than Micronair filters.

#### 5.6.4 Pb Concentrations of Standard Particle Filters from Two Different Suppliers in Two Different Car Models.

Figure 5.6.4 Shows a comparison of Pb levels on Micronair standard particle filters taken at kilometerages of 15,000 km, 30,000 km and 45,000 km from a Toyota Aventis.

A moderate difference is observed between blank filter samples and those taken at 15,000 km, from  $1,325.7 \pm 454.41$  ng to  $1,761.3 \pm 313.11$  ng. No observable difference is noted between 15,000 km,  $1,761.3 \pm 313.11$  ng, 30,000 km,  $1,679.58 \pm 555.48$  ng and 45,000 km,  $1,662.84 \pm 430.11$  ng, indicating that Micronair standard particle filters in a Toyota Aventis are ineffective at extracting lead.

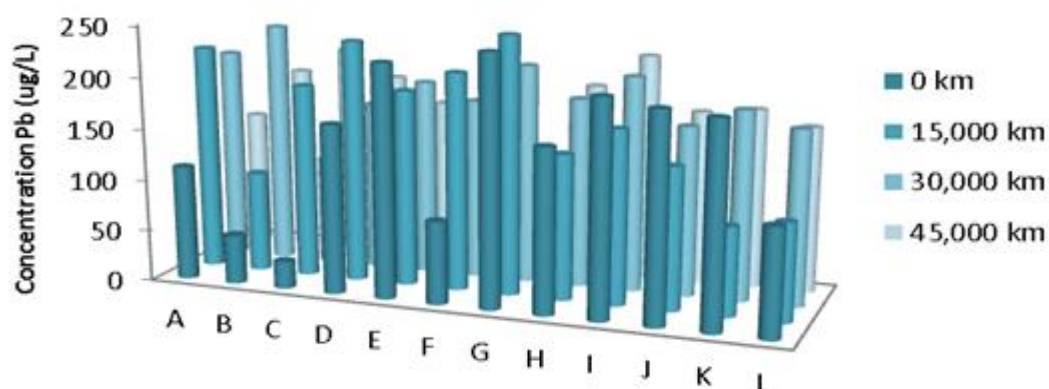


Figure 5.6.4: Average Pb concentrations for a Toyota Aventis, standard particle filter from 0 km to 45,000 km in increments of 15,000 km, manufactured by Micronair. The legend key for the x axis is shown in Table 1.4.2. All samples were collected in triplicate.



Table 5.6.4: The average concentrations of Pb for filters samples, with standard deviation errors between replicates are shown in column 2. With corrected concentrations based on percentage recoveries from SRM samples shown in column 3. Column 4 shows recoveries for the entire area of the filter.

Kilometerage (km)	Pb concentrations from filter sample (ng)	Corrected based on SRM % recovery (ng)	Recovery of Pb for entire filter area ( $\mu\text{g}$ )
0 km	$1,325.7 \pm 454.41$	1,518.57	485.91
15,000 km	$1,761.3 \pm 313.11$	2,017.53	645.57
30,000 km	$1,679.58 \pm 555.48$	1,923.93	615.6
45,000 km	$1,662.84 \pm 430.11$	1,904.76	609.48

Comparing concentrations for the same filter make, over the same kilometerage range for a Skoda Octavia and a Toyota Aventis shows that Micronair filters in a Skoda Octavia are more effective at lead extraction. From 0 km to 15,000 km Micronair standard particle filters in a Skoda Octavia extract  $1,303.2 \pm 198.63$  ng while in a Toyota Aventis they extract  $435.6 \pm 141.3$  ng. Between 15,000 km and 30,000 km the filter in a Skoda Octavia yields a concentration of  $820.17 \pm 321.73$  but a filter from the same manufacturer in a Toyota Aventis over the same kilometerage shows a de-absorption of  $81.72 \pm 242.27$  ng. From 15,000 km to 30,000 km and 30,000 km to 45,000 km in a Toyota Aventis de-absorption occurs with a decrease in lead concentrations of  $81.72 \pm 242.27$  ng and  $16.74 \pm 125.37$  ng, loss of particulates doesn't occur in a Skoda Octavia from 15,000 km to 30,000 km and 30,000 km to 45,000 km.

Filters in a Toyota Aventis are positioned horizontally while filters in a Skoda Octavia are placed vertically. This suggests that filter orientation plays a significant role in extraction efficiency. Vertical filters have higher extraction efficiencies. De-absorption of lead must occur in horizontally orientated filters.

### 5.6.5: Concentrations for a Third Standard Particle Filter Manufacturer in a Toyota Aventis.

Figure 5.6.5 shows a comparison of Nip & Denso standard particle filters taken at 15,000 km, 30,000 km and 45,000 km from a Toyota Aventis.

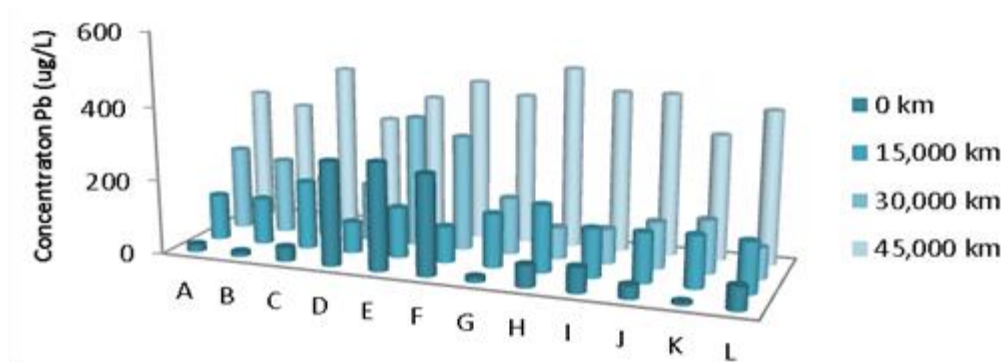


Figure 5.6.5: Average Pb concentrations for a Toyota Aventis, standard particle filter from 0 km to 45,000 km in increments of 15,000 km, manufactured by Nip & Denso. All samples were collected in triplicate.

Table 5.6.5: The average concentrations of Pb for filters samples, with standard deviation errors between replicates are shown in column 2. With corrected concentrations based on percentage recoveries from SRM samples shown in column 3. Column 4 shows recoveries for the entire area of the filter.

Kilometerage (km)	Pb concentrations from filter sample (ng)	Corrected based on SRM % recovery (ng)	Recovery of Pb for entire filter area (μg)
0 km	218.16 ± 135.36	249.93	79.92
15,000 km	1,648.53 ± 397.26	1,888.38	604.26
30,000 km	1,947.96 ± 123.2	2,231.37	713.97
45,000 km	3,595.32 ± 102.04	4,118.4	1,317.87

A difference of  $1430.37 \pm 261.9$  ng is observed between blank filters samples and those taken at 15,000 km. A moderate difference is not observed between samples taken at 15,000 km and 30,000 km,  $299.43 \pm 274.06$  ng but a significant increase is observed for samples taken at 45,000 km,  $1,647.36 \pm 21.16$  ng indicating that for lead filters become more effective with use, perhaps due to filter particulate blockage.

### Lead Conclusions:

A significant increase is observed from 0 km to 15,000 km of  $1,303.2 \pm 198.63$  ng and from 15,000 km to 30,000 km of  $820.17 \pm 321.03$  ng. A moderate increase of  $136.53 \pm 84.06$  ng is observed from 30,000 km to 45,000 km. Indicating that the extraction efficiency of Micronair standard particle filters diminishes with use.

Micronair standard particle filters yield higher concentrations from 0 km to 15,000 km ( $1,303.2 \pm 199.71$  ng) than Airforce standard particle filters over the same kilometerage ( $533.86 \pm 36.63$  ng).

Unlike standard particle filters Airforce combination filters yield higher concentrations ( $1138.95 \pm 136.17$  ng) from 0 km to 15,000 km than Micronair combination filters ( $763.47 \pm 123.84$  ng).

A significant concentration of  $435.6 \pm 141.3$  ng is observed from 0 km to 15,000 km for Micronair standard particle filters run in a Toyota Aventis. A decrease is observed from 15,000 km to 30,000 km (from  $1,761.3 \pm 313.11$  ng to  $679.58 \pm 555.48$  ng) and from 30,000 km to 45,000 km (from  $1,679.58 \pm 555.48$  ng to  $1,662.84 \pm 430.11$  ng). Indicating that the efficiency of Micronair particle filters in a Skoda Octavia is superior when compared to a Toyota Aventis, this shows that filters placed vertically have higher extraction efficiencies than filter placed horizontally.

An increase in concentration for Nip and Denso filters run in a Toyota Aventis is observed from 0 km to 15,000 km (from  $218.16 \pm 135.36$  ng to  $1,648.53 \pm 397.26$  ng), from 15,000 km to 30,000 km (from  $1,648.53 \pm 397.26$  ng to  $1,947.96 \pm 123.2$  ng) and from 30,000 km to 45,000 km (from  $1,947.96 \pm 123.2$  ng to  $3,595.32 \pm 102.04$  ng). Concentrations improve with use, as particulates build up on the filter the extraction efficiency improves.

#### **5.6.6: Pb concentrations at 15,000 km less blanks for all filter makes.**

All makes of standard particle and combination filters were run to a minimum of 15,000 km in their respective car models. 15,000 km is the replacement interval recommended by filter manufactures. A comparison was made between all car models and filter manufacturers up to a kilometerage of 15,000 km, shown in Table 5.6.6.

The concentrations are relatively low for all filters tested. The most efficient filter is Nip & Denso standard particle filter (a Toyota Aventis),  $1,430.37 \pm 21.16$  ng. Followed closely by Micronair standard particle filters (in a Skoda Octavia),  $1,303.2 \pm 198.63$  ng and Airforce combination filters (in a Skoda Octavia) filters,  $1,138.95 \pm 136.17$  ng. Micronair Particle Filter (in a Toyota Aventis),  $435.6 \pm 141.3$  ng is poor relative to Nip & Denso Particle (in a Toyota Aventis),  $1,430.37 \pm 21.16$  ng.

Table 5.6.6 Filter concentrations from filters run to 15,000 km minus blank filter concentrations, for all filter types tested, extrapolated over the surface area of the filter.

Car and filter make	ng
Micronair Particle Filter - Skoda Octavia	$1,303.2 \pm 198.63$
Airforce Particle Filter - Skoda Octavia	$533.86 \pm 36.63$
Airforce Combination filters – Skoda Octavia	$1,138.95 \pm 136.17$
Micronair Combination filters – Skoda Octavia	$422.01 \pm 123.84$
Micronair Particle Filter - Toyota Aventis	$435.6 \pm 141.3$
Nip & Denso Particle - Toyota Aventis	$1,430.37 \pm 21.16$

Filter manufacturer appears to play a significant role in lead extraction up to 15,000 km. Nip & Denso filters are the most effective filters. Airforce filters (standard particle and combination) have comparable extraction efficiencies to Nip & Denso. Micronair filters are the least effective, with extraction efficiency approximately half that of other manufacturers.

## 5.7 Manganese:

### 5.7.1: Concentrations of Mn at Different Kilometerages in Car Model 1 (a Skoda Octavia).

Figure 5.7.1 shows a comparison between Micronair particle filters taken from a Skoda Octavia at kilometerages of 15,000 km, 30,000 km and 45,000 km.

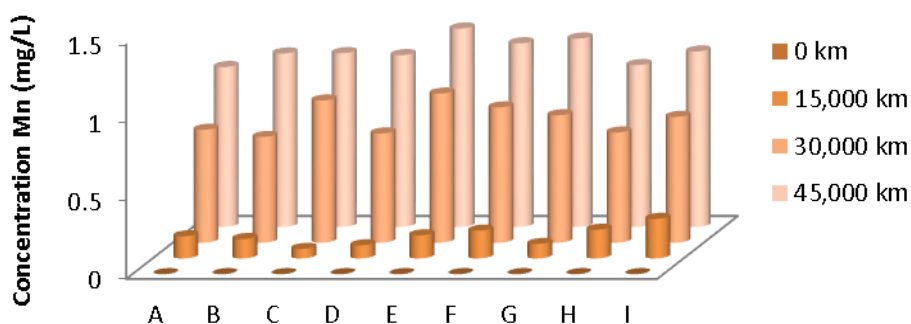


Figure 5.7.1: Average Mn concentrations for a Skoda Octavia, standard particle filter from 0 km to 45,000 km in increments of 15,000 km, manufactured by Micronair. All samples were collected in triplicate.

Table 5.7.1 shows corrected concentrations based on SRM recoveries of manganese using Method 3, estimated to be 82.1% of the overall quantities of manganese on the filter. Column 3 shows concentrations for one square inch of a filter. All filter samples were collected in triplicate.

Table 5.7.1: The average concentrations of Mn for filters samples, with standard deviation errors between replicates are shown in column 2. With concentrations based on percentage recoveries from SRM samples shown in column 3. Column 4 shows recoveries for the entire area of the filter.

Kilometerage (km)	Mn concentrations from filter sample ( $\mu\text{g}$ )	Corrected based on SRM % recovery ( $\mu\text{g}$ )	Recovery of Mn for entire filter area (mg)
0	0	0	0
15,000	$1.26 \pm 0.45$	1.53	0.45
30,000	$7.11 \pm 3.33$	8.73	2.53
45,000	$10.17 \pm 2.34$	12.33	3.59

A blank filter was analysed as a reference. An increase in manganese levels is observed between the blank sample and the sample taken at 15,000 km,  $1.26 \pm 0.45 \mu\text{g}$ . An increase in manganese is observed between samples taken at 15,000 km and 30,000 km,  $5.85 \pm 2.88 \mu\text{g}$  and samples taken at 30,000 km and 45,000 km,  $3.06 \pm 0.99 \mu\text{g}$ , indicating that filter efficiency levels increase with use, to a point. Extraction efficiencies are best between 15,000 km and 30,000 km.

### 5.7.2: Concentrations of Mn between Different Standard Particle Filter Manufacturers.

Figure 5.7.2 shows a comparison of Mn Levels between Airforce and Micronair standard particle filters taken at 15,000 km from a Skoda Octavia filters.

A moderate difference is observed between blank filter samples and those taken at 15,000 km for Micronair filters,  $1.26 \pm 0.45 \mu\text{g}$  with a greater difference observed between blank samples and 15,000 km samples for Airforce filter,  $6.12 \pm 2.52 \mu\text{g}$ . A difference of  $4.48 \pm 2.07 \mu\text{g}$  is observed between Micronair filters and Airforce filters at 15,000 km. This

indicating that Micronair filters are significantly less efficient than Airforce at manganese extraction up to 15,000 km.

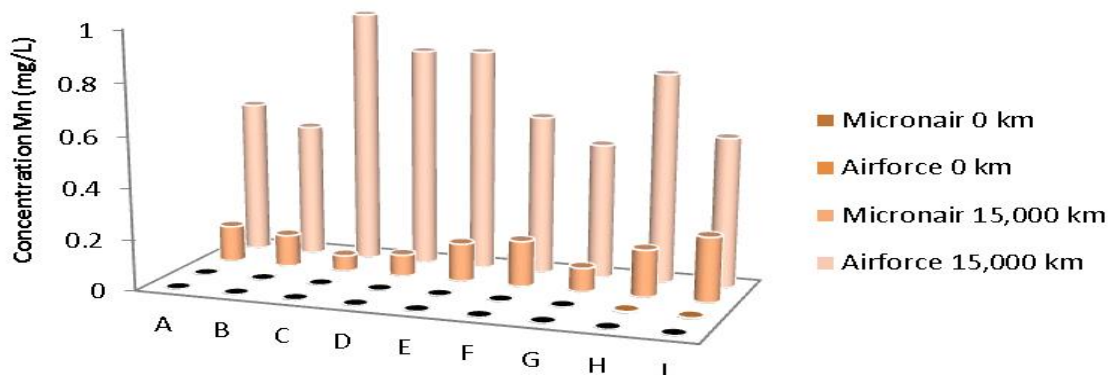


Figure 5.7.2: A comparison of average Mn concentrations from standard particle filters manufacturers by comparing Micronair and Airforce from 0 km to 15,000 km for a Skoda Octavia. All samples were collected in triplicate.

Table 5.7.2: The average concentrations of Mn for filters samples, with standard deviation errors between replicates are shown in column 2. With corrected concentrations based on percentage recoveries from SRM samples shown in column 3. Column 4 shows recoveries for the entire area of the filter.

Kilometerage (km)	Mn concentrations from filter sample ( $\mu\text{g}$ )	Corrected based on SRM % recovery ( $\mu\text{g}$ )	Recovery of Mn for entire filter area (mg)
0 km - Airforce	0	0	0
0 km - Micronair	0	0	0
15,000 km - Airforce	$6.12 \pm 2.52$	7.47	2.16
15,000 km - Micronair	$1.26 \pm 0.45$	1.53	0.45

### 5.7.3 Mn Concentrations from Combination Filters from Two Different Manufactures.

Figure 5.7.3 shows a comparison between Airforce and Micronair combination filters taken at 15,000 km from a Skoda Octavia.

A moderate difference is observed between blank filters samples and those taken at 15,000 km for both Micronair and Airforce filter samples,  $2.07 \pm 0.18 \mu\text{g}$  and  $2.43 \pm 0.81 \mu\text{g}$ , respectively. A significant difference not observed between the different brands of

combination filter indicating that for manganese analysis using combination filters, filter make does not play a significant role.

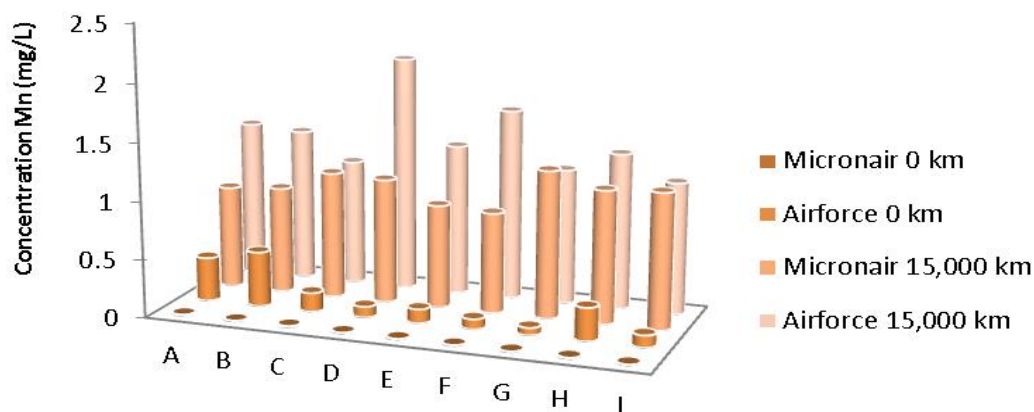


Figure 5.7.3: A comparison of average Mn concentrations from combination filters manufacturers by comparing Micronair and Airforce from 0 km to 15,000 km for a Skoda Octavia. All samples were collected in triplicate.

Table 5.7.3: The average concentrations of Mn for filters samples, with standard deviation errors between replicates are shown in column 2. With corrected concentrations based on percentage recoveries from SRM samples shown in column 3. Column 4 shows recoveries for the entire area of the filter.

Kilometerage (km)	Mn concentrations from filter sample ( $\mu\text{g}$ )	Corrected based on SRM % recovery ( $\mu\text{g}$ )	Recovery of Mn for entire filter area (mg)
0 km - Airforce	$9.99 \pm 3.69$	12.15	3.53
0 km - Micronair	$7.29 \pm 2.52$	8.91	2.57
15,000 km - Airforce	$12.42 \pm 2.88$	15.12	4.38
15,000 km - Micronair	$9.36 \pm 2.7$	11.34	3.3

#### 5.7.4 Mn Concentrations of Standard Particle Filters from Two Different Suppliers in Two Different Car Models.

Figure 5.7.4 shows a comparison of Micronair particle filters taken at kilometerages of 15,000 km, 30,000 km and 45,000 km from Car Model 2 (a Toyota Aventis).

A significant difference is not observed between blank filters samples,  $8.82 \pm 3.42 \mu\text{g}$  and those taken at 15,000 km,  $10.62 \pm 2.43 \mu\text{g}$ , 30,000 km,  $11.07 \pm 2.61 \mu\text{g}$  and 45,000 km,  $11.07 \pm 1.35 \mu\text{g}$ . Micronair filters taken from a Toyota Aventis are not effective in manganese extraction.

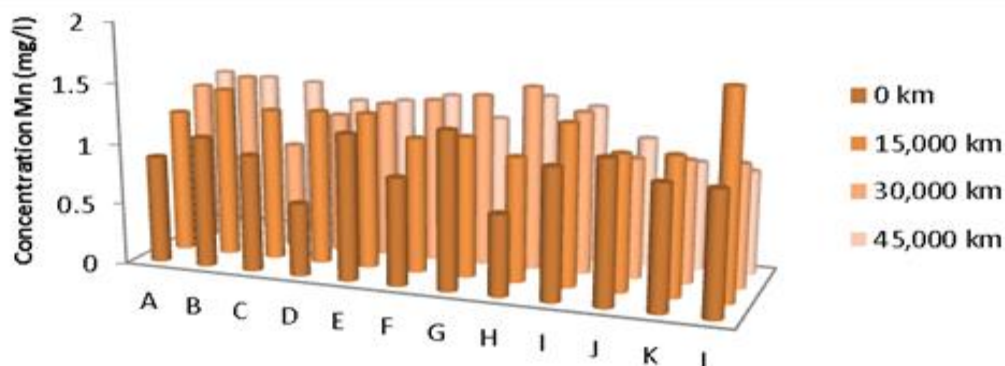


Figure 5.7.4: Average Mn concentrations for a Toyota Aventis, standard particle filter from 0 km to 45,000 km in increments of 15,000 km, manufactured by Micronair. All samples were collected in triplicate.

Table 5.7.4: The average percentage concentrations of Mn for filters samples, with standard deviation errors between replicates are shown in column 2. With corrected concentrations based on percentage recoveries from SRM samples shown in column 3. Column 4 shows recoveries for the entire area of the filter.

Kilometerage (km)	Mn concentrations from filter sample ( $\mu\text{g}$ )	Corrected based on SRM % recovery ( $\mu\text{g}$ )	Recovery of Mn for entire filter area (mg)
0 km	$8.82 \pm 3.42$	10.8	3.45
15,000 km	$10.62 \pm 2.43$	12.96	4.15
30,000 km	$11.07 \pm 2.61$	13.5	4.33
45,000 km	$11.07 \pm 1.35$	13.41	4.3

Concentrations from filters from a Toyota Aventis are comparable to the same filter make placed in a Skoda Octavia from 0 km to 15,000 km,  $1.8 \pm 0.99 \mu\text{g}$  and  $1.26 \pm 0.45 \mu\text{g}$ , respectively. Filters in a Skoda Octavia, however, show an increase between 15,000 km and 30,000 km and between 30,000 km and 45,000 km, while filters in a Toyota Aventis do not show any increase in concentrations over these kilometre ranges.



Filters in a Toyota Aventis are positioned horizontally while filters in a Skoda Octavia are placed vertically. The improved extraction efficiency of filters placed in a Skoda Octavia over filters placed in a Toyota Aventis, implies that vertically orientated filters are more efficient at manganese extraction than horizontally places filters.

### 5.7.5: Concentrations for a Third Standard Particle Filter Manufacturer in a Toyota Aventis.

Figure 5.7.5 shows a comparison of Mn levels on Nip & Denso standard particle filters taken at 15,000 km, 30,000 km and 45,000 km from a Toyota Aventis.

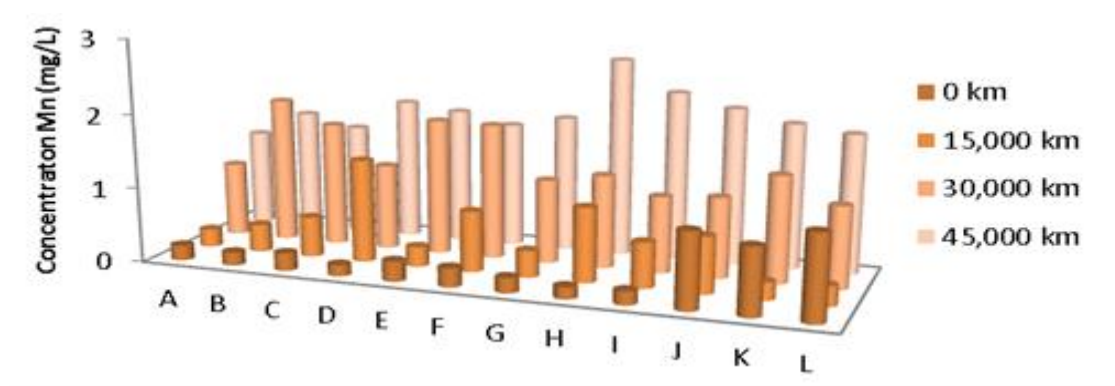


Figure 5.7.6: Average Mn concentrations for a Toyota Aventis, standard particle filter from 0 km to 45,000 km in increments of 15,000 km, manufactured by Nip & Denso. All samples were collected in triplicate.

Table 5.7.5: The average concentrations of Mn for filters samples, with standard deviation errors between replicates are shown in column 2. With corrected concentrations based on percentage recoveries from SRM samples shown in column 3. Column 4 shows recoveries for the entire area of the filter.

Kilometerage (km)	Mn concentrations from filter sample ( $\mu\text{g}$ )	Corrected based on SRM % recovery ( $\mu\text{g}$ )	Recovery of Mn for entire filter area (mg)
0 km	$1.89 \pm 1.26$	2.34	3.45
15,000 km	$5.4 \pm 3.33$	6.57	4.15
30,000 km	$12.78 \pm 6.39$	15.57	4.33
45,000 km	$16.83 \pm 7.02$	20.52	4.30

A significant difference is not observed between blank filters samples and those taken at 15,000 km,  $3.51 \pm 2.07 \mu\text{g}$ . A greater difference is observed between 15,000 km and 30,000 km,  $7.38 \pm 3.06 \mu\text{g}$ . However a decrease in extraction efficiency occurs between 30,000 km and 45,000 km,  $4.05 \pm 0.63 \mu\text{g}$ . For manganese Nip & Denso filters in a Toyota Aventis are most efficient between 15,000 km and 30,000 km but decreases after 30,000 km.

### **Manganese Conclusion:**

An increase in manganese levels is observed from 0 km to 15,000 km ( $1.26 \pm 0.45 \mu\text{g}$ ), from 15,000 km to 30,000 km ( $5.85 \pm 2.88 \mu\text{g}$ ) and from 30,000 to 45,000 km ( $3.06 \pm 0.99 \mu\text{g}$ ) for Micronair standard particle filters run in a Skoda Octavia.

Airforce standard particle filters yield higher concentrations than Micronair standard particle filters run in a Skoda Octavia,  $6.12 \pm 2.52 \mu\text{g}$  and  $1.26 \pm 0.45 \mu\text{g}$ , respectively. Airforce and Micronair combination filters run in a Skoda Octavia yield comparable results,  $2.43 \pm 0.81 \mu\text{g}$  and  $2.07 \pm 0.18 \mu\text{g}$ , respectively.

An increase of  $1.8 \pm 0.99 \mu\text{g}$  is observed between Micronair standard particle filters from 0 km to 15,000 km. No significant difference in manganese levels is observed between 15,000 km, 30,000 km and 45,000 km.

An increase of  $3.52 \pm 2.07 \mu\text{g}$  is observed between 0 km and 15,000 km for Nip and Denso filters run in a Toyota Aventis. An increase of  $7.38 \pm 3.06 \mu\text{g}$  was observed between 15,000 km and 30,000 km and an increase of  $4.05 \pm 0.63$  is observed between 30,000 km and 45,000 km.

### **5.7.6: Mn concentrations at 15,000 km less blanks for all filter makes.**

Table 5.7.6 shows filter concentrations from filters run to 15,000 km minus blank filter concentrations, for all filter types tested, extrapolated over the surface area of the filter.

Car and filter make	$\mu\text{g}$
Micronair Particle Filter - Skoda Octavia	$1.26 \pm 0.45$
Airforce Particle Filter - Skoda Octavia	$6.12 \pm 2.52$
Airforce Combination filters –Skoda Octavia	$2.43 \pm 0.81$
Micronair Combination filters – Skoda Octavia	$2.07 \pm 0.18$
Micronair Particle Filter - Toyota Aventis	$1.8 \pm 0.99$
Nip & Denso Particle - Toyota Aventis	$3.52 \pm 2.07$

The concentrations for Airforce combination filters (in a Skoda Octavia) and Micronair combination filters (in a Skoda Octavia) are comparable,  $2.43 \pm 0.81 \mu\text{g}$  and  $2.07 \pm 0.18 \mu\text{g}$  respectively, with Airforce Combination filters (in a Skoda Octavia) yielding slightly higher concentrations. The concentrations for Micronair standard particle filters (in a Skoda Octavia) are the lowest at  $26 \pm 0.45 \mu\text{g}$ . Airforce standard particle filters have the highest efficiency,  $6.12 \pm 2.52 \mu\text{g}$ , followed by Nip & Denso standard particle (in a Toyota Aventis),  $3.52 \pm 2.07 \mu\text{g}$ . For manganese the extraction efficiency of combination filters is comparable, independent of manufacturer. Standard particle filters are more efficient than combination filters at 15,000 km, and their extraction efficiency is manufacturer dependant, with Airforce being the most efficient, followed by Nip & Denso and then Micronair.

## 5.8 Zinc:

### 5.8.1: Concentrations of Zn at Different Kilometerages in Car Model 1 (a Skoda Octavia).

Figure 5.8.1 shows a comparison of Zn levels between Micronair particle filters taken from a Skoda Octavia at kilometerages of 15,000 km, 30,000 km and 45,000 km.

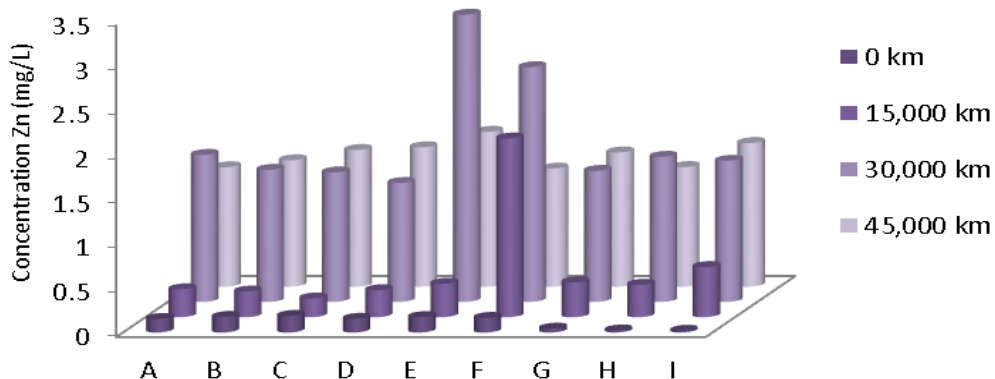


Figure 5.8.1: Average Zn concentrations for a Skoda Octavia, standard particle filter from 0 km to 45,000 km in increments of 15,000 km, manufactured by Micronair. All samples were collected in triplicate.

A moderate difference in zinc levels is observed between blank samples and those taken at 15,000 km,  $1.98 \pm 0.68 \mu\text{g}$ . Significant levels in zinc are observed between 15,000 km and 30,000 km samples,  $13.41 \pm 4.95 \mu\text{g}$  and a moderate decrease is observed between 30,000 km

and 45,000 km samples,  $3.06 \pm 2.25 \mu\text{g}$  indicating that filter efficiency levels off after 30,000 km and de-absorption occurs.

Table 5.8.1 shows corrected concentrations based on SRM recoveries of zinc using Method 3, estimated to be 83.5% of the overall quantities of zinc on the filter. Column 3 shows corrected concentrations for one square inch of a filter. All filter samples were collected in triplicate.

Table 5.8.1: The average concentrations of Zn for filters samples, with standard deviation errors between replicates are shown in column 2. With corrected concentrations based on percentage recoveries from SRM samples shown in column 3. Column 4 shows recoveries for the entire area of the filter.

Kilometerage (km)	Zn recovered from filter sample ( $\mu\text{g}$ )	Corrected based on SRM % recovery ( $\mu\text{g}$ )	Recovery of Zn for entire filter area (mg)
0 km	$1.08 \pm 2.11$	1.26	0.37
15,000 km	$3.06 \pm 2.79$	3.6	1.05
30,000 km	$16.47 \pm 7.74$	19.71	5.72
45,000 km	$13.41 \pm 5.49$	16.02	4.64

### 5.8.2: Concentrations of Zn between different standard particle filter manufacturers.

Figure 5.8.2 shows a comparison between Airforce and Micronair particle filters taken at 15,000 km from a Skoda Octavia filters.

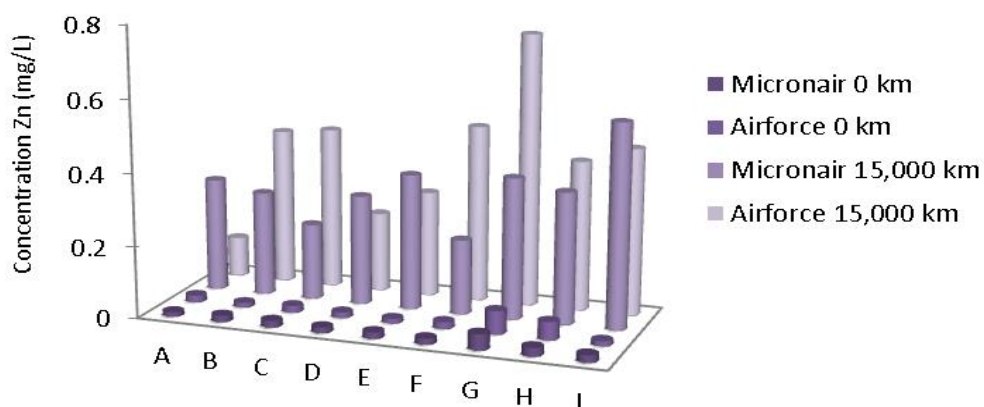


Figure 5.8.2: A comparison of average Zn concentrations from standard particle filters manufacturers by comparing Micronair and Airforce from 0 km to 15,000 km for a Skoda Octavia. All samples were collected in triplicate.

A moderate difference is observed between blank filter samples and those taken at 15,000 km for both Airforce and Micronair filters,  $4.5 \pm 2.52 \mu\text{g}$  and  $1.89 \pm 2.04 \mu\text{g}$ , respectively. A difference of  $2.61 \pm 0.48 \mu\text{g}$  is observed between Micronair filters and Airforce filters at 15,000 km. Airforce filters are moderately more efficient than Micronair filters for zinc extraction.

Table 5.8.2: The average concentrations of Zn for filters samples, with standard deviation errors between replicates are shown in column 2. With corrected concentrations based on percentage recoveries from SRM samples shown in column 3. Column 4 shows recoveries for the entire area of the filter.

Kilometerage (km)	Zn concentrations from filter sample ( $\mu\text{g}$ )	Corrected based on SRM % recovery ( $\mu\text{g}$ )	Recovery of Zn for entire filter area (mg)
0 km - Airforce	$1.08 \pm 1.11$	1.35	0.39
0 km - Micronair	$1.08 \pm 0.27$	1.26	0.37
15,000 km - Airforce	$5.58 \pm 2.79$	6.75	1.95
15,000 km - Micronair	$2.97 \pm 3.15$	3.6	1.05

### 5.8.3 Zn Concentrations from Combination Filters from Two Different Manufactures.

Figure 5.8.3 shows a comparison of Zn levels between Airforce and Micronair combination filters taken at 15,000 km from a Skoda Octavia.

A significant difference is observed between blank filter samples and those taken at 15,000 km for Micronair,  $16.92 \pm 5.76 \mu\text{g}$ . While a moderate difference is observed between blank samples and samples taken at 15,000 km for Airforce filter samples,  $6.66 \pm 4.05 \mu\text{g}$ . A significant difference is observed between the different brands of combination filter,  $10.26 \pm 1.71 \mu\text{g}$ , with Micronair filters having higher extraction efficiency. Implying that when using combination filters, filter make does play a significant role for zinc extraction.

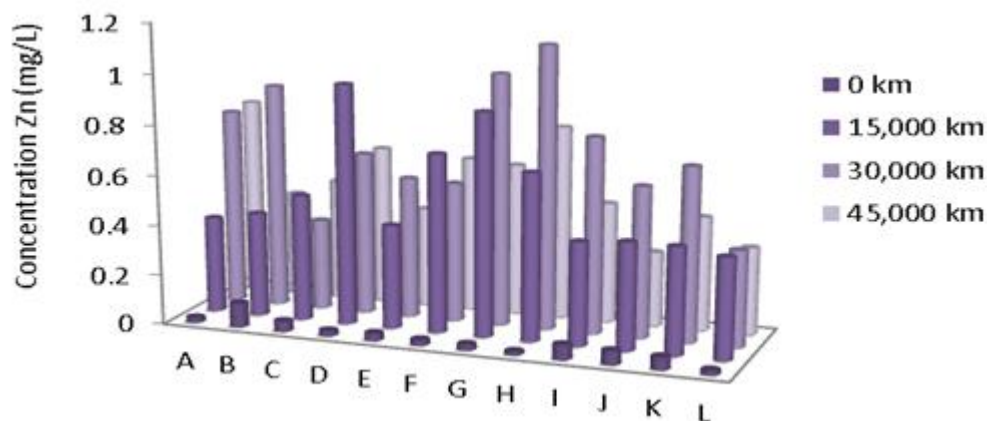


Figure 5.8.3: A comparison of average Zn concentrations from combination filters manufacturers by comparing Micronair and Airforce from 0 km to 15,000 km for a Skoda Octavia. All samples were collected in triplicate.

Table 5.8.3: The average concentrations of Zn for filters samples, with standard deviation errors between replicates are shown in column 2. With corrected concentrations based on percentage recoveries from SRM samples shown in column 3. Column 4 shows recoveries for the entire area of the filter.

Kilometerage (km)	Zn concentrations from filter sample ( $\mu\text{g}$ )	Corrected based on SRM % recovery ( $\mu\text{g}$ )	Recovery of Zn for entire filter area (mg)
0 km - Airforce	$1.98 \pm 0.36$	2.34	0.68
0 km - Micronair	$2.43 \pm 0.9$	2.97	0.85
15,000 km - Airforce	$8.64 \pm 4.41$	10.35	2.99
15,000 km - Micronair	$19.35 \pm 6.66$	23.22	6.73

#### 5.8.4 Zn Concentrations of Standard Particle Filters from Two Different Suppliers in Two Different Car Models.

Figure 5.8.4 shows a comparison of Micronair particle filters taken at kilometerages of 15,000 km, 30,000 km and 45,000 km from a Toyota Aventis.

Moderate differences are observed between blank filters samples and those taken at 15,000 km and between 15,000 km and 30,000 km,  $1.26 \pm 1.35 \mu\text{g}$  and  $2.88 \pm 0.09 \mu\text{g}$ , respectively. De-absorption occurs between 30,000 km and 45,000 km,  $1.53 \pm 0.43 \mu\text{g}$ . This indicates that the efficiency of Micronair filters in a Toyota Aventis increases to a point and de-absorption occurs when the filter becomes saturated.

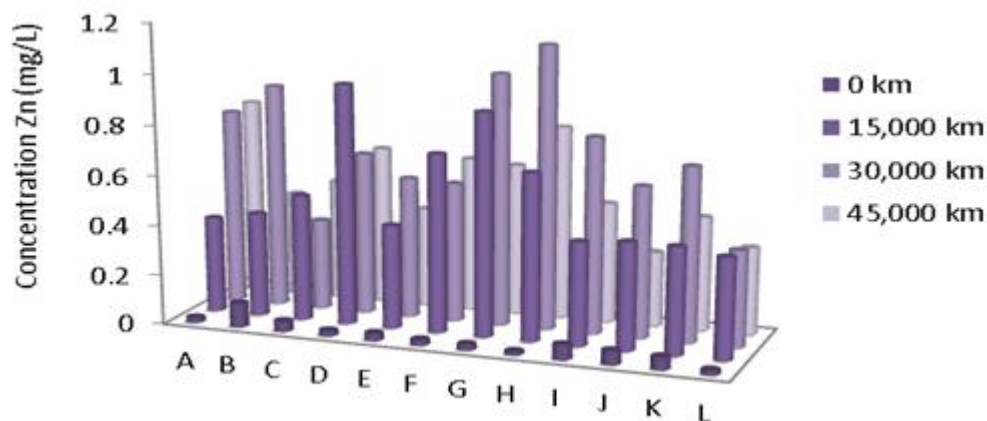


Figure 5.8.4: Average Zn concentrations for a Toyota Aventis, standard particle filter from 0 km to 45,000 km in increments of 15,000 km, manufactured by Micronair. All samples were collected in triplicate.

Table 5.8.4: The average concentrations of Zn for filters samples, with standard deviation errors between replicates are shown in column 2. With corrected concentrations based on percentage recoveries from SRM samples shown in column 3. Column 4 shows recoveries for the entire area of the filter.

Kilometerage (km)	Zn concentrations from filter sample ( $\mu\text{g}$ )	Corrected based on SRM % recovery ( $\mu\text{g}$ )	Recovery of Zn for entire filter area (mg)
0 km	$2.16 \pm 1.53$	2.61	0.76
15,000 km	$3.42 \pm 2.88$	4.05	1.19
30,000 km	$6.3 \pm 2.79$	7.56	2.19
45,000 km	$4.77 \pm 2.34$	5.67	1.64

### 5.8.5: Concentrations for a Third Standard Particle Filter Manufacturer in a Toyota Aventis.

Figure 5.8.5: Shows a comparison of Zn levels on Nip & Denso particle filters taken at 15,000 km, 30,000 km and 45,000 km from a Toyota Aventis.

A moderate difference is observed between blank filters samples and those taken at 15,000 km,  $2.43 \pm 1.62 \mu\text{g}$ . A significant difference is observed however between 15,000 km and 30,000 km,  $21.87 \pm 18.54 \mu\text{g}$  but only a moderate difference is observed between 30,000 km and 45,000 km,  $5.78 \pm 10.62 \mu\text{g}$  indicating that for zinc Nip and Denso filters become less effective after 30,000 km.

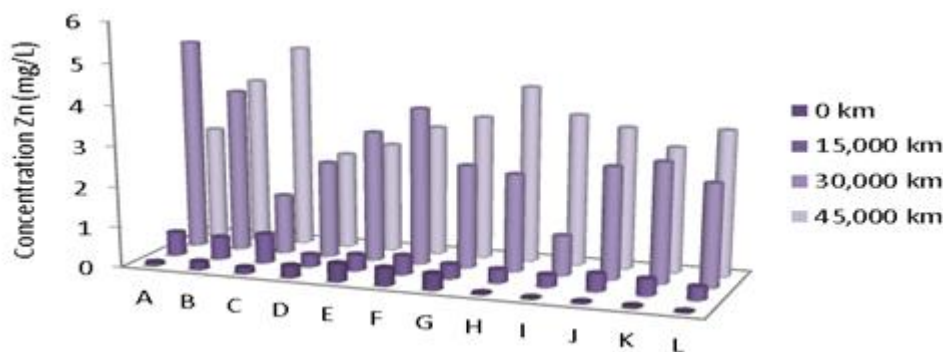


Figure 5.8.5: Average Zn concentrations for a Toyota Aventis, standard particle filter from 0 km to 45,000 km in increments of 15,000 km, manufactured by Nip & Denso. All samples were collected in triplicate.

Table 5.8.5: The average concentrations of Zn for filters samples, with standard deviation errors between replicates are shown in column 2. With corrected concentrations based on percentage recoveries from SRM samples shown in column 3. Column 4 shows recoveries for the entire area of the filter.

Kilometerage (km)	Zn concentrations from filter sample (µg)	Corrected based on SRM % recovery (µg)	Recovery of Zn for entire filter area (mg)
0 km	1.26 ± 0.54	1.53	0.44
15,000 km	3.69 ± 2.16	4.5	1.29
30,000 km	25.56 ± 20.7	30.6	8.89
45,000 km	31.32 ± 14.94	37.53	10.87

### Zinc Conclusion:

An increase of  $1.98 \pm 0.68 \mu\text{g}$  is observed between 0 km and 15,000 km for Micronair standard particle filters run in a Skoda Octavia. An increase of  $13.41 \pm 4.95 \mu\text{g}$  was observed between 15,000 km and 30,000 km and an decrease of  $3.06 \pm 2.25 \mu\text{g}$  is observed between 30,000 km and 45,000 km. indicating that zinc extraction improved with filter use to a point and the de-absorption occurs.

Airforce standard particle filters yield over four times more than Micronair standard particle filters from 0 km to 15,000 km in a Skoda Octavia,  $4.5 \pm 2.52 \mu\text{g}$  and  $1.89 \pm 2.04 .26 \text{ mg/L}$ , respectively. While, Micronair combinations filters yield over double the concentrations of Airforce combinations filters from 0 km to 15,000 km,  $16.93 \pm 5.76 .25 \mu\text{g}$  and  $6.66 \pm 4.05$



$\mu\text{g}$ , respectively. This indicates that Airforce standard particle filters are more effective than Micronair standard particle filters and Airforce combination filters are less effective than Micronair combination filters.

Micronair standard particle filters run in a Toyota Aventis show increases in concentrations from 0 km to 15,000 km,  $1.26 \pm 1.35 \mu\text{g}$ , from 15,000 km to 30,000 km of  $2.88 \pm 0.09 \mu\text{g}$  and a decrease from 30,000 km to 45,000 km of  $1.53 \pm 0.45 \mu\text{g}$ . The same pattern is observed for Micronair standard particle filters run in a Skoda Octavia. This indicates that for zinc extraction filters performance is consistent across different makes of cars.

Nip and Denso filters show an increase from 0 km to 15,000 km of  $2.13 \pm 1.62 \mu\text{g}$ , from 15,000 km to 30,000 km of  $21.87 \pm 18.54 \mu\text{g}$  and unlike Micronair filters they show an increase from 30,000 km to 45,000 km,  $5.76 \pm 5.76 \mu\text{g}$ . This indicates that Nip and Denso filters show a superior performance with increased use.

#### 5.8.6: Zn Concentrations at 15,000 km less blanks for all filter makes.

All makes of standard particle and combination filters were run to a minimum of 15,000 km in their respective car models. 15,000 km is the replacement interval recommended by filter manufacturers. A comparison was made between all car models and filter manufacturers up to a kilometerage of 15,000 km, shown in Table 5.8.6

Table 5.8.6. Filter concentrations from filters run to 15,000 km minus background filter concentrations, for all filter types tested, extrapolated over the surface area of the filter.

Car and filter make	$\mu\text{g}$
Micronair Particle Filter - Skoda Octavia	$1.98 \pm 0.68$
Airforce Particle Filter - Skoda Octavia	$4.5 \pm 2.52$
Airforce Combination filters – Skoda Octavia	$6.66 \pm 4.05$
Micronair Combination filters – Skoda Octavia	$16.92 \pm 5.76$
Micronair Particle Filter - Toyota Aventis	$1.26 \pm 1.35$
Nip & Denso Particle - Toyota Aventis	$2.43 \pm 1.62$

The concentrations for Micronair combination filters a Skoda Octavia at 15,000 km are significantly higher than all other filters tested,  $16.92 \pm 5.76 \mu\text{g}$ . Both standard particle and combination Airforce filters perform well at  $4.5 \pm 2.52 \mu\text{g}$  and  $6.66 \pm 4.05 \mu\text{g}$ , respectively. Micronair standard particle filters concentrations are comparable in a Skoda Octavia and a

Toyota Aventis,  $1.98 \pm 0.68 \mu\text{g}$  and  $1.26 \pm 1.35 \mu\text{g}$ , respectively, indicating that vertically and horizontally positioned filters have comparable extraction efficiencies.

### **Conclusions for all analytes analysis on filters:**

Standard particle Micronair filters were run in a Skoda Octavia with the same filter manufacturer and car make but with varying kilometerage. Generally an increase is observed between blank filters and 15,000 km and between 15,000 km and 30,000 km filter samples. However no significant difference is observed between 30,000 km and 45,000 km samples. Indicating that for a Skoda Octavia filter samples, the extraction efficiency decreases between 30,000 km and 45,000 km (but that de-absorption does not occur when the filters become saturated with particulates).

Micronair & Airforce standard particle filters were run with the same kilometerage and car make but with varying filter manufacturers. Generally a significant increase is observed between blank samples and those taken at 15,000 km for both filter makes (Micronair and Airforce). This demonstrates that both filter makes are effective at analyte extraction. The observed difference in extraction efficiency between filter manufacturers is dependent on the analyte in question. For Al, Cr and Zn, no significant difference is observed between filter makes, implying that the extraction capacity for both filter makes is comparable. For Cu, Fe, Pb and Mn a significant difference is observed, with Airforce filters showing improved extraction efficiencies over Micronair filters between 0 and 15,000 km.

Micronair & Airforce combination filters were run in a Skoda Octavia at the same kilometerage and with the same car make but with varying filter manufacturers. Filters show an increase in analyte concentrations between blank filters and those taken at 15,000 km for both filter makes. A difference in filter extraction efficiency between different filter makes is observed for certain analytes but not for others as for particle filters. No significant difference is observed for Al and Mn but a significant difference is observed for Cr, Cu, Fe, Pb and Zn. In general, Airforce combination filters are more effective at analyte extraction than Micronair combination filters.

Micronair standard particle filters were run in a Toyota Aventis, i.e. particle filters with the same filter manufacturer and car make but with varying kilometerages. Generally, an increase is observed between blank samples and those taken at 15,000 km. However no significant

difference is observed between 15,000 km and 30,000 km samples or between 30,000 km and 45,000 km samples. This indicates that for Micronair filters, in a Toyota Aventis cars, the extraction efficiency levels off after 15,000 km, unlike Skoda Octavia samples where the extraction efficiency levels off after 30,000 km. This also indicates that car make, or more specifically filter design/orientation, plays a significant role in extraction efficiency. Skoda Octavia filters are located horizontally behind the footwell in a separate compartment, with incoming air coming up through the bottom of the filter. Filters in a Toyota Aventis are positioned horizontally, located in a drop down compartment at the back of the glove box, with air circulating from the back to the front. The filters from a Skoda Octavia and a Toyota Aventis have a different physical design. Therefore since the filter materials are the same, as both filters are manufactured by Micronair, the difference in extraction efficiencies can be attributed to filter orientation, design or location.

Nip and Denso standard particle filters were run in a Toyota Aventis with varying kilometerages. As for Micronair filters an increase in analyte concentrations is observed between 0 and 15,000 km filter samples and no noticeable difference is observed between 15,000 km and 30,000 km samples. However, unlike Micronair filters a significant difference is observed between 30,000 km and 45,000 km, implying that for Nip and Denso filters in a Toyota Aventis the extraction efficiency improves as the filters become blocked for certain analytes, namely Cu, Cr, Fe and Pb. No significant increase is observed between 30,000 km and 45,000 km filters for Al, Mn and Zn. For all analytes tested, the concentration levels from Nip and Denso filters is higher than for Micronair filters, indicating that Nip and Denso filters have a significantly higher extraction efficiency than Micronair filters.

### **5.9: Analyte concentrations in relation to particulate sizes.**

Legislation changes regarding air emissions have been implemented in recent years in an attempt to reduce the presence of particulate matter in ambient air. Samet *et al.*, showed that the main effect of legislation changes has been a reduction in PM<sub>10</sub> but PM<sub>2.5</sub> levels have increased.[99] Samara *et al.*, confirmed this, reporting that ambient air tested consists of ~52% particle matter <0.8  $\mu\text{m}$  and ~20% >6.7  $\mu\text{m}$ . Indicating that the majority of particulate matter is <0.8  $\mu\text{m}$ . They found that Fe was present in higher concentrations on PM >2.5  $\mu\text{m}$ , Ni, Cu and Mn were found in higher concentrations on PM <2  $\mu\text{m}$  and Pb, Cd were found on

PM <1  $\mu\text{m}$ . [100] Riediker *et al.*, demonstrated that exposure to PM <2.5  $\mu\text{m}$  results in damage to the cardiovascular and respiratory system, due to its ability to progress deep into the lungs, even over short periods of exposure. [101]

Table 5.9.1 shows analyte concentrations for all filters tested from 0 km to 15,000 km. The most abundant analyte was found to be copper. Copper is not classed as a human carcinogen but it competes with zinc for absorption, so high copper levels can cause zinc deficiencies. The highest copper value obtained from filters run to 15,000 km was  $566.1 \pm 11.67 \mu\text{g}$ , from Airforce combination filters run in a Skoda Octavia. This figure is alarmingly high considering the recommended maximum limit for copper in drinking water is 1.3 mg/L. [28] Iron was found to be the second most abundant analyte. Iron, like copper, is not classed as a human carcinogen but can cause corrosive toxicity in the gastrointestinal tract. It also acts on muscle tissues and in extreme cases it can cause cellular death. The liver is mainly affected but exposure can also cause damage in the kidneys, lungs and heart. The maximum iron levels found on filters run to 15,000 km was  $270.18 \pm 88.56 \mu\text{g}$ , also from Airforce combination filters run in a Skoda Octavia. Aluminium, the third most abundant, is not classified as a carcinogen by the EPA but is thought to play a role in the onset of Alzheimer's disease. The recommended maximum level of aluminium in drinking water is 50-200  $\mu\text{g/L}$ , which is of concern considering it is considerably lower than the highest level of aluminium observed on filter samples,  $188.59 \pm 63.72 \mu\text{g}$ . [28] Mn and Zn were present but in significantly lower concentrations. The levels of Pb and Cr were similar and relatively low when compared to the other 5 analytes tested. However, given their potential harmful effects, their cumulative concentrations are significant.

Several studies on the relationship between particulate size and PTE concentrations have been carried out. Riediker *et al.*, found that Fe was the most abundant analyte followed closely by Cu. Pb, Mn, Ni, Cr and Cd were found to be the least abundant (Aluminium was not tested). [101] Cavanagh *et al.*, found that for PM 10, Fe and Cu concentrations are similar and are higher than Pb and Zn concentrations, which are comparable to each other. For PM2.5, Pb was found in higher concentrations than Fe, followed by Zn, Mn and finally Cu. [102] Allen *et al.*, found that fine particles had higher concentrations of Cd, Pb, and that intermediate particles contained Ni, Zn, Cu, Mn and course particulate matter contributed the highest concentration of Fe. [103] Rajšić *et al.*, found that Fe was the most abundant analyte on

PM<sub>10</sub>, followed closely by Zn. Al concentrations observed on PM<sub>10</sub> are lower than Fe concentrations,  $\sim 1/2$ . Mn, Cr, Pb, Cd, Ni are observed but in significantly low concentrations. On PM<sub>2.5</sub>, unlike PM<sub>10</sub>, Zn concentrations are significantly higher than Fe concentrations,  $\sim$  double. Fe and Al concentrations are equal. Cu, Pb, Mn and Cr concentrations are low but higher than their respective concentrations in PM<sub>10</sub>. [104] Srivastava *et al.*, found particulate matter  $<0.7 \mu\text{m}$  was the main source of Mn, Cr, Cd, Pb, Ni and Fe and coarse particulate matter  $>0.7 \mu\text{m}$  was the main source of Cu.[105]

Particle size therefore plays a significant role in the concentrations of analytes present in ambient air. Indicating that the maximum/minimum size of particulate matter being retained by filters plays a significant role in the extraction of analytes.

Looking at SEM imagery from Chapter 7, particulates present on standard particle and combination filters run to 15,000 km can be observed in Figure 7.1.14 and Figure 7.2.8, respectively. Figure 7.1.14 shows a Micronair standard particle filter taken at a kilometerage of 15,000 km from a Skoda Octavia. The smallest particles observed are  $\sim 2 \mu\text{m}$  and the largest particles observed are  $\sim 10 \mu\text{m}$ . Figure 7.2.8 shows a Micronair combination filter taken at a kilometerage of 15,000 km from a Skoda Octavia. The smallest particles observed are  $<1 \mu\text{m}$  and the largest particles observed are  $\sim 4 \mu\text{m}$ . Analyte concentrations on Micronair combination filters are at least twice those of Micronair standard particle filters for all analytes tested except Pb. Combination filters can extract particulates down to  $\sim 1 \mu\text{m}$  and particle filters can extract particulates down to  $\sim 2 \mu\text{m}$ . Indicating that PM  $<2 \mu\text{m}$  contains higher PTE concentrations of the majority of PTE tested. Pb concentrations are higher on standard particle filters, standard particle filters are capable of extracting particulates up to  $10 \mu\text{m}$  while the maximum particulate size combination filters can extract is  $4 \mu\text{m}$ . This may indicate that PM  $>4 \mu\text{m}$  contains more lead than PM  $<4 \mu\text{m}$ .

Table 5.9.1 shows that Airforce combination filters run in a Skoda Octavia yield the highest concentrations for Cu, Fe and Al and Micronair combination filters run in a Skoda Octavia show the highest concentrations for Zn. The other analytes tested, Cr, Pb and Mn, show higher concentrations from standard particle filters. Combination filters tend to extract smaller particle  $>1 \mu\text{m}$  and  $<4 \mu\text{m}$  and standard particle filters tend to extract larger particles  $>2 \mu\text{m}$  and  $<10 \mu\text{m}$ . The difference in analyte concentrations between combination and standard

particle filters and the relationship between particle size and analyte concentrations indicates that smaller particles, <2 µm, contain more Cu, Fe, Al and Zn and larger particles >4 µm contain more Cr, Pb and Mn.

Table 5.9.1: Analytes concentrations from all filter makes tested between 0 km and 15,000 km. Highest values are highlighted in bold.

Car and filter make	Micronair Particle Filter - Skoda Octavia	Airforce Particle Filter - Skoda Octavia	Airforce Combi filters – Skoda Octavia	Micronair Combi Filter– Skoda Octavia	Micronair Particle Filter - Toyota Aventis	Nip & Denso Particle - Toyota Aventis
Al (µg)	53.64 ± 8.91	72.09 ± 5.15	<b>188.59 ± 63.72</b>	117.95 ± 71.82	72.45 ± 18.9	151.92 ± 112.23
Cr (ng)	367.56 ± 64.35	347.67 ± 48.96	<b>1,231.38 ± 118.98</b>	696.96 ± 398.16	431.19 ± 65.25	1,572.03 ± 979.74
Cu (µg)	26.01 ± 6.38	161.91 ± 96.65	<b>566.1 ± 11.67</b>	148.05 ± 45.99	4.32 ± 3.87	4.86 ± 2.16
Fe (µg)	53.64 ± 15.07	105.66 ± 10.62	117.9 ± 54.72	<b>270.18 ± 88.56</b>	96.39 ± 62.28	129.33 ± 81.36
Pb (ng)	1,303.2 ± 198.63	533.86 ± 36.63	1,138.95 ± 136.17	422.01 ± 123.84	435.6 ± 141.3	<b>1,430.37 ± 21.16</b>
Mn (µg)	1.26 ± 0.45	<b>6.12 ± 2.52</b>	2.43 ± 0.81	2.07 ± 0.18	1.8 ± 0.99	3.52 ± 2.07
Zn (µg)	1.98 ± 0.68	4.5 ± 2.52	6.66 ± 4.05	<b>16.92 ± 5.76</b>	1.26 ± 1.35	2.43 ± 1.62

Table 5.9.2 shows a comparison between two different standard particle filter manufacturers, Micronair and Nip & Denso, run at varying kilometerages 15,000 km, 30,000 km and 45,000 km. Micronair standard particle filters run in a Skoda Octavia and a Toyota Aventis and Nip and Denso standard particle filters run in a Toyota Aventis.

SEM imagery of Micronair standard particle filters is shown in Chapter 7, Figure 7.1.14 to 7.1.16. Figure 7.1.14 shows that a Micronair standard particle filter at 15,000 km can extract a minimum particulate matter size of ~2 µm and a maximum particle size of 10 µm. Figure 7.1.15 shows a Micronair standard particle filter taken at a kilometerage of 30,000 km can extract particles down to ~1.5 µm and a maximum of 7.5 µm. Figure 7.1.16 shows a Micronair standard particle filter run to 45,000 km, similar to filters run to 30,000 km, these filters can extract particles down to ~1.5 µm and up to 4 µm.

The results in Table 5.9.2 show that Micronair standard particle filters, run in a Skoda Octavia show an increased extraction efficiency from 15,000 km to 30,000 km when compared to concentrations extracted from 0 to 15,000 km and a decrease from 30,000 km to 45,000 km when compared to extracts between 15,000 km and 30,000 km for all analytes, except Pb. Pb shows a decrease in extraction efficiency between 15,000 km and 30,000 km compared to concentrations extracted between 0 km and 15,000 km. A further decrease in extraction efficiency is observed between 30,000 km and 45,000 km.

Table 5.9.2: Comparison of different filter makes over different kilometre intervals.

	Kilometerage	Micronair Standard Particle Filter in a Skoda Octavia	Micronair Standard Particle Filter in a Toyota Aventis	Nip & Denso Standard Particle Filter in a Toyota Aventis
Al	15,000 km ( $\mu\text{g}$ )	$53.64 \pm 8.91$	$72.45 \pm 18.9$	$152.92 \pm 112.23$
	30,000 km ( $\mu\text{g}$ )	$125.82 \pm 52.29$	$18.45 \pm 10.44$	$13.68 \pm 83.61$
	45,000 km ( $\mu\text{g}$ )	$5.76 \pm 22.23$	$-11.34 \pm 9.63$	$-16.74 \pm 50.58$
Cr	15,000 km (ng)	$367.56 \pm 64.35$	$431.19 \pm 65.25$	$1,572.03 \pm 979.74$
	30,000 km (ng)	$1,009.17 \pm 352.62$	$382.5 \pm 400.68$	$534.6 \pm 525.78$
	45,000 km (ng)	$-20.61 \pm 135.81$	$-240.39 \pm 262.18$	$1,952.37 \pm 171.45$
Cu	15,000 km ( $\mu\text{g}$ )	$26.01 \pm 6.38$	$4.32 \pm 3.87$	$4.86 \pm 2.16$
	30,000 km ( $\mu\text{g}$ )	$325.26 \pm 140.23$	$1.08 \pm 1.53$	$4.95 \pm 2.52$
	45,000 km ( $\mu\text{g}$ )	$-80.37 \pm 131.49$	$0.9 \pm 0.45$	$49.68 \pm 13.5$
Fe	15,000 km ( $\mu\text{g}$ )	$53.01 \pm 15.07$	$96.39 \pm 62.28$	$129.33 \pm 81.36$
	30,000 km ( $\mu\text{g}$ )	$156.06 \pm 98.69$	$52.65 \pm 3.51$	$146.97 \pm 28.17$
	45,000 km ( $\mu\text{g}$ )	$-3.78 \pm 28.35$	$-47.7 \pm 34.92$	$665.64 \pm 57.42$
Pb	15,000 km (ng)	$1,303.2 \pm 198.63$	$435.6 \pm 141.3$	$1,430.37 \pm 261.9$
	30,000 km (ng)	$820.17 \pm 322.11$	$-81.72 \pm 242.37$	$299.43 \pm 274.06$
	45,000 km (ng)	$136.53 \pm 84.06$	$-16.74 \pm 125.37$	$1,647.36 \pm 21.16$
Mn	15,000 km ( $\mu\text{g}$ )	$1.26 \pm 0.45$	$1.8 \pm 0.99$	$3.52 \pm 2.07$
	30,000 km ( $\mu\text{g}$ )	$5.85 \pm 2.88$	$0.45 \pm 0.18$	$7.38 \pm 3.06$
	45,000 km ( $\mu\text{g}$ )	$3.06 \pm 0.99$	0	$4.05 \pm 0.63$
Zn	15,000 km ( $\mu\text{g}$ )	$1.98 \pm 0.68$	$1.26 \pm 1.35$	$2.43 \pm 1.62$
	30,000 km ( $\mu\text{g}$ )	$13.41 \pm 4.95$	$2.88 \pm 0.09$	$21.87 \pm 18.54$
	45,000 km ( $\mu\text{g}$ )	$-3.06 \pm 2.25$	$-1.53 \pm 0.45$	$5.76 \pm 5.76$

Looking at Figures 7.1.14 to 7.1.16, there appears to be degradation in the filter structure with use. A breakdown in the structure is observed between blank filters and those extracted at 15,000 km. This degradation continues between 15,000 km and 30,000 km. However, the

level of degradation between 30,000 km and 45,000 km is comparable. Filters run to 15,000 km have a greater ability to retain larger particles but a diminished capacity to retain smaller particles, when compared to filters run to 30,000 km. Filters run to 30,000 km and filters run to 45,000 km can both extract particles down to  $\sim 1.5 \mu\text{m}$  but filters run to 45,000 km have a diminished capacity to extract larger particles when compared to filters run to 30,000 km.

The results in Table 5.9.2. show that the majority of analyte extraction occurs between 15,000 km and 30,000 km for all analytes tested except Pb. Indicating that most PTEs are attached to particulates  $>1.5 \mu\text{m}$  and  $<7.5 \mu\text{m}$ . Pb appears to be attached to larger particles because concentrations decrease with the absence of larger particulates. The break down in the filter structure with use increases the ability to extract smaller particles to a point but decreases the ability to extract larger particles.

Looking at results for a Micronair standard particle filters run in a Toyota Aventis, shown in Table 5.9.2, the optimum extraction range is from 0 km to 15,000 km for all analytes tested except Cu and Zn. Pb extraction only occurs from 0 km to 15,000 km, indicating that large particles are extracted over this range, based on previous knowledge of Pb extraction. Pb extraction decreases with use, this indicates that the ability to extract large particles decreases with use. Cu and Zn extraction increases with use, indicating that Cu and Zn are attached to smaller particles and that Micronair standard particle filters run in a Toyota Aventis, like in a Skoda Octavia, have an increased capacity to retain smaller particles with time.

The results of Nip & Denso standard particle filters run in a Toyota Aventis, generally show higher extraction concentrations with use, between 15,000 km and 30,000 km for Mn and Zn and between 30,000 km and 45,000 km for Cr, Fe, Pb. Al and Cu show higher extraction concentrations between 0 km to 15,000 km. The increase in Pb concentrations between 30,000 km and 45,000 km indicates that Nip & Denso standard particle filters run in a Toyota Aventis, unlike Micronair standard particle filters, extract larger particles with use. The decrease in the extraction of the other 5 analytes of interest indicates that smaller particles are lost with use. Presumably the filter surface degrades with use but the degradation of Nip and Denso filters has the opposite effect on PTE extraction than the degradation of Micronair filters.



**Chapter 6:**  
**Analysis of Internal Cabin Filters and Cycle Filters for Analytes**  
**Deposition using Inductively Coupled Plasma Spectrometry**

## Chapter 6:

### Analysis of Internal Cabin Filters and Cycle Filters for Analyte Deposition using Inductively Coupled Plasma Spectrometry

#### 6.1 Internal filtration filters Introduction:

The main objective of this section of the study was to determine the concentrations of analytes entering the cabin with and without particle filters in place. An internal filtration system, shown in Figure 2.5.2 was placed on the passenger seat headrest in a Ford Fiesta for 1,000 km intervals firstly with no cabin filter in place, then with a standard particle filter in place and finally with a combination filter in place. The filter system was powered by the electrical socket in the vehicle. The filters from the internal filtration system, the standard particle filters and combination filters were analysed using microwave acid digestion Method 3, shown in Table 6.1.1 developed in Chapter 3 using the following acid combination 6ml HNO<sub>3</sub>, 2 ml HF and 1 ml HCl. All filter samples were collected in triplicate.

Table 6.1.1: Microwave digestion method used to analyse internal, standard particle and combination filters.

Power (W)	Ramp (mins)	Time (mins)	Fan
500	5.00	10	1
1000	5.00	10	1
1400	5.00	10	1
0		15	3

The air velocity was measured for all demister/heater settings in a Ford Fiesta using a Kestrel 4000 - Air Velocity Meter AVM-4000 [106]. While internal filtration filters were run in a Ford Fiesta the setting was held at setting 2, a velocity of 0.6ms<sup>-1</sup>, shown in Table 6.1.2.

Table 6.1.2: Ford Fiesta demister/heater air velocities

Setting	0	1	2	3	4
Velocity (ms <sup>-1</sup> )	0	0.3	0.6	1	1.4

Representative samples were collected from all filter types to accurately represent the dispersal of analyte carrying particulates over the surface of the filter. Table 6.1.3. shows representative sampling for Ford Fiesta filters: Ford Fiesta filters have 50 folds which are 1" high and the filter is 7" wide. Samples were taken from fold number 12, 24, 36 and 48 at 2", 4" and 6" along the width of the filter, creating 1" square filter samples.

Table 6.1.3.: Representative analysis of Ford Fiesta particle filters.

	2"	4"	6"
Fold 12	A*	B*	C*
Fold 24	D*	E*	F*
Fold 36	G*	H*	I*
Fold 48	J*	K*	L*

1" square samples were collected and digested. Once digested the samples were filtered through a 25 mm syringe filter with 0.45  $\mu\text{m}$  filter cellulose acetate membrane.

## 6.2 Aluminium:

### 6.2.1 Concentrations of Al from standard particle filters between 0 km and 1,000 km in a Ford Fiesta.

Figure 6.2.1 shows a comparison between Airforce standard particle filters taken from a Ford Fiesta at a kilometers of 0 km and 1,000 km.

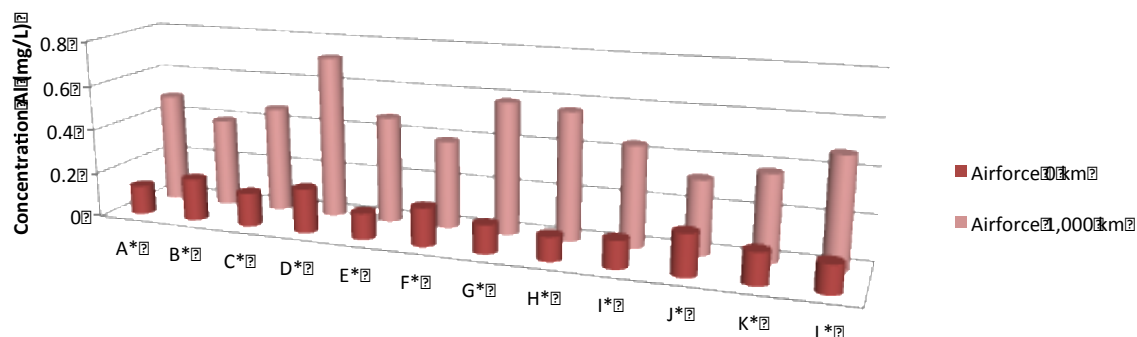


Figure 6.2.1: Al average concentrations for a Ford Fiesta, standard particle filters from 0 km to 1,000 km, manufactured by Airforce. The legend key for the x axis is shown in Table 1.4.3. All samples were collected in triplicate.

A significant difference is observed between blank filters and samples collected at 1,000 km,  $1.35 \pm 0.27 \mu\text{g}$  and  $4.5 \pm 0.9 \mu\text{g}$ , respectively. This indicates that even at low kilometerages a notable difference in aluminium concentrations is observed for standard particle filters in a Ford Fiesta.

Column 2 of Table 6.2.1 shows concentrations for one square inch of a filter. Column 3 of Table 6.2.1 shows concentrations corrected to 100%, based on SRM recoveries of aluminium using Method 3, shown in Table 3.2.4. This is estimated to be 57.03% of the overall quantities of aluminium on the filter. Three different filter samples were collected for each kilometerage.

Table 6.2.1: The average filter concentrations of Al for filters samples are shown in column 2 (with standard deviation errors) and corrected Al concentrations based on percentage recoveries from SRM samples are shown in column 3. Column 4 shows recoveries for the entire area of the filter.

Kilometerage (km)	Concentrations from filter sample ( $\mu\text{g}$ )	Corrected based on SRM % recovery ( $\mu\text{g}$ )	Recovery of Al for entire filter area (mg)
0 km	$1.35 \pm 0.27$	2.34	0.79
1,000 km	$4.5 \pm 0.9$	7.83	2.74

### 6.2.2 Concentrations of Al from combination filters between 0 km and 1,000 km in Ford Fiesta.

Figure 6.2.2 shows a comparison between Airforce combination filters taken from a Ford Fiesta at a kilometerages of 0 km and 1,000 km. The legend key for the x axis is shown in Table 1.4.3.

A significant difference in aluminium concentrations is observed for combination filters in a Ford Fiesta. The concentrations of aluminium from filters collected at 1,000 km,  $150.21 \pm 52.2 \mu\text{g}$  is over twice that of blank filter samples,  $73.26 \pm 9 \mu\text{g}$ .

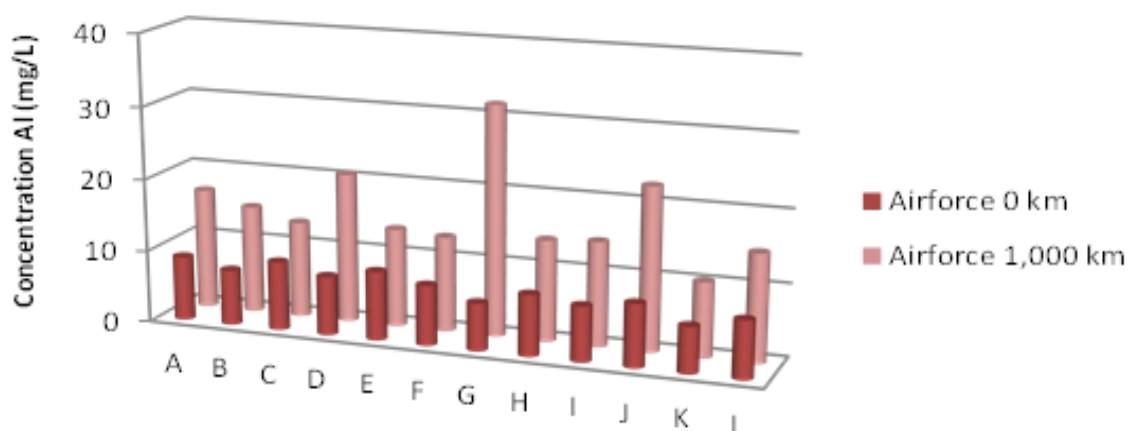


Figure 6.2.2: Al average concentrations for a Ford Fiesta, combination filters from 0 km to 1,000 km, manufactured by Airforce. The legend key for the x axis is shown in Table 1.4.3. All samples were collected in triplicate.

Table 6.2.2: The average filter concentrations of Al for filters samples are shown in column 2 (with standard deviation errors between replicates) and corrected Al concentrations based on percentage recoveries from SRM samples are shown in column 3. Column 4 shows recoveries for the entire area of the filter.

Kilometerage (km)	Concentrations from filter sample ( $\mu\text{g}$ )	Corrected based on SRM % recovery ( $\mu\text{g}$ )	Recovery of Al for entire filter area (mg)
0 km	$73.26 \pm 9$	128.43	44.91
1,000 km	$150.21 \pm 52.2$	263.43	91.8

Table 6.2.3 shows concentrations from all filters tested over 1,000 km and 15,000 km.

Car and filter make	At 1,000 km	At 15,000 km
	$\mu\text{g}$	
Micronair Particle Filter - Skoda Octavia	$3.57 \pm 0.59$	<b><math>53.64 \pm 8.91</math></b>
Airforce Particle Filter - Skoda Octavia	$4.8 \pm 0.34$	<b><math>72.09 \pm 5.15</math></b>
Micronair Particle Filter - Toyota Aventis	$4.83 \pm 1.26$	<b><math>72.45 \pm 18.9</math></b>
Nip & Denso Particle - Toyota Aventis	$10.13 \pm 7.48$	<b><math>151.92 \pm 112.23</math></b>
Airforce Particle Filter – Ford Fiesta	<b><math>3.15 \pm 0.63</math></b>	$47.25 \pm 9.45$
Airforce Combination filters – Skoda Octavia	$12.57 \pm 4.24$	<b><math>188.59 \pm 63.72</math></b>
Micronair Combination filters – Skoda Octavia	$7.86 \pm 4.78$	<b><math>117.95 \pm 71.82</math></b>
Airforce Combination filters - Ford Fiesta	<b><math>76.95 \pm 43.2</math></b>	$1,154.25 \pm 648$

Table 6.2.3 shows measured values for standard particle and combination filters at 15,000 km and 1,000 km, shown in bold. The table also shows extrapolated and interpolated figures, to determine approximate values at 15,000 km for filters run to 1,000 km and approximate values at 15,000 km for filters run to 1,000 km.

Aluminium quantities on combination filters, taken at 1,000 km are significantly higher than interpolated figures for other combination filters at the same kilometerage, Airforce Combination filters in a Skoda Octavia ( $188.59 \pm 63.72 \mu\text{g}$ ) and Micronair Combination filters in a Skoda Octavia ( $117.95 \pm 71.82 \mu\text{g}$ ) yield comparable concentrations, these concentrations are significantly lower than Airforce Combination filters in a Ford Fiesta ( $1,154.25 \pm 648 \mu\text{g}$ ) extrapolated to 15,000 km. This can be attributed to either the areas travelled by the Ford Fiesta while the combination filter was in place being high in aluminium or to how particles build up on combination filters.

The concentrations on standard particle filters are comparable and correlate well, indicating that for aluminium particulate build up is consistent over 15,000 km.

### 6.2.3 Al Concentrations from internal cabin filters with and without particle filters in place.

Figure 6.2.3 shows a comparison between filters taken from an internal filtration system at a kilometerages 0 km and of 1,000 km with and without a particle filter fitted.

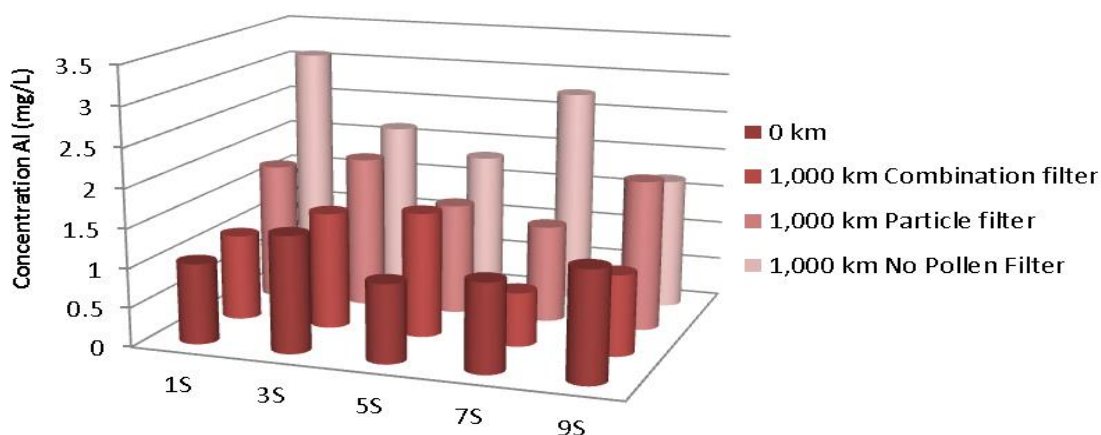


Figure 6.2.3: Al average concentrations for filters taken from an internal extraction system at a kilometerage of 0 km and 1,000 km. The legend key for the x axis is shown in Table 2.4.2. All samples were collected in triplicate.

A significant difference of  $11.61 \pm 2.61 \mu\text{g}$  is observed between the blank filter samples and filters run without a particle filter at 1,000 km. A decrease in Al concentrations is observed on internal filters when comparing filters collected without a standard particle filter present, with a standard particle filter in place and with a combination filter in place, ( $22.5 \pm 4.59 \mu\text{g}$ ,  $14.94 \pm 2.79 \mu\text{g}$ ,  $10.62 \pm 3.33 \mu\text{g}$ , respectively). This indicates that there is a decrease in aluminium concentrations in the cabin when using a standard particle filter and a further decrease occurs when using a combination filter.

Figure 6.2.3 shows a comparison of internal filters taken from a Ford Fiesta. A blank filter was analysed at 0 km as a reference, an internal filter was then placed in the cabin for 1,000 km with no standard particle filter in place, then with a standard particle filter in place for 1,000 km and finally with a combination filter in place for 1,000 km.

Table 6.2.4: The average filter concentrations of Al for filters samples are shown in column 2 (with standard deviation errors between replicates) and corrected Al concentrations based on percentage recoveries from SRM samples are shown in column 3. Column 4 shows recoveries for the entire area of the filter.

Kilometerage (km)	Concentrations from filter sample ( $\mu\text{g}$ )	Corrected based on SRM % recovery ( $\mu\text{g}$ )	Recovery of Al for entire filter area ( $\mu\text{g}$ )
0 Km	$10.89 \pm 1.98$	19.17	172.17
No Particle Filter 1,000 km	$22.5 \pm 4.59$	39.42	354.78
Standard Particle Filter 1,000 km	$14.94 \pm 2.79$	26.19	235.8
Combination Filter 1,000 km	$10.62 \pm 3.33$	18.63	167.49

#### **6.2.4 Al Concentrations from internal cabin filters from three different car makes, Ford Fiesta, Peugeot 307 and Toyota Starlet.**

Figure 6.2.4 shows a comparison between filters taken from an internal filtration system at a kilometerages of 0 km and 1,000 km from three different car models, Ford Fiesta, Peugeot 307 and Toyota Starlet. Representative sampling of internal filters is illustrated in Figure 2.4.2.

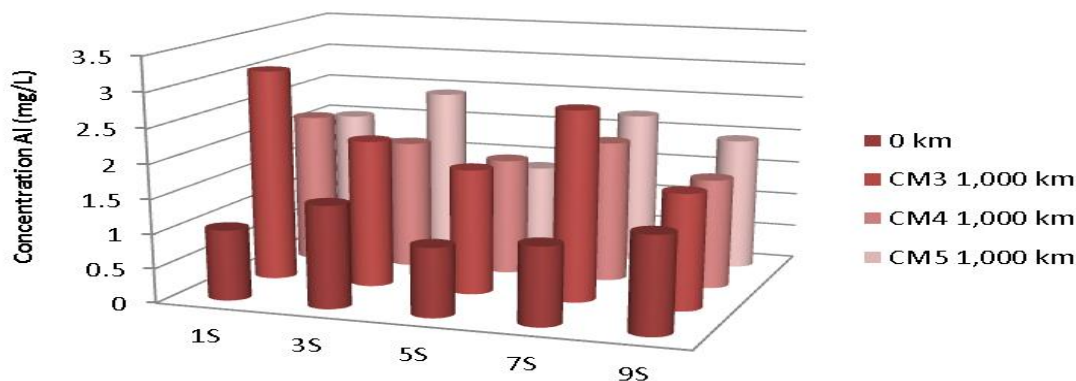


Figure 6.2.4: Average Al concentrations for filters taken from an internal extraction system, run without particle filters in place, from a kilometerage of 0 km to 1,000 km. The legend key for the x axis is shown in Table 2.4.2. All samples were collected in triplicate.

Table 6.2.5: The average filter concentrations of Al for filters samples are shown in column 2 (with standard deviation errors between replicates) and corrected Al concentrations based on percentage recoveries from SRM samples are shown in column 3. Column 4 shows recoveries for the entire area of the filter.

Kilometerage (km)	Concentrations from filter sample ( $\mu\text{g}$ )	Corrected based on SRM % recovery ( $\mu\text{g}$ )	Recovery of Al for entire filter area ( $\mu\text{g}$ )
0 Km	10.62 $\pm$ 2.97	18.63	167.67
Ford Fiesta 1,000 km	22.68 $\pm$ 3.15	39.69	357.30
Peugeot 307 1,000 km	17.01 $\pm$ 2.16	29.79	268.47
Toyota Starlet 1,000 km	17.91 $\pm$ 3.69	31.41	282.51

A significant difference is observed between blank samples and those run in Ford Fiesta, Peugeot 307 and Toyota Starlet, the concentrations are approximately double that of the blank filter. A significant difference is not observed however between filters collected at 1,000 km from a Ford Fiesta (22.68  $\pm$  3.15  $\mu\text{g}$ ), Peugeot 307 (17.01  $\pm$  2.16  $\mu\text{g}$ ), and Toyota Starlet (17.91  $\pm$  3.69  $\mu\text{g}$ ), implying that without particle filters in place the exposure level, for aluminium, is independent of car make.



### 6.3 Chromium

#### 6.3.1 Concentrations of Cr from standard particle filters between 0 km and 1,000 km in a Ford Fiesta).

Figure 6.3.1 shows a comparison between Airforce standard particle filters taken from a Ford Fiesta at a kilometers of 0 km and 1,000 km.

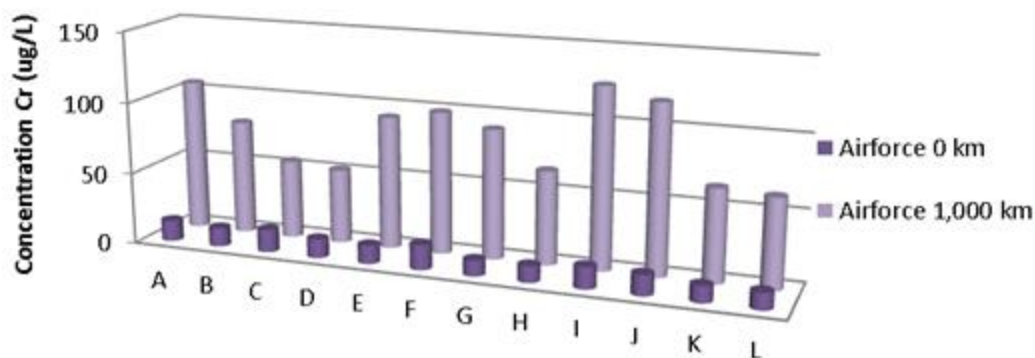


Figure 6.3.1: Average Cr concentrations for a Ford Fiesta, standard particle filters from 0 km to 1,000 km, manufactured by Airforce. The legend key for the x axis is shown in Table 1.4.3. All samples were collected in triplicate.

At a kilometerage of 1,000 km a difference of  $521.82 \pm 99.18$  ng is observed between blank standard particle filters and filter samples collected at 1,000 km,  $236.52 \pm 142.11$  ng and  $758.34 \pm 241.29$  ng, respectively.

Table 6.3.1: The average filter concentrations of Cr for filters samples are shown in column 2 (with standard deviation errors between replicates) and corrected Cr concentrations based on percentage recoveries from SRM samples are shown in column 3. Column 4 shows recoveries for the entire area of the filter.

Kilometerage (km)	Concentrations from filter sample (ng)	Corrected based on SRM % recovery (ng)	Recovery of Cr for entire filter area (µg)
0 km	$236.52 \pm 142.11$	259.02	90.00
1,000 km	$758.34 \pm 241.29$	830.61	290.70

Column 2 shows concentrations for one square inch of a filter with standard deviation errors between replicates. Column 3 of Table 6.3.1 shows concentrations corrected to 100% based on SRM recoveries of chromium using Method 3 shown in Table 3.2.4, estimated to be 91.3% of

the overall quantities of chromium on the filter. Three different filter samples were collected for each kilometerage.

### 6.3.2 Concentrations of Cr from combination filters between 0 km and 1,000 km in a Ford Fiesta.

Figure 6.3.2 shows a comparison between Airforce combination filters taken from a Ford Fiesta at a kilometerages of 0 km and 1,000 km.

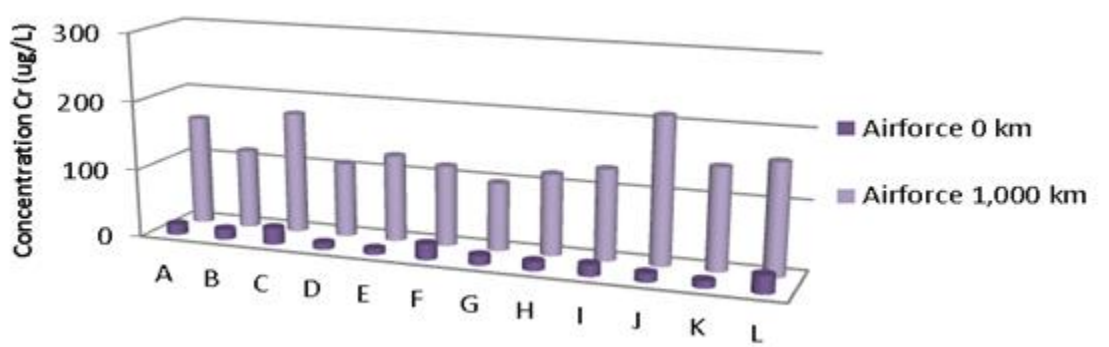


Figure 6.3.2: Average Cr concentrations for a Ford Fiesta, combination filters from 0 km to 1,000 km, manufactured by Airforce. The legend key for the x axis is shown in Table 1.4.3. All samples were collected in triplicate.

A significant difference is observed for combination filters, (as for standard particle filters) between blank filters and those collected at 1,000 km. Chromium levels for blank combination filters are  $172.08 \pm 71.64$  ng and are  $1,254.42 \pm 406.26$  ng for filters collected at 1,000 km. The increase observed on combination filters is twice that of standard particle filters.

Table 6.3.2: The average filter concentrations of Cr for filters samples are shown in column 2 (with standard deviation errors between replicates) and corrected Cr concentrations based on percentage recoveries from SRM samples are shown in column 3. Column 4 shows recoveries for the entire area of the filter.

Kilometerage (km)	Concentrations from filter sample (ng)	Corrected based on SRM % recovery (ng)	Recovery of Cr for entire filter area ( $\mu$ g)
0 km	$172.08 \pm 71.64$	188.55	65.97
1,000 km	$1,254.42 \pm 406.26$	1,373.94	439.65

Table 6.3.3 shows measured values for standard particle and combination filters at 15,000 km and 1,000 km. The table also shows calculated figures, to determine approximate values at 15,000 km for filters run to 1,000 km and approximate values at 15,000 km for filters run to 1,000 km.

Table 6.3.3 shows concentrations from all filters tested over 1,000 km and 15,000 km.

Car and filter make	At 1,000 km	At 15,000 km
	ng	
Micronair Particle Filter - Skoda Octavia	$24.5 \pm 4.29$	<b><math>367.56 \pm 64.35</math></b>
Airforce Particle Filter - Skoda Octavia	$23.18 \pm 3.26$	<b><math>347.67 \pm 48.96</math></b>
Micronair Particle Filter - Toyota Aventis	$28.75 \pm 4.35$	<b><math>431.19 \pm 65.25</math></b>
Nip & Denso Particle - Toyota Aventis	$104.8 \pm 65.31$	<b><math>1,572.03 \pm 979.74</math></b>
Airforce Particle Filter - Ford Fiesta	<b><math>521.82 \pm 99.18</math></b>	$7,827.3 \pm 1,487.7$
Airforce Combination filters – Skoda Octavia	$82.09 \pm 7.93$	<b><math>1,231.38 \pm 118.98</math></b>
Micronair Combination filters – Skoda Octavia	$46.46 \pm 26.54$	<b><math>696.96 \pm 398.16</math></b>
Airforce Combination filters - Ford Fiesta	<b><math>1,082.34 \pm 334.62</math></b>	$16,235.1 \pm 5,019.3$

Airforce standard particle filters analysed at 1,000 km show significantly lower levels of chromium than filters run to 15,000 km, when figures are extrapolated up to 15,000 km. Indicating that for standard particle filters the majority of chromium build up is after 1,000 km as the filter becomes blocked. Airforce combination filters run to 1,000 km in a Ford Fiesta show similar concentrations to Airforce combination filters run in a Ford Fiesta for 15,000 km, thus indicating that the majority of chromium extraction on a combination filter occurs in the first 1,000 km or the area travelled by the Ford Fiesta was higher in chromium than the area travelled by a Skoda Octavia.

Figure 6.3.3: shows a comparison between internal filters taken from a Ford Fiesta. A blank filter was analysed at 0 km as a reference, an internal filter was then placed in the cabin with no standard particle filter in place for 1,000 km, then with a standard particle filter in place for 1,000 km and finally with a combination filter in place for 1,000 km.

Figure 6.3.3 shows a comparison between filters taken from an internal filtration system at a kilometerages 0 km and of 1,000 km.

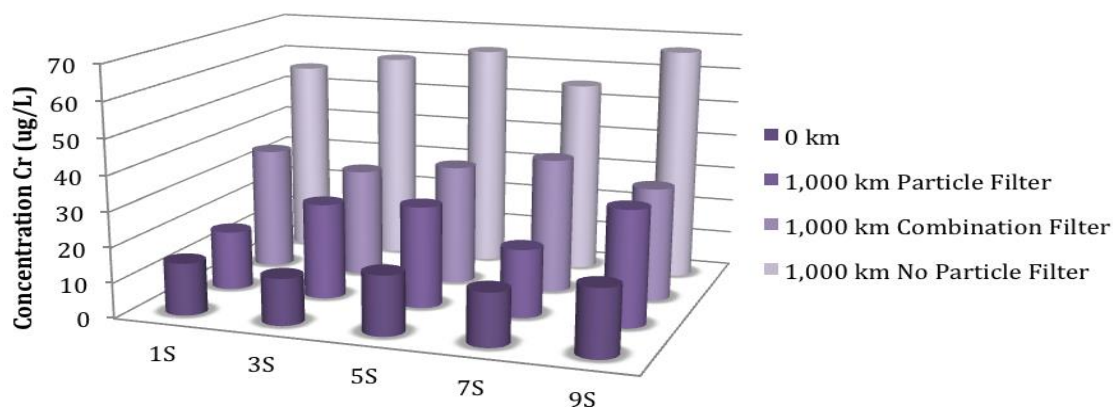


Figure 6.3.3: Average Cr concentrations for filters taken from an internal extraction system at a kilometerage of 0 km and 1,000 km. The legend key for the x axis is shown in Table 2.4.2. All samples were collected in triplicate.

Table 6.3.4: The average filter concentrations of Cr for filters samples are shown in column 2 (with standard deviation errors between replicates) and corrected Cr concentrations based on percentage recoveries from SRM samples are shown in column 3. Column 4 shows recoveries for the entire area of the filter.

Kilometerage (km)	Concentrations from filter Sample (ng)	Corrected based on SRM % recovery (ng)	Recovery of Cr for entire filter area (μg)
0 Km	171.09 ± 109.17	187.38	1.69
No Particle Filter 1,000 km	513.45 ± 91.17	562.41	5.06
Particle Filter 1,000 km	326.52 ± 63.09	357.66	2.28
Combination Filter 1,000 km	231.57 ± 55.26	253.71	3.22

An increase of  $342.36 \pm 18$  ng is observed between the blank filter,  $171.09 \pm 109.17$  ng and the internal filter run with no particle filter,  $513.45 \pm 91.17$  ng. There is a decrease in concentrations between internal filters run with no particle filter and both standard particle filters,  $326.52 \pm 63.09$  ng and combination filters of  $231.57 \pm 55.26$  ng. There is difference of  $94.95 \pm 7.83$  ng observed between standard particle filters and combination filters. This indicates a moderate but measureable amount of chromium is present on internal filters and that the use of a particle/combination filters reduces chromium levels within the cabin.

Figure 6.3.4 shows a comparison between filters taken from an internal filtration system at a kilometers 0 km and of 1,000 km from three different car models, Ford Fiesta, Peugeot 307 and Toyota Starlet.

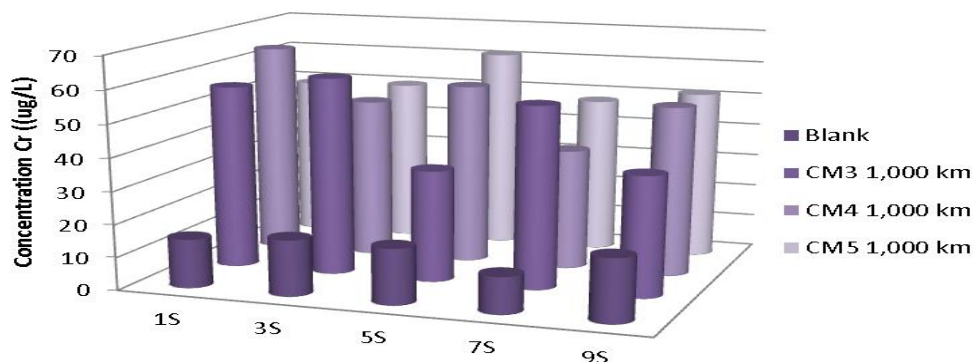


Figure 6.3.4: Average Cr concentrations for filters taken from an internal extraction system, run without particle filters in place, from a kilometerage of 0 km to 1,000 km. The legend key for the x axis is shown in Table 2.4.2. All samples were collected in triplicate.

Table 6.3.5: The average filter concentrations of Cr for filters samples are shown in column 2 (with standard deviation errors between replicates) and corrected Cr concentrations based on percentage recoveries from SRM samples are shown in column 3. Column 4 shows recoveries for the entire area of the filter.

Kilometerage (km)	Concentrations from filter sample (ng)	Corrected based on SRM % recovery (ng)	Recovery of Cr for entire filter area (µg)
0 Km	310.05 ± 22.86	339.66	3.06
Ford Fiesta 1,000 km	513.45 ± 91.17	562.41	5.06
Peugeot 307 1,000 km	498.51 ± 157.77	545.94	4.91
Toyota Starlet 1,000 km	504.27 ± 127.89	552.33	4.97

A moderate difference is observed between blank samples,  $310.05 \pm 22.86$  ng and those run in Ford Fiesta,  $513.45 \pm 91.17$  ng, Peugeot 307,  $498.51 \pm 157.77$  ng and Toyota Starlet for 1,000 km,  $504.27 \pm 127.89$  ng but there is no observable difference between different car makes. This implies that there is an observable level of chromium on the internal filters tested and that this level is independent of car make.

## 6.4: Copper:

### 6.4.1 Concentrations of Cu from standard particle filters between 0 km and 1,000 km in a Ford Fiesta.

Figure 6.4.1 shows a comparison between Airforce standard particle filters taken from a Ford Fiesta at a kilometerages of 0 km and 1,000 km.

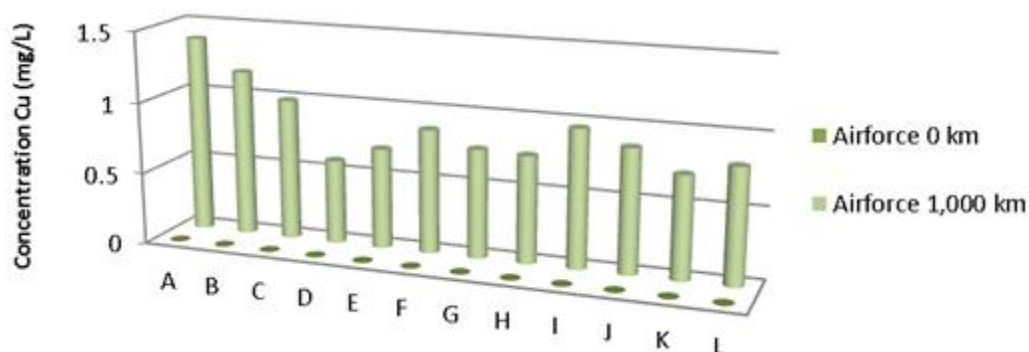


Figure 6.4.1: Average Cu concentrations for a Ford Fiesta, standard particle filters from 0 km to 1,000 km, manufactured by Airforce. The legend key for the x axis is shown in Table 1.4.3. All samples were collected in triplicate.

Table 6.4.1: The average filter concentrations of Cu for filters samples are shown in column 2 (with standard deviation errors) and corrected Cu concentrations based on percentage recoveries from SRM samples are shown in column 3. Column 4 shows recoveries for the entire area of the filter.

Kilometerage (km)	Concentrations from filter sample ( $\mu\text{g}$ )	Corrected based on SRM % recovery ( $\mu\text{g}$ )	Recovery of Cu for entire filter area (mg)
0 km	0	0	0
1,000 km	$6.21 \pm 4.23$	7.65	2.46

Column 2 shows concentrations for one square inch of a filter, with replicate errors. Column 3 of Table 6.4.1 shows concentrations corrected to 100% based on SRM recoveries of copper using Method 3 shown in Table 3.2.4, estimated to be 80.5% of the overall quantities of copper on the filter. Three different filter samples were collected for each kilometerage.

A significant difference is observed between blank filters and filters collected at 1,000 km, 0 mg/L and  $6.21 \pm 4.23 \mu\text{g}$ , respectively. Indicating that at low kilometerages a notable difference in copper concentrations is observed on standard particle filters.

#### 6.4.2 Concentrations of Cu from combination filters between 0 km and 1,000 km in a Ford Fiesta.

Figure 6.4.2 shows a comparison between Airforce combination filters taken from a Ford Fiesta at a kilometerages of 0 km and 1,000 km.

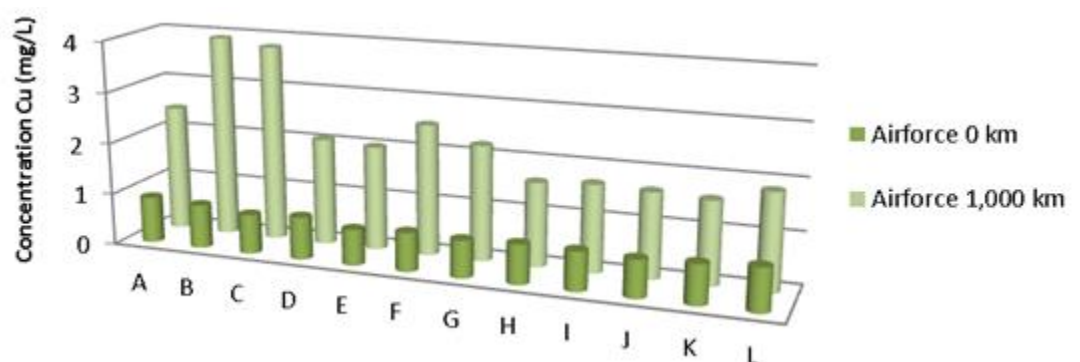


Figure 6.4.2: Average Cu concentrations for a Ford Fiesta, combination filters from 0 km to 1,000 km, manufactured by Airforce. The legend key for the x axis is shown in Table 1.4.3. All samples were collected in triplicate.

Table 6.4.2: The average filter concentrations of Cu for filters samples are shown in column 2 (with standard deviation errors between replicates) and corrected Cu concentrations based on percentage recoveries from SRM samples are shown in column 3. Column 4 shows recoveries for the entire area of the filter.

Kilometerage (km)	Concentrations from filter sample ( $\mu\text{g}$ )	Corrected based on SRM % recovery ( $\mu\text{g}$ )	Recovery of Cu for entire filter area (mg)
0 km	$7.02 \pm 0.54$	8.64	2.77
1,000 km	$21.33 \pm 11.52$	26.46	8.48

A difference of  $14.31 \pm 10.98 \mu\text{g}$  is observed between blank filters and samples collected at 1,000 km,  $7.02 \pm 0.54 \mu\text{g}$  and  $21.33 \pm 11.52 \mu\text{g}$ , respectively. Indicating that even at low kilometerages a notable difference in copper concentrations is observed on combination filters.

A significant difference is observed between combination filters and standard particle filter samples,  $6.21 \pm 4.23 \mu\text{g}$  for standard particle filters and  $14.31 \pm 10.98 \mu\text{g}$  for combination filters. Demonstrating that over this kilometerage combination filters are more efficient at copper extraction.

Table 6.4.3 shows measured values for standard particle and combination filters at 15,000 km and 1,000 km. The table also shows calculated figures, to determine approximate values at 15,000 km for filters run to 1,000 km and approximate values at 15,000 km for filters run to 1,000 km.

Table 6.4.3 shows concentrations from all filters tested over 1,000 km and 15,000 km.

Car and filter make	At 1,000 km	At 15,000 km
	$\mu\text{g}$	
Micronair Particle Filter - Skoda Octavia	$1.74 \pm 0.43$	$26.01 \pm 6.38$
Airforce Particle Filter - Skoda Octavia	$10.79 \pm 6.44$	$161.91 \pm 96.65$
Micronair Particle Filter - Toyota Aventis	$0.28 \pm 0.25$	$4.32 \pm 3.87$
Nip & Denso Particle - Toyota Aventis	$0.32 \pm 0.14$	$4.86 \pm 2.16$
Airforce Particle Filter - Ford Fiesta	$6.21 \pm 4.23$	$93.15 \pm 63.45$
Airforce Combination filters –Skoda Octavia	$37.74 \pm 0.78$	$566.1 \pm 11.67$
Micronair Combination filters – Skoda Octavia	$9.87 \pm 3.06$	$148.05 \pm 45.99$
Airforce Combination filters - Ford Fiesta	$14.31 \pm 10.98$	$214.65 \pm 164.7$

Copper levels on Airforce standard particle filters collected at 1,000 km in a Ford Fiesta are generally consistent with levels on filters collected at 15,000 km from a Skoda Octavia, when interpolated back to 1,000 km. Indicating that Airforce standard particle filter performance is consistent from 0 km to 15,000km and is independent of car make. The levels of copper on Airforce combination filters run in a Ford Fiesta are  $\sim 1/2$  the levels observed in Airforce combination filters run in a Skoda Octavia and are over double the levels observed on Micronair filters run in a Skoda Octavia. Demonstrating that Airforce filters have a higher extraction efficiency over Micronair filters from 0 km to 15,000 km and that particulate matter build up is not consistent over this range, that build up increases with use.



### 6.4.3 Cu concentrations from internal cabin filters with and without particle filters in place.

Figure 6.4.3 shows a comparison between filters taken from an internal filtration system at a kilometerages 0 km and of 1,000 km.

Figure 6.4.3 shows a comparison of internal filters taken from a Ford Fiesta. A blank filter was analysed at 0 km as a reference, an internal filter was then placed in the cabin for 1,000 km with no standard particle filter in place, then with a standard particle filter in place and finally with a combination filter fitted for 1,000 km.

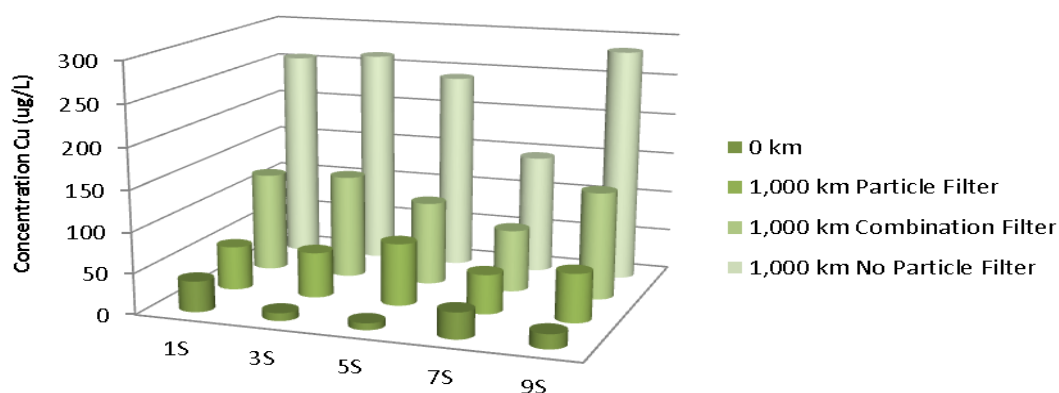


Figure 6.4.3: Average Cu concentrations for filters taken from an internal extraction system at a kilometerage of 0 km and 1,000 km. The legend key for the x axis is shown in Table 2.4.2 All samples were collected in triplicate.

A significant difference in average Cu concentrations is observed between the blank filters and the filter run without a particle filters,  $408.96 \pm 430.92$  ng and  $2,272.77 \pm 123.19$  ng, respectively. A difference of  $1,565.19 \pm 233.31$  ng is also observed between the internal filter run with no particle filter and the internal filters run with a standard particle filter. A moderate difference of  $242.82 \pm 40.14$  ng is observed between internal filters run with a standard particle filter and a combination filter. This implies that for copper, a significant increase in copper concentrations is observed in the absence of a standard particle filter when compared to when using a standard particle filter. These levels further decrease when using a combination filter.

Table 6.4.4: The average filter concentrations of Cu for filters samples are shown in column 2 (with standard deviation errors between replicates) and corrected Cu concentrations based on

percentage recoveries from SRM samples are shown in column 3. Column 4 shows recoveries for the entire area of the filter.

Kilometerage (km)	Concentrations from filter sample (ng)	Corrected based on SRM % recovery (ng)	Recovery of Cu for entire filter area ( $\mu\text{g}$ )
0 Km	$408.96 \pm 430.92$	508.05	4.50
No Particle Filter 1,000 km	$2,272.77 \pm 123.19$	2,823.39	25.38
Particle Filter 1,000 km	$950.4 \pm 396.54$	1,180.62	7.83
Combination Filter 1,000 km	$707.58 \pm 356.4$	878.94	10.62

#### 6.4.4 Cu concentrations from internal cabin filters from three different car makes, Ford Fiesta, Peugeot 307 and Toyota Starlet.

Figure 6.5.4 shows a comparison between internal filters taken from an internal filtration system at a kilometerages 0 km and of 1,000 km from three different car models, Ford Fiesta, Peugeot 307 and Toyota Starlet.

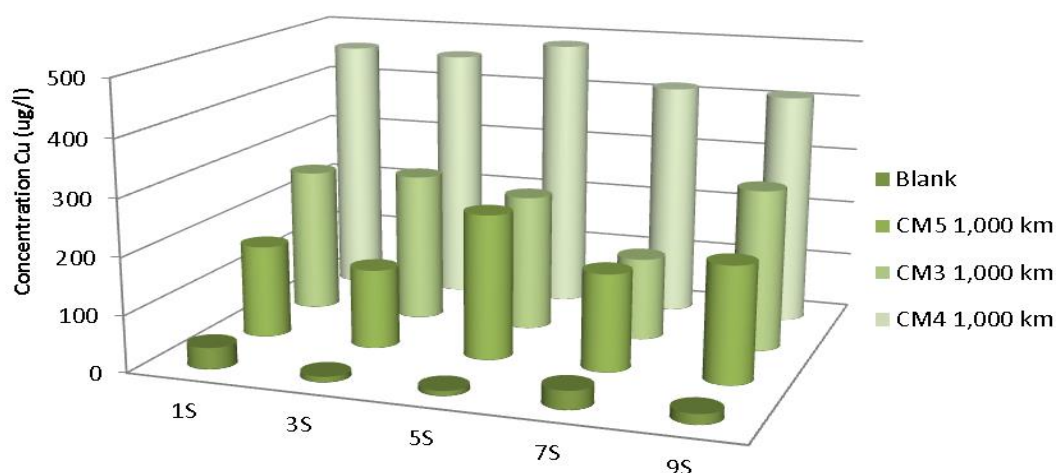


Figure 6.4.4: Average Cu recoveries for filters taken from an internal extraction system, run without particle filters in place, from a kilometerage of 0 km to 1,000 km. The legend key for the x axis is shown in Table 2.4.2. All samples were collected in triplicate.

A significant difference is observed between blank samples,  $408.96 \pm 430.92$  ng and those run in a Ford Fiesta,  $2,272.77 \pm 123.19$  ng, a Peugeot 307,  $3,887.64 \pm 1,016.91$  ng and a Toyota Starlet,  $1,683 \pm 686.25$  ng at 1,000 km. No significant difference is observed between a Ford Fiesta and a Toyota Starlet at 1,000 km but recoveries from a Peugeot 307 are almost double those of a Ford Fiesta and a Toyota Starlet. Implying that without particle filters in place the

exposure level to copper is significantly increased. The areas travelled by the Ford Fiesta and the Toyota Starlet appear to have similar copper levels in but levels in areas travelled by the Peugeot 307 are significantly higher resulting in higher exposure levels.

Table 6.4.5: The average filter recoveries of Cu for filters samples are shown in column 2 (with standard deviation errors) and corrected Cu recoveries based on percentage recoveries from SRM samples are shown in column 3. Column 4 shows recoveries for the entire area of the filter.

### 6.5: Iron:

Kilometerage (km)	Recovered from filter sample (ng)	Corrected based on SRM % recovery (ng)	Recovery of Fe for entire filter area (µg)
0 Km	408.96 ± 430.92	508.05	4.50
Ford Fiesta 1,000 km	2,272.77 ± 123.19	2,823.39	25.38
Peugeot 307 1,000 km	3,887.64 ± 1,016.91	4,829.31	43.47
Toyota Starlet 1,000 km	1,683 ± 686.25	2,090.7	18.90

#### 6.5.1 Recoveries of Fe from standard particle filters between 0 km and 1,000 km in a Ford Fiesta.

Figure 6.5.1 shows a comparison between Airforce standard particle filters taken from a Ford Fiesta at a kilometerages of 0 km and 1,000 km.

A significant difference of  $7.47 \pm 2.61 \mu\text{g}$  is observed between blank filters and filters collected at 1,000 km,  $2.61 \pm 0.54 \mu\text{g}$  and  $10.08 \pm 3.15 \mu\text{g}$  respectively. This indicates at this kilometerage a notable difference in iron concentrations is observed.

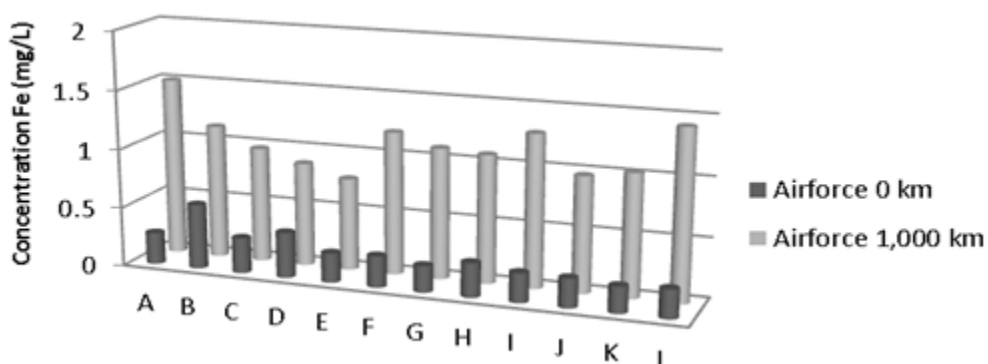


Figure 6.5.1: Average Fe concentrations for a Ford Fiesta, standard particle filters from 0 km to 1,000 km, manufactured by Airforce. The legend key for the x axis is shown in Table 1.4.3. All samples were collected in triplicate.

Table 6.5.1: The average filter concentrations of Fe for filters samples are shown in column 2 (with standard deviation errors between replicates) and corrected Fe concentrations based on percentage recoveries from SRM samples are shown in column 3. Column 4 shows recoveries for the entire area of the filter.

Kilometerage (km)	Concentrations from filter sample ( $\mu\text{g}$ )	Corrected based on SRM % recovery ( $\mu\text{g}$ )	Recovery of Fe for entire filter area (mg)
0 km	$2.61 \pm 0.54$	3.15	1.01
1,000 km	$10.08 \pm 3.15$	12.15	3.90

Column 2 of Table 6.5.2 shows concentrations for one square inch of a filter. Column 3 shows concentrations corrected to 100% based on SRM recoveries of iron using Method 3 shown in Table 3.2.4, estimated to be 82.4% of the overall quantities of iron on the filter. Three different filter samples were collected for each kilometerage.

### 6.5.2 Concentrations of Fe from combination filters between 0 km and 1,000 km in a Ford Fiesta.

Figure 6.5.2 shows a comparison between Airforce combination filters taken from a Ford Fiesta at a kilometerages of 0 km and 1,000 km.

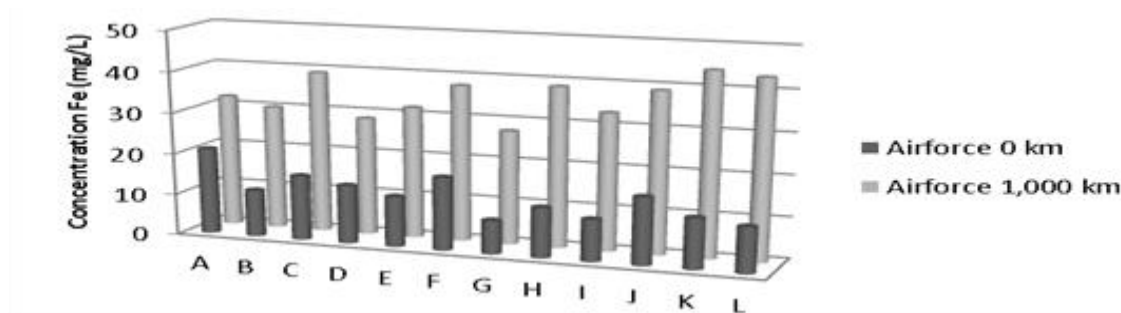


Figure 6.5.2: Average Fe concentrations for a Ford Fiesta, combination filters from 0 km to 1,000 km, manufactured by Airforce. The legend key for the x axis is shown in Table 1.4.3. All samples were collected in triplicate.

Concentrations for blank filter samples,  $121.95 \pm 25.83 \mu\text{g}$  almost half those of samples taken at 1,000 km,  $319.59 \pm 79.56 \mu\text{g}$ . This indicates that even at low kilometerages a significant difference in iron concentrations is observed. A significant difference is observed in Fe concentrations between both standard particle filters and combination filter samples, indicating that combination filters are more efficient at iron extraction.

Table 6.5.2: The average filter concentrations of Fe for filters samples are shown in column 2 (with standard deviation errors between replicates) and corrected Fe concentrations based on percentage recoveries from SRM samples are shown in column 3. Column 4 shows recoveries for the entire area of the filter.

Kilometerage (km)	Concentrations from filter sample ( $\mu\text{g}$ )	Corrected based on SRM % recovery ( $\mu\text{g}$ )	Recovery of Fe for entire filter area (mg)
0 km	$121.95 \pm 25.83$	148.05	47.34
1,000 km	$319.59 \pm 79.56$	387.81	124.02

Table 6.5.3 shows measured values for standard particle and combination filters at 15,000 km and 1,000 km. The table also shows extrapolated and interpolated figures, to determine approximate values at 15,000 km for filters run to 1,000 km and approximate values at 15,000 km for filters run to 1,000 km, for comparison.

There is a general consistency between standard particle filters run to 1,000 km and extrapolated figures, calculated from filters run to 15,000 km. Indicating that iron extraction on standard particle filters is consistent from 0 km to 15,000 km. Concentrations from combination filters run to 1,000 km are comparable to quantities extracted from filters run to 15,000 km, implying that iron build up on combination filters is not consistent over 15,000 km and the majority of iron is extracted in the first 1,000 km or like chromium, the area travelled by the Ford Fiesta was higher in iron than the area travelled by a Skoda Octavia.

Table 6.5.3 shows concentrations from all filters tested over 1,000 km and 15,000 km.

Car and filter make	At 1,000 km	At 15,000 km
	$\mu\text{g}$	
Micronair Particle Filter - Skoda Octavia	<b><math>3.57 \pm 1</math></b>	<b><math>53.64 \pm 15.07</math></b>
Airforce Particle Filter - a Skoda Octavia	<b><math>7.04 \pm 0.7</math></b>	<b><math>105.66 \pm 10.62</math></b>
Airforce Particle Filter - Ford Fiesta	<b><math>7.47 \pm 2.61</math></b>	$112.05 \pm 39.15$
Micronair Particle Filter - Toyota Aventis	$6.42 \pm 4.15$	<b><math>96.39 \pm 62.28</math></b>
Nip & Denso Particle - Toyota Aventis	$8.62 \pm 5.42$	<b><math>129.33 \pm 81.36</math></b>
Airforce Combination filters – Skoda Octavia	$7.86 \pm 3.64$	<b><math>117.9 \pm 54.72</math></b>
Micronair Combination filters – Skoda Octavia	$18.01 \pm 5.9$	<b><math>270.18 \pm 88.56</math></b>
Airforce Combination filters - Ford Fiesta	<b><math>197.64 \pm 53.73</math></b>	$2,964.9 \pm 805.95$

### 6.5.3 Fe Concentrations from internal cabin filters with and without particle filters in place.

Figure 6.5.3 shows a comparison of representative Fe concentrations between filters taken from internal filtration systems, in a Ford Fiesta, at kilometerages of 0 km and 1,000 km. A blank filter was analysed at 0 km as a reference, an internal filter was then placed in the cabin for 1,000 km with no standard particle filter in place, the with a standard particle filter in place for 1,000 km and finally with a combination filter in place for 1,000 km.

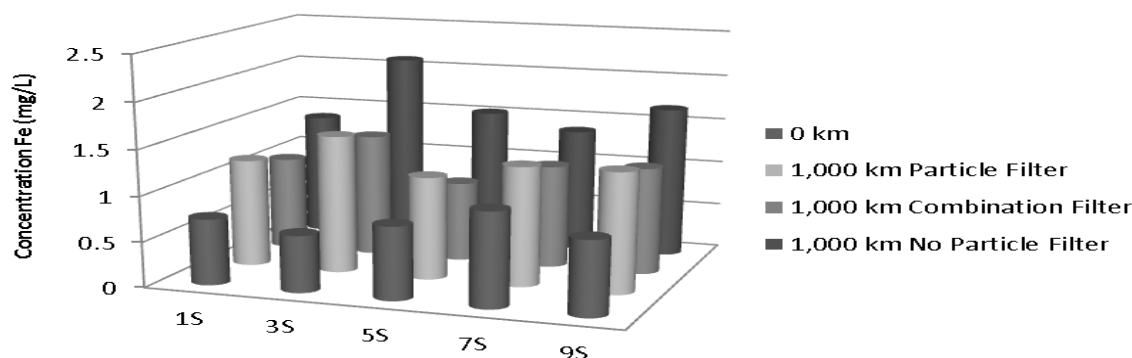


Figure 6.5.3: Average Fe concentrations for filters taken from an internal extraction system at a kilometerage of 0 km and 1,000 km. The legend key for the x axis is shown in Table 2.4.2. All samples were collected in triplicate.

A moderate increase is observed between the blank filter,  $8.1 \pm 1.35 \mu\text{g}$  and the filters run without particle filters  $13.86 \pm 3.51 \mu\text{g}$ . A moderate decrease is also observed between the internal filter run with no particle filter,  $13.86 \pm 3.51 \mu\text{g}$  and the internal filters run with a standard particle filter,  $11.7 \pm 3.87 \mu\text{g}$  and a combination filter,  $9.36 \pm 3.06 \mu\text{g}$ . This indicates

that exposure occurs in the absence of a particle filter. The use of a standard particle filters reduces the exposure levels and the exposure levels decrease further when using combination filters.

Table 6.5.4: The average filter concentrations of Fe for filters samples are shown in column 2 (with standard deviation errors) and corrected Al concentrations based on percentage recoveries from SRM samples are shown in column 3. Column 4 shows recoveries for the entire area of the filter.

Kilometerage (km)	Concentrations from filter sample ( $\mu\text{g}$ )	Corrected based on SRM % recovery ( $\mu\text{g}$ )	Recovery of Fe for entire filter area ( $\mu\text{g}$ )
0 Km	$8.1 \pm 1.35$	9.81	88.65
No Particle Filter 1,000 km	$13.86 \pm 3.51$	16.83	151.38
Particle Filter 1,000 km	$11.7 \pm 3.87$	14.13	127.35
Combination Filter 1,000 km	$9.36 \pm 3.06$	11.34	102.15

#### 6.5.4 Fe concentrations from internal cabin filters from three different car makes, Ford Fiesta, Peugeot 307 and Toyota Starlet.

Figure 6.5.4 shows a comparison between filters taken from an internal filtration system at a kilometerages 0 km and of 1,000 km from three different car models, Ford Fiesta, Peugeot 307 and Toyota Starlet.

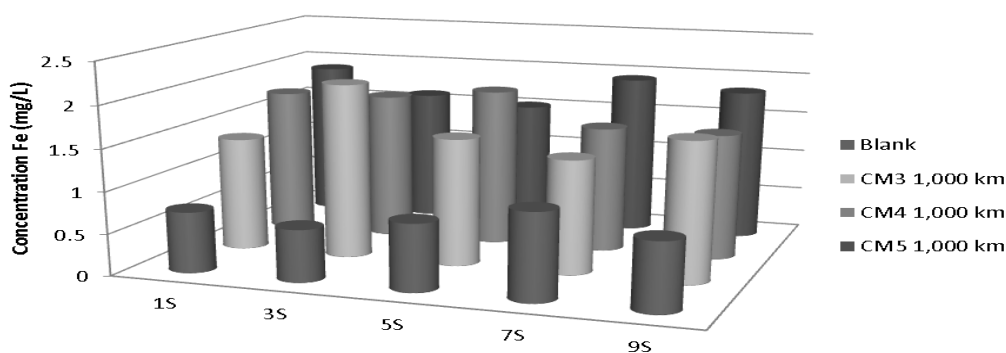


Figure 6.5.4: Average Fe concentrations for filters taken from an internal extraction system, run without particle filters in place, from a kilometerage of 0 km to 1,000 km. The legend key for the x axis is shown in Table 2.4.2. All samples were collected in triplicate.

Iron concentrations between blank samples are approximately half,  $7.38 \pm 1.35 \mu\text{g}$  of those from samples run to 1,000 km. The observed concentrations are  $7.38 \pm 1.35 \mu\text{g}$  for blank samples and  $13.86 \pm 3.51 \mu\text{g}$  for those run in a Ford Fiesta, Peugeot 307 ( $15.84 \pm 1.71 \mu\text{g}$ ) and Toyota Starlet ( $15.21 \pm 1.53 \mu\text{g}$ ) for 1,000 km. There is no significant difference observed between 1,000 km samples from different car makes, implying that without particle filters in place the exposure level is independent of car make.

Table 6.5.5: The average filter concentrations of Fe for filters samples are shown in column 2 (with standard deviation errors between replicates) and corrected Pb concentrations based on percentage concentrations from SRM samples are shown in column 3. Column 4 shows recoveries for the entire area of the filter.

Kilometerage (km)	Concentrations from filter sample ( $\mu\text{g}$ )	Corrected based on SRM % recovery ( $\mu\text{g}$ )	Recovery of Fe for entire filter area ( $\mu\text{g}$ )
0 Km	$7.38 \pm 1.35$	9	80.82
Ford Fiesta 1,000 km	$13.86 \pm 3.51$	16.83	151.38
Peugeot 307 1,000 km	$15.84 \pm 1.71$	19.17	172.89
Toyota Starlet 1,000 km	$15.21 \pm 1.53$	18.45	165.87

## 6.6: Lead:

### 6.6.1 Concentrations of Pb from standard particle filters between 0 km and 1,000 km in a Ford Fiesta.

Figure 6.6.1 shows a comparison between Airforce standard particle filters taken from a Ford Fiesta at a kilometerages of 0 km and 1,000 km.

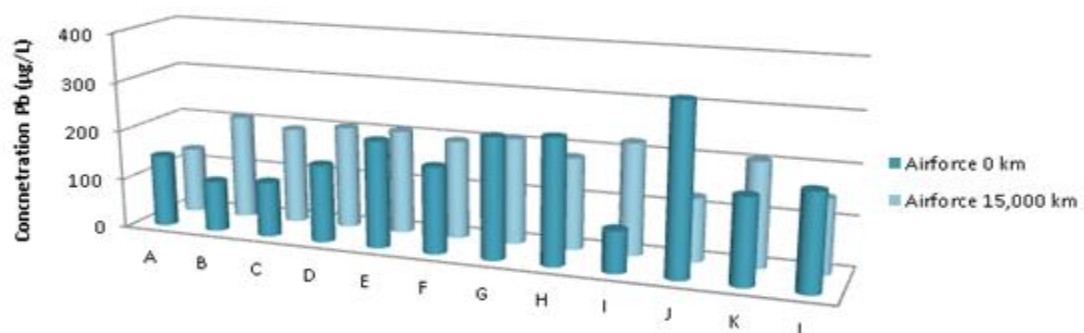


Figure 6.6.1: Average Pb concentrations for a Ford Fiesta, standard particle filters from 0 km to 1,000 km, manufactured by Airforce. The legend key for the x axis is shown in Table 1.4.3. All samples were collected in triplicate.



A significant difference is not observed between blank filters,  $1,631.34 \pm 270.36$  ng and samples collected at 1,000 km,  $1,684.35 \pm 175.95$  ng. Indicating that at low kilometerages no notable difference in lead concentrations is observed.

Table 6.6.1: The average filter concentrations of Pb for filters samples are shown in column 2 (with standard deviation errors) and corrected Pb concentrations based on percentage recoveries from SRM samples are shown in column 3. Column 4 shows recoveries for the entire area of the filter.

Kilometerage (km)	Concentrations from filter sample (ng)	Corrected based on SRM % recovery (ng)	Recovery of Pb for entire filter area ( $\mu\text{g}$ )
0 km	$1,631.34 \pm 270.36$	1,868.58	654.03
1,000 km	$1,684.35 \pm 175.95$	1,929.33	675.00

Column 3 of Table 6.6.1 shows concentrations corrected to 100% based on SRM recoveries of lead using Method 3 shown in Table 3.2.4, estimated to be 87.3% of the overall quantities of lead on the filter. Column 2 shows concentrations for one square inch of a filter, with standard deviation errors between replicates. Three different filter samples were collected for each kilometerage.

### 6.6.2 Concentrations of Pb from combination filters between 0 km and 1,000 km in a Ford Fiesta.

Figure 6.6.2 shows a comparison between Airforce combination filters taken from a Ford Fiesta at a kilometerages of 0 km and 1,000 km.

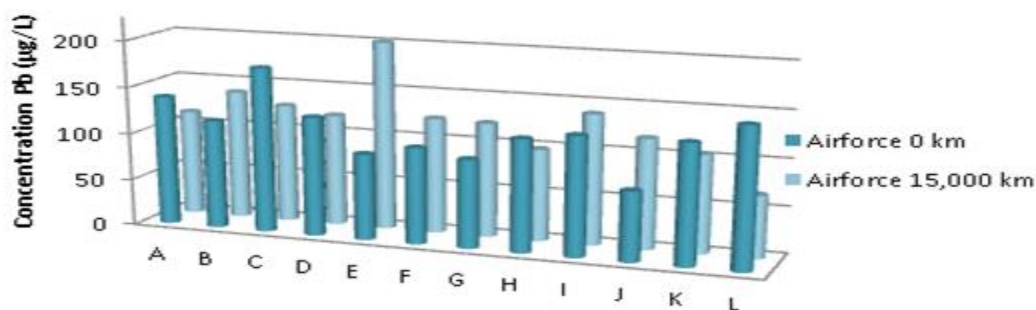


Figure 6.6.2: Average Pb concentrations for a Ford Fiesta, combination filters from 0 km to 1,000 km, manufactured by Airforce. The legend key for the x axis is shown in Table 1.4.3. All samples were collected in triplicate.

Table 6.6.2: The average filter concentrations of Pb for filters samples are shown in column 2 (with standard deviation errors between replicates) and corrected Pb concentrations based on percentage recoveries from SRM samples are shown in column 3. Column 4 shows recoveries for the entire area of the filter.

Kilometerage (km)	Concentrations from filter sample (ng)	Corrected based on SRM % recovery (ng)	Recovery of Pb for entire filter area ( $\mu\text{g}$ )
0 km	$1,021.05 \pm 43.2$	1,169.55	374.22
1,000 km	$1,206 \pm 225$	1,381.41	441.99

Table 6.6.3 shows measured values for standard particle and combination filters at 15,000 km and 1,000 km. The table also shows calculated figures, to determine approximate values at 15,000 km for filters run to 1,000 km and approximate values at 15,000 km for filters run to 1,000 km.

A moderate increase is observed between blank filters,  $1,021.05 \pm 43.2$  ng and those collected at 1,000 km,  $1,206 \pm 225$  ng. This indicates, due to elevated background of the blank filters, that at low kilometerages a less significant quantity of lead is not observed on combination filters. The high background for Pb is equivalent to that for the standard particle filter.

Table 6.6.3 shows concentrations from all filters tested over 1,000 km and 15,000 km.

Car and filter make	At 1,000 km	At 15,000 km
	ng	
Micronair Particle Filter - Skoda Octavia	$86.88 \pm 13.24$	<b><math>1,303.2 \pm 198.63</math></b>
Airforce Particle Filter - Skoda Octavia	$35.59 \pm 2.44$	<b><math>533.86 \pm 36.63</math></b>
Airforce Particle Filter - Ford Fiesta	<b><math>53.01 \pm 94.41</math></b>	$795.15 \pm 1,416.15$
Micronair Particle Filter - Toyota Aventis	$70.92 \pm 9.42$	<b><math>435.6 \pm 141.3</math></b>
Nip & Denso Particle - Toyota Aventis	$95.35 \pm 1.41$	<b><math>1,430.37 \pm 21.16</math></b>
Airforce Combination filters – Skoda Octavia	$75.93 \pm 9.07$	<b><math>1,138.95 \pm 136.17</math></b>
Micronair Combination filters – Skoda Octavia	$28.13 \pm 8.25$	<b><math>422.01 \pm 123.84</math></b>
Airforce Combination filters - Ford Fiesta	<b><math>184.95 \pm 181.8</math></b>	$2,774.25 \pm 2,727$

Lead concentrations for standard particle filters extracted at 1,000 km are comparable to levels from filters extracted at 15,000 km, when figures are extrapolated back. Indicating that, for standard particle filters, extraction is consistent from 0 km to 15,000 km. Concentrations from

combination filters taken from a Ford Fiesta show no significant quantities of Pb, while combination filter run in a Skoda Octavia show significant Pb concentrations. Indicating that there isn't a continuous extraction from 0 km to 15,000 and that the concentration increase with use or that the ambient air in the area travelled by the Skoda Octavia is higher in lead than the area travelled by a Ford Fiesta.

### 6.6.3 Pb concentrations from internal cabin filters with and without particle filters in place.

Figure 6.6.3 shows a comparison between filters taken from an internal filtration system at a kilometers 0 km and of 1,000 km.

Figure 6.6.3: shows a comparison of internal filters taken from a Ford Fiesta. A blank filter was analysed at 0 km as a reference, an internal filter was then placed in the cabin for 1,000 km with no standard particle filter in place for 1,000 km, then with a standard particle filter in place for 1,000 km and finally with a combination filter in place for 1,000 km.

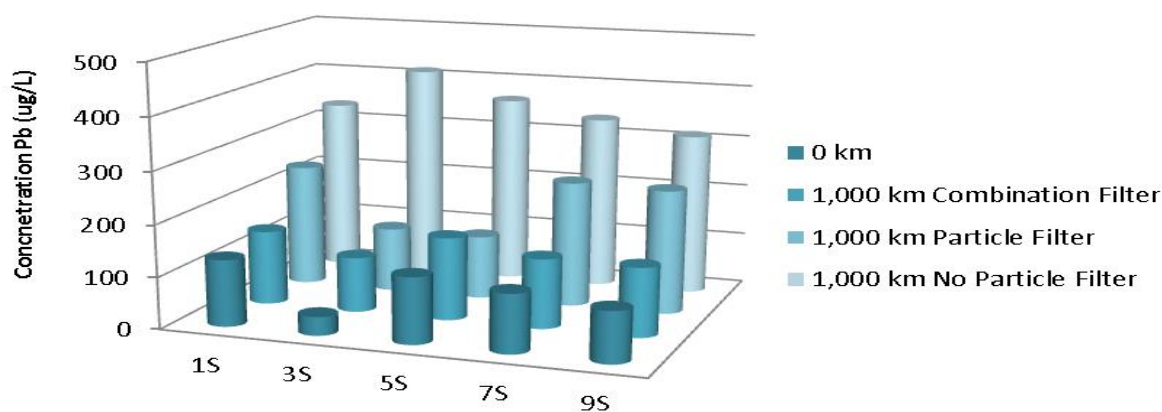


Figure 6.6.3: Average Pb concentrations for filters taken from an internal extraction system at a kilometerage of 0 km and 1,000 km. The legend key for the x axis is shown in Table 2.4.2. All samples were collected in triplicate.

A difference of  $2,442.24 \pm 120.42$  ng is observed between the blank filter and the internal filter run without a particle filter. A significant difference is also observed between the internal filter run with no particle filter,  $3,347.19 \pm 464.85$  ng and internal filters run with a standard particle filter yield  $1,917.36 \pm 452.61$  ng and a combination filter  $1,218.87 \pm 174.96$  ng. This

implies that the use a standard particle filter reduces exposure to lead and that exposure is further reduced with the use of a combination filter.

Table 6.6.4: The average filter concentrations of Pb for filters samples are shown in column 2 (with standard deviation errors between replicates) and corrected Pb concentrations based on percentage recoveries from SRM samples are shown in column 3. Column 4 shows recoveries for the entire area of the filter.

Kilometerage (km)	Concentrations from filter sample (ng)	Corrected based on SRM % recovery (ng)	Recovery of Pb for entire filter area ( $\mu\text{g}$ )
0 Km	904.95 $\pm$ 344.43	1,036.62	9.27
No Particle Filter 1,000 km	3,347.19 $\pm$ 464.85	3,834.18	34.47
Particle Filter 1,000 km	1,917.36 $\pm$ 452.61	2,196.27	19.71
Combination Filter 1,000 km	1,218.87 $\pm$ 174.96	1,396.17	12.51

#### 6.6.4 Pb concentrations from internal cabin filters from three different car makes, Ford Fiesta, Peugeot 307 and Toyota Starlet.

Figure 6.6.4 shows a comparison between filters taken from an internal filtration system at a kilometerages 0 km and of 1,000 km from three different car models Ford Fiesta, Peugeot 307 and a Toyota Starlet.

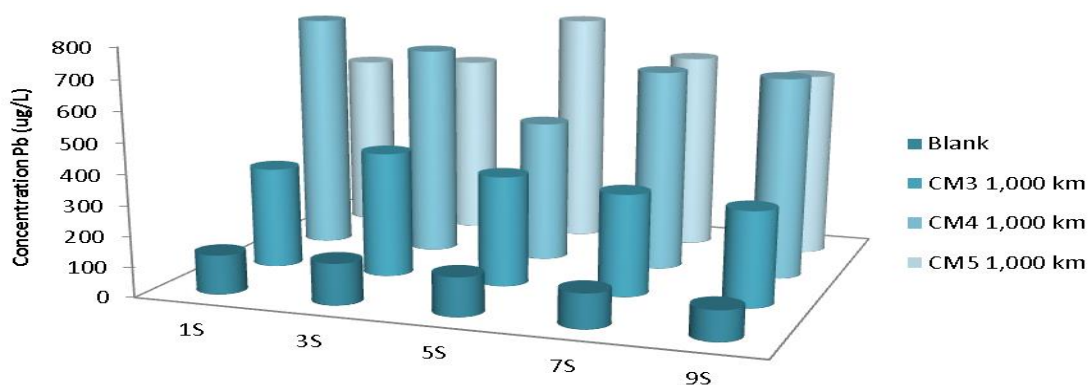


Figure 6.6.4: Average Pb concentrations for filters taken from an internal extraction system, run without particle filters in place, from a kilometerage of 0 km to 1,000 km. The legend key for the x axis is shown in Table 2.4.2. All samples were collected in triplicate.

Table 6.6.5: The average filter concentrations of Pb for filters samples are shown in column 2 (with standard deviation errors) and corrected Pb concentrations based on percentage

recoveries from SRM samples are shown in column 3. Column 4 shows recoveries for the entire area of the filter.

Kilometerage (km)	Concentrations from filter sample (ng)	Corrected based on SRM % recovery (ng)	Recovery of Pb for entire filter area (mg)
0 Km	904.95 $\pm$ 344.34	419.49	3.78
Ford Fiesta 1,000 km	2,447.19 $\pm$ 1,064.34	1,296.45	11.67
Peugeot 307 1,000 km	5,836.77 $\pm$ 662.58	807.12	7.26
Toyota Starlet 1,000 km	5,910.12 $\pm$ 1,037.07	1,263.24	11.37

A moderate difference is observed between blank samples, 904.95  $\pm$  344.34 ng and those run in a Ford Fiesta, 2,447.19  $\pm$  1,064.34 ng. With a greater difference between blank samples and Peugeot 307 samples, 5,836.77  $\pm$  662.58 ng & Toyota Starlet, 5,910.12  $\pm$  1,037.07 ng for 1,000 km. No significant difference is observed between 1,000 km samples for a Peugeot 307 and a Toyota Starlet but a significant difference is observed between a Ford Fiesta and Peugeot 307/Toyota Starlet. This may indicate that areas travelled by a Peugeot 307 and a Toyota Starlet are significantly higher in lead than areas travelled by a Ford Fiesta.

## **.7: Manganese:**

### **6.7.1 Concentrations of Mn from standard particle filters between 0 km and 1,000 km in a Ford Fiesta.**

Figure 6.7.1 shows a comparison between Airforce standard particle filters taken from a Ford Fiesta at a kilometerages of 0 km and 1,000 km.

A moderate difference of 1.98  $\pm$  7.65 ng is observed between blank filters and samples collected at 1,000 km, 7.74  $\pm$  1.98 ng and 9.63  $\pm$  9.63 ng, respectively. Background values for Mn are significantly high and levels observed at 1,000 km are marginally higher with no de-absorption evident.

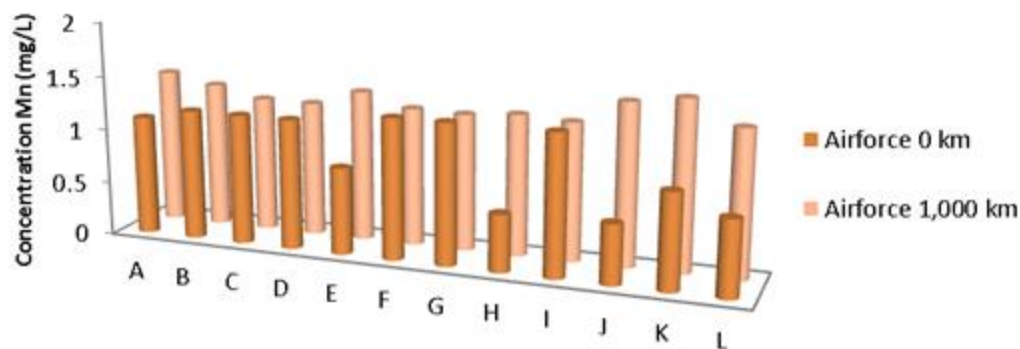


Figure 6.7.1: Average Mn concentrations for a Ford Fiesta, standard particle filters from 0 km to 1,000 km, manufactured by Airforce. The legend key for the x axis is shown in Table 1.4.3. All samples were collected in triplicate.

Table 6.7.1: The average filter concentrations of Mn for filters samples are shown in column 2 (with standard deviation errors between replicates) and corrected Mn concentrations based on percentage recoveries from SRM samples are shown in column 3. Column 4 shows recoveries for the entire area of the filter.

Column 3 of Table 6.7.1 shows concentrations corrected to 100% based on SRM recoveries of manganese using Method 3 shown in Table 3.2.4, estimated to be 82.1% of the overall quantities of manganese on the filter. Column 2 shows concentrations for one square inch of a filter, with standard deviation errors. Three different filter samples were collected for each kilometerage.

Kilometerage (km)	Concentrations from filter sample (ng)	Corrected based on SRM % recovery (ng)	Recovery of Mn for entire filter area (mg)
0 km	7.74 ± 1.98	9.45	3.01
1,000 km	9.63 ± 9.63	11.7	3.75

### 6.7.2 Concentrations of Mn from combination filters between 0 km and 1,000 km in a Ford Fiesta.

Figure 6.7.2 shows a comparison between Airforce combination filters taken from a Ford Fiesta at a kilometerages of 0 km and 1,000 km.

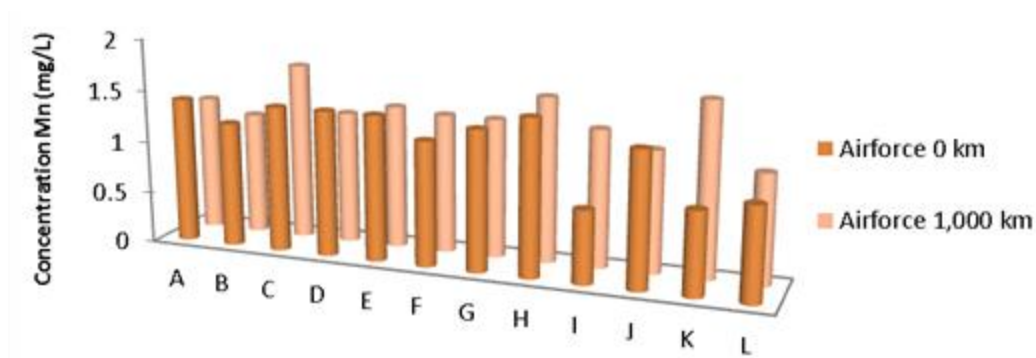


Figure 6.7.2: Average Mn concentrations for a Ford Fiesta, combination filters from 0 km to 1,000 km, manufactured by Airforce. The legend key for the x axis is shown in Table 1.4.3. All samples were collected in triplicate.

Table 6.7.2: The average filter concentrations of Mn for filters samples are shown in column 2 (with standard deviation errors between replicates) and corrected Mn concentrations based on percentage recoveries from SRM samples are shown in column 3. Column 4 shows recoveries for the entire area of the filter.

Kilometerage (km)	Concentrations from filter sample (ng)	Corrected based on SRM % recovery (ng)	Recovery of Mn for entire filter area (mg)
0 km	11.88 ± 3.51	14.49	4.62
1,000 km	11.61 ± 3.33	14.13	4.51

Table 6.7.3 shows measured values for standard particle and combination filters at 15,000 km and 1,000 km. The table also shows calculated figures, to determine approximate values at 15,000 km for filters run to 1,000 km and approximate values at 15,000 km for filters run to 1,000 km.

As for standard particulate filters, a significant difference is not observed between both filter samples,  $11.88 \pm 3.51$  ng for blank samples and  $11.61 \pm 3.33$  ng for samples taken at 1,000 km. Indicating that at low kilometerages a notable difference in manganese concentrations is not observed, due to high background concentrations.

Manganese concentrations are low for all filters tested. Both combination and standard particle filters show no manganese present at 1,000 km, with high background levels. They do however show manganese levels at 15,000 km, implying that with filter use the extraction

efficiency of manganese increases or areas travelled by Skoda Octavias and Toyota Aventis are higher in manganese.

Table 6.7.3 shows concentrations from all filters tested over 1,000 km and 15,000 km.

Car and filter make	At 1,000 km	At 15,000 km
	$\mu\text{g}$	
Micronair Particle Filter - Skoda Octavia	$0.084 \pm 0.03$	<b><math>1.26 \pm 0.45</math></b>
Airforce Particle Filter - Skoda Octavia	$0.408 \pm 0.168$	<b><math>6.12 \pm 2.52</math></b>
Airforce Particle Filter - Ford Fiesta	<b><math>0.002 \pm 0.007</math></b>	$0.028.35 \pm 0.12$
Micronair Particle Filter - Toyota Aventis	$0.12 \pm 0.066$	<b><math>1.8 \pm 0.99</math></b>
Nip & Denso Particle - Toyota Aventis	$0.24 \pm 0.138$	<b><math>3.52 \pm 2.07</math></b>
Airforce Combination filters – Skoda Octavia	$0.162 \pm 0.054$	<b><math>2.43 \pm 0.81</math></b>
Micronair Combination filters – Skoda Octavia	$0.138 \pm 0.012$	<b><math>2.07 \pm 0.18</math></b>
Airforce Combination filters - Ford Fiesta	<b>0</b>	0

### 6.7.3 Mn concentrations from internal cabin filters with and without particle filters in place

Figure 6.7.3 shows a comparison between filters taken from an internal filtration system at a kilometerages 0 km and of 1,000 km.

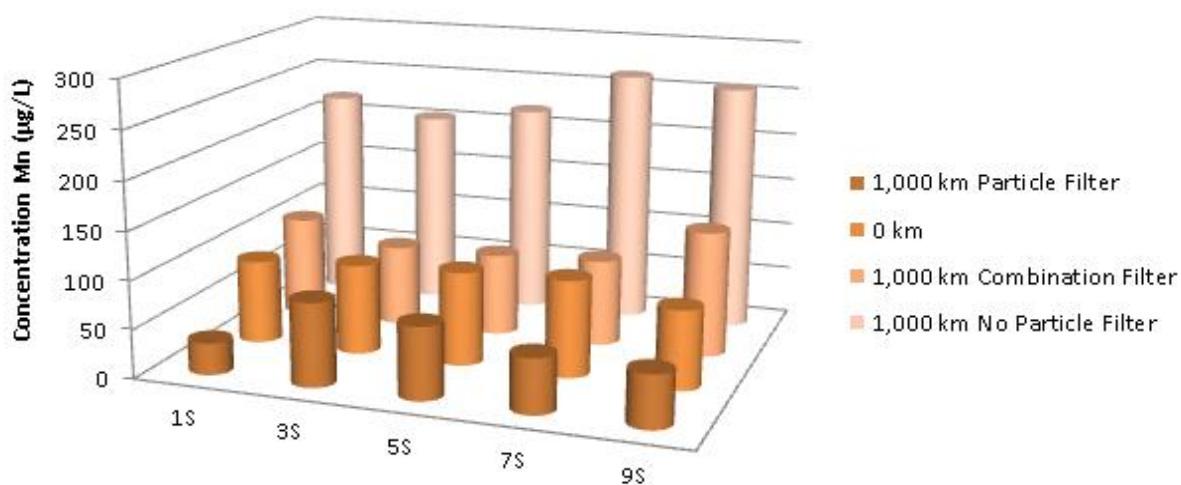


Figure 6.7.3: Average Mn concentrations for filters taken from an internal extraction system at a kilometerage of 0 km and 1,000 km. The legend key for the x axis is shown in Table 2.4.2. All samples were collected in triplicate.



A difference in manganese concentrations is observed between the blank filters,  $124.47 \pm 67.14$  ng and the filters run without a particle filter,  $2,098.98 \pm 225.36$  ng, run with a standard particle filter,  $547.38 \pm 185.22$  ng and run with a combination filter,  $908.46 \pm 163.62$  ng. A measureable quantity of manganese is present with a particle filter (standard particle filter or a combination filter) despite high background levels, in their absence there is a significant increase in Mn.

Table 6.7.4: The average filter recoveries of Mn for filters samples are shown in column 2 (with standard deviation errors between replicates) and corrected Mn recoveries based on percentage recoveries from SRM samples are shown in column 3.

Kilometerage (km)	Concentrations from filter sample (ng)	Corrected based on SRM % recovery (ng)	Recovery of Mn for entire filter area ( $\mu\text{g}$ )
0 Km	$124.47 \pm 67.14$	1,006.65	9.09
No Particle Filter 1,000 km	$2,098.98 \pm 225.36$	2,554.38	22.95
Particle Filter 1,000 km	$547.38 \pm 185.22$	666.81	6.03
Combination Filter 1,000 km	$908.46 \pm 163.62$	1,106.55	12.51

#### 6.7.4 Mn Recoveries from internal cabin filters from three different car makes, Ford Fiesta, Peugeot 307 and Toyota Starlet.

Figure 6.7.4 shows a comparison between filters taken from an internal filtration system at a kilometerages 0 km and of 1,000 km from three different car models Ford Fiesta, Peugeot 307 and Toyota Starlet.

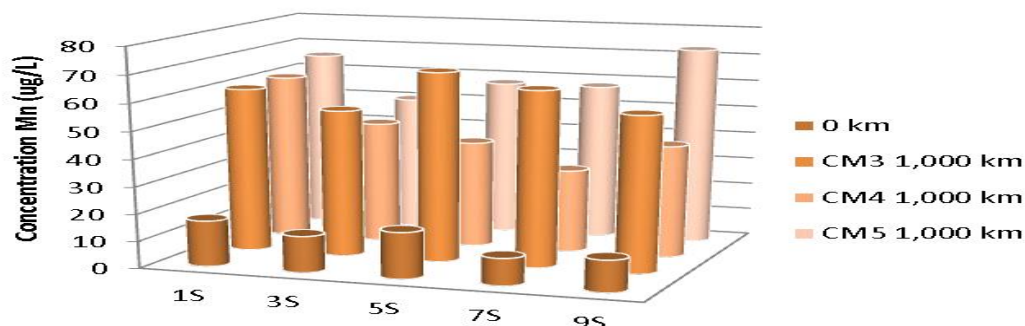


Figure 6.7.4: Average Mn concentrations for filters taken from an internal extraction system, run without particle filters in place, from a kilometerage of 0 km to 1,000 km. The legend key for the x axis is shown in Table 2.4.2. All samples were collected in triplicate.

Table 6.7.5: The average filter concentrations of Mn for filters samples are shown in column 2 (with standard deviation errors between replicates) and corrected Mn concentrations based on percentage recoveries from SRM samples are shown in column 3. Column 4 shows recoveries for the entire area of the filter.

Kilometerage (km)	Recovered from filter sample (ng)	Corrected based on SRM % recovery (ng)	Recovery of Mn for entire filter area ( $\mu\text{g}$ )
0 Km	$124.47 \pm 89.01$	151.65	1.36
Ford Fiesta 1,000 km	$550.98 \pm 86.98$	671.13	6.04
Peugeot 307 1,000 km	$391.86 \pm 168.12$	477.27	4.30
Toyota Starlet 1,000 km	$548.46 \pm 397.17$	668.07	6.01

Moderate increases are observed between blank samples,  $124.47 \pm 89.01$  ng and those run in a Peugeot 307,  $391.86 \pm 168.12$  ng, a Ford Fiesta,  $550.98 \pm 86.98$  ng and a Toyota Starlet,  $548.46 \pm 397.17$  ng over 1,000 km, implying that without particle filters in place an increase in manganese concentrations is observed between blanks and filters run to 1,000 km. A significant difference is not observed between samples taken from different car models implying that without a particle filter in place manganese exposure is independent of car make.

## 6.8: Zinc:

### 6.8.1 Concentrations of Zn from standard particle filters between 0 km and 1,000 km in a Ford Fiesta.

Figure 6.8.1 shows a comparison between Airforce standard particle filters taken from a Ford Fiesta at a kilometerages of 0 km and 1,000 km.

A difference of  $4.5 \pm 0.99$   $\mu\text{g}$  is observed between blank filters,  $1.71 \pm 0.9$   $\mu\text{g}$  and samples collected at 1,000 km,  $6.21 \pm 1.89$   $\mu\text{g}$ . At low kilometerages a moderate difference in zinc concentrations is observed.

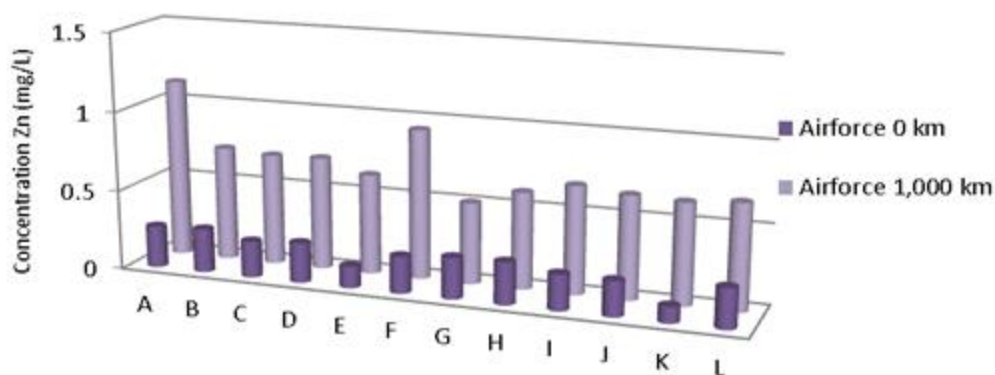


Figure 6.8.1: Average Zn concentrations for a Ford Fiesta, standard particle filters from 0 km to 1,000 km, manufactured by Airforce. The legend key for the x axis is shown in Table 1.4.3. All samples were collected in triplicate.

Column 3 of Table 6.8.1 shows concentrations corrected to 100% based on SRM recoveries of zinc using Method 3 shown in Table 3.2.4, estimated to be 83.5% of the overall quantities of zinc on the filter. Column 2 shows concentrations for one square inch of a filter, with standard deviation errors. Three different filter samples were collected for each kilometerage.

Table 6.8.1: The average filter concentrations of Zn for filters samples are shown in column 2 (with standard deviation errors between replicates) and corrected Zn concentrations based on percentage recoveries from SRM samples are shown in column 3. Column 4 shows recoveries for the entire area of the filter.

Kilometerage (km)	Concentrations from filter sample ( $\mu\text{g}$ )	Corrected based on SRM % recovery ( $\mu\text{g}$ )	Recovery of Zn for entire filter area (mg)
0 km	$1.71 \pm 0.9$	2.07	0.67
1,000 km	$6.21 \pm 1.89$	7.38	2.37

### 6.8.2 Concentrations of Zn from combination filters between 0 km and 1,000 km in a Ford Fiesta.

Figure 6.8.2 shows a comparison between Airforce combination filters taken from a Ford Fiesta at a kilometerages of 0 km and 1,000 km.

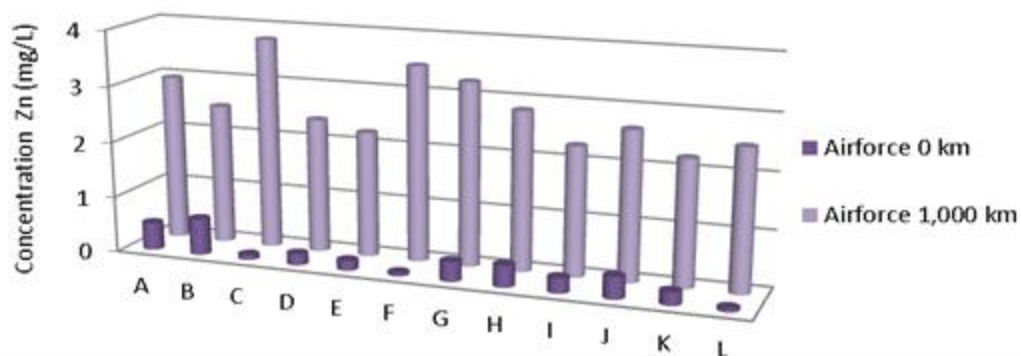


Figure 6.8.2: Average Zn concentrations for a Ford Fiesta, combination filters from 0 km to 1,000 km, manufactured by Airforce. The legend key for the x axis is shown in Table 1.4.3. All samples were collected in triplicate.

A difference ( $18.9 \pm 2.61 \mu\text{g}$ ) is observed between both filter samples. Concentrations for blank filters are  $10.44 \pm 6.48 \mu\text{g}$  and concentrations for samples collected at 1,000 km are  $29.34 \pm 9.09 \mu\text{g}$ . This indicates that at this kilometerage a significant difference in zinc concentrations is observed.

Table 6.8.2: The average filter concentrations of Zn for filters samples are shown in column 2 (with standard deviation errors between replicates) and corrected Zn concentrations based on percentage recoveries from SRM samples are shown in column 3. Column 4 shows recoveries for the entire area of the filter.

Kilometerage (km)	Concentrations from filter sample ( $\mu\text{g}$ )	Corrected based on SRM % recovery ( $\mu\text{g}$ )	Recovery of Zn for entire filter area (mg)
0 km	$10.44 \pm 6.48$	12.51	4.00
1,000 km	$29.34 \pm 9.09$	35.19	11.26

Table 6.8.3 shows measured values for standard particle and combination filters at 15,000 km and 1,000 km. The table also shows calculated figures, to determine approximate values at 15,000 km for filters run to 1,000 km and approximate values at 15,000 km for filters run to 1,000 km.

Concentrations for both standard particle filters and combination filters at 1,000 km are comparable to or higher than concentrations at 15,000 km. Implying that the majority of zinc extraction occurs over the first 1,000 km or more likely the ambient air in the areas travelled

by a Ford Fiesta are higher in zinc than areas travelled by a Skoda Octavia with the same make of pollen filter in place.

Table 6.8.3 shows concentrations from all filters tested over 1,000 km and 15,000 km.

Car and filter make	At 1,000 km	At 15,000 km
	$\mu\text{g}$	
Micronair Particle Filter - Skoda Octavia	$0.132 \pm 0.045$	$1.98 \pm 0.68$
Airforce Particle Filter - Skoda Octavia	$0.3 \pm 0.168$	$4.5 \pm 2.52$
Airforce Particle Filter - Ford Fiesta	$4.5 \pm 0.99$	$67.5 \pm 14.85$
Micronair Particle Filter - Toyota Aventis	$0.084 \pm 0.09$	$1.26 \pm 1.35$
Nip & Denso Particle - Toyota Aventis	$0.162 \pm 0.108$	$2.43 \pm 1.62$
Airforce Combination filters – Skoda Octavia	$0.444 \pm 0.27$	$6.66 \pm 4.05$
Micronair Combination filters – Skoda Octavia	$1.13 \pm 0.38$	$16.92 \pm 5.76$
Airforce Combination filters - Ford Fiesta	$18.9 \pm 2.61$	$283.5 \pm 39.15$

### 6.8.3 Zn concentrations from internal cabin filters with and without particle filters in place

Figure 6.8.3 shows a comparison between filters taken from an internal filtration system at a kilometerages 0 km and of 1,000 km.

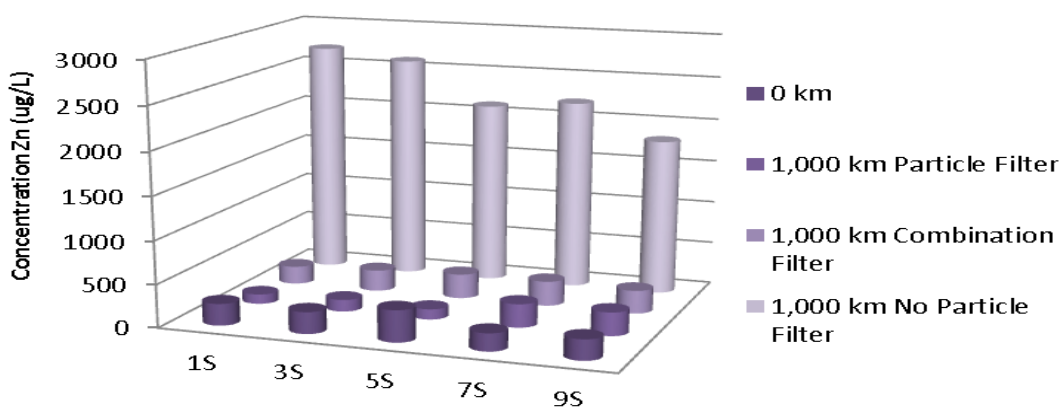


Figure 6.8.3: Average Zn concentrations for filters taken from an internal extraction system at a kilometerage of 0 km and 1,000 km. The legend key for the x axis is shown in Table 2.4.2. All samples were collected in triplicate.

Figure 6.8.3: shows a comparison of internal filters taken from a Ford Fiesta. A blank filter was analysed at 0 km as a reference, an internal filter was then placed in the cabin for 1,000

km with no standard particle filter in place, then with a standard particle filter in place for 1,000 km and finally with a combination filter in place for 1,000 km.

A significant difference is observed between the blank filter,  $2.34 \pm 0.54 \mu\text{g}$  and the filter run without a particle filter,  $20.61 \pm 20.61 \mu\text{g}$ . A decrease in concentrations is observed between the internal filter run with no particle filter,  $20.61 \pm 20.61 \mu\text{g}$  and the internal filters run with a standard particle filter,  $12.78 \pm 12.78 \mu\text{g}$  and a combination filter,  $2.34 \pm 2.34 \mu\text{g}$ . Indicating that zinc exposure is reduced with the use of a standard particle filter and is reduced further with the use of a combination filter. Levels observed on filters run with a combination filter in place yield the same concentrations as blank filters, implying that any zinc present is removed when using a combination filter.

Table 6.8.4: The average filter concentrations of Zn for filters samples are shown in column 2 (with standard deviation errors between replicates) and corrected Zn concentrations based on percentage recoveries from SRM samples are shown in column 3. Column 4 shows recoveries for the entire area of the filter.

Kilometerage (km)	Concentrations from filter sample ( $\mu\text{g}$ )	Corrected based on SRM % recovery ( $\mu\text{g}$ )	Recovery of Zn for entire filter area ( $\mu\text{g}$ )
0 Km	$2.34 \pm 0.54$	2.88	25.92
No Particle Filter 1,000 km	$20.61 \pm 20.61$	25.11	225.99
Particle Filter 1,000 km	$12.78 \pm 12.78$	15.48	139.68
Combination Filter 1,000 km	$2.34 \pm 2.34$	2.88	25.65

#### **6.8.4 Zn concentrations from internal cabin filters from three different car makes, Ford Fiesta, Peugeot 307 and Toyota Starlet.**

Figure 6.8.4 shows a comparison between filters taken from an internal filtration system at a kilometerages 0 km and of 1,000 km from three different car models a Ford Fiesta, Peugeot 307 and Toyota Starlet.

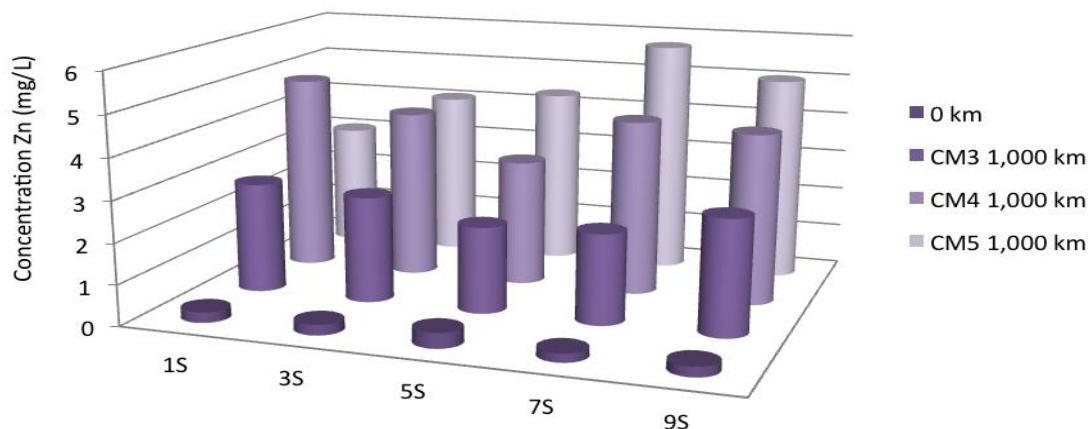


Figure 6.8.4: Average Zn concentrations for filters taken from an internal extraction system, run without particle filters in place, from a kilometerage of 0 km to 1,000 km. The legend key for the x axis is shown in Table 2.4.2. All samples were collected in triplicate.

Table 6.8.5: The average filter concentrations of Zn for filters samples are shown in column 2 (with standard deviation errors between replicates) and corrected Zn concentrations based on percentage recoveries from SRM samples are shown in column 3. Column 4 shows recoveries for the entire area of the filter.

Kilometerage (km)	Concentrations from filter sample ( $\mu\text{g}$ )	Corrected based on SRM % recovery ( $\mu\text{g}$ )	Recovery of Zn for entire filter area ( $\mu\text{g}$ )
0 Km	$2.34 \pm 0.54$	2.88	25.92
Ford Fiesta 1,000 km	$20.61 \pm 3.33$	25.11	225.99
Peugeot 307 1,000 km	$37.08 \pm 5.67$	45.18	406.26
Toyota Starlet 1,000 km	$44.64 \pm 5.76$	54.36	489.24

A difference of  $18.27 \pm 2.79 \mu\text{g}$  is observed between blank samples and those run in a Ford Fiesta and a difference of  $34.74 \pm 5.13 \mu\text{g}$  and  $42.3 \pm 5.25 \mu\text{g}$  is observed between blank samples and those run in a Peugeot 307 and Toyota Starlet, respectively, for 1,000 km. A difference is observed between 1,000 km samples from a Ford Fiesta and Peugeot 307/Toyota Starlet of  $10 \mu\text{g}$ , which may indicate implying that a travelled in an area where zinc levels in the ambient air are lower than the area travelled by the Peugeot 307 and the Toyota Starlet.

### 6.9: Analysis of PTE extraction relative to particle size.

SEM/EDX analysis was not carried out on filters from a Ford Fiesta but conclusions regarding the relationship between analyte extraction and particulate size can be made based on the findings in Section 5.9. Cu, Fe, Al and Zn were found to bind to particulates  $<2\ \mu\text{m}$ , Cr and Mn were found to bind to particulates  $>1.5\ \mu\text{m}$  and  $<7.5\ \mu\text{m}$  and Pb tends to be attracted to larger particulates from  $7.5\ \mu\text{m}$  to  $10\ \mu\text{m}$ .

Internal filters were run in a Ford Fiesta for 1,000 km without a pollen filter, then with a standard particle filter and finally with a combination filter. Column 2 of Table 6.9.1. shows the concentrations for a square inch of an internal filter run without a particle filter. Column 3 shows concentrations for a square inch of an internal filter run with a particle filter plus the concentrations from the square inch of the corresponding particle filter. Column 4 shows concentrations for a square inch of an internal filter run with a combination filter plus the concentrations from the square inch of the corresponding combination filter.

Table 6.9.1 – Internal Air purifier filters run for 1,000 km in a Ford Fiesta.

	With no particle filter	With a standard particle filter	With a combination particle filter
Al ( $\mu\text{g}$ )	$11.61 \pm 2.61$	$7.2 \pm 1.26$	<b><math>76.95 \pm 43.2</math></b>
Cr (ng)	$342.36 \pm 18$	$677.25 \pm 145.26$	<b><math>1,142.82 \pm 388.53</math></b>
Cu ( $\mu\text{g}$ )	$1.86 \pm 0.3$	$6.75 \pm 4.26$	<b><math>14.6 \pm 11.05</math></b>
Fe ( $\mu\text{g}$ )	$5.76 \pm 2.16$	$15.57 \pm 5.13$	<b><math>198.9 \pm 55.44</math></b>
Pb (ng)	<b><math>2,442.24 \pm 120.42</math></b>	$1,065.42 \pm 202.59$	$498.87 \pm 351.27$
Mn ( $\mu\text{g}$ )	<b><math>1,974.51 \pm 158.22</math></b>	$424.8 \pm 126.03$	$783.99 \pm 96.48$
Zn ( $\mu\text{g}$ )	$18.27 \pm 20.07$	$14.95 \pm 13.23$	<b><math>18.9 \pm 2.61</math></b>

Ideally, if all filters performed equally and had a comparable ability to extract particulates of all sizes the figures from columns 2, 3 and 4 would be equal. Combination filters paired with internal filters have the higher extraction rates for Al, Cr, Cu, Fe and Zn. In Section 5.9 it was determined that Al, Cr, Cu, Fe and Zn bind to fine particulates  $<2\ \mu\text{m}$ , indicating that internal filters and standard particle filters have reduced capacity to extract fine particulates relative to combination filters. Internal filters with no particle filter in place have the highest extraction concentration for Mn and Pb. From Section 5.9 we know that Pb tends to bind to larger



particulates from 7.5  $\mu\text{m}$  to 10  $\mu\text{m}$ , indicating that internal filters have a greater ability to extract larger particulates relative to standard particle and combination filters.

### **Internal Filters Conclusion:**

Airforce standard particle filters were run (in triplicate) in a Ford Fiesta for 1,000 km with internal cabin filters placed within the cabin. An increase is observed between all blank standard particle filters and standard particle filters run to 1,000 km for Al, Cr, Cu, Pb, Fe and Zn. However a difference is not observed for Mn due to high background levels. This indicates that for a Ford Fiesta using particle filters, at low kilometerages, the majority of analytes tested show an increase.

Airforce combination filters were run in a Ford Fiesta for 1,000 km (in triplicate) with internal cabin filters in place. An increase is observed between blank filters and those run for 1,000 km for Al, Cr, Cu, Fe, Pb and Zn but not for Mn. Indicating that for a Ford Fiesta using combination filters, at low kilometerages, the majority of analyte tested shows an increase.

When comparing standard particle and combination filter concentrations to concentrations from filters run to 15,000 km, extrapolated back to 1,000 km, analyte concentrations differ. Al, Cu and Pb standard particle filters are comparable to concentrations taken at 15,000 km but combination filters are significantly higher. Cr standard particle filters show significantly lower concentrations at 1,000 km and combination filters are comparable. For Fe and Zn the levels on standard particle filter and combination filters are comparable to levels on filters collected at 15,000 km. Manganese combination filters show no manganese present but standard particle filters show a higher concentration on filters collected at 1,000 km.

Generally standard particle filters behave similarly from 0 km to 1,000 km and from 0 km to 15,000 km but combination filters show significantly higher Al, Cu and Pb concentrations from 0 km to 1,000 km when compared to figures extrapolated back from 15,000 km. The difference in PTE concentrations on combination filters can perhaps be attributed to how particles build up on filters. SEM images were not taken of Airforce combination filters run to 1,000 km, in a Ford Fiesta, it is not therefore possible to observe particulate build up. From previous discussions in Chapter 5, it has been determined that lead generally binds to courser particles and that Al and Cu generally bind to finer particles. This therefore implies that particle size is not a reasonable explanation for the higher concentrations of Al, Cu and Pb.

It is possible that the areas travelled by a Ford Fiesta with combination filters in place were high in certain analytes, namely Al, Cu and Pb. The Ford Fiesta travelled mainly in Cork city centre and a Skoda Octavia and a Toyota Aventis travelled in both urban and rural areas. Harrison *et al.*, carried out PM analysis in four different UK cities and found PTE concentrations differed significantly between them due to the difference in concentrations of course/fine particulates. [107] Harrison *et al.*, also found that urban sites have less course particles than rural sites. Fine particles generally originate from regulated sources. Course particles mainly from natural (sources/construction/mining/quarrying). [108] The variation in PTE concentrations may also be due to the time of year the filters were collected. Filters collected at 15,000 km were in place for approximately 12 months, considering a motorist's average annual kilometerage is 15,000 km. Taking 15,000 km as an annual kilometerage then filters run to 1,000 km are in place for less than a month. It is therefore important to take into account the time of year when the filters were in place. Marcazzan *et al.*, found that on PM<sub>10</sub> Mn, Zn values are constant year round, Fe, Pb less during the summer months and Al, increases during the summertime. Also, on PM<sub>2.5</sub> Mn, Cu have similar values all year long, Zn, Pb decrease in in summer and Al and Fe increase (agricultural sources). [109] Melaku *et al.*, found that during the summer months all analytes are present in higher concentrations except Cr. [110] Cavanagh *et al.*, found that PTE are higher in July in two cities which is attributed to the variation in PM composition. [111]

Internal cabin filters were run in a Ford Fiesta for 1,000 km with the following filter set ups, no particle filter, then a standard particle filter and finally a combination filter. An increase is observed between blank filters and filters run with no particle filter in place for all analytes tested. This implies that measureable quantities of all analytes are present in cabin air. A decrease is observed between filters run with no particle filter and filters run with a standard particle filter in place for all analytes tested. Showing that using a standard particle filter reduces analyte exposure levels. A decrease is observed between filters run with no particle filter and filters run with a combination filter in place for all analytes, a further decrease in analyte concentrations is observed between standard particle filters and combination filters. This indicates that analyte exposure is decreased further with the use of combination filters.

Internal cabin filters were run for 1,000 km without particle filters in place in different car makes, Ford Fiesta, Peugeot 307 and Toyota Starlet. An increase is observed between blank filters and filters run without a particle filter in place for all analytes tested. This indicates that measureable quantity of all analytes are present in ambient air at 1,000 km. Concentrations from a Ford Fiesta and a Peugeot 307 are comparable for Al, Cr, Fe and Mn but the exposure levels in a Peugeot 307 are greater for Cu, Pb and Zn. Concentrations from a Ford Fiesta and a Toyota Starlet are comparable for Al, Cr, Cu, Fe and Mn, but the exposure levels in a Toyota Starlet are greater for Pb and Zn. Concentrations from a Peugeot 307 and a Toyota Starlet vehicles are comparable for analytes analysed Al, Cr, Fe, Pb, Mn and Zn except Cu. Therefore the extraction efficiency of a Peugeot 307 and a Toyota Starlet are comparable for the majority of analytes but the exposure levels in a Ford Fiesta are less than for Peugeot 307 and Toyota Starlet vehicles. Considering the general consistencies between different car models concentrations are dependent on areas travelled and not on car model.

## **6.9: Filters collected from cycling masks.**

Particulate matter exposure levels, at the roadside, are significantly less than those experienced while driving in traffic, ~83.3% less, due to the tunnel effect. Analysis of filters worn by cyclists was carried out in an attempt to determine if this is the case.

Cycling masks may be considered as passive filters in comparison to the motorized air flow associated with cabin particle filters and internal filters in chapter 5. When looking at exposure levels, the inhalation rate of a cyclist should however be taken into consideration when comparing the exposure levels of a cyclist and a motorist.

### **6.9.1: Aluminium: Concentrations from cycle mask filters.**

Figure 6.9.1: shows a comparison between filters taken from cycle masks worn by two different cyclists (C1 & C2), cycling in urban areas for a kilometerage of 0 km and 500 km.

A blank sample (0 km) was run as a reference. A moderate difference is observed between blank filter samples and those taken at 500m,  $445.95 \pm 527.49 \mu\text{g}$ ,  $655.2 \pm 83.43 \mu\text{g}$  and  $577.62 \pm 20.88 \mu\text{g}$ , respectively. No significant difference is observed between samples taken from difference cyclists.

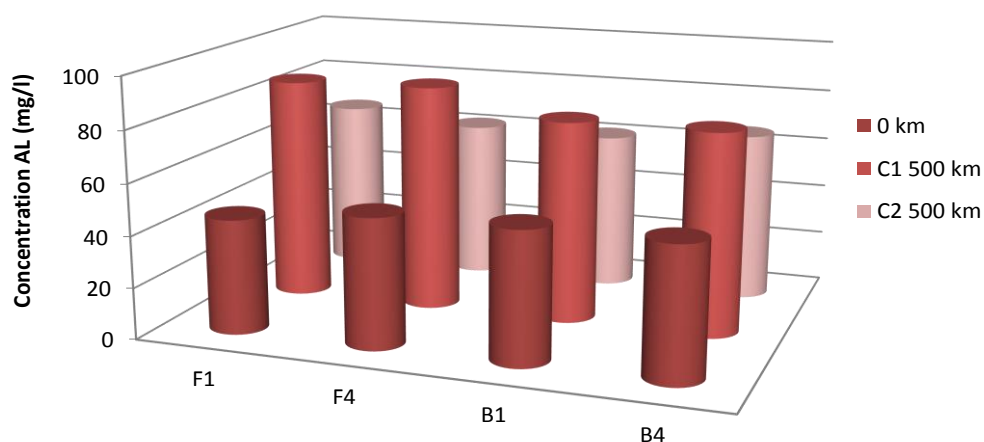


Figure 6.9.1: Average Al concentrations for cycle mask filters, from 0 km to 1,000 km worn by two different cyclists, cyclist 1 (C1) and cyclist 2 (C2). The legend key for the x axis is shown in Table 2.5.2. All samples were collected in triplicate.

Table 6.9.1: The average filter concentrations of Al for filters samples, corrected Al concentrations and overall filter concentrations of Al extrapolated over the area of the entire filter. Column 4 shows recoveries for the entire area of the filter.

Kilometerage (km)	Concentrations from filter sample ( $\mu\text{g}$ )	Corrected based on SRM % recovery ( $\mu\text{g}$ )	Recovery of Al for entire filter area (mg)
0 km	$445.95 \pm 527.49$	782.28	7.02
500 km C1	$655.2 \pm 83.43$	1,149.3	10.26
500 km C2	$577.62 \pm 20.88$	1,013.13	9.09

### 6.9.2: Chromium: Concentrations from cycle mask filter.

Chromium: Figure 6.9.2: shows a comparison between filters taken from cycle masks worn by two different cyclists (C1 & C2), cycling in urban areas for a kilometerage of 0 km and 500 km.

A blank sample (0 km) was run as a reference. No difference is observed between blank filter samples,  $1,946.61 \pm 132.57$  ng and those taken at 500m,  $1,532.16 \pm 439.92$  ng and  $1,338.66 \pm 62.64$  ng. No significant level of chromium was extracted from cyclist filters.

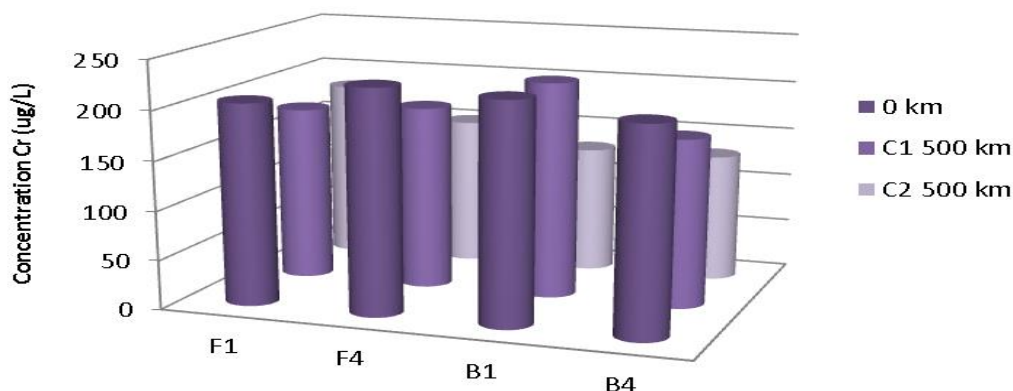


Figure 6.9.2: Average Cr concentrations for cycle mask filters, from 0 km to 1,000 km worn by two different cyclists, cyclist 1 (C1) and cyclist 2 (C2). The legend key for the x axis is shown in Table 2.5.2. All samples were collected in triplicate.

Table 6.9.2: The average filter concentrations of Cr for filters samples, corrected Cr concentrations and overall filter concentrations of Cr extrapolated over the area of the entire filter. Column 4 shows recoveries for the entire area of the filter.

Kilometerage (km)	Concentrations from filter sample (ng)	Corrected based on SRM % recovery (ng)	Recovery of Cr for entire filter area (μg)
0 km	1,946.61 ± 132.57	2,132.1	17.01
500 km C1	1,532.16 ± 439.92	1,678.14	13.41
500 km C2	1,338.66 ± 62.64	1,466.28	11.70

### 6.9.3: Copper: Recoveries from cycle mask filter.

Copper: Figure 6.9.3: shows a comparison between filters taken from cycle masks worn by two different cyclists (C1 & C2), cycling in urban areas for a kilometerage of 0 km and 500 km.

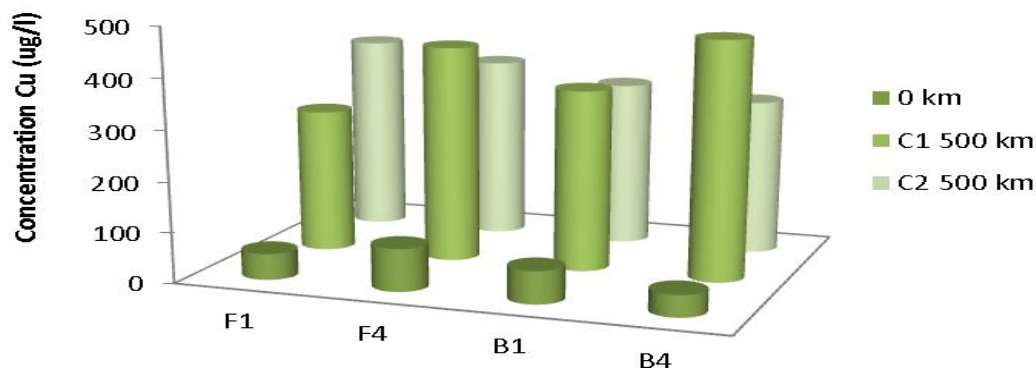


Figure 6.9.3: Average Cu recoveries for cycle mask filters, from 0 km to 1,000 km worn by two different cyclists, cyclist 1 (C1) and cyclist 2 (C2). The legend key for the x axis is shown in Table 2.5.2. All samples were collected in triplicate.

Table 6.9.3: The average filter concentrations of Cu for filters samples and corrected Cu concentrations based on SRM % recoveries. Column 4 shows recoveries for the entire area of the filter.

Kilometerage (km)	Concentrations from filter sample (ng)	Corrected based on SRM % recovery (ng)	Recovery of Cr for entire filter area (μg)
0 km	540 ± 1.17	670.77	5.31
500 km C1	2,790 ± 0.45	3,465.81	27.72
500 km C2	3,195 ± 9.99	3,968.91	31.50

A blank sample (0 km) was run as a reference. A significant difference is observed between blank filter samples,  $540 \pm 1.17$  ng and those taken at 500m,  $2,790 \pm 0.45$  ng and  $3,195 \pm 9.99$  ng, for cyclist 1 and 2, respectively. Copper concentrations on filters collected from different cyclists are comparable.

#### 6.9.4: Iron: Concentrations from cycle mask filter.

Iron: Figure 6.9.4: shows a comparison between filters taken from cycle masks worn by two different cyclists (C1 & C2), cycling in urban areas for a kilometerage of 0 km and 500 km.

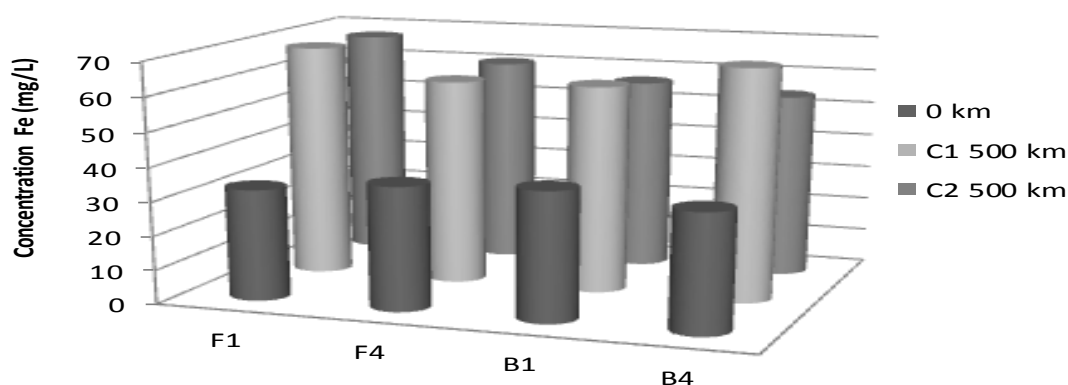


Figure 6.9.4: Average Fe concentrations for cycle mask filters, from 0 km to 1,000 km worn by two different cyclists, cyclist 1 (C1) and cyclist 2 (C2). The legend key for the x axis is shown in Table 2.5.2. All samples were collected in triplicate.

Table 6.9.4: The average filter concentrations of Fe for filters samples corrected Fe concentrations and overall filter concentrations of Fe extrapolated over the area of the entire filter. Column 4 shows recoveries for the entire area of the filter.

Kilometerage (km)	Concentrations from filter sample ( $\mu\text{g}$ )	Corrected based on SRM % recovery ( $\mu\text{g}$ )	Recovery of Fe for entire filter area (mg)
0 km	$318.87 \pm 22.41$	387	3.10
500 km C1	$434.79 \pm 54.63$	527.67	4.22
500 km C2	$537.21 \pm 164.79$	651.96	5.22

A blank sample (0 km) was run as a reference. A moderate difference is observed between blank filter samples,  $318.87 \pm 22.41 \mu\text{g}$  and those taken at 500m,  $434.79 \pm 54.63 \mu\text{g}$  and  $537.21 \pm 164.79 \mu\text{g}$ . No significant difference is observed between samples taken from difference cyclists.

#### 6.9.5: Lead: Concentrations from cycle mask filter.

Lead: Figure 6.9.5: shows a comparison between filters taken from cycle masks worn by two different cyclists (C1 & C2), cycling in urban areas for a kilometerage of 0 km and 500 km.

A blank sample (0 km) was run as a reference. No difference is observed between blank filter samples,  $2,267.19 \pm 285.57$  ng and those taken at 500m,  $2,297.25 \pm 168.66$  ng and  $1,982.7 \pm 239.13$  ng.

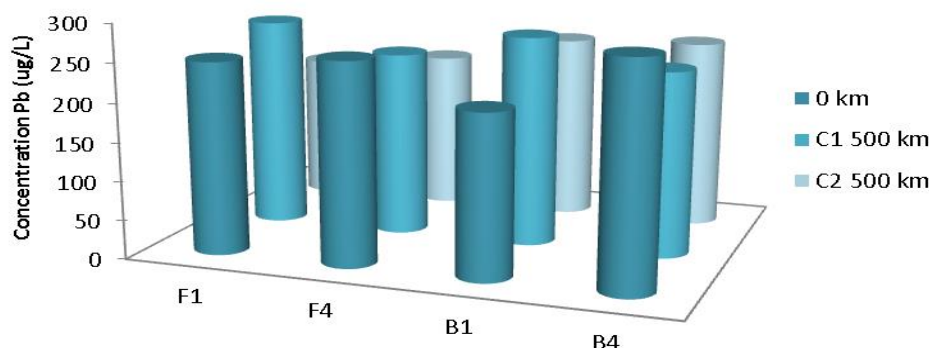


Figure 6.9.5: Average Pb concentrations for cycle mask filters, from 0 km to 1,000 km worn by two different cyclists, cyclist 1 (C1) and cyclist 2 (C2). The legend key for the x axis is shown in Table 2.5.2. All samples were collected in triplicate.

Table 6.9.5: The average filter concentrations of Pb for filters samples, corrected Pb concentrations and overall filter concentrations of Pb extrapolated over the area of the entire filter. Column 4 shows recoveries for the entire area of the filter.

Kilometerage (km)	Concentrations from filter sample (ng)	Corrected based on SRM % recovery (ng)	Recovery of Pb for entire filter area (mg)
0 km	$2,267.19 \pm 285.57$	2,596.95	20.78
500 m C1	$2,297.25 \pm 168.66$	2,631.42	21.05
500 m C2	$1,982.7 \pm 239.13$	2,271.15	18.17

#### 6.9.6: Manganese: Concentrations from cycle mask filter.

Manganese: Figure 6.10.6: shows a comparison between filters taken from cycle masks worn by two different cyclists (C1 & C2), cycling in urban areas for a kilometerage of 0 km and 500 km. A blank sample (0 km) was run as a reference.



A difference is not observed between blank filter samples,  $2,228.85 \pm 120.69$  ng and those taken at 500m,  $2,509.74 \pm 849.51$  ng for C2 but a significant difference is observed for blank filter samples,  $2,228.85 \pm 120.69$  ng and those taken at 500m,  $5,172.93 \pm 1,058.58$  ng for C1. Indicating that cyclist 1 experiences higher manganese exposure than cyclist 2 over the same kilometerage, due to areas travelled by C1.

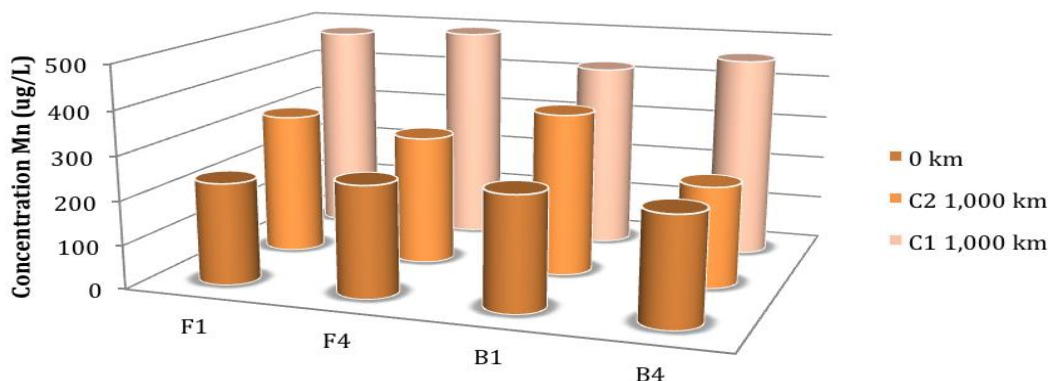


Figure 6.9.6: Average Mn concentrations for cycle mask filters, from 0 km to 1,000 km worn by two different cyclists, cyclist 1 (C1) and cyclist 2 (C2). The legend key for the x axis is shown in Table 2.5.2. All samples were collected in triplicate.

Table 6.9.6: The average filter concentrations of Mn for filters samples, corrected Mn concentrations and overall filter concentrations of Mn extrapolated over the area of the entire filter. Column 4 shows recoveries for the entire area of the filter.

Kilometerage (km)	Recovered from filter sample (ng)	Corrected based on SRM % recovery (ng)	Recovery of Mn for entire filter area (µg)
0 km	$2,228.85 \pm 120.69$	2,714.85	21.69
500 m C1	$5,172.93 \pm 1,058.58$	6,300.81	50.40
500 m C2	$2,509.74 \pm 849.51$	3,056.94	24.30

### 6.9.7: Zinc: Concentrations from cycle mask filter.

Figure 6.9.7: shows a comparison between filters taken from cycle masks worn by two different cyclists (C1 & C2), cycling in urban areas for a kilometerage of 0 m and 500 m.

A blank sample (0 km) was run as a reference. A moderate difference is observed between blank filter samples,  $2,206.71 \pm 828$  ng and those taken at 500m,  $5,051.16 \pm 370.26$  ng and  $4,810.68 \pm 786.06$  ng. No significant difference is observed between samples taken from different cyclists.

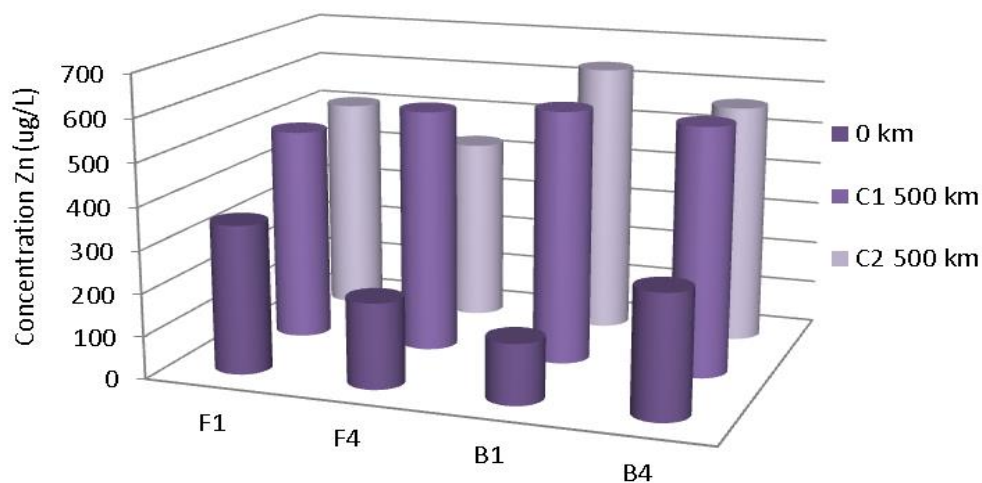


Figure 6.9.7: Average Zn concentrations for cycle mask filters, from 0 km to 1,000 km worn by two different cyclists, cyclist 1 (C1) and cyclist 2 (C2). The legend key for the x axis is shown in Table 2.5.2. All samples were collected in triplicate.

Table 6.9.7: The average filter concentrations of Zn for filters samples and corrected Zn concentrations. Column 4 shows recoveries for the entire area of the filter.

Kilometerage (km)	Recovered from filter sample (ng)	Corrected based on SRM % recovery (ng)	Recovery of Zn for entire filter area (µg)
0 km	$2,206.71 \pm 828$	2,636.46	2.34
500 m C1	$5,051.16 \pm 370.26$	6,034.86	5.36
500 m C2	$4,810.68 \pm 786.06$	5,747.49	5.1

### Conclusion Cycle filters:

Filters worn by two cyclists (one male, one female) for 500 km. An increase is not observed between blank samples and male/female cyclist samples run for 500 km for all analytes tested, except for manganese, where cyclist 1 experienced a higher manganese exposure. Implying that the ambient air in areas travelled by cyclist 1 are higher in manganese.

### 6.10 A comparison between cycle filters and internal cabin filters:

Internal filters were run in a Ford Fiesta from 0 km to 1,000 km and were then compared to cycle mask filters run from 0 km to 500 km, shown in Table 6.10.1.

According to Micronair [61] and the tunnel effect theory discussed in chapter 1 Figure 1.4.15, indicates roadside exposure levels should be considerably less than levels in the traffic stream (e.g. up to 6 times less). Boogaard *et al.*, agreed with Micronair, they found that PTE exposure was higher when travelling in a car when compared to a cyclist's exposure. [111]

Harrison *et al.*, found that fine particles are generally generated from road traffic and that coarse particles are generated from other sources. [108] Therefore, PTE present on fine particulates will be present in higher concentrations in the traffic stream and analytes present on coarse particulates will be present in the traffic stream and at the roadside. Allen *et al.*, found that exhaust emissions contain Pb, Fe, Cu, Zn, Ni and Cd. [113] Panis *et al.*, agreed that the composition of PM<sub>2.5</sub> depends on area/traffic source. They suggested also looking at the inhalation source not mode of transport. A higher inhalation rate is experienced by cyclists when compared to a stationary car occupant. Therefore more particles enter the nasal tract. [112]

Table 6.10.1 shows a comparison between the maximum in car exposure taken from Table 6.9.1 and cycle mask filters. The figures in column 2 represent the highest in car exposure from 0 km to 1,000 km (extrapolated back to 500 km) and the figures in column 3 represent cyclist exposure from 0 to 500 km. All figures are representative of one square inch of the filter.

Table 6.10.1: A comparison between the maximum exposure in a car and a cyclists exposure from 0 km to 500 km.

	Maximum in car exposure	Cyclist exposure
Al (µg)	38.47 ± 21.6	0.17 ± 0.05
Cr (ng)	571.41 ± 194.26	0
Cu (µg)	918.4 ± 153.86	2,992.5 ± 4.05
Fe (µg)	99.45 ± 27.72	0.17 ± 0.087
Pb (ng)	1,221.12 ± 60.21	0
Mn (µg)	978.25 ± 79.11	1,612.48 ± 833.35
Zn (µg)	9.45 ± 1.3	2,724.21 ± 249.79

There is a significant difference between the physical design and the material composition of cycle mask filters and standard particle/combination filters. It is therefore difficult to draw a direct comparison between extraction figures from each filter type. Table 6.10.1 does however give an indication of potential exposure to analyte containing particulates in absence of a filter.

In reality the differences in exposure appear to be analyte specific. Exposure levels for Al, Cr, Fe and Pb are considerably less at the roadside, concentrations of Cu, and Zn are significantly higher at the roadside and Mn concentrations are similar at the roadside and in the traffic stream.

**Chapter 7:**  
SEM Imagery & EDX Quantitative Analysis  
of Cabin Air Filters

## **Chapter 7:**

### **SEM Imagery & EDX quantitative analysis of Cabin Air Filters**

#### **SEM Imagery:**

As discussed previously in section 1.2, ambient air contains course and fine particulate matter. The ability of these particles to enter the respiratory system is dependent on the size of the particles. Course materials between 2.5  $\mu\text{m}$  and 10  $\mu\text{m}$  are generally eliminated in the nasal cavity through coughing and sneezing but fine particle  $<2.5 \mu\text{m}$  can enter the respiratory system, deep into the lungs causing lung damage. Particles  $<1 \mu\text{m}$  can enter the bloodstream, through the alveoli causing heart problems and releasing harmful chemicals into the bloodstream. SEM imagery was used to carry out analysis on the size of particles trapped by different filters. Standard particle filters and combination filters, run in CM1, were examined at different kilometerages 0 km, 15,000 km, 30,000 km and 45,000 km.

#### **7.1: SEM imagery of Micronair Standard Particle Filters: 0 km, 15,000 km, 30,000 km and 45,000 km**

##### **Standard Particle Filter at a kilometerage of 0 km.**

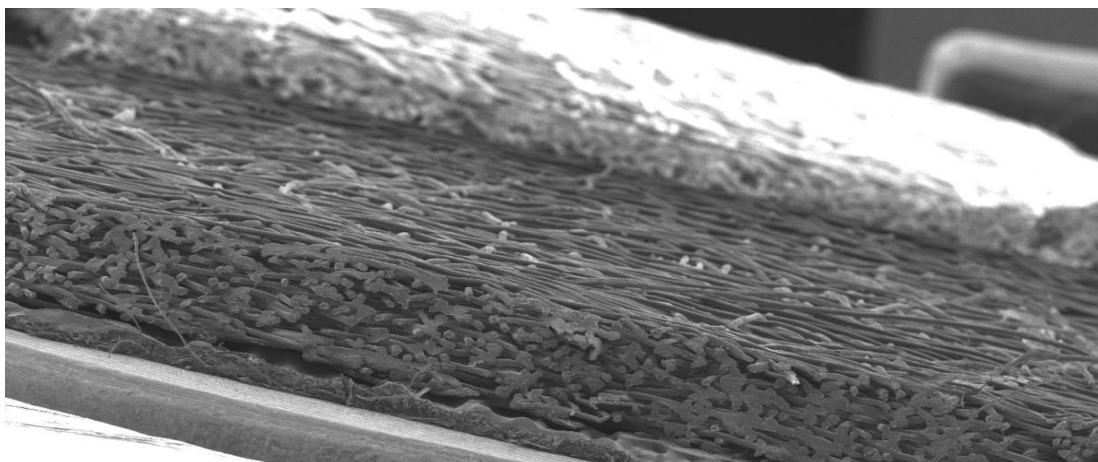


Figure 7.1.1: SEM image of a blank Micronair standard particle filter from CM1, at a magnification x 25.

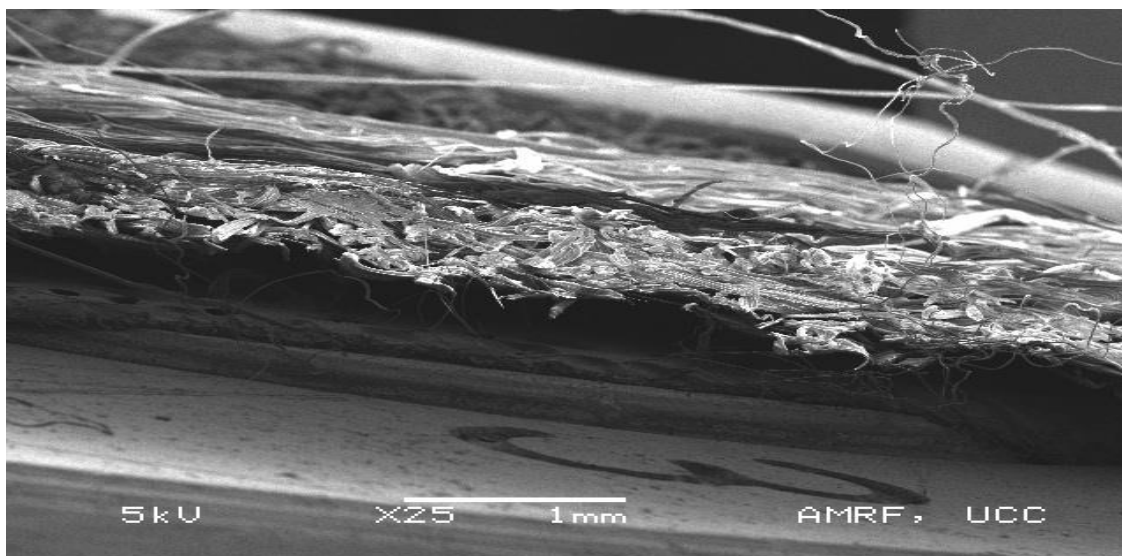
**Standard Particle Filter at a kilometerage of 15,000 km.**

Figure 7.1.2: SEM image of a Micronair standard particle filter taken at a kilometerage of 15,000 km from CM1, at a magnification x 25.

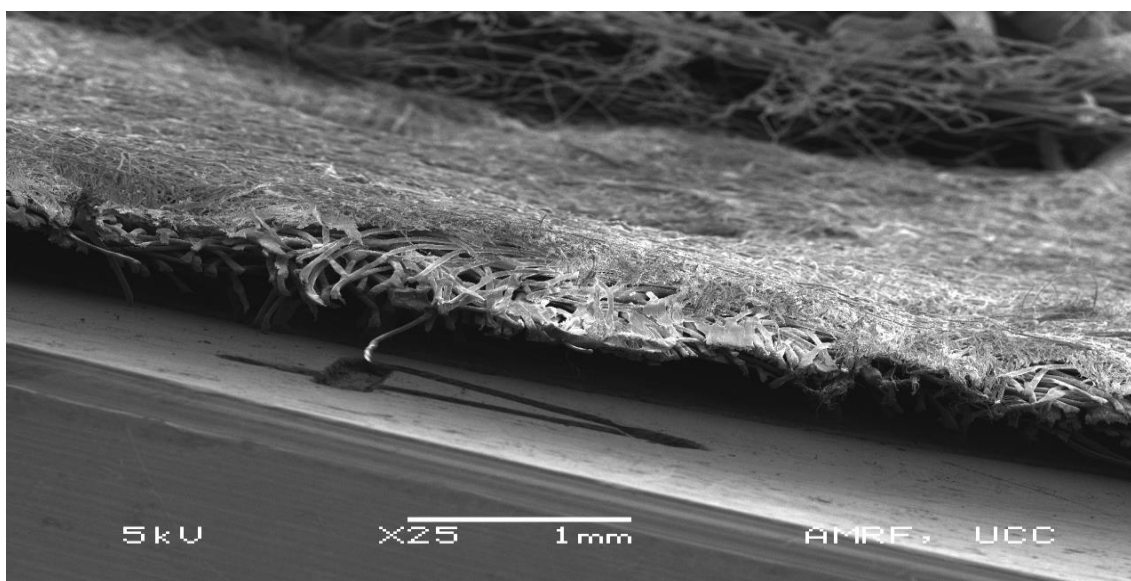
**Standard Particle Filter at a kilometerage of 30,000 km.**

Figure 7.1.3: SEM image of a Micronair standard particle filter taken at a kilometerage of 30,000 km from CM1, at a magnification x 25.

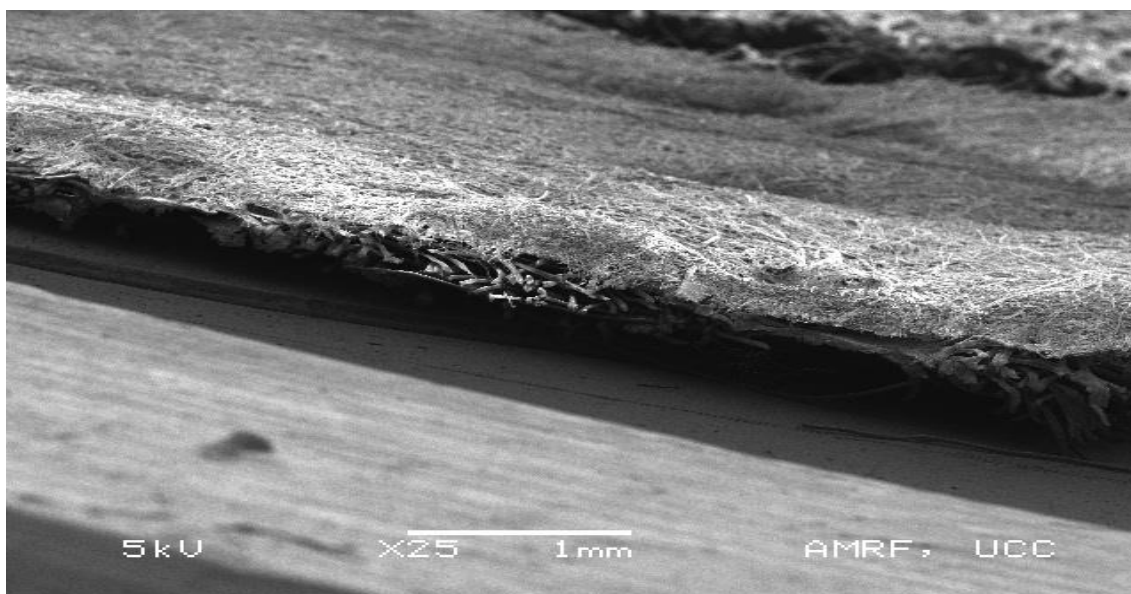
**Standard Particle Filter at a kilometerage of 45,000 km.**

Figure 7.1.4: SEM image of a Micronair standard particle filter taken at a kilometerage of 45,000 km from CM1, at a magnification x 25.

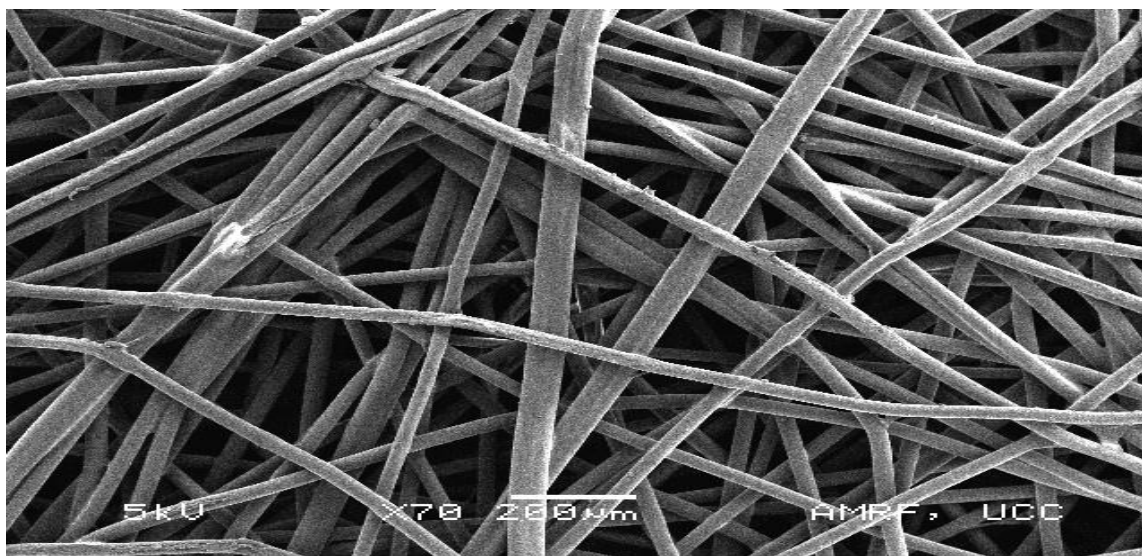
**Standard Particle Filter at a kilometerage of 0 km.**

Figure 7.1.5: SEM image of a blank Micronair standard particle filter from CM1, at a magnification x 70.



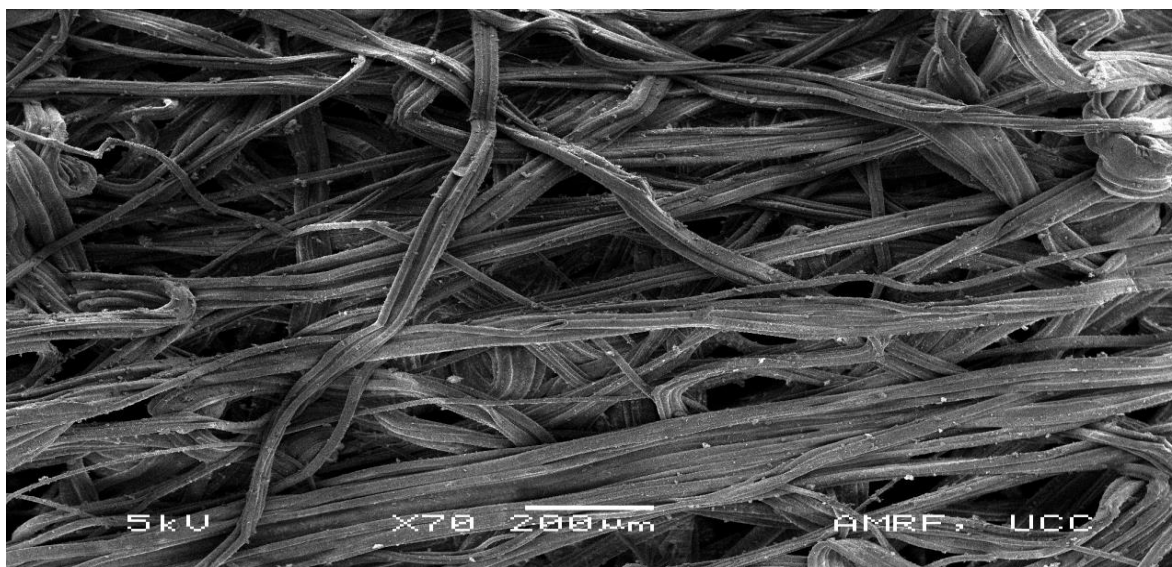
**Standard Particle Filter at a kilometerage of 15,000 km.**

Figure 7.1.6: SEM image of a Micronair standard particle filter taken at a kilometerage of 15,000 km from CM1, at a magnification x 70. The filter fibres show a degradation when compared to Figure 7.1.5.

**Standard Particle Filter at a kilometerage of 30,000 km.**

Figure 7.1.7: SEM image of a Micronair standard particle filter taken at a kilometerage of 30,000 km from CM1, at a magnification x 70. The filter fibres show a further degradation when compared to Figure 7.1.6.

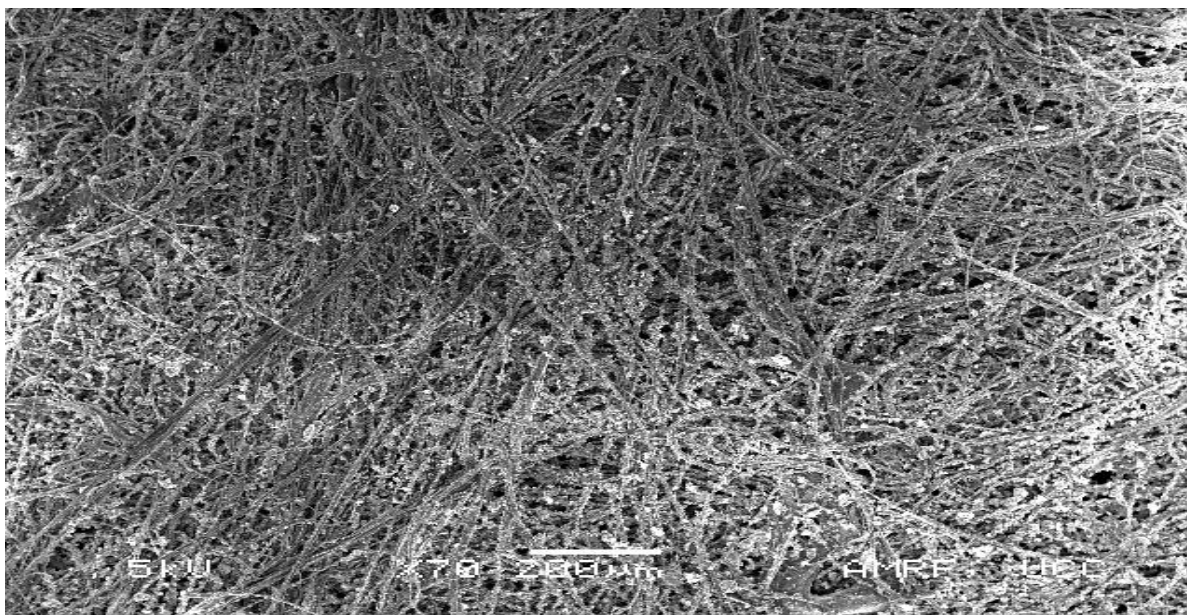
**Standard Particle Filter at a kilometerage of 45,000 km.**

Figure 7.1.8: SEM image of a Micronair standard particle filter taken at a kilometerage of 45,000 km from CM1, at a magnification x 70. The filter fibres show no further degradation when compared to Figure 7.1.7.

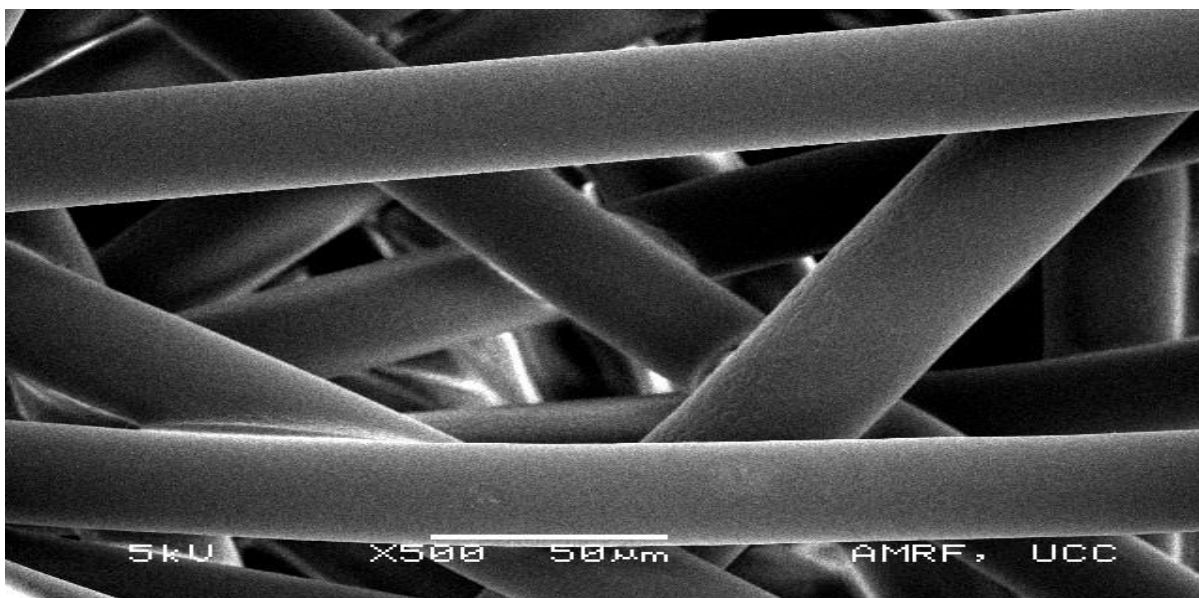
**Standard Particle Filter at a kilometerage of 0 km.**

Figure 7.1.9: SEM image of a blank Micronair standard particle filter from CM1, at a magnification x 500.

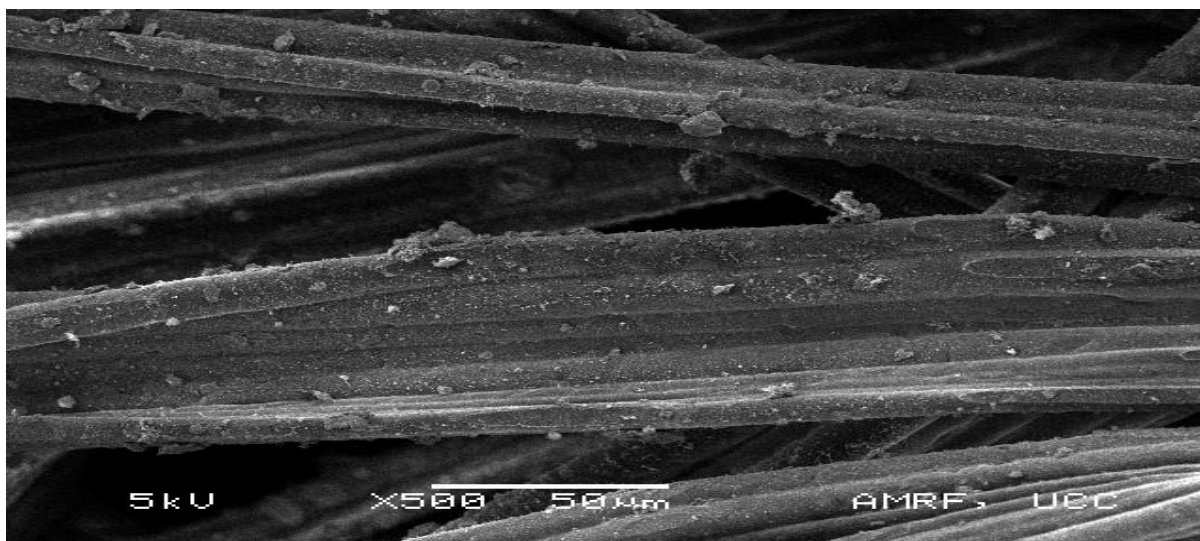
**Standard Particle Filter at a kilometerage of 15,000 km.**

Figure 7.1.10: SEM image of a Micronair standard particle filter taken at a kilometerage of 15,000 km from CM1, at a magnification x 500. A greater appreciation of the amount of particles present on the filter can be observed at this magnification.

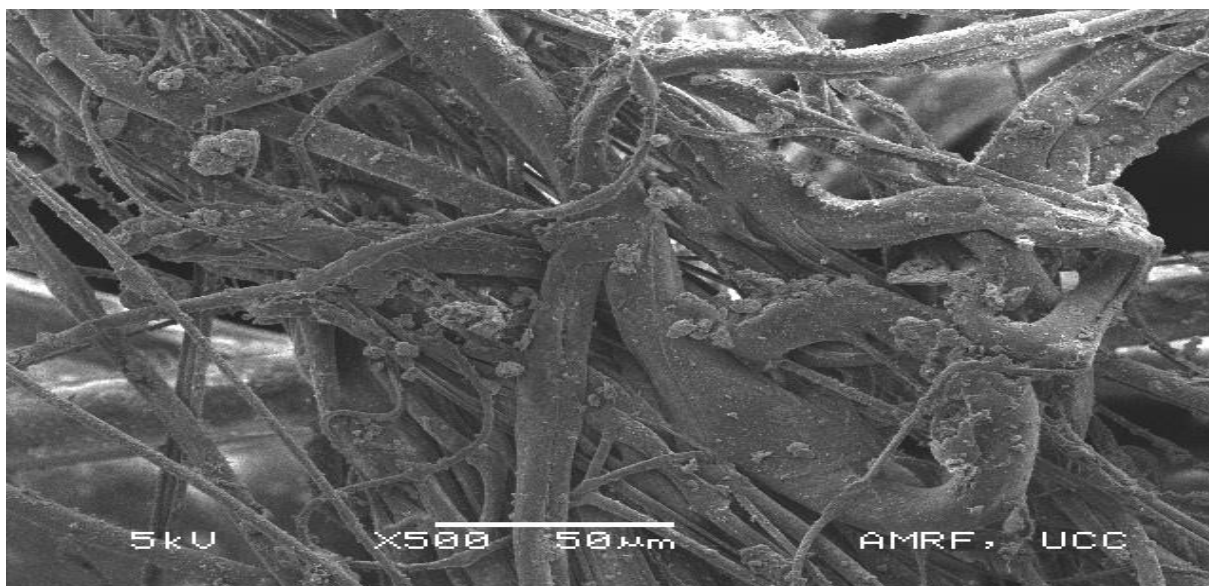
**Standard Particle Filter at a kilometerage of 30,000 km.**

Figure 7.1.11: SEM image of a Micronair standard particle filter taken at a kilometerage of 30,000 km from CM1, at a magnification x 500. A further increase in particulate concentrations can be observed in Figure 7.1.11 when compared to Figure 7.1.10.

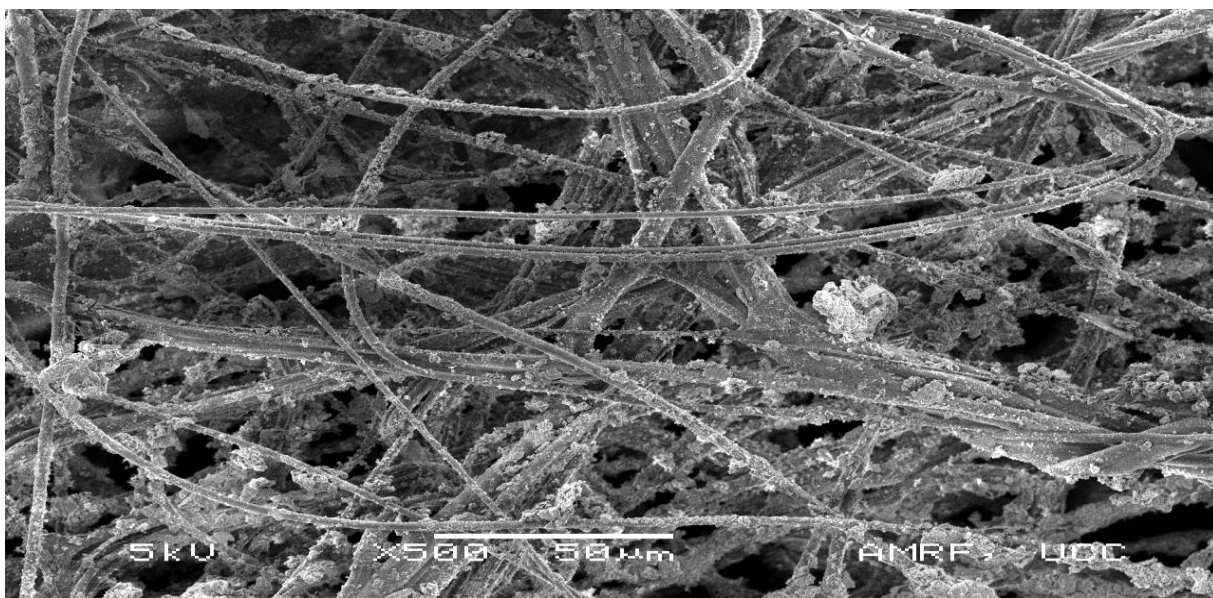
**Standard Particle Filter at a kilometerage of 45,000 km.**

Figure 7.1.12: SEM image of a Micronair filter standard particle taken at a kilometerage of 45,000 km from CM1, at a magnification x 500. Particulate concentrations are comparable to concentration observed in Figure 7.1.11.

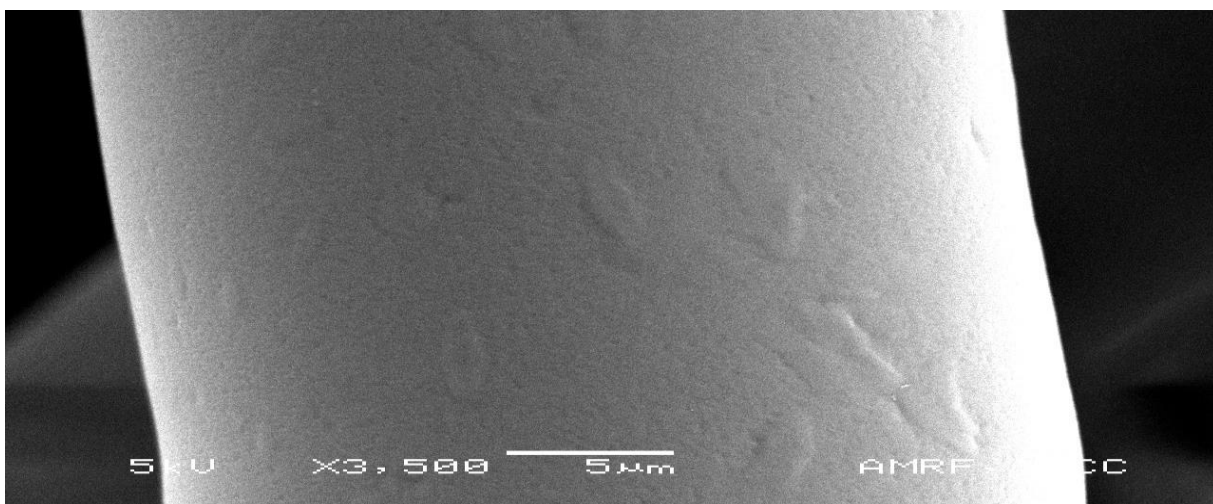
**Standard Particle Filter at a kilometerage of 0 km.**

Figure 7.1.13: SEM image of a blank Micronair standard particle filter from CM1, at a magnification x 3,500.



### Standard Particle Filter at a kilometerage of 15,000 km.

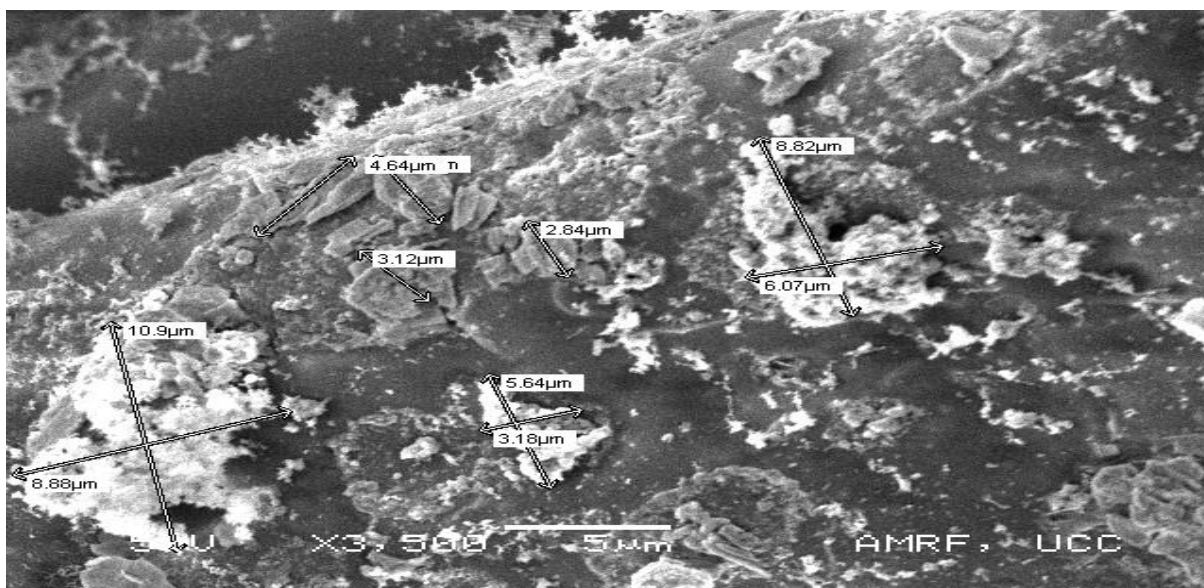


Figure 7.1.14: SEM image of a Micronair standard particle filter taken at a kilometerage of 15,000 km from CM1, at a magnification x 3,500, with particle sizes. The smallest particles observed are ~2  $\mu\text{m}$ , implying that particles <2  $\mu\text{m}$  can pass through a Micronair filter at 15,000 km in CM1.

### Standard Particle Filter at a kilometerage of 30,000 km.

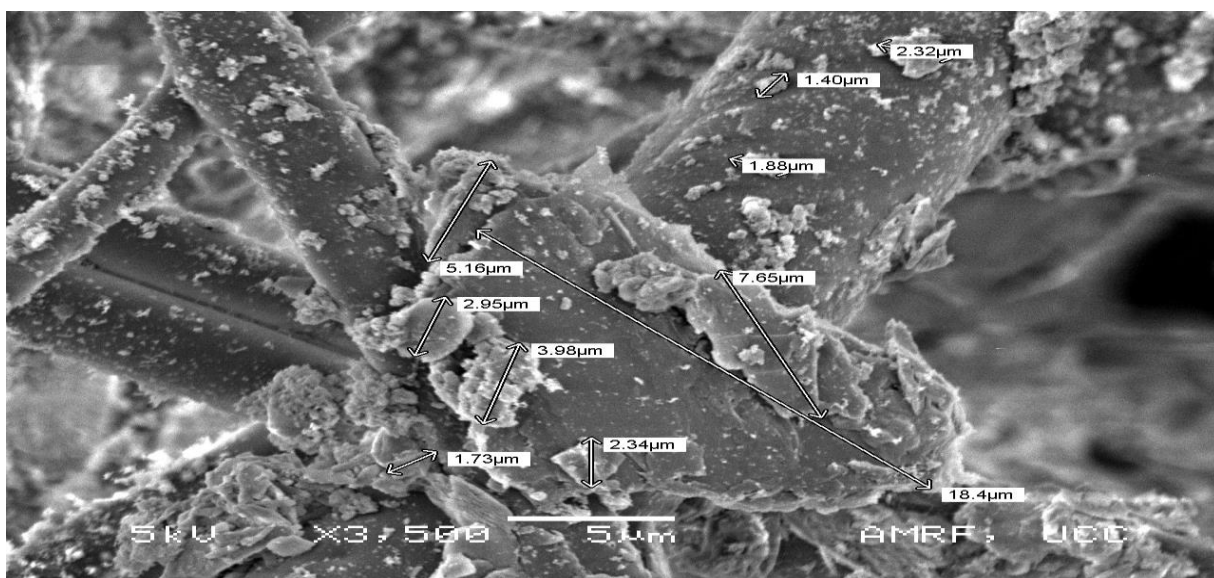


Figure 7.1.15: SEM image of a Micronair standard particle filter taken at a kilometerage of 30,000 km from CM1, at a magnification x 3,500, with particle sizes. The smallest particles observed are <1.5  $\mu\text{m}$ , implying that particles >1  $\mu\text{m}$  and <2  $\mu\text{m}$  can be trapped by Micronair filters at 30,000 km in CM1.

### Standard Particle Filter at a kilometerage of 45,000 km.

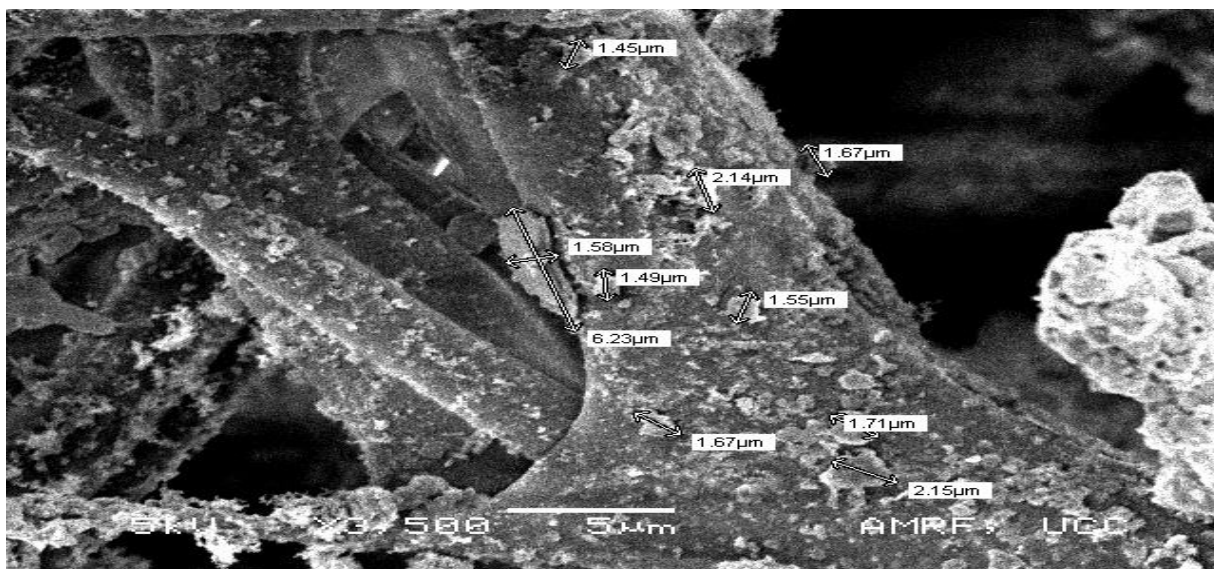


Figure 7.1.16: SEM image of a Micronair standard particle filter taken at a kilometerage of 45,000 km from CM1, at a magnification x 3,500, with particle sizes. The smallest particles observed are  $<1.5 \mu\text{m}$ . This indicates that particles  $>1 \mu\text{m}$  and  $<2 \mu\text{m}$  can be trapped by Micronair filters at 45,000 km in CM1.

### Conclusion:

There appears to be degradation in the filter structure with use. A notable breakdown in the structure is observed between blank filters and those extracted at 15,000 km. This degradation continues between 15,000 km and 30,000 km. However, the level of degradation between 30,000 km and 45,000 km is comparable.

Particle sizes: images taken from 15,000 km filter samples show particles between  $>2$  &  $<10 \mu\text{m}$ , with several large particles present. Images taken from 30,000 km filters show particles between  $>1 \mu\text{m}$  &  $<8 \mu\text{m}$ , with several large particles also present. However, images taken from 45,000 km filter samples show particles generally  $>1 \mu\text{m}$  and  $<2 \mu\text{m}$ , with a reduced number of large particles present. This implies that as filter integrity deteriorates the capacity for retaining large particles is diminished, while the ability to retain smaller particles improves.

## 7.2: SEM imagery of Micronair Combination Filters Blank v 15,000 km in CM1

**Combination Filter at a kilometerage of 0 km.**

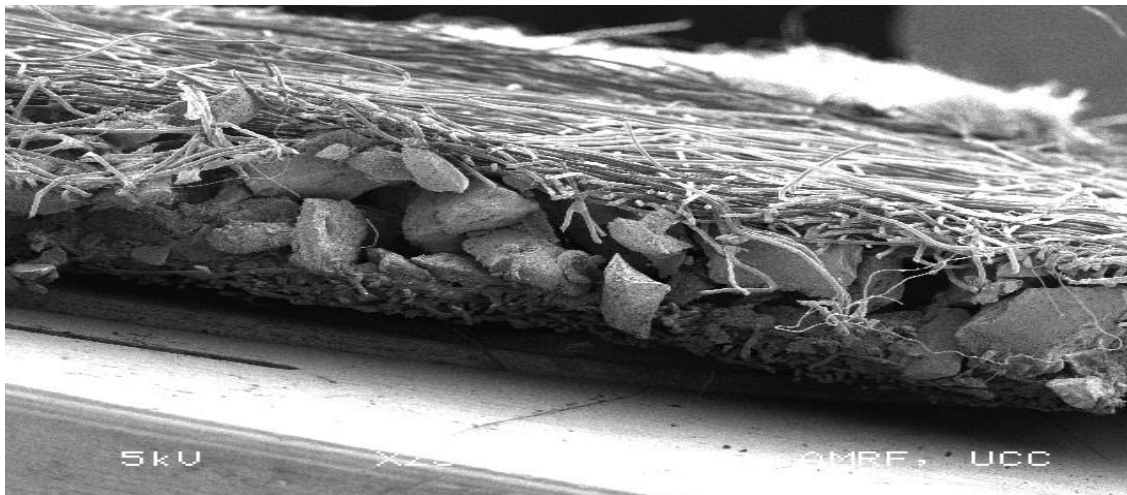


Figure 7.2.1: SEM image of a blank Micronair combination filter from CM1, at a magnification x 25. The carbon fibre layer on the combination filter is clearly visible in Figure 7.2.1.

**Combination Filter at a kilometerage of 15,000 km.**

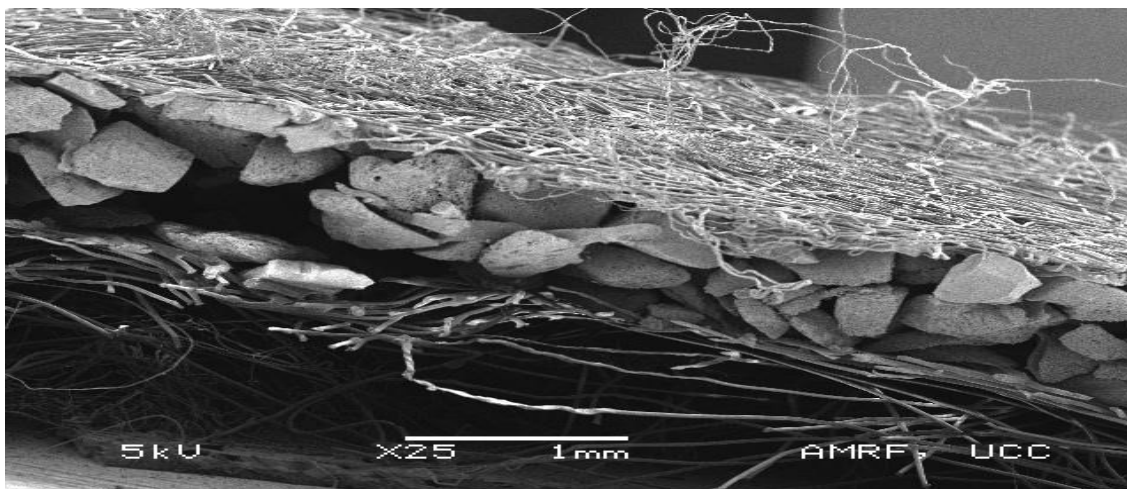


Figure 7.2.2: SEM image of a Micronair combination filter taken at a kilometerage of 15,000 km from CM1, at a magnification x 25.

**Combination Filter at a kilometerage of 0 km.**

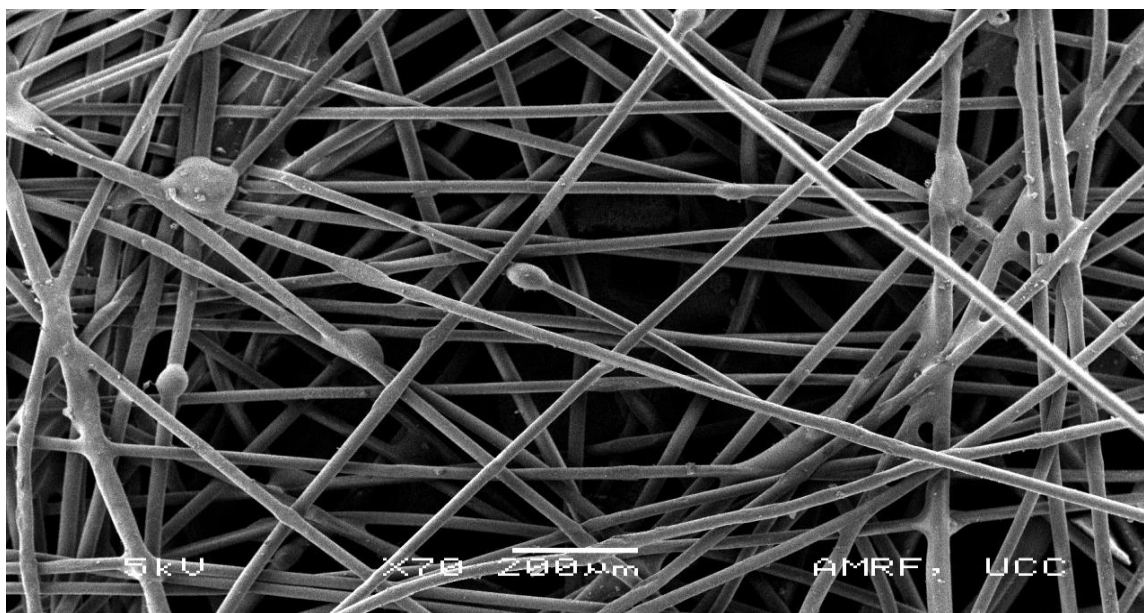


Figure 7.2.3: SEM image of a blank Micronair combination filter from CM1, at a magnification x 70.

**Combination Filter at a kilometerage of 15,000 km.**

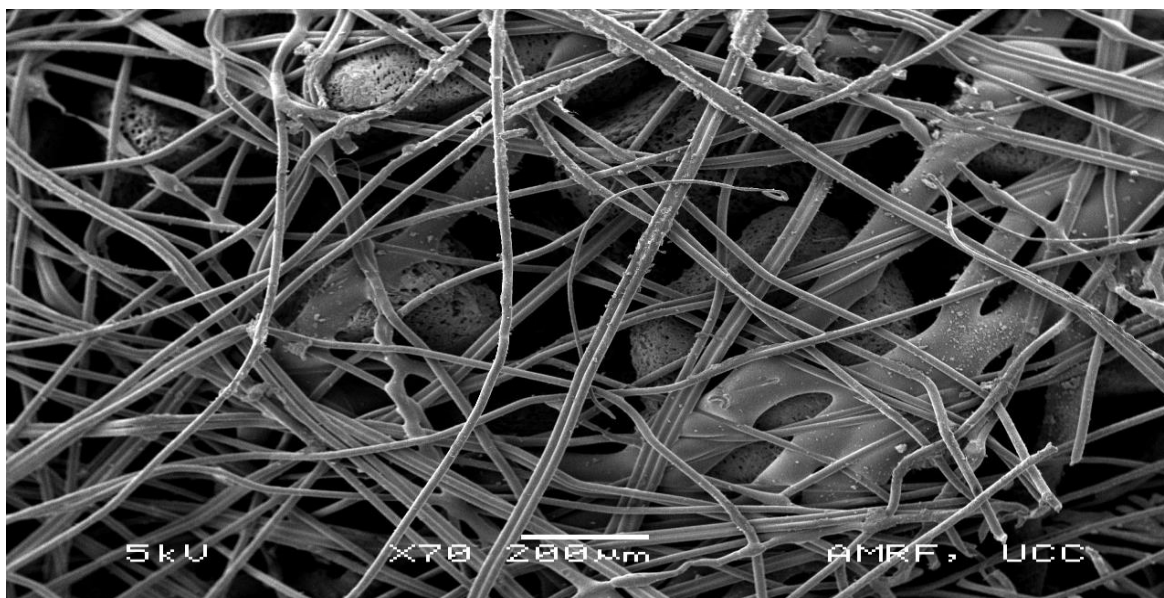


Figure 7.2.4: SEM image of a Micronair combination filter taken at a kilometerage of 15,000 km from CM1, at a magnification x 70.



**Combination Filter at a kilometerage of 0 km.**

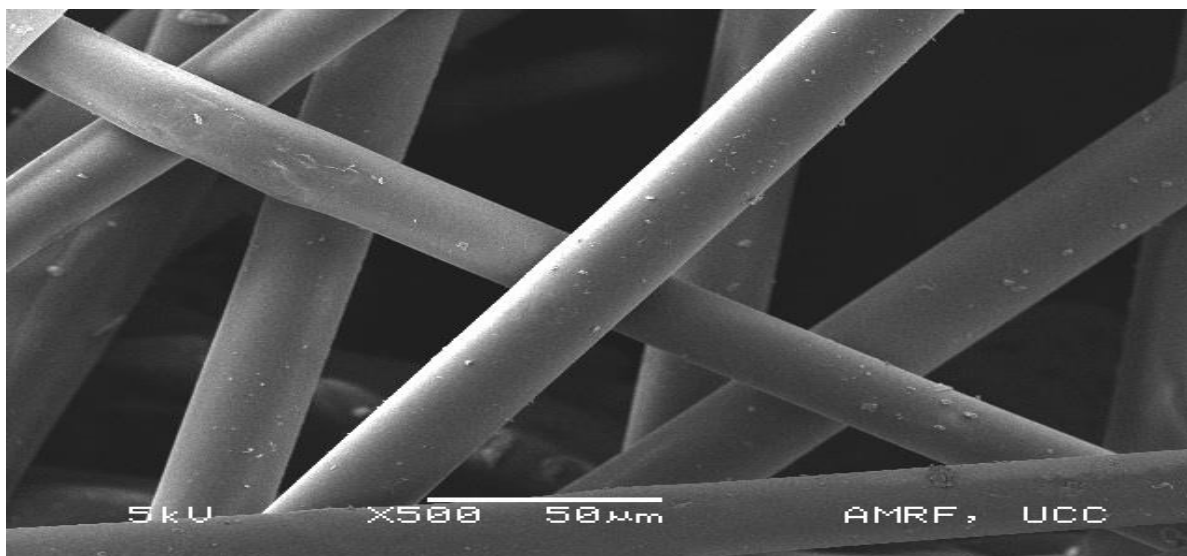


Figure 7.2.5: SEM image of a blank Micronair combination filter from CM1, at a magnification x 500.

**Combination Filter at a kilometerage of 15,000 km.**



Figure 7.2.6: SEM image of a Micronair combination filter taken at a kilometerage of 15,000 km from CM1, at a magnification x 500.

### Combination Filter at a kilometerage of 0 km.

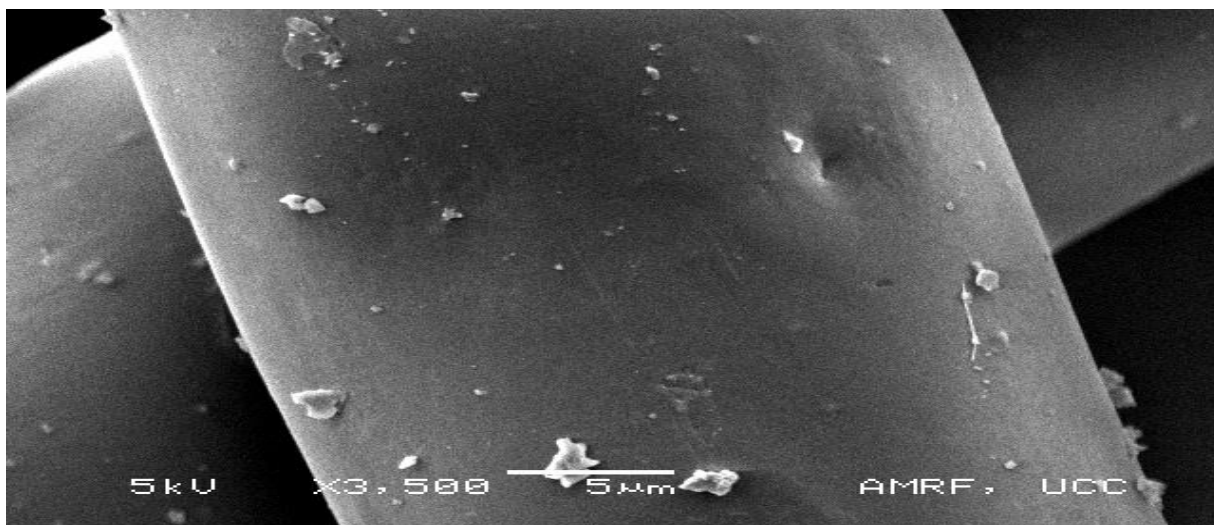


Figure 7.2.7: SEM image of a blank Micronair combination filter from CM1, at a magnification x 3,500.

### Combination Filter at a kilometerage of 15,000 km.

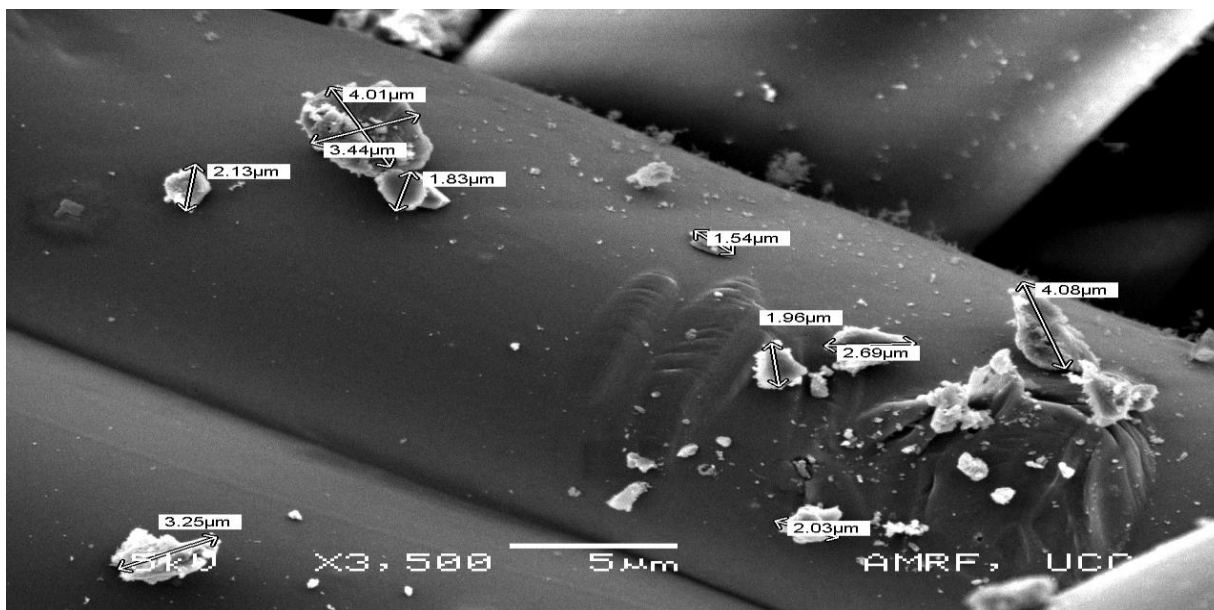


Figure 7.2.8: SEM image of a Micronair combination filter taken at a kilometerage of 15,000 km from CM1, at a magnification x 3,500, with particle sizes indicated. The smallest particles observed are  $>1$  and  $<2$   $\mu\text{m}$ , implying that particles  $<2$   $\mu\text{m}$  can be trapped by Micronair combination filters at 15,000 km in CM1.

**Conclusion:**

Filter degradation is also observed using combination filters. A notable breakdown in the structure is observed between blank filters and those extracted at 15,000 km.

Particle sizes: images taken from 15,000 km combination filter samples show particles between  $<2$  &  $>5$   $\mu\text{m}$ , with few large particles present. This implies that combination filters are more efficient at extracting smaller particles.

**EDX: Elemental quantitative/qualitative analysis.**

When using an ICP-OES or a GFAAS to analyse samples they need to be liquefied for injection, as discussed previously in Chapter 3. An analysis of filters recoveries using EDX was carried out to determine if comparable sample recoveries could be detected using solid samples, eliminating the need for a digestion step.

**7.3: EDX: Elemental quantitative/qualitative analysis of standard particle filters.**

EDX analysis of blank, uncoated, Micronair standard particle filters, from CM1, shown in Figure 7.3.1, show mainly carbon, 17.3 mg/L with small concentrations of calcium and copper, 0.01 mg/L and 0.02 mg/L respectively.

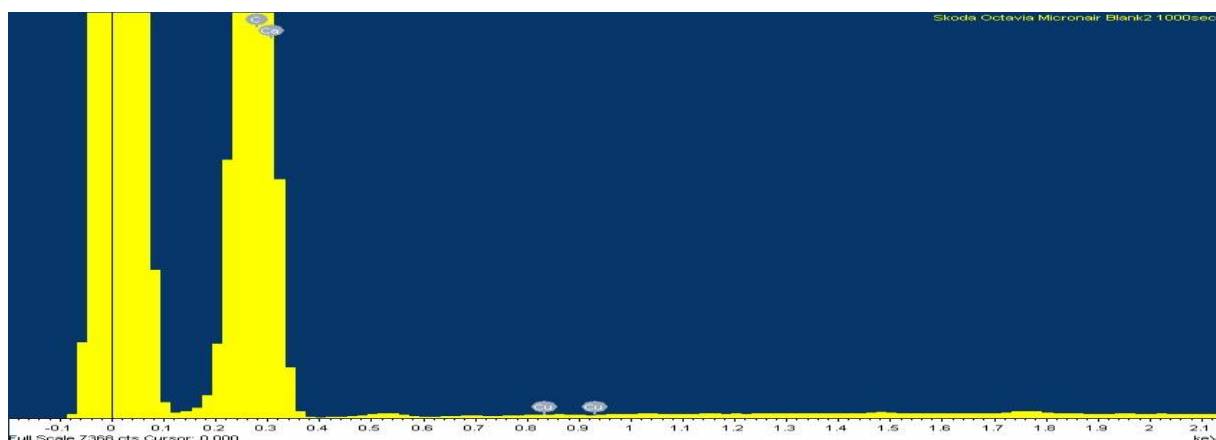


Figure 7.3.1: Standard particle filter, EDX metal profile from blank uncoated Micronair filter from CM1.

EDX analysis of uncoated Micronair standard particle filters extracted at 15,000, shown in Figure 7.3.2, show mainly carbon, 13.84 mg/L with small concentration of Na (0.01 mg/L), Al (0.01 mg/L), Si (0.02 mg/L) chlorine (0.01 mg/L) and Ca (0.01 mg/L).

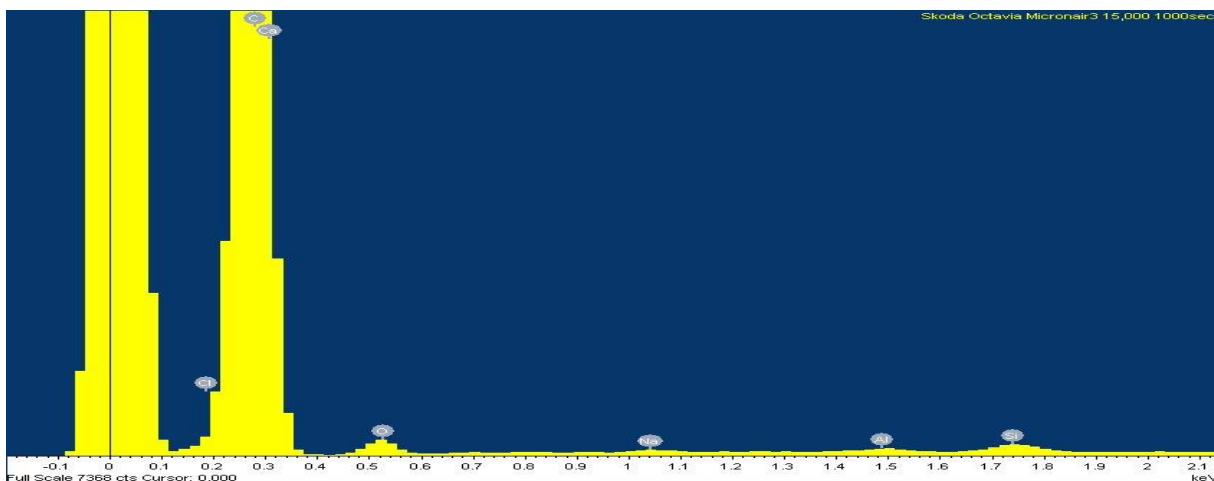


Figure 7.3.2: Standard particle filter, EDX metal profile from 15,000 km, uncoated, Micronair filter from CM1.

EDX analysis of uncoated Micronair standard particle filters extracted at 30,000, shown in Figure 7.3.3, show mainly carbon, 10.17 mg/L with small concentration of Na (0.01 mg/L), Mg (0.02 mg/L), Al (0.06 mg/L), Si (0.19 mg/L) Cl (0.15 mg/L), K (0.03 mg/L), Ca (0.11 mg/L) and Cu (0.06 mg/L).

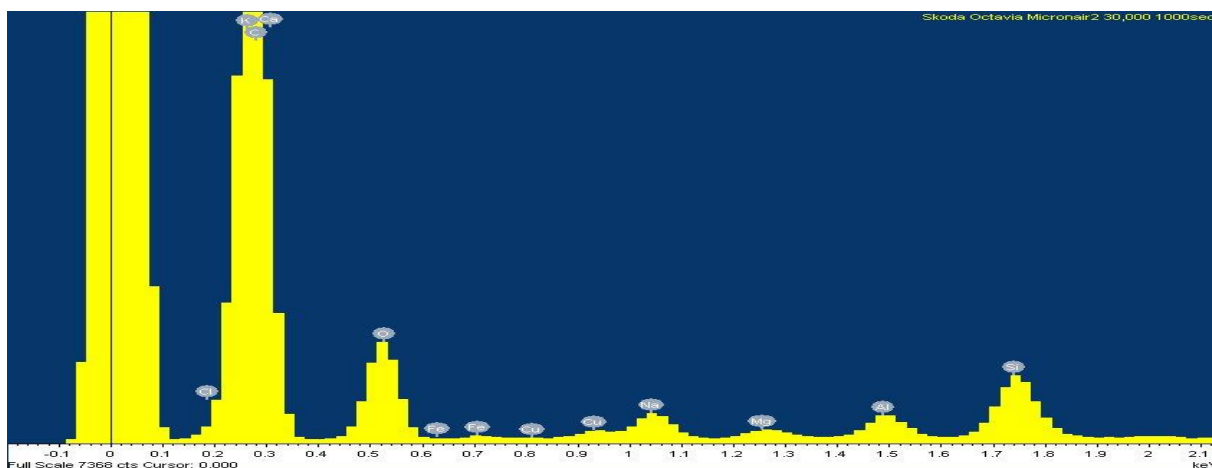


Figure 7.3.3: Standard particle filter, EDX metal profile from 30,000 km, uncoated, Micronair filter from CM1.

EDX analysis of uncoated Micronair standard particle filters extracted at 45,000, shown in Figure 7.3.4, show mainly carbon, 10.7 mg/L with small concentration of Na (0.1 mg/L), Mg

(0.03 mg/L), Al (0.08 mg/L), Si (0.24 mg/L) Cl (0.16 mg/L), K (0.04 mg/L), Ca (0.23 mg/L) Fe (0.09 mg/L) and Cu (0.08 mg/L).

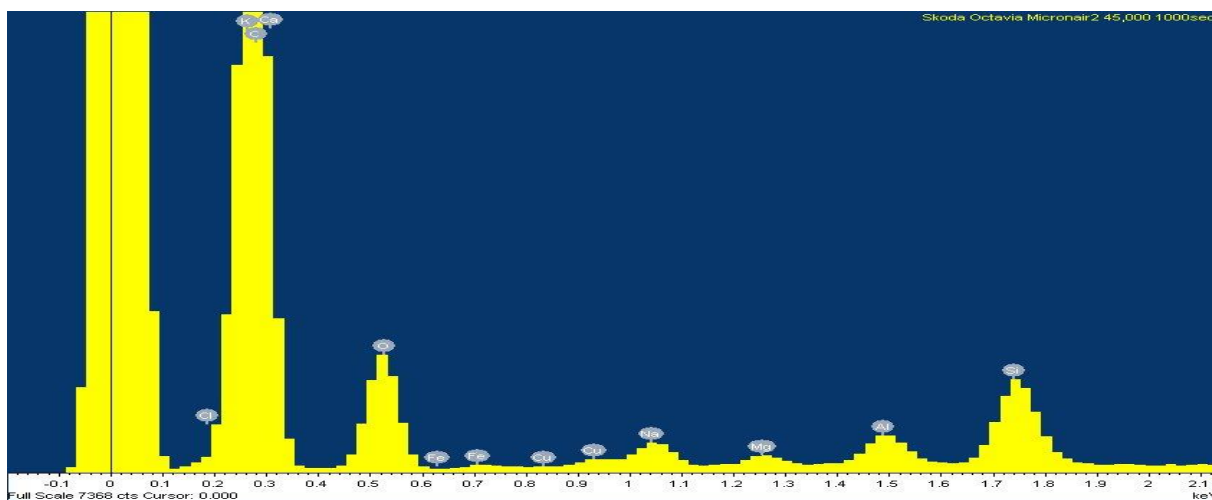


Figure 7.3.4 Standard particle filter, EDX metal profile from 45,000 km, uncoated, Micronair filter from CM1.

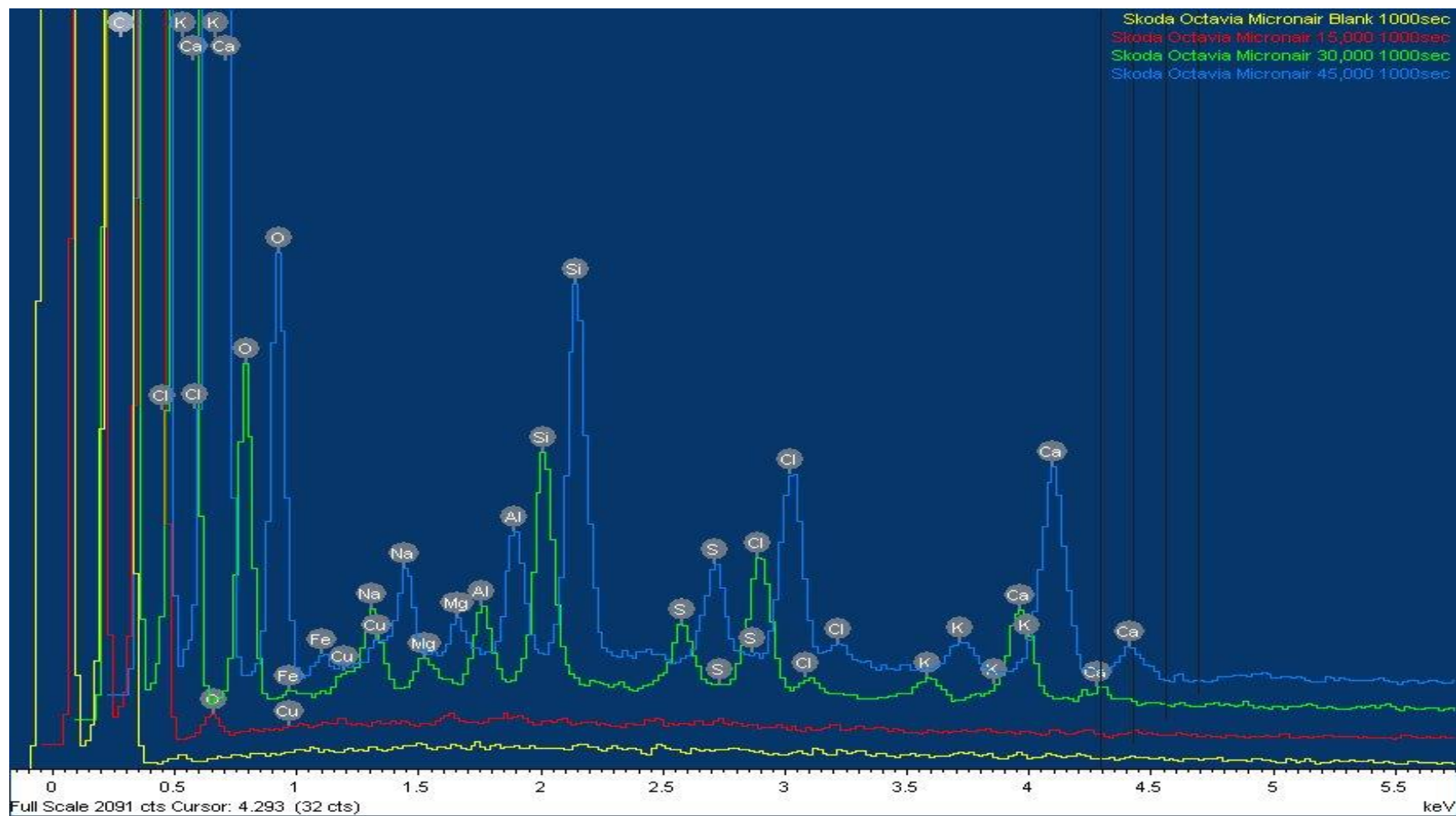


Figure 7.3.5: Standard particle filter, EDX metal profile comparison between 0 km, 15,000 km, 30,000 km and 45,000 km, uncoated, Micronair filter from CM1.

**Conclusion:**

Table 7.3.1: Recoveries using EDX analysis compared to ICP-OES analysis.

	0 km		15,000 km		30,000 km		45,000 km	
	mg/L							
	EDX	ICP	EDX	ICP	EDX	ICP	EDX	ICP
Cu (mg/L)	0.02	0.01		4	0.06	48	0.08	34
Al (mg/L)		3.5	0.01	0.01	0.06	22	0.08	22
Fe (mg/L)		0.4		8		29	0.09	29

**EDX Copper Analysis:** For EDX analysis an increase is observed, as for ICP-OES analysis, between 0 km samples and samples taken at 30,000 km and 45,000 km. Samples taken at 15,000 km do not show any copper present. A difference of ~34 mg/L was observed between 0 km and 45,000 km using ICP-OES, whereas a difference of 0.06 mg/L was observed using EDX.

**EDX Aluminium Analysis:** No aluminium is observed in blank samples and increase of 0.07 mg/L is observed between 15,000 km and 45,000 km using EDX analysis. Using ICP-OES analysis, aluminium is detected in blank samples and an increase of ~20 mg/L is observed between blank samples and samples taken at 45,000 km.

**EDX Iron Analysis:** No iron is detected in blank samples, samples taken at 15,000 km or 30,000 km but ~0.09 mg/L was measured at 45,000 km using EDX analysis. Using ICP-OES detection iron is detected in blank samples, those taken at 15,000 km, at 30,000 km and at 45,000 km, going from 0.4 mg/L in blank samples to 29 mg/L in 45,000 km samples.

The sample recoveries for ICP-OES and EDX are not quantifiably comparable; recoveries for all metals are higher using ICP-OES. However, the recovery patterns are comparable.

Unlike for ICP-OES analysis no measurable amounts of chromium, lead, zinc and manganese were observed using EDX analysis.

**Conclusion:**

Recoveries using EDX analysis are not comparable to ICP-OES analysis for samples taken from Micronair combination filters taken at 0 km and 15,000 km. No measureable quantities of Al, Cr,

Cu, Fe, Mn, Pb and Zn are observed using EDX analysis. Therefore EDX is not a viable option for filter analysis for either particle or combination filters.

EDX analysis is carried out on the surface of solid samples, it is therefore only capable of monitoring the top layer of particulate matter absorbed by particle filters. ICP-OES analysis requires complete liquidation of solid samples, whole sample analysis is therefore carried out. Comparing EDX and ICP-OES figures it is apparent that whole sample analysis is necessary to obtain accurate representation of metal concentrations retained by the particle filters.



## Conclusion

An investigation into the concentration of heavy metals on filter samples was carried out by initially digesting them using a Microwave Multiwave 3000 and then analysing them using a inductively coupled plasma oscillating emission spectroscopy (ICP-OES). The optimum digestion method used an acid combination of 1 ml HCl, 2 ml HF and 6 ml HNO<sub>3</sub> with a digestion method that had a gradual increase in power to 14,000 W.

The extraction efficiency of the filters was analysed with respect to the following variables: filter manufacturer, car make, filter type (particle and combination) and varying kilometerages (1,000 km, 15,000 km, 30,000 km and 45,000 km). Air purifiers were placed in car cabins to analyse the concentrations of metals passing through standard particle and combination filters into the cabin. The majority of filters showed an increase in metal concentrations from 0 km to 15,000 km and from 15,000 km to 30,000 km. No significant increase in concentrations was generally observed from 30,000 km to 45,000 km. Some filters tested showed high background levels for certain metals, e.g. Pb on Micronair Standard Particle filters. A significant increase was not observed between blank filter and those run to 45,000 km but de-absorption was not observed. These filters do not appear to have the ability to retain Pb but they also do not appear to add to the levels of Pb entering the cabin through de-absorption.

Scanning Electron Microscope and Energy Dispersive X-ray (SEM/EDX) analysis was carried out on the Micronair standard particle and combination filters to investigate the size of particulates retained by the filter. The size of particulates being retained is of interest because particulates <2.5 µm can enter the lungs and particulates <1 µm can enter the bloodstream but also because heavy metal retention is dependent on particle size. Cycling filters were also worn by cyclists to analyse the difference between exposures in a vehicle compared to at the roadside.

From SEM analysis it was observed that standard particle Micronair filters degrade with use and this degradation has an impact on particle retention. As the filter degrades the filter's ability to retain large particulates diminishes and its ability to retain fine particulates increases. Images were obtained from Micronair Combination filters at 15,000 km. These images showed that combination filters have a greater capacity to retain fine particulates, while standard particle filters have greater capacity to retain coarser particulates. Considering the majority of metals tested, besides Pb, tend to attach to fine particulates combination filters should be used in place of standard particle filters.

Results from SEM and ICP-OES analysis of Micronair standard particle and combination filters shows that there is a significant relationship between a filter's ability to extract particulate matter based on particle size and the concentration of heavy metals extracted. Cu, Fe, Al and Zn are present in higher concentrations on particles  $>2\text{ }\mu\text{m}$  and particles  $<4\text{ }\mu\text{m}$  contain more Cr and Mn. Pb is present in higher concentrations on PM  $>7.5\text{ }\mu\text{m}$ .

Table 5.9.1 shows metal concentrations for all filters tested from 0 km to 15,000 km, this is an indication of annual exposure given that the average motorist drives approximately 15,000 km per year.

The highest copper value obtained from filters run to 15,000 km was 22.97 g/L. This figure is alarmingly high considering the recommended maximum limit for copper in drinking water is 1.3 mg/L. The recommended maximum limit for iron in drinking water is 0.3 mg/L considerably lower than the level of 13.1 g/l observed on filter samples run to 15,000 km.

The recommended maximum level of aluminium in drinking water is 50-200  $\mu\text{g/L}$ , which is of concern considering it is considerably lower than the highest level of aluminium observed on filter samples, 10.7 g/L. The highest levels of chromium observed on filters tested were 60 mg/L. This figure is representative of total chromium present. Exposure limits in drinking water are set specifically for  $\text{Cr}^{+6}$ , set out by the US EPA is 100  $\mu\text{g/L}$ . A potential annual exposure of 60 mg/L is a concern but it not as alarming as the high levels of Al, Cu or Fe. The level of lead allowed in drinking water as set out by the Irish EPA is 10  $\mu\text{g/L}$  and the maximum lead exposure observed on filters run to 15,000 km was 60 mg/L. The levels of lead present are a concern to human health. Permissible levels of manganese in drinking water are set by the US EPA at 50  $\mu\text{g/L}$  and the highest concentration observed on filters run to 15,000 km was 240 mg/L. The levels of manganese present, when considered relative to other metals present, don't appear to be alarmingly high but are of concern when taking into account the recommended exposure limits. For zinc the recommended exposure limit set by the US EPA is 5 mg/L and the maximum level of Zinc found on filters run to 15,000 km was 650 mg/L. The levels of zinc found are of concern but are not alarmingly high, relative to the recommended exposure limit.

The potential annual exposure observed on filters run to 15,000 km is of concern for all metals tested and demonstrates the necessity for the installation and regular replacement of particle filters.

## Further study

Harrison *et al.*, found that in London road traffic is responsible for 86% of PM<sub>10</sub> while in California Motor vehicles account for 30-42% of PM<sub>10</sub>. [114] Harrison *et al.*, also found that while testing four UK, heavy metal concentration from city to city were consistent.[107] Filters were collected in and around Cork city for this study. To determine if heavy metal concentrations differ from city to city future study should include the analysis of filters collected in several sites around the country. An international study should also be carried out to compare metal concentrations in several European cities, comparing exposure levels in cities by population/area.

Marcazzan *et al.*, found that for PM<sub>10</sub>, Mn and Zn values are constant year round, that Fe and Pb levels are reduced and Al levels increase during the summer months. For PM<sub>2.5</sub>, Mn and Cu concentrations are consistent all year long but Zn and Pb concentrations decrease and Al and Fe increase in the summer. Lack of some metals is due to better dispersion of motor vehicle emissions. [109] Cavanagh *et al.*, found that heavy metal concentrations are higher in July in two cities tested, attributed to the variation in PM composition [102] Melaku *et al.*, tested for As, Cd, Cr, Pb and found that in the Summer the concentration of most metals was consistent except for Cr.[110] Most of the filters collected as part of this study were collected over periods equal to or exceeding 12 months. Future study should include running filters at specific times of the year.

It is recommend as a result of this study that combination filters should be used in place of standard particle filters due to the size of particulates being retained. Further study should include ICP-OES and SEM analysis of combination filters at kilometerages of 30,000 and 45,000 to determine if, like standard particle filters, the filters structure breaks down and if this breakdown occurs what impact it has on particulate retention.

Further study should look at how potentially toxic elements are bound to particulates, to determine if they are chemically absorbed to the particles or if they are physically adsorbed onto the particle surface. As discribed in section 1.4 combination filter manufacturers suggest that particles are adsorbed onto the filters surface by electrostatic forces. The first layer of the filter extracts the largest particles to an electrostatically charged surface. It is suggested that when this layer becomes loaded with particles the efficiency of this layer is increased because the particles themselves act as a filter. The second layer of the filter consists of finer electrostatically charged fibres that are densely packed, attracting fine particle. The final layer, a carbon layer, consists of tiny granules of porous, activated carbon. Pollutant gases are

absorbed in this layer. It has a large surface layer within the microscopic pores of the activated carbon. Pollutant gases are attracted to the activated carbon surface by Van Der Waal's forces. Further study should include an investigation into how particles adhere to filter surfaces. Looking at the electrostatic forces between filters and particles and how these bonds breakdown during digestion. The toxicity of potentially toxic elements is dependant on the species present, e.g.  $\text{Cr}^{3+}$  is an essential nutrient but  $\text{Cr}^{6+}$  is carcinogenic. Further study should look at the form of potentially toxic elements and the possibility that they are chemically absorbed to particles by looking at anionic concentrations and how these chemical bonds breakdown, e.g. using HF will breakdown silica bonds, so increased HF use could lead to an increase in the extraction of cations bound to silica.

1. Safety, U.E.H.a. *Toxicology and Exposure Guidelines*. 2002; Available from: <http://ehs.unl.edu>.
2. Kaiser, J., *Evidence mounts that tiny particles can kill*. Science, 2000. **289**(5476): p. 22.
3. Ministry of Water, L.a.A.P., Cranbrook, B.C. *Winter Fine Particulate Air Quality in Cranbrook*. 1999; Available from: [http://www.env.gov.bc.ca/epd/regions/kootenay/aq\\_reports/pdf/cranbrook\\_air\\_quality\\_report.pdf](http://www.env.gov.bc.ca/epd/regions/kootenay/aq_reports/pdf/cranbrook_air_quality_report.pdf).
4. EPA. *Air Trends - Basic Information* Available from: <http://www.epa.gov/airtrends/sixpoll.html>.
5. Sydenham, T., *Air pollution*. 2009.
6. Borough, F.N.S., *Health - Particle Pollution*.
7. pentz, B., *Fine Dust Properties*, 2007.
8. <http://qz.com/#307176/thirteen-of-the-20-most-polluted-cities-in-the-world-are-indian/>
9. HSE, E., *Development of the Air Quality Index for Health (AQIH)*. 2013.
10. EPA, *Air Quality in Ireland 2012 Key Indicators of Ambient Air Quality*. 2013.
11. EPA. *Air quality standards*. 2013; Available from: <http://www.epa.ie/air/quality/standards/>
12. Kjellstrom, T., *World Energy Assessment: Energy and the Challenge of Sustainability*.
13. Adachi, K. and Y. Tainosho, *Characterization of heavy metal particles embedded in tire dust*. Environment international, 2004. **30**(8): p. 1009-1017.
14. Sternbeck, J., A.Å. Sjödin, and K. Andréasson, *Metal emissions from road traffic and the influence of resuspension--results from two tunnel studies*. Atmospheric Environment, 2002. **36**(30): p. 4735-4744.
15. Ozaki, H., I. Watanabe, and K. Kuno, *Investigation of the heavy metal sources in relation to automobiles*. Water, Air, & Soil Pollution, 2004. **157**(1): p. 209-223.
16. Shakya, P.R.A.J., et al., *Studies and Determination of Heavy Metals in Waste Tyres and their Impacts on the Environment*. Pak. J. Anal. & Envir. Chem. Vol, 2006. **7**(2): p. 70-76.
17. Napier, F., B. D'Arcy, and C. Jefferies, *A review of vehicle related metals and polycyclic aromatic hydrocarbons in the UK environment*. Desalination, 2008. **226**(1-3): p. 143-150.
18. <https://www.thermoscientific.com/content/dam/tfs/ATG/CMD/cmd-support/icap/7000/datasheets/7000%20Accessories%20Guide.pdf>
19. Kommana, K., *Pollution in River Ganga Problems and Prospects in Varanasi, India*. 2011.
20. Peralta-Videa, J.R., et al., *The biochemistry of environmental heavy metal uptake by plants: implications for the food chain*. The International Journal of Biochemistry & Cell Biology, 2009. **41**(8-9): p. 1665-1677.
21. Whitby, L. and T. Hutchinson, *Heavy-metal pollution in the Sudbury mining and smelting region of Canada, II. Soil toxicity tests*. Environmental Conservation, 1974. **1**(03): p. 191-200.
22. Christie, N.T. and M. Costa, *In vitro assessment of the toxicity of metal compounds*. Biological Trace Element Research, 1984. **6**(2): p. 139-158.
23. Bearer, C.F., *How are children different from adults?* Environmental Health Perspectives, 1995. **103**(Suppl 6): p. 7.
24. Almeida, P. and L.B. Stearns, *Political opportunities and local grassroots environmental movements: The case of Minamata*. Social Problems, 1998: p. 37-60.

25. Kaye, P., H. Young, and I. O'sullivan, Metal fume fever: a case report and review of the literature. *Emergency Medicine Journal: EMJ*, 2002. 19(3): p. 268.
26. Birchall, J. D., et al. "Acute toxicity of aluminium to fish eliminated in silicon-rich acid waters." (1989): 146-148.
27. Darbre, P., Environmental oestrogens, cosmetics and breast cancer. *Best practice & research clinical endocrinology & metabolism*, 2006. 20(1): p. 121-143.
28. Nordberg, G., *Handbook on the Toxicology of Metals*. 2007: Academic Pr.
29. Das, P., S. Samantaray, and G. R. Rout. "Studies on cadmium toxicity in plants: a review." *Environmental pollution* 98.1 (1997): 29-36.
30. Shanker, Arun K., et al. "Chromium toxicity in plants." *Environment international* 31.5 (2005): 739-753.
31. Gaetke, Lisa M., and Ching Kuang Chow. "Copper toxicity, oxidative stress, and antioxidant nutrients." *Toxicology* 189.1 (2003): 147-163.
32. Medscape. *Iron Toxicity*. Available from: <http://emedicine.medscape.com/article/815213-overview>.
33. Patrick, Lyn. "Lead toxicity, a review of the literature. Part 1: Exposure, evaluation, and treatment." *Alternative medicine review: a journal of clinical therapeutic* 11.1 (2006): 2-22.
34. Crossgrove, Janelle, and Wei Zheng. "Manganese toxicity upon overexposure." *NMR in Biomedicine* 17.8 (2004): 544.
35. Melita, L. and F. Gumrah, *Studies on transport of vanadium (V) and nickel (II) from wastewater using activated composite membranes*. *Waste and Biomass Valorization*, 2010. 1(4): p. 461-465.
36. Supplements, O.O.D. *Zinc Toxicity*. Available from: <http://ods.od.nih.gov/factsheets/zinc.asp>.
37. Micronair. *Particle Filter*. 2013; Available from: [http://micronair.aw-con.de/en/products/desc\\_partikelfilter.php](http://micronair.aw-con.de/en/products/desc_partikelfilter.php).
38. Micronair, *Micronair particle filter*.
39. Micronair, *Micronair - Combination Filter*.
40. Micronair, *How Our Filters Work*.
41. Maus, R. and H. Umhauer, *Collection efficiencies of coarse and fine dust filter media for airborne biological particles*. *Journal of Aerosol Science*, 1997. 28(3): p. 401-415.
42. KG, H.R.F.V. and U.S.F.V. KG, *Recent Developments in Cabin Air Filtration*. 2006.
43. Reinhardt, H., *Experience - Driven Cabin Air Filter Development*. 1996.
44. Puravent. *Particle filter Design*; Available from: <http://www.puravent.co.uk/filters/puraventfilterdesign.htm>.
45. Larson, S.D., et al., *Postnatal remodeling of the neural components of the epithelial-mesenchymal trophic unit in the proximal airways of infant rhesus monkeys exposed to ozone and allergen*. *Toxicology and applied pharmacology*, 2004. 194(3): p. 211-220.
46. Micronair. *CM2 filter design*. Available from: <http://www.micronair.us/assets/pics/125.jpg>.
47. Micronair. *CM1 Particle filter*. Available from: [www.micronair.com.br/press/pictures/index.php](http://www.micronair.com.br/press/pictures/index.php).
48. Micronair. *Customer Research Study conducted for Freudenberg non-wovens*. Available from: [http://www.micronair.com/en/press/pressreleases/detail\\_english\\_07.php?prinTable](http://www.micronair.com/en/press/pressreleases/detail_english_07.php?prinTable).
49. Autoglass. Available from: <http://www.autoglassontheweb.com/whats-new?offset=35&max=5>.

50. Mahle. *Demand for particle filters all year round.*; Available from: <http://www.mahle-aftermarket.com/C12570B3006C0D49/CurrentBaseLink/W27ENGX6914STULEN>.
51. Micronair. *Ozone levels are rising a combination filter can protect you.*; Available from: [http://www.micronair.com/en/press/pressreleases/detail\\_english\\_05.php](http://www.micronair.com/en/press/pressreleases/detail_english_05.php).
52. Saranow, J., *Your Car as a Shelter From Allergies*. Wall Street Journal, 2005.
53. SARANOW, J., *Your Car as a Shelter From Allergies*. 2005.
54. Micronair. *Protection against small particles and fine dust*. Available from: [http://www.micronair.de/en/products/article\\_feinstaub.php](http://www.micronair.de/en/products/article_feinstaub.php).
55. Schmidt, F. *Dynamic Absorption behaviour of Cabin Air Filters*. 2002; Available from: [http://www.sciencedirect.com/science?\\_ob=MIImg&imagekey=B6VJM-4783K52-N-2&cdi=6098&user=77869&orig=search&coverDate=09%2F30%2F2002&sk=999609992&view=c&wchp=dGLbVtb-zSkzS&valck=1&md5=bbe76743a6037e59d4f374d09b87ee4a&ie=/sdarticle.pdf](http://www.sciencedirect.com/science?_ob=MIImg&imagekey=B6VJM-4783K52-N-2&cdi=6098&user=77869&orig=search&coverDate=09%2F30%2F2002&sk=999609992&view=c&wchp=dGLbVtb-zSkzS&valck=1&md5=bbe76743a6037e59d4f374d09b87ee4a&ie=/sdarticle.pdf).
56. Bräunling, V. *New filtration concepts for cabin air filters*. 2004.
57. Genf, *DIN EN ISO 846: Plastics – Evaluation of the action of microorganisms*. 1997.
58. Micronair. *The Road Test of Cabin Air Filters in Japan*. 1997; Available from: <http://www.micronair.com/files/publications/road.pdf>.
59. Namork, E., B.V. Johansen, and M. Løvik, *Detection of allergens adsorbed to ambient air particles collected in four European cities*. Toxicology Letters, 2006. 165(1): p. 71-78.
60. Namork, *Detection of allergens adsorbed to ambient air particles collected in four European cities*. Elsevier, 2006.
61. Micronair. *Tunnel Effect*. Available from: <http://www.micronair.de/en/products/index.php?prinTable>.
62. Micronair, *Particle arrestance performance: VW particle filter*.
63. Micronair, *Replacement demand for cabin air filters in Europe*.
64. *micronAir cabin air filters earn Greenguard certification*. Filtration & Separation. 44(1): p. 7-7.
65. Filter, M. *Mann-Filter Cabin Filter*. Available from: <http://www.mann-hummel.com/mannfilter/upload/doc/HBRPBK8agzp.pdf>.
66. Spectrometry, G.F.A.A. *Graphite Furnace Atomic Absorption Spectrometry*. Available from: <http://www.clu-in.org/characterization/technologies/graphite.cfm>.
67. Components, D.o.G., .
68. Fifield, F. and D. Kealey, *Principles and practice of analytical chemistry*. 2000: Wiley-Blackwell.
69. MANNING, T. and W. GROW, *Inductively Coupled Plasma-Atomic Emission Spectrometry*. The Chemical Educator, 1997. 2(1): p. 1-19.
70. *Schematic Diagram of ICP Plasma Torch*. Available from: <http://www.sas.upenn.edu/~seanjw/Inductive%20Heating%20and%20Plasma%20Index.html>.
71. Elmer, P. *Dual View ICP the best of both worlds*. Available from: [http://www.perkinelmer.com/CMSResources/Images/44-74835TCH\\_DualViewICP.pdf](http://www.perkinelmer.com/CMSResources/Images/44-74835TCH_DualViewICP.pdf).
72. Bradford, T.C., N, *Inductively Coupled Plasma (ICP)*. 1997.

73. Elmer, P. *The Optima 2000: a unique double-monochromator optical system.*; Available from: [http://las.perkinelmer.com/content/TechnicalInfo/TCH\\_Optima2000.pdf](http://las.perkinelmer.com/content/TechnicalInfo/TCH_Optima2000.pdf).
74. Elmer, P. *The Clear Solution For High-Throughput Microwave-Assisted Sample Preparation.* Available from: [http://las.perkinelmer.com/content/RelatedMaterials/Brochures/bro\\_multiwave3000.pdf](http://las.perkinelmer.com/content/RelatedMaterials/Brochures/bro_multiwave3000.pdf).
75. Paar, A., *Multiwave Sample Preparation System*. 1998.
76. Group, E.A., *Scanning Electron Microscope Schematic*, 2008.
77. 7300, N.I., *Elements by ICP 7300*.
78. Elmer, P. *Microwave Multiwave.* Available from: <http://las.perkinelmer.com/Catalog/ProductInfoPage.htm?ProductID=N3141000>.
79. Technology., N.I.o.S.a. *SRM 1648a*. Available from: <https://www-s.nist.gov/srmors/certificates/1648A.pdf?CFID=1214088&CFTOKEN=6d69536228c6500-B46B2D4F-F3A8-8F9F-F4F05056241B8E11&jsessionid=f0307cc3e40efebc3bea533c6a46701b3533>.
80. *PorTable Car Air Purifier.* Available from: [http://www.airpurifiersforhome.com/products/car\\_air\\_purifier.htm](http://www.airpurifiersforhome.com/products/car_air_purifier.htm).
81. *Cycle Mask.* Available from: [http://www.ukbikestore.co.uk/product/100/respro\\_city/respro-city-cycle-mask.html](http://www.ukbikestore.co.uk/product/100/respro_city/respro-city-cycle-mask.html).
82. 7301, N.I., *ELEMENTS by ICP 7301 (Aqua Regia Ashing)*.
83. Callen, B. W., et al. "Nitric acid passivation of Ti6Al4V reduces thickness of surface oxide layer and increases trace element release." *Journal of biomedical materials research* 29.3 (1995): 279-290.
84. Eastern Research Group, I., *Standard Operating Procedure for Determination of Lead in TSP by Inductively Coupled Plasma Mass Spectrometry (ICP-MS) with Hot Block Dilute Acid and Hydrogen Peroxide Filter Extraction*.
85. Hill, S.J., et al., *Atomic spectrometry update. Environmental analysis*. Journal of Analytical Atomic Spectrometry, 2002. **17**(3): p. 284-317.
86. Robache, A., et al., *Multi-element analysis by inductively coupled plasma optical emission spectrometry of airborne particulate matter collected with a low-pressure cascade impactor*. The Analyst, 2000. **125**(10): p. 1855-1859.
87. Pekney, N.J. and C.I. Davidson, *Determination of trace elements in ambient aerosol samples*. Analytica Chimica Acta, 2005. **540**(2): p. 269-277.
88. Link, D., P. Walter, and H. Kingston, *Development and validation of the new EPA microwave-assisted leach method 3051A*. Environ. Sci. Technol, 1998. **32**(22): p. 3628-3632.
89. Wang, C.-F., J.-Y. Yang, and C.-H. Ke, *Multi-element analysis of airborne particulate matter by various spectrometric methods after microwave digestion*. Analytica Chimica Acta, 1996. **320**(2-3): p. 207-216.
90. Sandroni, V., C.M.M. Smith, and A. Donovan, *Microwave digestion of sediment, soils and urban particulate matter for trace metal analysis*. Talanta, 2003. **60**(4): p. 715-723.
91. Zhou, C.Y., et al., *Orthogonal array design for the optimization of closed-vessel microwave digestion parameters for the determination of trace metals in sediments*. Analytica Chimica Acta, 1995. **314**(1-2): p. 121-130.



92. Sivakumar, V., L. Ernyei, and R. Obenauf, *Guide for Determining ICP/ICP-MS Method Detection Limits and Instrument Performance*. Spectroscopy-Springfield Then Eugene Then Duluth-, 2006. **21**(9): p. 13.
93. Karthikeyan, S., U.M. Joshi, and R. Balasubramanian, *Microwave assisted sample preparation for determining water-soluble fraction of trace elements in urban airborne particulate matter: Evaluation of bioavailability*. *Analytica Chimica Acta*, 2006. **576**(1): p. 23-30.
94. Alfantazi, A., and V. J. Gelling. *Corrosion (general)-217th ECS Meeting*. Electrochemical Soc., 2010.
95. Yang, K.X., K. Swami, and L. Husain, *Determination of trace metals in atmospheric aerosols with a heavy matrix of cellulose by microwave digestion-inductively coupled plasma mass spectroscopy*. *Spectrochimica Acta Part B: Atomic Spectroscopy*, 2002. **57**(1): p. 73-84.
96. Karanasiou, A.A., et al., *Comparative study of pretreatment methods for the determination of metals in atmospheric aerosol by electrothermal atomic absorption spectrometry*. *Talanta*, 2005. **65**(5): p. 1196-1202.
97. Kulkarni, P., et al., *Microwave digestion--ICP-MS for elemental analysis in ambient airborne fine particulate matter: Rare earth elements and validation using a filter borne fine particle certified reference material*. *Analytica Chimica Acta*, 2007. **599**(2): p. 170-176.
98. Melaku, S., et al., *Multi-element analysis of Tinishu Akaki River sediment, Ethiopia, by ICP-MS after microwave assisted digestion*. *Can. J. Ana. Sci. Spectrosc*, 2004. **50**(1): p. 31-40.
99. Samet, Jonathan M., et al. "Fine particulate air pollution and mortality in 20 US cities, 1987–1994." *New England journal of medicine* 343.24 (2000): 1742-1749.
100. Samara, Constantini, and Demetra Voutsas. "Size distribution of airborne particulate matter and associated heavy metals in the roadside environment." *Chemosphere* 59.8 (2005): 1197-1206.
101. Riediker, Michael, et al. "Particulate matter exposure in cars is associated with cardiovascular effects in healthy young men." *American journal of respiratory and critical care medicine* 169.8 (2004): 934-940.
102. Cavanagh, J. A. E., Trought, K., Brown, L., & Duggan, S. (2009). Exploratory investigation of the chemical characteristics and relative toxicity of ambient air particulates from two New Zealand cities. *Science of the total environment*, 407(18), 5007-5018.
103. Allen, A. G., et al. "Size distributions of trace metals in atmospheric aerosols in the United Kingdom." *Atmospheric Environment* 35.27 (2001): 4581-4591.
104. Rajšić, S., Mijić, Z., Tasić, M., Radenković, M., & Joksić, J. (2008). Evaluation of the levels and sources of trace elements in urban particulate matter. *Environmental Chemistry Letters*, 6(2), 95-100.
105. Srivastava, Arun, and V. K. Jain. "Size distribution and source identification of total suspended particulate matter and associated heavy metals in the urban atmosphere of Delhi." *Chemosphere* 68.3 (2007): 579-589.
106. <http://www.industrial-needs.com/technical-data/anemometer-avm-40.htm>
107. Harrison, Roy M., and Jianxin Yin. "Particulate matter in the atmosphere: which particle properties are important for its effects on health?." *Science of the total environment* 249.1 (2000): 85-101.
108. Harrison M. Roy et al. "Studies of the coarse particle (2.5 - 10µm) component in UK urban atmospheres" *Atmospheric Environment* 35 (2001): 3667-3679.

- 109 Marcazzan, Grazia M., et al. "Characterisation of PM10 and PM2. 5 particulate matter in the ambient air of Milan (Italy)." *Atmospheric Environment* 35.27 (2001): 4639-4650.
- 110 Melaku, S., Morris, V., Raghavan, D., & Hosten, C. (2008). Seasonal variation of heavy metals in ambient air and precipitation at a single site in Washington, DC. *Environmental Pollution*, 155(1), 88-98.
- 111 Boogaard, H., Borgman, F., Kamminga, J., & Hoek, G. (2009). Exposure to ultrafine and fine particles and noise during cycling and driving in 11 Dutch cities. *Atmospheric Environment*, 43(27), 4234-4242.
- 112 Panis, L. I., De Geus, B., Vandenbulcke, G., Willems, H., Degraeuwe, B., Bleux, N., ... & Meeusen, R. (2010). Exposure to particulate matter in traffic: a comparison of cyclists and car passengers. *Atmospheric Environment*, 44(19), 2263-2270.
- 113 Allen, A. G., et al. "Size distributions of trace metals in atmospheric aerosols in the United Kingdom." *Atmospheric Environment* 35.27 (2001): 4581-4591.
- 114 Harrison, Roy M., et al. "Sources and processes affecting concentrations of PM 10 and PM 2.5 particulate matter in Birmingham (UK)." *Atmospheric Environment* 31.24 (1997): 4103-4117.

% Metal Recoveries from SRM NIST 1648a using Microwave digestion Method 3 shown in Table 5.1.1. and acid combination 2 ml HF, 1 ml HCl and 6ml HNO<sub>3</sub>.

Below are concentrations of metals analysed from filter samples corrected to 100%, calculated based on % recoveries from SRM analysis. SRM % recoveries were used to calculate corrected filter recoveries by taking recoveries from filter samples and correcting them to 100% .

**Aluminium filter sample recoveries corrected to 100% based an SRM recovery of 57.03%**

Micronair standard particle filter - CM1				
	0 km	15,000 km	30,000 km	45,000 km
	mg/L			
A	3.41	7.49	17.55	20.96
B	3.86	7.04	18.49	25.6
C	3.5	7.5	22.32	24.02
D	3.6	7.67	23.14	20.46
E	3.05	7.74	24.47	24.69
F	3.62	9.23	25.5	19.77
G	4.23	5.01	22.68	20.03
H	3.2	9.61	21.88	26.13
I	3.41	10.5	21.58	21.76
Airforce standard particle filter - CM1				
		0 km	15,000 km	
		mg/L		
A		0.39	23.64	
B		0.84	14.28	
C		0.53	22.16	
D		1.03	15.82	
E		0.62	11.59	
F		0.89	15.14	
G		0.88	8.4	

H		0.61		7.14	
I		0.48		14.47	
Airforce combination filter – CM1					
		0 km		15,000 km	
		mg/L			
A		12.39		47.78	
B		5.97		34.78	
C		8.80		34.03	
D		8.59		61.34	
E		12.57		43.29	
F		16.55		55.90	
G		17.58		44.02	
H		14.46		64.98	
I		13.97		57.67	
Micronair combination filter – CM1					
		0 km		15,000 km	
		mg/L			
A		12.14		29.56	
B		8.28		33.09	
C		20.26		30.57	
D		10.88		30.55	
E		8.60		38.30	
F		14.09		51.80	
G		14.65		35.89	
H		13.74		35.39	
I		12.61		34.72	
Micronair standard particle filter - CM2					
	0 km	15,000 km	30,000 km	45,000 km	
	mg/L				
A	0.53	19.20	22.35	19.98	
B	0.78	18.36	25.42	19.62	

C	0.63	18.72	16.29	16.30
D	0.51	16.34	20.13	18.64
E	0.50	12.40	14.89	15.72
F	0.46	13.63	13.84	16.97
G	0.63	17.49	25.20	17.89
H	0.58	18.18	26.05	22.60
I	0.74	16.08	20.86	20.05
J	0.52	12.05	12.33	10.83
K	0.84	11.10	12.69	9.33
L	0.56	3.29	9.89	5.42
<b>Nip &amp; Denso standard particle filter - CM2</b>				
	0 km	15,000 km	30,000 km	45,000 km
	mg/L			
A	0.61	22.63	28.47	31.00
B	0.45	17.84	24.26	31.64
C	1.39	39.02	37.83	46.74
D	1.05	16.59	33.28	24.68
E	0.52	26.58	33.02	30.72
F	0.78	45.79	29.68	18.31
G	0.81	32.72	38.14	23.92
H	0.57	38.50	39.11	25.06
I	0.66	44.49	32.42	50.32
J	0.75	26.71	40.20	18.90
K	0.98	25.18	30.82	32.72
L	0.51	28.13	28.91	23.05

	Airforce Particle Filter - CM3				Airforce Combination Filter - CM3					
	0		15000		0		15000			
A	131.4	230.5	490.3	860.2	8907.2	15626.7	16701.2	29300.4		
B	189.9	333.2	395.4	693.6	7667.5	13451.8	14880.5	26106.2		
C	151.3	265.5	471.2	826.7	9501.3	16669.0	13295.7	23325.8		
D	198.8	348.8	722.9	1268.2	8131.0	14265.0	20654.9	36236.7		
E	118.5	207.8	474.2	831.9	9509.7	16683.7	13598.8	23857.5		
F	171.2	300.3	390.7	685.5	8295.1	14552.9	13122.8	23022.5		
G	127.3	223.4	585.2	1026.7	6571.7	11529.3	31757.2	55714.4		
H	107.7	188.9	566.5	993.8	8457.6	14838.0	14000.4	24562.2		
I	124.0	217.5	445.4	781.4	7602.3	13337.3	14438.3	25330.4		
J	184.4	323.5	326.8	573.4	8678.8	15226.0	22544.6	39551.9		
K	140.7	246.9	378.6	664.2	6360.0	11158.0	10359.4	18174.3		
L	125.6	220.3	480.5	842.9	7939.0	13928.0	14888.6	26120.4		
Cycle Filters										
	F1		F4		B1		B4			
0	44660.7	78352.1	50613.2	88795.1	51394.0	90165.0	51542.9	90426.2		
F500	87047.9	152715.6	88425.9	155133.1	78709.8	138087.4	78886.8	138397.9		
T500	66488.8	116647.0	62193.3	109111.0	61745.1	108324.8	66275.6	116273.0		
Internal Filters – Different Car Makes										
	1S		3S		5S		7S		9S	
Blank	1028.8	1805.0	1487.3	2609.4	1002.9	1759.5	1135.1	1991.5	1406.5	2467.6
CM3	3088.1	5417.7	2146.0	3764.9	1822.0	3196.6	2754.3	4832.1	1680.3	2948.0
CM4	2197.6	3855.5	1881.7	3301.3	1708.2	2996.8	2059.6	3613.4	1604.1	2814.3
CM5	2000.4	3509.5	2423.1	4251.1	1343.6	2357.3	2239.0	3928.2	1940.4	3404.2
Internal Filters – CM3										
	1S		3S		5S		7S		9S	
Blank	1028.8	1805.0	1487.3	2609.4	1002.9	1759.5	1135.1	1991.5	1406.5	2467.6
NPF	3088.1	5417.7	2146.0	3764.9	1822.0	3196.6	2754.3	4832.1	1680.3	2948.0
Particle	1766.1	3098.3	1946.8	3415.5	1424.5	2499.1	1240.4	2176.1	1924.4	3376.1
Combi	1100.5	1930.7	1491.0	2615.8	1591.0	2791.2	686.4	1204.2	1027.4	1802.5

**Chromium filter sample recoveries corrected to 100% based an SRM recovery of 91.3%**

Micronair standard particle filter - CM1				
	0 km	15,000 km	30,000 km	45,000 km
	µg/L			
A	0	41.42	123.24	114.38
B	0	37.76	127.59	150.23
C	0	36.02	154.31	276.85
D	0	36.84	159.3	194.98
E	0	53.03	204.55	209.48
F	0	54.98	185.59	165.76
G	0	31.12	216.26	128.95
H	0	53.99	124.98	138.94
I	0	57.41	212.15	106.23
Airforce standard particle filter - CM1				
	0 km		15,000 km	
	µg/L			
A	6.08		53.21	
B	7.67		108.36	
C	8.27		166.7	
D	7.59		77.32	
E	9.07		91.14	
F	7.6		47.31	
G	6.61		106.73	
H	8.06		100.16	
I	5.12		78.6	
Airforce combination filter – CM1				
	0 km		15,000 km	
	µg/L			
A	15.65		114.81	

B		42.59		182.15
C		67.33		201.71
D		11.64		165.65
E		13.52		253.91
F		11.45		211.6
G		37.27		198.71
H		28.27		181.53
I		49.48		115.92
Micronair combination filter – CM1				
		0 km		15,000 km
		µg/L		
A		6.08		53.21
B		7.67		108.36
C		8.27		166.7
D		7.59		77.32
E		9.07		91.14
F		7.6		47.31
G		6.61		106.7
H		8.06		100.16
I		5.12		78.6
Micronair standard particle filter - CM2				
	0 km	15,000 km	30,000 km	45,000 km
	µg/L			
A	0	57.53	129.14	94.81
B	0	58.15	94.42	42.59
C	0	75.82	57.44	130.31
D	5.72	46.7	83.64	68.05
E	0	39.02	118.44	43.83
F	0	74.35	124.20	108.49
G	14.91	99.32	150.85	64.98
H	0	65.51	156.81	46.37



I	44.72	32.16	121.28	34.26
J	12.13	33.04	61.72	130.47
K	0	38.01	69.56	64.33
L	0	48.23	58.86	46.95
<b>Nip &amp; Denso standard particle filter - CM2</b>				
	0 km	15,000 km	30,000 km	45,000 km
	µg/L			
A	31.4	43.82	121.69	199.86
B	0	66.07	315.14	573.42
C	0	92.38	280.23	405.84
D	0	335.04	283.07	540.91
E	21.44	214.1	281.94	617.94
F	23.72	240.14	295.4	241.49
G	0	231.83	156.37	653.39
H	0	268.91	488.31	638.85
I	0	254.59	240.45	531.47
J	0	218.26	142.78	630.18
K	0	233.5	325.2	486.3
L	0	174.5	222.8	484.6

	<b>Airforce Particle Filter – CM3</b>				<b>Airforce Combination Filter - CM3</b>			
	0		15000		0		15000	
A	14.6	16.0	106.2	116.3	15.7	17.2	159.3	174.4
B	13.1	14.3	80.0	87.6	15.2	16.7	115.3	126.3
C	15.9	17.5	54.9	60.1	24.4	26.8	176.7	193.5
D	13.1	14.4	52.1	57.0	9.5	10.4	108.3	118.7
E	12.9	14.2	92.7	101.5	8.3	9.0	126.1	138.1
F	17.4	19.1	99.2	108.6	22.9	25.1	117.0	128.1
G	11.0	12.0	90.4	99.0	14.1	15.5	98.8	108.2
H	11.5	12.6	65.3	71.5	13.2	14.5	118.1	129.4
I	15.2	16.6	125.8	137.8	17.0	18.6	132.0	144.5

J	14.4	15.8	117.8	129.1	12.6	13.8	212.6	232.8		
K	11.5	12.6	64.5	70.7	10.4	11.4	147.6	161.6		
L	11.7	12.9	62.2	68.2	26.1	28.6	160.9	176.2		
Cycle Filters										
	F1		F4		B1		B4			
0	205.3	224.9	227.7	249.4	223.4	244.6	208.8	228.7		
F500	178.2	195.2	187.1	204.9	220.0	240.9	171.7	188.1		
T500	183.1	200.6	151.4	165.9	129.8	142.2	130.6	143.1		
Internal Filters – Different Car Makes										
	1S		3S		5S		7S		9S	
Blank	1028.8	1126.9	1487.3	1629.1	1002.9	1098.5	1135.1	1243.3	1406.5	1540.6
CM3	3088.1	3382.4	2146.0	2350.5	1822.0	1995.7	2754.3	3016.7	1680.3	1840.5
CM4	2197.6	2407.0	1881.7	2061.0	1708.2	1871.0	2059.6	2255.9	1604.1	1757.0
CM5	2000.4	2191.0	2423.1	2654.0	1343.6	1471.7	2239.0	2452.4	1940.4	2125.3
Internal Filters – CM3										
	1S		3S		5S		7S		9S	
Blank	14.8	16.3	13.3	14.6	16.9	18.5	15.1	16.5	19.1	20.9
NPF	56.1	61.5	60.3	66.0	64.1	70.2	55.3	60.6	66.7	73.0
Particle	16.9	18.6	27.3	29.9	28.9	31.7	19.4	21.2	32.9	36.0
Combi	35.2	38.5	31.1	34.0	34.3	37.6	38.5	42.2	32.4	35.5

## Copper filter sample recoveries corrected to 100% based an SRM recovery of 80.6%

Micronair standard particle filter - CM1				
	0 km	15,000 km	30,000 km	45,000 km
	mg/L			
A	0.02	1.45	26.28	19.05
B	0.01	2.30	25.03	25.28
C	0.01	1.41	32.17	19.09
D	0.02	4.33	36.63	38.09
E	0.02	3.12	50.79	41.78
F	0.03	6.11	56.21	27.03
G	0.04	4.39	63.21	53.42
H	0.01	3.86	78.26	40.75
I	0.01	6.55	68.35	43.00
Airforce standard particle filter - CM1				
	0 km		15,000 km	
	mg/L			
A	0.01		36.70	
B	0.01		26.36	
C	0.01		29.69	
D	0.00		20.64	
E	0.00		16.37	
F	0.00		23.51	
G	0.00		12.00	
H	0.00		10.01	
I	0.00		25.64	
Airforce combination filter – CM1				
	0 km		15,000 km	
	mg/L			
A	1.09		120.99	
B	1.02		69.24	

C		1.20		69.37	
D		1.13		45.61	
E		1.12		91.56	
F		0.90		100.18	
G		0.96		49.20	
H		0.98		106.68	
I		1.12		59.06	
Micronair combination filter – CM1					
		0 km		15,000 km	
		mg/L			
A		0.83		6.54	
B		1.02		8.63	
C		0.91		7.37	
D		0.91		16.18	
E		0.77		18.01	
F		1.00		14.31	
G		1.08		26.95	
H		0.84		7.30	
I		0.94		20.28	
Micronair standard particle filter - CM2					
	0 km	15,000 km	30,000 km	45,000 km	
	mg/L				
A	0.00	0.61	0.93	0.99	
B	0.00	0.71	1.05	0.86	
C	0.00	0.88	0.67	0.79	
D	0.00	0.86	0.90	0.61	
E	0.00	0.58	0.60	0.35	
F	0.00	0.64	0.57	0.08	
G	0.00	0.62	1.16	0.45	
H	0.00	0.72	1.03	0.46	
I	0.00	0.63	0.81	0.37	

J	0.00	0.61	0.45	0.56
K	0.00	0.35	0.46	0.52
L	0.00	0.08	0.37	0.33
<b>Nip &amp; Denso standard particle filter - CM2</b>				
	0 km	15,000 km	30,000 km	45,000 km
	mg/L			
A	0.00	0.48	1.21	6.83
B	0.00	0.48	1.34	5.58
C	0.00	0.68	1.16	6.82
D	0.00	0.81	1.34	7.75
E	0.00	0.54	1.30	8.38
F	0.00	0.49	1.29	12.17
G	0.00	0.58	1.76	10.19
H	0.00	0.64	1.36	8.94
I	0.00	0.63	1.15	8.88
J	0.00	0.49	1.43	8.45
K	0.00	0.51	1.63	6.10
L	0.00	0.53	1.25	8.32

	<b>Airforce Particle Filter – CM3</b>				<b>Airforce Combination Filter - CM3</b>			
	0		15000		0		15000	
A	0	0	1382.4	1717.2	895.6	1112.5	2448.8	3042.0
B	0	0	1166.1	1448.6	843.5	1047.8	3918.6	4867.8
C	0	0	989.6	1229.3	758.4	942.1	3806.1	4728.1
D	0	0	588.6	731.2	822.8	1022.1	2073.9	2576.3
E	0	0	701.6	871.5	693.6	861.6	2015.4	2503.6
F	0	0	866.4	1076.3	749.0	930.5	2532.3	3145.7
G	0	0	760.9	945.2	718.1	892.1	2229.8	2770.0
H	0	0	748.7	930.1	760.7	945.0	1621.0	2013.6
I	0	0	963.4	1196.8	751.2	933.1	1687.8	2096.7

J	0	0	864.4	1073.7	721.4	896.2	1649.0	2048.4		
K	0	0	715.8	889.2	763.4	948.3	1601.5	1989.5		
L	0	0	803.4	998.0	827.4	1027.9	1862.8	2314.1		
Cycle Filters										
	F1		F4		B1		B4			
0	52.3	65.0	85.2	105.8	65.1	80.8	43.6	54.1		
F500	287.1	356.6	431.5	536.1	361.0	448.5	473.8	588.6		
T500	391.5	486.3	362.5	450.3	330.1	410.0	310.6	385.8		
Internal Filters – Different Car Makes										
	1S		3S		5S		7S		9S	
Blank	37.6	46.7	9.5	11.8	8.3	10.3	32.1	39.9	17.8	22.1
CM3	256.8	319.1	264.2	328.2	241.5	300.0	146.1	181.5	285.0	354.1
CM4	461.1	572.7	454.5	564.6	484.3	601.6	416.7	517.6	412.2	512.0
CM5	164.2	204.0	140.0	173.9	255.2	317.0	171.0	212.4	204.7	254.3
Internal Filters – CM3										
	1S		3S		5S		7S		9S	
Blank	37.6	46.7	9.5	11.8	8.3	10.3	32.1	39.9	17.8	22.1
NPF	256.8	319.1	264.2	328.2	241.5	300.0	146.1	181.5	285.0	354.1
Particle	53.7	66.7	55.6	69.1	76.1	94.6	48.1	59.7	59.5	73.9
Combi	122.1	151.7	127.2	158.1	102.1	126.9	76.4	94.9	131.8	163.7

**Iron filter sample recoveries corrected to 100% based an SRM recovery of 82.5%**

Micronair standard particle filter - CM1				
	0 km	15,000 km	30,000 km	45,000 km
	mg/L			
A	0.82	8.98	24.62	29.31
B	0.41	8.52	23.48	28.69
C	0.37	2.99	33.54	21.42
D	0.30	4.69	23.46	31.43
E	0.55	9.48	38.77	35.54
F	0.18	4.57	34.23	31.89
G	0.58	4.65	26.26	27.48
H	0.23	10.76	27.01	27.92
I	0.26	14.98	26.49	27.68
Airforce standard particle filter - CM1				
	0 km		15,000 km	
	mg/L			
A	0.23		21.91	
B	0.79		16.41	
C	0.37		19.45	
D	0.38		13.09	
E	0.66		13.38	
F	0.56		15.16	
G	0.34		8.85	
H	0.22		7.88	
I	0.13		15.67	
Airforce combination filter – CM1				
	0 km		15,000 km	
	mg/L			

A	8.47	47.67		
B	5.87	34.22		
C	6.66	32.15		
D	6.56	58.11		
E	10.23	46.12		
F	11.03	52.92		
G	10.09	46.90		
H	9.61	45.66		
I	9.22	41.47		
Micronair combination filter – CM1				
	0 km	15,000 km		
	mg/L			
A	5.19	17.39		
B	8.08	20.82		
C	6.04	20.71		
D	3.61	22.94		
E	5.00	21.96		
F	5.06	20.12		
G	4.00	25.02		
H	5.32	24.64		
I	5.50	17.14		
Micronair standard particle filter - CM2				
	0 km	15,000 km	30,000 km	45,000 km
	mg/L			
A	0.34	15.34	24.13	18.05
B	0.37	17.94	27.48	16.73
C	0.35	19.23	17.74	15.51
D	0.32	19.50	23.38	16.67
E	0.57	11.45	16.00	14.48
F	0.18	13.14	15.41	13.69
G	0.73	14.17	29.56	15.37



H	0.48	15.69	30.48	18.16
I	0.31	14.89	23.41	16.82
J	0.37	13.55	15.32	10.58
K	0.75	15.56	12.50	7.93
L	0.37	8.54	10.49	4.96
<b>Nip &amp; Denso standard particle filter - CM2</b>				
	0 km	15,000 km	30,000 km	45,000 km
	mg/L			
A	1.02	14.27	37.16	119.21
B	0.24	6.93	43.14	108.39
C	0.48	22.48	36.10	118.55
D	0.14	24.38	33.50	129.95
E	0.21	14.23	34.04	134.94
F	0.12	25.86	33.95	138.92
G	0.43	17.77	44.85	133.89
H	0.07	20.68	35.30	139.98
I	0.02	21.90	30.18	134.14
J	0.31	14.73	42.59	132.87
K	0.58	14.47	44.99	108.60
L	0.04	14.99	34.46	126.59

	Airforce Particle Filter - CM3				Airforce Combination Filter - CM3			
			15000		0		15000	
A	268.0	324.8	1506.9	1826.5	21003.2	25458.4	32212.2	39045.1
B	550.9	667.7	1134.7	1375.4	11403.0	13821.9	30105.3	36491.3
C	298.8	362.1	974.1	1180.8	15783.2	19131.1	39165.4	47473.2
D	384.9	466.5	877.2	1063.2	14205.4	17218.7	28595.8	34661.5
E	248.6	301.3	779.5	944.9	12292.2	14899.7	31909.7	38678.4
F	264.2	320.3	1205.1	1460.8	17768.4	21537.4	37827.3	45851.3
G	223.7	271.2	1104.0	1338.1	8148.8	9877.4	27574.6	33423.8
H	289.2	350.5	1081.6	1311.0	12155.5	14734.0	38783.4	47010.1
I	246.8	299.2	1288.3	1561.6	10151.2	12304.5	33224.3	40271.9
J	245.2	297.2	975.8	1182.8	16349.5	19817.6	39064.2	47350.6
K	221.9	269.0	1035.7	1255.4	12281.4	14886.5	44338.0	53743.0
L	241.8	293.1	1433.2	1737.2	11070.3	13418.6	43289.6	52472.2

**Cycle Filters**

	F1		F4		B1		B4	
0	32753.2	39700.9	36337.6	44045.6	37861.5	45892.8	34773.3	42149.5
F500	68413.2	82925.1	60214.5	72987.3	60762.3	73651.3	68068.8	82507.7
T500	67266.2	81534.7	60597.0	73450.9	56598.0	68603.6	54288.7	65804.5

**Internal Filters – Different Car Makes**

	1S		3S		5S		7S		9S	
Blank	729.0	883.7	624.9	757.5	802.0	972.1	1036.9	1256.9	818.1	991.6
CM3	1365.8	1655.5	2099.6	2544.9	1526.5	1850.3	1367.1	1657.1	1674.0	2029.1
CM4	1745.2	2115.4	1767.4	2142.4	1897.6	2300.2	1515.3	1836.7	1513.3	1834.3
CM5	1899.7	2302.7	1606.4	1947.2	1519.5	1841.9	1934.3	2344.6	1835.7	2225.1

**Internal Filters – CM3**

	1S		3S		5S		7S		9S	
Blank	729.0	883.7	624.9	757.5	802.0	972.1	1036.9	1256.9	818.1	991.6
NPF	1365.8	1655.5	2099.6	2544.9	1526.5	1850.3	1367.1	1657.1	1674.0	2029.1
Particle	1189.2	1441.5	1517.6	1839.6	1131.6	1371.7	1314.9	1593.8	1325.0	1606.1
Combi	1030.4	1249.0	1355.1	1642.6	880.3	1067.0	1137.7	1379.0	1180.5	1430.9

Lead filter sample recoveries corrected to 100% based an SRM recovery of 87.3%

Micronair standard particle filter - CM1				
	0 km	15,000 km	30,000 km	45,000 km
	µg/L			
A	0	173.67	256.31	286.26
B	0	176.51	236.61	291.59
C	0	130.51	245.96	300.62
D	0	146.88	244.52	285.98
E	0	148.88	272.77	266.43
F	0	208.98	311.33	239.59
G	0	138.69	273.56	298
H	0	176.2	309.43	262.39
I	0	192.37	281.7	357.79
Airforce standard particle filter - CM1				
	0 km		15,000 km	
	µg/L			
A	200.98		295.14	
B	184.14		246.83	
C	167.29		203.48	
D	195.47		248.71	
E	159.84		263.88	
F	203.56		172.82	
G	183.5		231.29	
H	30.46		212.53	
I	223.73		308.77	
Airforce combination filter – CM1				
	0 km		15,000 km	
	µg/L			
A	199.84		403.8	

B		155.88		267.12
C		167.01		363.17
D		196.17		352.63
E		216.81		392.34
F		158.9		385.83
G		109.99		405.92
H		242.55		221.03
I		227.65		187.56
Micronair combination filter – CM1				
		0 km		15,000 km
		µg/L		
A		104.56		164.33
B		132.32		180.97
C		113.47		241.49
D		190.58		139.82
E		213.25		140.98
F		155.75		129.64
G		110.61		210.46
H		160.52		218.48
I		91.23		188.11
Micronair standard particle filter - CM2				
	0 km	15,000 km	30,000 km	45,000 km
	µg/L			
A	127.62	250.72	235.53	152.01
B	54.56	111.65	268.99	208.26
C	30.24	215.48	120.3	236.41
D	188.03	268.17	188.02	208.21
E	258.26	217.7	216.25	182.1
F	91.88	241.19	199.45	142.97
G	276.53	285.03	242.59	138.96
H	182.1	161.48	209.63	213.29

I	238.28	193.09	237.63	250.39
J	229.9	157.92	188.02	192.311
K	224.97	98.79	210	199.11
L	119.4	108.57	193.8	184.03
<b>Nip &amp; Denso standard particle filter - CM2</b>				
	0 km	15,000 km	30,000 km	45,000 km
	µg/L			
A	22.42	141.36	257.2	414.73
B	14.07	142.93	231.9	380.99
C	43.88	210.68	191.25	511.45
D	32.75	96.85	179.86	358.38
E	33.7	156.71	405.48	439.22
F	31.1	111.72	356.49	499.73
G	15.05	166.14	176.29	465.42
H	67.97	207.76	98.51	560.48
I	77.9	151.08	107.9	498.29
J	40.33	154.01	145.25	501.77
K	8.4	160.8	165.7	387.9
L	72.2	158.1	97.1	472.8

	<b>Airforce Particle Filter - CM3</b>				<b>Airforce Combination Filter - CM3</b>			
	0		15000		0		15000	
A	500.5	609.6	1428.9	1740.4	505.4	615.6	1304.4	1588.8
B	516.1	628.6	1343.9	1636.9	510.5	621.8	1179.9	1437.2
C	522.3	636.2	1246.6	1518.4	533.2	649.5	1704.2	2075.8
D	555.0	676.0	1242.5	1513.4	566.9	690.5	1271.8	1549.0
E	581.5	708.3	1389.3	1692.2	486.5	592.6	1374.5	1674.1
F	597.5	727.8	1270.3	1547.2	518.4	631.4	1333.0	1623.7
G	595.5	725.3	1258.7	1533.2	502.6	612.2	1332.0	1622.4
H	528.3	643.5	1297.5	1580.4	533.5	649.8	1582.2	1927.2

I	552.1	672.5	1270.3	1547.3	545.9	664.9	1319.1	1606.7
J	440.7	536.8	1492.7	1818.2	539.6	657.3	1170.4	1425.6
K	486.3	592.3	1562.8	1903.6	656.7	799.8	1671.0	2035.3
L	522.1	635.9	1346.2	1639.7	518.1	631.1	1049.9	1278.8
<b>Cycle Filters</b>								
	F1		F4		B1		B4	
0	232.0	282.6	253.5	308.8	259.6	316.2	245.5	299.1
F500	478.4	582.7	492.6	600.0	422.6	514.7	458.7	558.7
T500	322.6	393.0	293.9	358.0	368.6	448.9	230.3	280.5

Internal Filters – Different Car Makes										
	1S		3S		5S		7S		9S	
Blank	16.9	20.6	13.4	16.3	17.1	20.8	10.0	12.2	11.7	14.3
CM3	60.6	73.8	54.2	66.0	69.5	84.6	64.5	78.6	57.3	69.8
CM4	61.1	74.4	45.0	54.8	39.4	48.0	30.7	37.3	41.6	50.6
CM5	65.9	80.3	50.2	61.1	57.8	70.4	57.9	70.5	72.9	88.9
Internal Filters – CM3										
	1S		3S		5S		7S		9S	
Blank	86.9	105.9	93.4	113.8	97.1	118.2	100.0	121.8	81.7	99.5
NPF	220.6	268.7	204.2	248.7	219.5	267.4	264.5	322.2	257.3	313.4
Particle	32.7	39.9	86.3	105.1	74.7	91.0	56.4	68.7	54.0	65.8
Combi	104.8	127.7	83.9	102.2	85.5	104.2	90.0	109.6	130.4	158.8

Manganese filter sample recoveries corrected to 100% based an SRM recovery of 82.1%

Micronair standard particle filter - CM1				
	0 km	15,000 km	30,000 km	45,000 km
	mg/L			
A	0.00	0.17	0.88	1.25
B	0.00	0.15	0.82	1.35
C	0.00	0.07	1.11	1.35
D	0.00	0.10	0.85	1.34
E	0.00	0.18	1.16	1.55
F	0.00	0.22	1.05	1.43
G	0.00	0.11	0.99	1.47
H	0.00	0.22	0.86	1.26
I	0.00	0.31	0.98	1.37
Airforce standard particle filter - CM1				
	0 km		15,000 km	
	mg/L			
A	0.00		0.72	
B	0.00		0.63	
C	0.00		1.20	
D	0.00		1.03	
E	0.00		1.05	
F	0.00		0.75	
G	0.00		0.64	
H	0.01		0.99	
I	0.00		0.71	
Airforce combination filter – CM1				
	0 km		15,000 km	
	mg/L			
A	0.46		1.65	

B		0.58		1.61
C		0.20		1.33
D		0.11		2.47
E		0.15		1.59
F		0.10		2.01
G		0.08		1.43
H		0.35		1.64
I		0.13		1.39
Micronair combination filter – CM1				
		0 km		15,000 km
		mg/L		
A		0.01		1.08
B		0.01		1.12
C		0.02		1.33
D		0.01		1.31
E		0.01		1.09
F		0.01		1.06
G		0.01		1.55
H		0.01		1.40
I		0.01		1.43
Micronair standard particle filter - CM2				
	0 km	15,000 km	30,000 km	45,000 km
	mg/L			
A	1.07	1.43	1.61	1.66
B	1.31	1.69	1.73	1.64
C	1.17	1.52	1.06	1.62
D	0.73	1.54	1.41	1.46
E	1.46	1.55	1.56	1.49
F	1.07	1.35	1.63	1.58
G	1.57	1.40	1.71	1.38
H	0.81	1.24	1.83	1.64



I	1.31	1.61	1.61	1.57
J	1.43	1.36	1.19	1.29
K	1.24	1.38	1.22	1.09
L	1.23	2.06	1.23	1.04
<b>Nip &amp; Denso standard particle filter - CM2</b>				
	0 km	15,000 km	30,000 km	45,000 km
	mg/L			
A	0.25	0.29	1.22	1.59
B	0.21	0.45	2.38	2.00
C	0.29	0.66	2.03	1.81
D	0.18	1.68	1.40	2.31
E	0.33	0.33	2.22	2.21
F	0.31	0.99	2.21	2.04
G	0.25	0.44	1.37	2.22
H	0.19	1.22	1.52	3.23
I	0.22	0.74	1.25	2.75
J	1.24	0.92	1.32	2.56
K	1.09	0.29	1.74	2.37
L	1.39	0.33	1.34	2.27

	Airforce Particle Filter - CM3				Airforce Combination Filter - CM3				Appendix
	0		15000		0		15000		
A	94.9	108.7	238.4	273.1	39.0	44.7	161.7	185.2	
B	102.1	117.0	229.5	262.8	26.4	30.2	131.7	150.9	
C	80.5	92.2	216.7	248.2	16.4	18.8	126.3	144.6	
D	96.0	109.9	215.1	246.4	27.4	31.4	130.4	149.4	
E	94.5	108.3	207.7	238.0	31.8	36.4	172.6	197.7	
F	93.5	107.1	230.5	264.1	22.6	25.9	125.8	144.0	
G	91.3	104.6	229.3	262.7	26.6	30.5	138.6	158.8	
H	90.9	104.1	205.7	235.7	9.9	11.3	124.4	142.5	
I	83.2	95.3	237.7	272.3	21.8	25.0	139.1	159.3	
J	97.6	111.8	210.5	241.1	24.3	27.8	119.1	136.5	
K	97.1	111.3	203.1	232.7	26.3	30.1	134.1	153.6	
L	94.3	108.0	205.6	235.5	18.9	21.6	104.2	119.3	
<b>Cycle Filters</b>									
	F1		F4		B1		B4		
0	248.8	285.0	260.9	298.9	210.8	241.4	287.1	328.9	
F500	271.5	311.0	239.0	273.8	271.5	311.0	239.0	273.8	
T500	190.3	218.0	205.7	235.6	240.2	275.1	245.0	280.7	

Internal Filters – Different Car Makes										
	1S		3S		5S		7S		9S	
Blank	128.8	147.5	135.8	155.6	127.3	145.8	112.8	129.2	98.1	112.4
CM3	334.7	383.4	413.1	473.3	363.6	416.5	335.3	384.1	312.8	358.3
CM4	785.5	899.8	697.8	799.3	470.4	538.9	664.9	761.6	664.8	761.5
CM5	588.6	674.3	606.9	695.2	772.1	884.4	658.3	754.1	616.7	706.5
Internal Filters – CM3										
	1S		3S		5S		7S		9S	
Blank	128.8	147.5	35.8	41.0	127.3	145.8	112.8	129.2	98.1	112.4
NPF	334.7	383.4	413.1	473.3	363.6	416.5	335.3	384.1	312.8	358.3
Particle	236.4	270.8	124.1	142.2	122.5	140.3	242.4	277.7	239.8	274.6
Combi	143.6	164.5	106.2	121.7	159.6	182.9	134.2	153.7	133.4	152.8

Zinc filter sample recoveries corrected to 100% based an SRM recovery of 83.5%

Micronair standard particle filter - CM1				
	0 km	15,000 km	30,000 km	45,000 km
	µg/L			
A	0.18	0.38	1.98	1.61
B	0.21	0.35	1.78	1.70
C	0.22	0.25	1.74	1.84
D	0.18	0.36	1.60	1.87
E	0.21	0.45	3.86	2.08
F	0.20	2.40	3.16	1.59
G	0.05	0.47	1.76	1.80
H	0.03	0.44	1.95	1.61
I	0.02	0.67	1.90	1.93
Airforce standard particle filter - CM1				
	0 km		15,000 km	
	µg/L			
A	0.02		0.13	
B	0.02		0.52	
C	0.02		0.54	
D	0.02		0.26	
E	0.01		0.35	
F	0.02		0.59	
G	0.08		0.90	
H	0.06		0.50	
I	0.02		0.55	
Airforce combination filter – CM1				
	0 km		15,000 km	
	µg/L			
A	0.31		2.58	

B		0.28		2.14
C		0.26		1.85
D		0.28		2.87
E		0.27		2.61
F		0.50		3.21
G		0.28		2.18
H		0.34		2.51
I		0.25		3.25
Micronair combination filter – CM1				
		0 km		15,000 km
		µg/L		
A		0.20		0.47
B		0.25		0.94
C		0.23		1.77
D		0.13		0.77
E		0.30		1.02
F		0.33		0.44
G		0.34		1.13
H		0.34		1.42
I		0.26		0.65
Micronair standard particle filter - CM2				
	0 km	15,000 km	30,000 km	45,000 km
	µg/L			
A	0.02	0.46	0.93	0.94
B	0.11	0.50	1.08	0.50
C	0.05	0.60	0.43	0.58
D	0.02	1.15	0.78	0.76
E	0.03	0.50	0.67	0.48
F	0.03	0.85	0.67	0.74
G	0.03	1.06	1.20	0.73
H	0.01	0.80	1.35	0.93

I	0.07	0.49	0.94	0.58
J	0.06	0.51	0.72	0.36
K	0.06	0.51	0.83	0.55
L	0.02	0.48	0.46	0.42
<b>Nip &amp; Denso standard particle filter - CM2</b>				
	0 km	15,000 km	30,000 km	45,000 km
	$\mu\text{g/L}$			
A	0.09	0.68	6.19	3.33
B	0.22	0.64	4.79	4.90
C	0.16	0.85	1.73	5.96
D	0.34	0.34	2.82	2.82
E	0.52	0.45	3.83	3.21
F	0.51	0.54	4.61	3.82
G	0.47	0.41	3.03	4.21
H	0.03	0.37	2.87	5.18
I	0.02	0.34	1.16	4.45
J	0.03	0.50	3.29	4.17
K	0.04	0.46	3.52	3.68
L	0.01	0.36	3.01	4.27

	<b>Airforce Particle Filter - CM3</b>				<b>Airforce Combination Filter - CM3</b>			
	0		15000		0		15000	
A	261.6	313.3	1125.3	1347.6	493.2	590.7	2966.4	3552.6
B	275.1	329.4	719.2	861.3	656.4	786.1	2504.4	2999.3
C	228.1	273.1	699.4	837.6	87.4	104.7	3774.1	4519.9
D	250.3	299.8	707.8	847.7	201.5	241.3	2396.1	2869.6
E	135.5	162.3	628.0	752.1	176.2	211.0	2238.1	2680.3
F	232.2	278.1	938.3	1123.7	57.2	68.5	3482.2	4170.2
G	259.0	310.1	509.4	610.1	355.9	426.3	3265.1	3910.3

H	264.2	316.4	605.2	724.8	388.4	465.1	2836.4	3396.9
I	224.6	269.0	676.2	809.8	267.8	320.8	2299.8	2754.2
J	219.7	263.1	646.5	774.3	392.9	470.5	2653.4	3177.7
K	101.0	121.0	634.1	759.4	234.8	281.2	2240.9	2683.7
L	249.3	298.5	662.2	793.1	61.5	73.7	2510.3	3006.4
<b>Cycle Filters</b>								
	F1		F4		B1		B4	
0	349.6	418.7	200.8	240.5	142.0	170.0	288.3	345.3
F500	501.0	600.0	570.8	683.6	592.7	709.9	580.4	695.0
T500	508.4	608.9	429.5	514.3	635.9	761.5	564.3	675.8

<b>Internal Filters – Different Car Makes</b>										
	1S		3S		5S		7S		9S	
Blank	252.8	302.8	251.1	300.7	368.3	441.1	205.1	245.7	238.4	285.6
CM3	2710.3	3245.9	2604.7	3119.4	2115.2	2533.2	2206.7	2642.7	2814.7	3370.9
CM4	4841.6	5798.3	4144.1	4963.0	3103.5	3716.8	4304.9	5155.5	4194.8	5023.7
CM5	3050.6	3653.4	4082.2	4888.9	4340.5	5198.2	5743.4	6878.3	5027.6	6021.0
<b>Internal Filters – CM3</b>										
	1S		3S		5S		7S		9S	
Blank	252.8	302.8	251.1	300.7	368.3	441.1	205.1	245.7	238.4	285.6
NPF	2710.3	3245.9	2604.7	3119.4	2115.2	2533.2	2206.7	2642.7	1814.7	2173.3
Particle	112.5	134.7	138.2	165.6	119.9	143.6	272.6	326.5	271.5	325.1
Combi	208.7	250.0	247.8	296.7	285.5	341.9	287.1	343.9	268.6	321.7